STUDY OF THE ROLE OF VIRAL COAT PROTEIN AND HOST FACTOR HSP70 HOMOLOGS IN THE ASSEMBLY AND DISASSEMBLY OF *CUCUMBER NECROSIS VIRUS* PARTICLES

by

SYED BENAZIR ALAM

B.Sc. in Chemistry, University of Calcutta, India, 2008

M.Sc. in Biochemistry, University of Calcutta, India, 2010

A THESIS SUBMITTED IN THE PARTIAL FULFILLMENT OF THE REQUIREMENTS FOR THE DEGREE OF

DOCTOR OF PHILOSOPHY

in

The Faculty of Graduate and Postdoctoral Studies

(Plant Science)

The University of British Columbia

(Vancouver)

May 2017

Abstract

Virion assembly and disassembly are crucial aspects of the virus multiplication cycle, however, relatively little is known about these processes in plant viruses. While the former helps to produce multiple copies of stable infectious progeny virions, the latter is required for release of the encapsidated viral genome into a host cell for initiating new rounds of virus multiplication. In this thesis, I aimed to study *Cucumber necrosis virus* (CNV) particle assembly and disassembly and the role of CNV coat protein (CP) and host HSP70 homologs in these processes. I found that CNV infection of *Nicotiana benthamiana* causes a significant upregulation of HSP70 homologs, and that, in turn, HSP70 is co-opted by the virus at several stages of the multiplication cycle to promote various aspects of the infection cycle including viral RNA, CP and particle accumulation. HSP70 homologs were also found to assist CNV CP in chloroplast targeting possibly to attenuate chloroplast-mediated plant defence and thereby allow further spread of the virus. I also determined that the HSP70 homologue, Hsc70-2 is bound to CNV virions and that this association appears to facilitate the uncoating efficiency of CNV particles likely via triggering a conformational change in particles. This is the first report that a plant virus utilizes HSP70 homologs for disassembly.

A highly basic "KGRKPR" sequence in the ε region of the CNV CP arm was also examined for its role in virion assembly and encapsidation of viral RNA. Through mutational analysis, it was found that the basic residues promote T=3 versus T=1 virion formation and encapsidation of full-length viral RNA *in vivo*. Moreover, mutants lacking two to four of the basic residues encapsidated proportionately greater amounts of host RNA suggesting the role of these basic residues in selection of viral RNA during assembly.

I also showed that heat shock enhances transcription of heat-inducible ONSEN-like retro-transposons known to be induced during CNV infection. Since retrotransposons are known to play an important role in genome variation, the described studies may be helpful in understanding the importance of plant viruses in inducing genome variation and perhaps adaptation of plants to changes in the environment.

Lay Summary

CNV is a plant virus that naturally infects cucumbers, reducing their marketability. The objective of this research is to understand how CNV induces disease with the overall aim of using the knowledge to generate new methods for virus disease control. Our studies have focused on how CNV uncoats to release its genome to establish infection and how new virions are assembled in cells, two essential aspects of the CNV infection cycle. CNV was found to induce and interact with the host protein HSP70, which is normally involved in protein folding and unfolding. Such interaction assists in CNV uncoating and also increases CNV RNA, coat protein and virion accumulation during infection. A short sequence in the CNV coat protein was also found to be essential for efficient and proper virion formation. It also ensures that viral rather than host RNA is encapsidated, and thereby assists in the formation of infectious virions.

Preface

The research work of this thesis was conducted under the able guidance of Dr. D'Ann Rochon at the Agriculture and Agri-Food Canada, Summerland Research and Development Center (SuRDC), Summerland, British Columbia, Canada from May 2012 to December 2016 by the Candidate. A list of manuscripts that are either published or in preparation are mentioned below which have resulted from the research conducted in this thesis. The contribution of the candidate is mentioned below.

Chapter 1: Literature review

The candidate wrote the chapter and Dr. D'Ann Rochon provided editorial support.

A version of information presented in this chapter has been published in *Virology*, http://dx.doi.org/10.1016/j.virol.2013.12.035. Rochon, D., Singh, B., Reade, R., Theilmann, J., Ghoshal, K., **Alam, S.B.** and Maghodia, A. (2014); "The p33 auxiliary replicase protein of *Cucumber necrosis virus* targets peroxisomes and infection induces de novo peroxisome formation from the endoplasmic reticulum" (Virology Highlights).

The candidate performed CNV inoculation experiments on 16C transgenic *N. benthamiana* plants, and performed confocal microscopy with the guidance of Dr. D'Ann Rochon.

Chapter 2: "*Cucumber necrosis virus* recruits cellular heat shock protein 70 homologs at several stages of infection" was modified from the manuscript published in the *Journal of Virology*: **Alam, S.B.** and Rochon, D. (2016) "*Cucumber necrosis virus* recruits cellular heat

shock protein 70 homologs at several stages of infection". J. Virol 90:3302–3317.doi:10.1128/JVI.02833-15.

The candidate and Dr. D'Ann Rochon designed the research. The candidate conducted experiments. Dr. D'Ann Rochon initially analysed the Next Generation Sequence Analysis raw data to obtain an Excel sheet containing a list of all the *N. benthamiana* host genes expressed during CNV infection. The candidate extracted and analysed all the data corresponding to upregulated HSP70 homologs, confirmed their annotation and prepared the Heat map. The candidate wrote the manuscript and Dr. D'Ann Rochon supervised the work, manuscript preparation and provided editorial support.

Chapter 3: "Evidence that Hsc70 is associated with *Cucumber necrosis virus* and plays a role in particle disassembly" was modified from the manuscript published in the *Journal of Virology*: **Alam, S.B.** and Rochon, D. (2017) "Evidence that Hsc70 is associated with *Cucumber necrosis virus* and plays a role in particle disassembly" J. Virol 91:e01555-16.https://doi.org/10.1128/JVI.01555-16. This article was chosen as a *Journal of Virology* Spotlight article, which are articles of significant interest selected by the editors.

The candidate and Dr. D'Ann Rochon designed the research. The candidate conducted experiments. The candidate wrote the manuscript and Dr. D'Ann Rochon supervised the work, manuscript preparation and provided editorial support.

Chapter 4: "Evidence for the role of basic amino acids in the coat protein arm region of *Cucumber necrosis virus* in particle assembly and encapsidation of viral versus host RNA" A version of this Chapter is under preparation for publication. Anticipated author list: **Alam, S.B.,** Reade, R., Theilmann, J. and Rochon, D.

The candidate and Dr. D'Ann Rochon designed the research. The candidate conducted all the experiments. Ron Reade and Jane Theilmann, research technicians in Dr. Rochon's lab technically assisted the candidate in cloning, contributing to approximately 1-2% of the research. The candidate wrote the manuscript and Dr. D'Ann Rochon supervised the work, manuscript preparation and provided editorial support.

Chapter 5: General discussion

The candidate wrote the chapter and Dr. D'Ann Rochon provided editorial support. A version of information presented in this Chapter is under preparation for publication. **"Targeting of Cucumber necrosis virus coat protein to chloroplasts is associated with a delay in the onset of necrotic symptoms during infection"** Anticipated author list: **Alam, S.B.,** Reade, R., Maghodia, A., Ghoshal, B., Theilmann, J. and Rochon, D.

Appendices

Appendix A: "Various HSP70 mRNA homologs are induced during CNV infection". (A.1) a version of this has been published in *Journal of Virology* as a supplementary figure in conjunction with Chapter 2. (A.2) the candidate constructed, sequenced and cloned *N.*

benthamiana Hsc70-2 (NbHsc70-2) into a binary vector pBin(+).(A.3) the candidate performed co-immunoprecipitation as well as virion extraction experiments as described in Sections 2.2.16 and 3.2.1 respectively. Mass spectrometry on the co-immunoprecipitate and CNV virion preparation was performed using the using the Proteomics Core Facility at the University of British Columbia Center for High-Throughput Biology as described in Sections 2.2.17 and 3.2.4 respectively.

Appendix B: "Induction of specific retrotransposons by *Cucumber necrosis virus* infection likely occurs through activation of the heat-shock response". A version of this along with additional experiments is anticipated to be prepared for publication. Anticipated author list: Reade, R., **Alam, S.B.**, Theilmann, J. and Rochon, D.

Dr. D'Ann Rochon, the candidate, Ron Reade and Jane Theilmann designed the research. The candidate conducted the analysis of HSEs in the LTRs of RTns along with Dr. Rochon and Ron Reade and performed the heat shock experiments and subsequent analyses. Ron Reade prepared samples for NGS analysis and constructed the pRTn5533-LTR/GFP/pBin(+) and pRTn0067-LTR/GFP/pBin(+) clones. Jane Theilmann prepared the HSFA2 primers and conducted ddPCR analyses on heat-shocked leaf samples supplied by the candidate to determine if HSFA2 is induced during heat treatment. Dr. D'Ann Rochon analysed the NGS data as summarized in Figure B.1 as well as identified the LTRs of the retrotransposons. The candidate wrote the Appendix B and Dr. D'Ann Rochon provided editorial support.

Table of Contents

Abstract…….. ii

Lay Summary. iv

Preface…… v

Table of Contents ix

List of Tables…. xvi

List of Figures xvii

List of Abbreviations xx

Acknowledgements xxiii

Dedication……. xxvi

Chapter 1: Literature review 1

1.1 Introduction 1

1.2 Identification and classification of CNV 3

1.3 CNV symptomatology and hosts 4

1.4 CNV as a model system 4

1.5 Virion properties 5

1.5.1 Genome structure and function 5

1.5.2 Virus morphology 8

1.5.3 Physical properties of virions 11

1.5.4 Transmission 11

1.5.5 Cytopathic effects 12

1.6 Stages of the multiplication cycle of CNV 12

1.6.1 Virus entry 12

1.6.2 Virus uncoating/disassembly 12

1.6.3 Primary translation of CNV RNA 13

1.6.4 Formation of sgRNA 15

1.6.5 Secondary translation of CNV RNA 16

1.6.6 Virus particle assembly 16

1.6.7 Movement to adjacent and systemic cells in the infected plant 17

1.6.8 Transmission to a new host 17
1.7 Research objectives 20
1.8 Discovery of heat shock proteins 21
1.9 Structure of HSP70 homologs 22
1.10 Mechanism of activation or induction of *HSP70* family of genes 22
1.11 Mechanism of action of the HSP70 family of proteins 23
1.11.1 The ATPase cycle 23
1.11.2 Induction of substrate unloading 26
1.11.3 Nucleotide stabilizing factors 26
1.11.4 Decision making between protein folding and degradation 27
1.12 Known cellular functions of HSP70 27
1.13 Why do viruses recruit HSP70 homologs? 29
1.14 Role of HSP70 homologs in virus disassembly 30
1.15 Role of HSP70 homologs in virus replication 30
1.16 Role of HSP70 homologs in virus assembly 31
1.17 Major strategies by which icosahedral viruses undergo assembly 32
1.17.1 Unassisted capsid self-assembly 33
1.17.2 Scaffold protein-assisted assembly 34
1.17.3 Viral nucleic acid-assisted assembly 35
1.18 Packaging of host RNA by viruses 35
1.19 Overview of factors involved in the assembly of plant viruses 36
1.19.1 Electrostatic interactions 36
1.19.2 Amino acid sequences on the CP 37
1.19.3 Conformational collapse of vRNA 41
1.19.4 CP-mediated capturing of RNA secondary structures is compatible with capsid geometry 42
1.19.5 Replication coupled encapsidation 42
1.19.5.1 Physical interaction between CP and the replication complex 43
1.19.5.2 Conformational change in the CP as a result of interaction with the replicase 44
1.19.5.3 Translation of CP in *cis* from replicating RNA and the microenvironment.. 44

1.19.5.4 Translation of the non-structural protein in *cis* from replicating viral RNA. 46
1.19.6 Packaging signals 47
1.19.7 Physical size constraint 49
1.19.8 CP-CP interactions in virus assembly 50
1.20 Background, hypothesis and synopsis of Chapters 50
1.20.1 Chapter 2 50
1.20.2 Chapter 3 52
1.20.3 Chapter 4 53
Chapter 2: *Cucumber necrosis virus* recruits cellular heat shock protein 70 homologs at several stages of infection 55
2.1 Introduction 55
2.2 Materials and methods 60
2.2.1 Transcript inoculation 60
2.2.2 SDS-PAGE and Western blot analysis 61
2.2.3 SYPRO Ruby and Ponceau S staining 61
2.2.4 Transcriptome analysis by next generation sequencing (NGS) 62
2.2.5 Heat shock of *Chenopodium quinoa* 63
2.2.6 Production and purification of CNV VLPs 64
2.2.7 Virus purification 65
2.2.8 Agarose gel electrophoresis of purified particles 65
2.2.9 TLR extraction and electrophoresis 66
2.2.10 ddPCR 66
2.2.11 Cloning of pNbHsc70-2 cDNA and construction of pNbHsc70-2/pBin(+) and pNbHsc70-2/GFP/pBin(+) 67
2.2.12 Cloning and purification of bacterially expressed *N. benthamiana* Hsc70-2 [pNbHsc70-2/His_7/pET24D(+)] 69
2.2.13 Agroinfiltration 70
2.2.14 *In vitro* CP solubilisation assay 70
2.2.15 Quercetin treatment 71
2.2.16 Co-immunoprecipitation 72
2.2.17 Mass spectrometry 73

2.2.18 Confocal microscopy 73
2.2.19 Temperature sensitivity assay 73
2.3 Results 76
2.3.1 Heat shock protein 70 (HSP70) family proteins are induced during CNV infection. 76
2.3.2 Both Hsp70 and Hsc70 mRNA levels increase during CNV infection 78
2.3.3 Increased levels of Hsp70 and/or Hsc70 in CNV infected plants is associated with enhanced CNV gRNA, CP and virion accumulation 82
2.3.4 Downregulation of Hsp70 or Hsc70 in CNV infected plants is associated with decreased CNV gRNA, CP and virions 87
2.3.5 Overexpression of Hsc70-2 is associated with increased CNV CP accumulation and VLP assembly 90
2.3.6 Hsc70-2 co-immunoprecipitates with CNV CP 94
2.3.7 *N. benthamiana* Hsc70-2 prevents aggregation of CNV CP *in vitro* 97
2.3.8 HSP70 facilitates targeting of CNV CP to chloroplasts 100
2.4 Discussion 102
Chapter 3: Evidence that Hsc70 is associated with *Cucumber necrosis virus* and plays a role in particle disassembly 105
3.1 Introduction 105
3.2 Materials and methods 109
3.2.1 Virus purification 109
3.2.2 SDS-PAGE and Western blot analysis 110
3.2.3 Ponceau S staining 111
3.2.4 Mass spectrometry 111
3.2.5 Purification of bacterially expressed *N. benthamiana* Hsc70-2 [pNbHsc70-2/His_7]. 111
3.2.6 Quantification of Hsc70-2 present in CNV virion preparations 112
3.2.7 Agarose gel electrophoresis of purified particles followed by Western blot analysis 113
3.2.8 Virus overlay assay 113
3.2.9 Immunogold labelling assay 114
3.2.10 Trypsin digestion of CNV preparations 115
3.2.11 Local lesion analysis following incubation with HSP70 antibody 115

3.2.12 Local lesion assay on *N. benthamiana* expressing Hsc70-2 116
3.2.13 Local lesion assays on heat-shocked *C. quinoa* 117
3.2.14 *In vitro* CNV/Hsc70-2 binding assay 118
3.2.15 Chymotrypsin sensitivity assay 118
3.3 Results 119
3.3.1 Hsc70-2 is present in CNV particle preparations 119
3.3.2 CNV particles bind Hsc70 *in vitro* 126
3.3.3 Hsc70-2 is bound to virions in purified CNV preparations 126
3.3.4 Hsc70-2 is associated with CNV virions as determined by immunogold labelling…. 129
3.3.5 The Hsc70-2 bound to CNV in purified virion preparations is partially protected from trypsin digestion 132
3.3.6 HSP70 antibody incubated virus particles or CsCl purified CNV virions having undetectable amounts of HSP70 produce a reduced number of local lesions on *C. quinoa* 136
3.3.7 Overexpression of Hsc70-2 or Hsp70 leads to enhanced CNV disassembly efficiency 139
3.3.8 Incubation of virus particles with *N. benthamiana* Hsc70-2 at pH 7.5 leads to partial disassembly and/or conformational change of CNV virions 143
3.4 Discussion 147
Chapter 4: Evidence for the role of basic amino acids in the coat protein arm region of *Cucumber necrosis virus* in particle assembly and selective encapsidation of viral RNA over host RNA……..... 156
4.1 Introduction 156
4.2 Materials and methods 160
4.2.1 Structural analysis of CNV CP C/C dimer 160
4.2.2 Site-directed mutagenesis 160
4.2.3 Transcript inoculation 161
4.2.4 TLR extraction and electrophoresis 161
4.2.5 SDS-PAGE and Western blot analysis 161
4.2.6 Virus purification by “midiprep” procedure 162
4.2.7 Agarose gel electrophoresis of purified particles 162
4.2.8 Virus yield 163

4.2.9 Percent RNA encapsidation 163
4.2.10 Transmission electron microscopy 164
4.2.11 Thermostability assay 164
4.2.12 RNaseA treatment of virions 164
4.2.13 vRNA extraction 165
4.2.14 Northern blot analysis 165
4.2.15 Percent relative encapsidation efficiency of viral versus host RNA 166
4.3 Results 168
4.3.1 The ε region of the CNV CP arm is rich in basic amino acid (aa) residues 168
4.3.2 Mutations in basic residues in the "KGRKPR" sequence affect genomic RNA, CP and particle accumulation 171
4.3.3 "KGRKPR" mutants encapsidate less RNA compared to WT CNV 175
4.3.4 Virions of "KGRKPR" mutants are polymorphic 179
4.3.5 Virion proteins of WT CNV and "KGRKPR" mutants contain cleaved species which may correspond to CP subunits of T=1 particles 183
4.3.6 Virions produced by "KGRKPR" mutants encapsidate full-length as well as truncated RNA of viral origin 186
4.3.7 Virions produced by "KGRKPR" mutants encapsidate relatively more host RNA than WT CNV 188
4.3.8 Host RNAs detected in vRNA extracted from "KGRKPR" mutant preparations are contained within virions 192
4.3.9 "KGRKPR" double mutants are thermally less stable than WT CNV 195
4.4 Discussion 198
Chapter 5: General discussion and future perspectives 206
5.1 Multiple roles played by the host factor HSP70 during CNV infection 207
5.2 Role of Hsc70-2 in CNV particle disassembly 211
5.2.1 Hypothetical model for CNV disassembly in the presence of HSP70 homologs…… 213
5.3 Evaluation of potential HSP70 binding sites on CNV CP 216
5.4 Role of basic residues in the CNV CP in CNV particle assembly 217
5.4.1 Examination of CP species that form T=1 particles 219
5.4.2 Proposed hypothetical model for CNV assembly 221

5.4.3 Host RNA encapsidation by WT CNV and "KGRKPR" mutants..... 227

5.5 Does the ability of CNV CP to target the stroma interfere with chloroplast-mediated plant defense response? 228

5.6 Does CNV acts as a beneficial microparasite for plants? 231

5.7 Evolution of a plant virus and its susceptible host..... 236

Bibliography… 239

Appendices…..... 262

Appendix A: Various HSP70 mRNA homologs are induced during CNV infection..... 262

A.1 Summary of induction levels of HSP70 mRNA homologs in CNV versus mock inoculated plants at 3 dpi..... 262

A.2 Nucleotide sequence of cloned *N. benthamiana* Hsc70-2 (NbHsc70-2) 268

A.3 Alignment of various peptides obtained via Mass Spectometry of the co-immunoprecipitate and CNV virion preparation with *N. benthamian* Hsc70-2 protein sequence 269

Appendix B: Induction of specific retrotransposons by *Cucumber necrosis virus* infection likely occurs through activation of the heat-shock response..... 270

B.1 Introduction……....270

B.2 Materials and methods……...275

B.2.1 Next generation sequencing……..275

B.2.2 Identification of LTR……276

B.2.3 Identification of HSEs in LTR……..276

B.2.4 Heat-shock experiment to determine if RTns are induced by heat treatment of *N. benthamiana*……277

B.2.5 Reporter expression assay to determine if RTn LTRs are heat inducible…….278

B.3 Results……281

B.3.1 Specific retrotransposon transcripts are induced during CNV infection……..281

B.3.2 LTRs of RTns induced by CNV contain putative HSEs……...283

B.3.3 *Ty-1/Copia*-type RTns induced by CNV are heat-shock inducible……...287

B.3.4 Heat treatment activates the LTR of CNV inducible RTn5533 resulting in the expression of the downstream reporter gene, GFP……..290

B.3.5 Heat treatment activates the LTR of CNV inducible RTn0067 resulting in the expression of the downstream reporter gene, GFP……..294

B.4 Discussion……....297

List of Tables

Table 2.1: Oligonucleotides used for RT-PCR, PCR and ddPCR 75

Table 4.1: Oligonucleotides used for PCR 167

Table B.1: List of oligonucleotide primers used in this study 280

List of Figures

Figure 1.1: Genome organization of CNV showing the five ORFs and their encoded proteins. ... 7

Figure 1.2: Structure of the CNV CP, particle and β-annulus. 10

Figure 1.3: Schematic representation of the multiplication cycle of CNV. 19

Figure 1.4: Structure and mechanism of function for HSP70 chaperones. 25

Figure 2.1: Features of CNV CP. 57

Figure 2.2: HSP70 is induced during CNV infection. 77

Figure 2.3: Hsc70 and Hsp70 mRNA isoforms are highly induced during CNV infection. 80

Figure 2.4: Increased levels of Hsp70 and/or Hsc70 in CNV infected plants is associated with enhanced CNV gRNA, CP and virion accumulation. 85

Figure 2.5: Downregulation of Hsp70 or Hsc70-2 in CNV infected plants is associated with decreased CNV gRNA, CP and virions. 89

Figure 2.6: Overexpression of Hsc70-2 via agroinfiltration increases both CNV CP and VLP accumulation. 93

Figure 2.7: Hsc70-2 co-immunoprecipitates with CNV CP. 96

Figure 2.8: Hsc70-2 assists in solublization of CNV CP. 99

Figure 2.9: Downregulation of HSP70 interferes with chloroplast targeting of the CNV CP in *N. benthamiana*. 101

Figure 3.1: Hsc70-2 is present in CNV virion preparations. 122

Figure 3.2: HSP70 co-purifies with CLSV. 125

Figure 3.3: Purified CNV particles bind to Hsc70 *in vitro and in vivo*. 128

Figure 3.4: Immunogold labelling experiment showing that purified CNV particles are bound to Hsc70. 131

Figure 3.5: The Hsc70-2 bound to virions is partially protected from protease digestion. 135

Figure 3.6: CNV particles incubated with HSP70 antibody or having undetectable amounts of HSP70 produce fewer local lesions on the local lesion host *Chenopodium quinoa*. 138

Figure 3.7: *N. benthamiana* leaves agroinfiltrated with Hsc70-2 show an increase in the number of local lesions produced by CNV in comparison to plants agroinfiltrated with EV. 140

Figure 3.8: Heat-shocked *C. quinoa leaves* show an increase in the number of local lesions in comparison to untreated plants when virions are used as inoculum but not when virion RNA is used. 142

Figure 3.9: Incubation of CNV with NbHsc70-2/His_7 at pH 7.5 leads to partial disassembly of virions. 145

Figure 4.1: The epsilon (ε) region of the CNV CP is conserved among *Tombusviruses*, being rich in basic amino acid residues which lie under the C/C dimer facing the interior of the particle. 170

Figure 4.2: Mutations of basic residues in the "KGRKPR" sequence of the CNV CP arm ε region affect CNV particle accumulation. 177

Figure 4.3: Virions of "KGRKPR" mutants are polymorphic. 182

Figure 4.4: Western blot analysis of proteins extracted from virions of mutants M1-M7. 185

Figure 4.5: Virions produced by "KGRKPR" mutants encapsidate full-length and truncated viral RNA as well as host RNA species. 190

Figure 4.6: Host RNAs detected in vRNA extracted from "KGRKPR" mutant preparations are contained within virions. 194

Figure 4.7: "KGRKPR" double mutants M3 and M7 are thermally less stable than WT CNV. 197

Figure 4.8: Pictorial representation showing the location of two putative RNA binding sites on the CP in CNV virions. 205

Figure 5.1: Hypothetical model for multiple roles played by HSP70 homologs during CNV infection. 210

Figure 5.2: Hypothetical model for CNV disassembly facilitated by HSP70 homologs. 215

Figure 5.3: Diagrammatic representation of a trimer of C/C dimers and a pentamer of A/B dimers. 222

Figure 5.4: Hypothetical model for CNV assembly. 226

Figure 5.5: Hypothetical model showing evolution of CNV and plants. 238

Figure A.1: RPKM values for individual transcripts were determined and then the ratios of CNV RPKM values to mock values were obtained. 267

Figure B.1: Retrotransposon (RTn) transcripts are induced during CNV infection. 282

Figure B.2: LTRs of RTns induced by CNV contain putative HSEs. 285

Figure B.3: *Ty-1/Copia*-type RTns induced by CNV are heat shock inducible. 289

Figure B.4: Heat treatment activates the LTR of CNV inducible RTn5533 inducing the expression of the downstream reporter gene, GFP. 292

Figure B.5: Heat treatment activates the LTR of CNV inducible RTn0067 promoting the expression of the downstream reporter gene, GFP. 295

List of Abbreviations

3’	Three prime in the context of nucleic acid
5’	Five prime in the context of nucleic acid
A	Alanine
Å	Angstrom
a	CP arm region
aa	Amino acid
ABA	Abscisic acid
ADP	Adenosine diphosphate
AMV	*Alfalfa mosaic virus*
ARM	Arginine rich motif
ASFV	*African swine fever virus*
ATP	Adenosine triphosphate
ATPase	Adenosine triphosphatase
AUG	Start codon
BMV	*Brome mosaic virus*
BSA	Bovine serum albumin
C. quinoa	*Chenopodium quinoa*
Ca^{2+}	Calcium cation
CarMV	*Carnation mottle virus*
CCMV	*Cowpea chlorotic mottle virus*
cDNA	Complementary DNA
CHIP	Carboxyl terminus of HSP70-interacting protein
CITE	Cap independent translational enhancer
CMV	*Cucumber mosaic virus*
CNV	*Cucumber necrosis virus*
CP	Coat protein
CsCl	Cesium chloride
C-terminal	Carboxyl terminal
DBD	DNA-binding hydrophobic repeat domain
ddPCR	Droplet digital PCR
DNA	Deoxyribonucleic acid
Double mutant	Mutant with two aa substitutions
dpai	Days post agroinfiltration
dpi	Days post inoculation
dsDNA	Double stranded DNA
dsRNA	Double stranded RNA
EM	Electron microscope
EP	Empty particle
ER	Endoplasmic reticulum
EV	Empty vector
FHV	*Flock house virus*
FIV	*Feline immunodeficiency virus*
G type HSE	Gap type HSE

GEMSA	Gel electrophoresis mobility shift assay
GFP	Green fluorescent protein
gRNA	Genomic RNA
h	Hinge region in the context of CNV CP
H	Histidine
HBV	*Hepatitis B virus*
Hip	HSP70 interacting protein
HIV I	*Human immunodeficiency virus I*
Hop	HSP70-HSP90 organising protein
hpt	Hours post treatment
Hsc70	Heat shock cognate 70 kDa protein
Hsc70-2	Heat shock cognate 70 kDa protein-2
HSE	Heat shock element
HSF	Heat shock factor
Hsp70	Heat shock 70 kDa protein
HSP70	Heat shock protein 70 family
IVM	*In vitro* mutagenesis
JDP	J-domain proteins
K	Lysine in the context of an amino acid
kb	Kilobase
kDa	Kilodalton
LDS	Lithium dodecyl sulphate
LINE	Long interspersed nuclear element
LTR	Long terminal repeat
MNSV	*Melon necrotic spot virus*
mRNA	Messenger RNA
MVB	Multivescicular body
N. benthamiana	*Nicotiana benthamiana*
N. clevelandii	*Nicotiana clevelandii*
NBD	Nucleotide binding domain
NbHsc70-2	*N. benthamiana* Hsc70-2 homologue
ng	Nanogram
NGS	Next generation sequencing
nm	Nanometer
nt	Nucleotide
N-terminal	Amino terminal
O. bornovanus	*Olpidium bornovanus*
ORF	Open reading frame
P	Protruding domain
P type	Perfect type HSE
PAGE	Polyacrylamide gel electrophoresis
PS	Packaging signal
PVDF	Polyvinylidine difluoride
R	Arginine in the context of an amino acid
R	CNV CP RNA binding domain
RCNMV	*Red clover necrotic mosaic virus*

RdDM	RNA-directed DNA methylation
RdRp	RNA dependent RNA polymerase
RID	RNA interacting domain
RJ1	Infectious cDNA clone of CLSV
RNA	Ribonucleic acid
RNaseA	RibonucleaseA
RNA-seq	RNA sequencing using NGS
RPKM	Reads per kilobase per million
RT	Room temperature
RTn	Retrotransposon
S	CP shell domain
S type HSE	Step type HSE
SBD	Substrate binding domain
SBMV	*Southern bean mosaic virus*
SDS	Sodium dodecyl sulphate
SeMV	*Sesbania mosaic virus*
sgRNA	Subgenomic RNA
SINE	Short interspersed nuclear element
ssRNA	Single-stranded RNA
STNV	*Satellite tobacco necrosis virus*
SV40	*Simian virus 40*
T	Triangulation number
TBSV	*Tomato bushy stunt virus*
TCV	*Turnip crinkle virus*
TE	Transposable element
TEM	Transmission electron microscopy
TIC	Translocon at inner envelope of chloroplast
TLP	Total leaf protein
TLR	Total leaf RNA
TMV	*Tobacco mosaic virus*
TNV	*Tobacco necrosis virus*
TOC	Translocon at outer envelope of chloroplast
tRNA	Transfer RNA
TRSV	*Tobacco ring spot virus*
TRV	*Tobacco rattle virus*
TuMV	*Turnip mosaic virus*
TYLCV	*Tomato yellow leaf curl virus*
UAG	Amber termination codon
UTR	Untranslated region
VLP	Virus-like particle
vRNA	Virion RNA
WT	Wild type
Zn^{2+}	Zinc cation

Acknowledgements

I would like to thank my supervisor Dr. D'Ann Rochon for giving me the wonderful opportunity to persue my doctoral studies in her lab. I am deeply obliged and thankful for her constant teachings, motivation, encouragement, support and warmth during the entire course of my Ph.D. She has always helped immensely to bring out the best in me. She has been a great guide to help me grow professionally. I also would like to express my gratitude to her and her family (Mike and Melissa) for their kind gestures, hospitality and friendship.

I am extremely thankful to my co-supervisor Dr. James Kronstad and my committee members Dr. David Theilmann, Dr. Nelly Panté and Dr. Xin Li for their critical suggestions, feedback and support. I would like to thank Dr. Hélène Sanfaçon and Dr. Eric Jan, for participating as external examiners for my comprehensive examination. I am also thankful to Dr. François Jean and Dr. Curtis Suttle for serving as university examiners as well as Dr. Peter Nagy for participating as external examiner for the Oral defense. As well I would like to thank as my Graduate Advisor Dr. Mahesh Upadhyaya for his time and contributions. I am also thankful to UBC and the entire staff of the Department of Plant Science, LFS especially Ronaldo Cerri, Mona Lee, Lia Maria Dragan and Shelley Small for their constant support in administrative work.

I am grateful to my lab members Ron Reade and Jane Theilmann for their enduring support, valuable suggestions and constant assistance with laboratory techniques. I specially want to thank Ron Reade for his tremendous help and all those brain storming questions as well as helpful critical discussions. I also would like to express my gratitude to Jane Theilmann and her family (Dave, Ann and Mark) for their constant homely warmth, love and support. I also would

like to sincerely thank Dr. Kankana Ghoshal and Dr. Basudev Ghoshal for being extremely supportive, helpful and kind seniors. I wish them good luck in every aspect of life. Heartfelt thanks to my friend Siddharth for his continuous support and encouragement throughout my Ph.D. tenure. I wish him good luck, success and prosperity in everything he seeks. I also thank my previous lab members; Dr. Ajay Maghodia, Wendy Lee and Carys Croft for their help and support. A special thanks to Joan Chisholm and Les Willis for their amazing friendship and of course the movies.

I also want to acknowledge SuRDC for allowing me to use their facilities. I thank Dr. Kenna MacKenzie, Research Manager and all the staff at SuRDC for their support. I specially thank Dr. Guus Bakkeren, Michael Weis and Melanie Walker for their help and support. I also would like to thank my dear friend Dr. Hala Khalil and Dr. Paul Wiersma for their kind help with the Next Generation Sequencing Analyses. I am thankful to my friends at the SuRDC and in the Okanagan Valley- Dinesh, Ana, Pranali, Rahul, Tammy, Eunice, Rob, Paul, Robyn, Sudarsana, Nadia, Julie, Krin, Ting, Rajita, Sushma, Caitlin, Mel, José, Yu Xiang and Murali.

I am thankful to all my teachers at the school and University of Calcutta especially Dr. Geetanjali Sundaram, Dr. Maitree Bhattacharya, Dr. Sanjay Ghosh, Dr. Krishanu Chakraborty, Dr. Prashanta kumaar Bag, Dr. Anirban Siddhanta and Dr. Anjan Dasgupta.

Finally, my deepest appreciation and acknowledgment would go towards my family for their continuous moral support. I am indebted to my father, Md. Shoib Alam; mother, Nazia Alam and brother, Zeeshan Syed. I wish to express my heartfelt gratitude towards them for understanding

my dreams and passion for science and motivating me to prosper in life. I absolutely would not be where I am today without their tremendous help, support and encouragement. My parents have always given their best to make me happy and supported me unconditionally. I wish my brother, Zeeshan, best wishes and good luck for his present and future endeavours. And finally I wish that the Almighty God blesses my family with sound health, happiness and peace in every aspect of life.

“Dedicated to my parents”

Chapter 1: Literature review[1]

1.1 Introduction

Viruses are obligate, intracellular microparasites that can multiply only within living cells. Virusesare composed of an outer protective proteinaceous layer called the capsid that encapsulates the nucleic acid. The capsid is made up of repeating units of structural proteins called the coat protein (CP). Some virions also have an envelope surrounding the capsid which contains glycoproteins (1). The interaction between different CP subunits along with CP-nucleic acid interactions play an important role in forming a complete stable virion, a process termed virus assembly. A stably assembled complete virion forms an infectious particle that can move to an adjacent uninfected cell and establish a new infection following virus disassembly. Some plant viruses do not require virus particle assembly for movement to adjacent cells, rather viral RNA/movement protein complexes, likely in conjunction with other virus and cellular components, assists in movement to an adjacent cell (2). Once the virion or the viral RNA/movement protein complex disassembles, the nucleic acid replicates and produces several copies of the genome which again is assembled into new progeny virions or RNA/movement protein complexes capable of infecting several uninfected cells. The nucleic acid that is encapsidated within virions is the genetic material that has coding capacity.

Viral genomes can be single or double stranded DNA or RNA molecules. Single stranded RNA genomes could further be divided into positive or negative polarity genomes, depending on

[1] A version of information presented in this Chapter has been published in *Virology* as a Highlight Article. Rochon, D., Singh, B., Reade, R., Theilmann, J., Ghoshal, K., **Alam, S.B.** and Maghodia, A. (2014) The p33 auxiliary replicase protein of *Cucumber necrosis virus* targets peroxisomes and infection induces *de novo* peroxisome formation from the endoplasmic reticulum. *Virology*, http://dx.doi.org/10.1016/j.virol.2013.12.035.

whether the RNA can directly be used as a template for translation of viral proteins (positive polarity) or if the RNA needs to be transcribed first before commencing protein translation (negative polarity). The majority of the viruses infecting plants have single stranded (ss) RNA molecules of positive polarity, as their genome.

In this thesis, I aimed to study specific aspects of the molecular biology of a positive polarity, ssRNA virus *Cucumber necrosis virus* (CNV) during infection of the laboratory host *Nicotiana benthamiana*. Single stranded RNA viruses generally have small genomes and limited coding capacity. Hence, these viruses rely heavily on their hosts for multiplication and spread. Viruses have evolved to co-opt host components at several stages of the multiplication cycle such as replication, assembly and disassembly. Virus assembly and disassembly are crucial aspects of the virus infection cycle, however, very little is known about mechanisms underlying these processes *in vivo* in non-enveloped viruses and in plant viruses in general. The studies described here will be helpful in providing deeper insight into these essential aspects of CNV infection. These studies are also expected to be applicable to other spherical plant viruses and possibly to non-enveloped animal viruses as well. Finally, these studies may enable the development of global antiviral strategies with novel mechanisms of action that target critical host or viral components that are essential to infection and disease. Focusing on novel host-directed therapeutics will help avert the development of drug-resistant viral strains. Hence, in this thesis, using CNV as a model system virus, I was also interested in the role of host factors in various aspects of the virus multiplication cycle. In particular, I discovered that CNV infection causes induction of HSP70 homologs which are co-opted by the virus at several stages of infection. Hence, the studies described in this thesis also will help to unravel the involvement of HSP70 in virus

multiplication and spread. I also discovered that CNV induces retrotransposons in *N. benthamiana* plants likely through its induction of heat shock factors that bind the long terminal repeats (LTRs) of retrotransposons inducing their transcription. Retrotransposons comprise a significant proportion of plant genomes and play an important role in shaping genome evolution. Thus, the studies described in this thesis also will help to unravel the importance of plant viruses in inducing genome variation and adaptation to the changing needs of the environment.

1.2 Identification and classification of CNV

CNV was isolated from infected greenhouse grown cucumber plants at the Harrow Research Centre laboratory in Ontario, Canada. The only known natural host so far for CNV is cucumber (*Cucumis sativus*). In 1959 *McKeen et al.* (3) was the first to describe the disease caused by CNV. Initially, based on the symptoms the disease, infection was thought to be caused by a virus closely related to *Tobacco ring spot virus* (TRSV), a *Nepovirus*, whereas detailed analyses of symptoms and the mode of fungal transmission of the virus led the researchers to group it with *Tobacco necrosis virus* (TNV), a *Necrovirus* (3). Later, serological studies revealed that it is unrelated to TNV (4, 5). *Rochon et al*. (1988) (6), reported that the genome sequence of CNV is highly similar to that of *Tomato bushy stunt virus* (TBSV), the type member of the *Tombusvirus* genus. Thus, CNV is currently grouped as a member of the genus *Tombusvirus* in the Family *Tombusviridae* (7).

1.3 CNV symptomatology and hosts

During natural infection, CNV infected cucumber plants produce necrotic symptoms throughout the plant that ultimately lead to death of the plant. Earlier in infection, the infected plant also shows stunting, along with malformed fruits with reduced size. CNV has a wide experimental host range including many dicotyledonous plants such as members of the *Cucurbitaceae*, *Solanaceae*, *Chenopodiaceae* and *Leguminosae*. *Nicotiana benthamiana*, *N. clevelandii*, *Chenopodium quinoa* and *Cucumis sativus* are the commonly used experimental hosts. CNV infected *N. benthamiana* plants show symptoms of stunting. Inoculated leaves show chlorosis early in infection at 3-4 days post inoculation (dpi) and a spreading necrosis phenotype is displayed at 5-6 dpi. This spreading necrosis ultimately leads to systemic necrosis in upper uninoculated leaves by 6-7 dpi and ultimate death of the plant by 9-12 dpi.

1.4 CNV as a model system

CNV is an excellent model system virus for characterizing basic aspects of the viral infection cycle. The small RNA genome, which is sequenced, is encapsidated within a capsid made up of identical copies of a single CP. Dr. Rochon's laboratory has produced an infectious cDNA clone of CNV RNA, which allows extensive manipulation of the genome to study the roles of different proteins and their substituent amino acids. The virus accumulates to high levels in infected plants (~0.3 mg virus/g leaf tissue). Plants can readily be infected by mechanical inoculation of leaves using carborundum as an abrasive to facilitate entry of virus into host cells. The preferred laboratory host for CNV, *N. benthamiana,* is highly convenient to work with: i.e., plants can be inoculated approximately 5-6 weeks after seeding, they are easily agroinfiltrated for transient

expression of protein (8, 9) and a draft genome and transcriptome is published and available (http://www.ncbi.nlm.nih.gov, http://solgenomics.net, http://benthgenome.qut.edu.au/). *Tombusviruses* are one of the most highly studied plant virus genera; hence much literature is available as background information. Specifics of the replication and translation processes of *Tombusviruses* have been studied extensively (10-12). An X-ray crystal structure and cryo-electron microscopy (cryo-EM) structure of CNV have been determined at 2.9Å and 12Å respectively (13, 14). Nevertheless, many questions are still unanswered and this model system virus provides an excellent opportunity for basic research in virology. An in-depth understanding of the molecular biology of CNV may provide insight into new strategies for virus disease control, not only for CNV but for other viruses as well.

1.5 Virion properties

1.5.1 Genome structure and function

As stated above, CNV is a positive-strand ssRNA virus in the genus *Tombusvirus*, Family *Tombusviridae*. Positive-stranded ssRNA viruses comprise a vast group, infecting plants, animals, insects, fungi and bacteria (7). The CNV genome is 4.7 kb and monopartite. The 5' end is presumably uncapped and the 3' end is not polyadenylated (1). The genome contains five open reading frames (ORFs) which encode five different proteins (Figure 1.1): namely the auxiliary replicase factor (p33), the RNA dependent RNA polymerase (RdRp) (p92), CP (p41), movement protein (p21) and the silencing suppressor (p20). The UAG stop codon of ORF1 is read through approximately 10% of the time to produce the RdRp (15). The products encoded by ORF1 and

ORF2 comprise part of the viral replicase, with remaining components being derived from the host (10, 16-19). ORF 1 and 2 are translated from genomic RNA (gRNA). The CP being present on an internal region of the genome is translated from a 3' co-terminal subgenomic RNA (sgRNA) of ~2.1 kb. Since, the CP is translated from sgRNA, which is distinct from the encapsidated gRNA within the virions, the CP molecules encapsidate CNV RNA in *trans*. The overlapping ORFs 4 and 5, which produce p21 and p20, respectively are expressed from distinct nested ORFs from a second 3' co-terminal sgRNA of ~0.9 kb (16) (Figure 1.1). p20 is translated following leaky scanning of the p21 AUG codon (20).

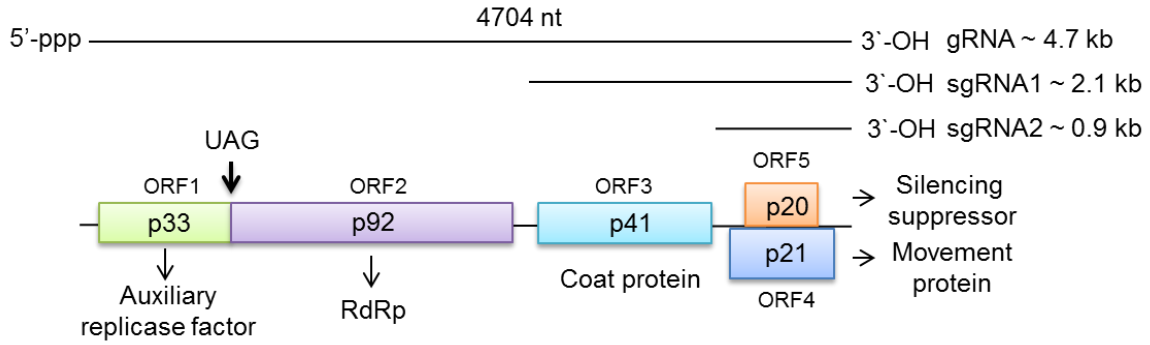

Figure 1.1: Genome organization of CNV showing the five ORFs and their encoded proteins.

The locations and sizes of sgRNA1 and 2 relative to gRNA are also shown. 5'-ppp represents the uncapped presumed triphosphate group at the 5' terminus and the 3'-OH represents the hydroxyl group at the 3' end of the gRNA and sgRNAs. The approximate sizes of gRNA and sgRNAs are indicated. Also the exact number of nucleotides (nt) constituting CNV gRNA is mentioned above gRNA (4704 nt).The UAG is an amber termination codon which is read through to produce p92. For further details see Section 1.5.1.

1.5.2 Virus morphology

The virus particle is a T=3 icosahedron consisting of 180 identical copies of the 41 kDa CP which occurs in three different conformations (A, B and C) in the icosahedron (Figure 1.2 A, B and C are shown in red, blue and green, respectively). Virions are non-enveloped with a diameter of 34 nm and have a rounded outline with a granular appearance when viewed by transmission electron microscopy (TEM). The CNV particle consists of an outer shell, as well as a structured inner shell, that may play an important role in the assembly of particles through forming a T=1-like scaffold for the formation of the T=3 outer shell (21).

Each of the CP subunits folds into three distinct structural domains: "R", the N-terminal RNA binding domain that interacts with viral RNA and forms the inner shell; "S", the shell domain constituting the capsid backbone, and "P", the protruding C-terminal domain, (Figure 1.2 A) which projects in pairs from A/B and C/C dimers from the surface of the particle and gives the virus its granular appearance (Figure 1.2 C). The P and the S domains are connected by a short five amino acid hinge, "h" region. The "a" or arm region flexibly tethers the R and S domains allowing, along with "h", for T=3 icosahedral symmetry. The β regions of the arms of three C subunits intertwine to form a β-annular structure at the particle 3-fold axis that contributes to particle stability (Figure 1.2 D) (22). The ε region of the C subunit arm lies along the inner face of the S domain antiparallel to the first β sheet. As described further in this thesis, the ε region may, like the R domain, bind viral RNA as it is rich in basic amino acids and its position in the particle is co-incident with RNA based on neutron scattering (23). The S domains form a beta-barrel structure made up of eight beta–strands oriented in an antiparallel fashion. Ca^{2+} binding

sites stabilize contacts between the adjacent S domains of the A, B and C subunits (16) (Figure 1.2 C).

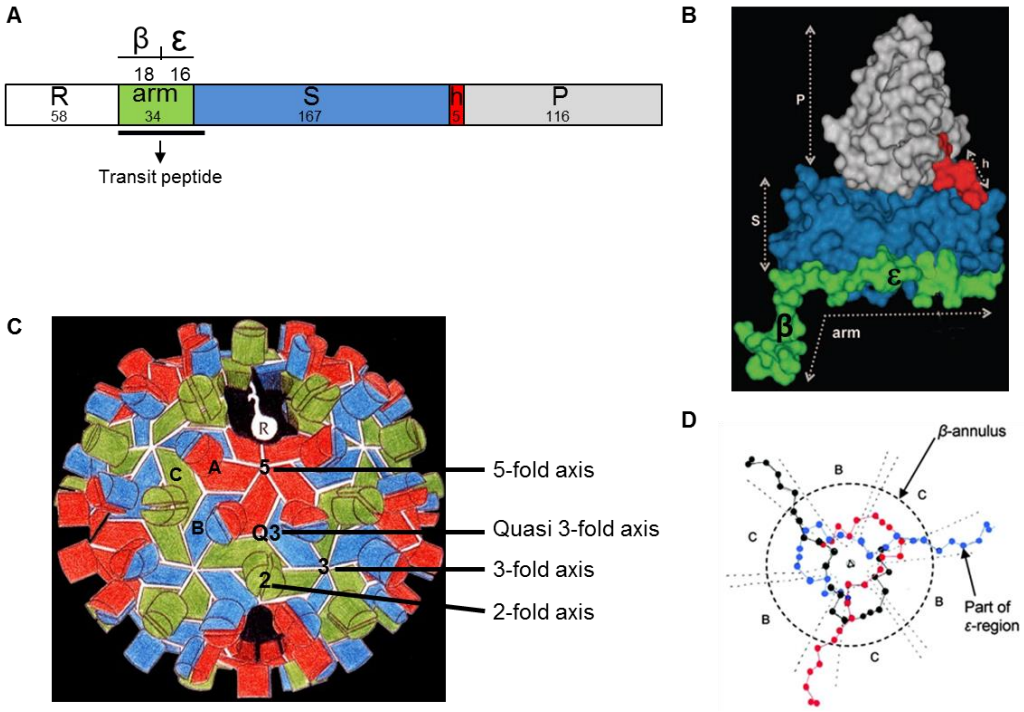

Figure 1.2: Structure of the CNV CP, particle and β-annulus.

(A) Linear structure of CNV CP subunit showing the different domains including the RNA binding (R), shell (S) and protruding (P) domains along with the arm and hinge (h) regions as well as the number of amino acids (aa) constituting them. The position of the β and ε regions within the arm is also shown, along with the number of aa that they are composed of. The CP transit peptide like sequence involved in chloroplast targeting (24) encompasses the entire arm along with four amino acids of the shell and is shown by a black line. (B) Tertiary structure of the CNV CP showing the different domains: arm, S, h and P. The R domain, not shown in the figure, is located in the interior of the particle and is shown diagrammatically in A and C; the modified structure is adopted from (25) [Reprinted from Induction of particle polymorphism by *Cucumber necrosis virus* coat protein mutants in vivo, 82, 3, 1547-1557, Kakani, K., Reade, R., Katpally, U., Smith, T., Rochon, D.; *Journal of Virology* (2008) with permission from American Society for Microbiology)] (21). (C) Diagrammatic representation of the CNV particle based on that of TBSV showing spatial arrangement of the three conformationally different subunits (A, B, C subunits are shown in red, blue and green, respectively). Particle 2-fold, 3-fold, 5-fold and the quasi 3-fold (Q3) axes are also shown. [Reprinted from *Tomato bushy stunt virus* at 2.9Å resolution, 276, 5686, 368-373, Harrison, S.C., Olson, A.J., Schutt, C.E., Winkler, F.K., Bricogne, G.; *Nature* (1978) with permission from Macmillan Publishers LTD-Nature Publishing Group] (26). The modified structure has been adopted from (25). A, B and C refer to the CP subunits. For details see Section 1.5.2. (D) Schematic representation of the β-annulus. This structure is formed by three interwined β regions of three C subunits and is shown in black, red and blue, respectively) The β -annulus is viewed down the particle 3-fold axis [Reprinted from: Evaluation of the roles of specific regions of the *Cucumber necrosis virus* coat protein arm in particle accumulation and fungus transmission, 80, 12, 5968-5975, Hui, E., Rochon, D.; *Journal of Virology* (2006) with permission from American Society for Microbiology)] (22).

1.5.3 Physical properties of virions

Virions are stable at acidic pH but expand above pH 7 in the presence of a Ca^{2+} chelator such as EDTA or EGTA. The isoelectric point of the virion is pH 5.2. Virions are resistant to elevated temperatures and thermal inactivation of infectivity occur above 80°C. Particles are insensitive to non-ionic detergents and organic solvents (such as phenol, chloroform). Ca^{2+} ions stabilize the interaction between adjacent CP Sdomains by bringing together adjacent aspartate residues at the particle Q3 axis (Figure 1.2B). There also appears to be a novel Zn^{2+} binding site at a histidine residue (H62) within the β-annulus (14) of unknown function. However, it was hypothesized that Zn^{2+} could play a role in stabilizing the capsid at the β-annulus or could help drive assembly in the cell as has been described for a *Rotavirus* (27). It was also suggested that the interaction of the Zn^{2+} ion with the imidazole ring of H62 might play a role in extrusion of the arms during fungus transmission and disruption of this interaction could lead to an altered conformation that could render defects in fungal transmission.

1.5.4 Transmission

CNV is transmitted under natural conditions to cucumber roots by zoospores of the *Chytridiomycete* fungus *Olpidium bornovanus* (28-30). In the laboratory, CNV can be transmitted by mechanically rubbing leaves of a variety of hosts with virus in buffer in the presence of the abrasive, carborundum. Infection can be achieved this way with either ground infected leaf exudate, purified particles, virion RNA (vRNA) or transcripts of the infectious cDNA clone, pK2/M5 (31).

1.5.5 Cytopathic effects

Tombusvirus virions are found predominantly in the cytoplasm of the infected host plant cell but virions have occassionally been observed in chloroplasts, mitochondria and peroxisomes, but at a lower level. Multivesicular bodies (MVBs) are found within infected cells, which are formed by remodelling of either peroxisomal or outer mitochondrial membranes (32-34) (see below for further details on CNV).

1.6 Stages of the multiplication cycle of CNV

1.6.1 Virus entry

CNV enters the plant cell either naturally through the roots by fungal zoospores (*O. bornovanus)* or mechanically under laboratory conditions by rub inoculation of leaves as described above (29, 35).

1.6.2 Virus uncoating/disassembly

It is believed that the virus uncoats (or disassembles) under conditions of high pH and/or in a calcium-deprived region within the host cell. Under these conditions the CP-CP interactions which are stabilized by Ca^{2+} at the Q3 axis become destabilized. This results in swelling of the virus particle by about 10% and subsequent partial or full release of the viral genome as has been suggested for other viruses (36, 37). The A and B subunit R and arms, which may be bound to

RNA due to their highly basic nature, are believed to exit through the hole created at the Q3 axis and this may facilitate exit of virion RNA.As described in this thesis, host factors such as HSP70 homologs appear to be involved in bringing about a conformational change in the particle, facilitating its disassembly (24). It has been suggested that some spherical plant viruses uncoat during *in vitro* translation in cell-free systems, such as the rabbit reticulocyte and wheat germ systems, following swelling of particles and exposure of the 5' end of the genome (37). Viral RNA, released or partially released from particles, is translated using the host translation machinery. However, numerous attempts to obtain translation products from swollen CNV particles were not successful (S.B. Alam, unpublished results).

1.6.3 Primary translation of CNV RNA

Translation of the CNV genome, in analogy to *Tomato bushy stunt virus,* is cap-independent and is controlled by elements in the 3' untranslated region of the genome (3'-UTR) (38). The 3'-UTR contains translational enhancers, which consist of a series of stems and loops termed the cap independent translational enhancer (CITE) (38). These elements form base pairs with sequences in the 5'- UTR to promote non-covalent circularization of the genome. Formation of this structure mimics the cap-polyA tail protein bridge formed during translation of cellular mRNA, and likewise facilitates viral mRNA translation (39).

Primary translation might accompany uncoating as has been suggested for other viruses as described above (36, 37). The first protein to be translated is the auxiliary replicase factor (p33) as well as its read through product, the RdRp (p92). The newly synthesized p33 and p92 proteins

along with host factors such as HSP70 homologs, physically co-ordinate to allow viral RNA replication (10, 11). Replication occurs in peroxisome-derived MVBs which are induced during virus infection. MVBs contain numerous 80-150 nm spherules or cup-shaped invaginations of the peroxisomal boundary membranes. Spherules serve a protective role against degradation of viral RNA and the replication complex by host enzymes. They also help to concentrate the viral RNA, replicase and host factors required for replication in a small region to facilitate the initiation of replication (16). It has been found that CNV p33 contains the targeting information required for peroxisomal localization of the replicase (17, 32). Also, I participated in a collaborative project where it was found that p33 induces *de novo* formation of peroxisomes from endoplasmic reticulum (32).

As the ssRNA genome is of positive polarity, it can act both as an mRNA for translation and a template for replication. Consequently, regulatory mechanisms must be in place to allow the switch from the translation mode to the replication mode to avoid collision of the ribosomes, travelling from the 5' to the 3' end of the viral RNA, and the viral RdRp which travels from the 3' to the 5' end of the viral RNA (16).

HSP70 is also associated with the replicase. It enhances viral RNA replication and, as well, assists in the assembly of the replicase complex (40). A complementary (-) strand is synthesized by the viral replicase using the (+) strand as a template. This involves the recognition of *cis-acting* elements in the genome by the replicase. The newly formed (-) strand forms doublestranded (ds) RNA intermediate with the (+) strand and this dsRNA then serves as a template for the synthesis of numerous progeny (+) strands. The replicase recognizes enhancer

elements located internally in the viral genome and places itself at the complementary genomic promoter located at the 3'end of the (-) strand intermediate. RNA replication is asymmetric in nature producing excess amounts of (+) strand progeny RNA as compared to (-) strands (34).

Tombusviruses do not encode a helicase as do many other (+)ssRNA viruses. In TBSV it has been found that host factors such as glyceraldehyde 3-phosphate dehydrogenase (GAPDH) and various DEAD-box RNA helicases are important for maintaining the asymmetry of viral RNA replication. DEAD-box RNA helicases help unwind secondary structures at the 3' end of TBSV (-) RNA facilitating plus-strand RNA synthesis (19, 41-43).

1.6.4 Formation of sgRNA

In addition to progeny (+) strand genome RNAs, CNV also produces two 3' co-terminal sgRNAs. The 2.1 kb sgRNA serves as a mRNA for the synthesis of the CP and the 0.9 kb sgRNA serves is a bicistronic mRNA for the synthesis of both the movement protein and the silencing suppressor from nested ORFs (Figure 1.1) (31). The templates for synthesis of sgRNAs are (-) strand RNAs that arise through premature synthesis of (-) strand RNA from genomic (+) strand in the vicinity of the sgRNA promoter. Plus-strand synthesis from the truncated (-) strand products ensues and the sgRNAs are formed (44). Sub genomic RNAs are 3'-coterminal with gRNA and allow the translation of otherwise internal ORFs by placing their initiator AUG codons at the proximal 5'-terminus, a position which is greatly favoured by eukaryotic ribosomes for initiation of translation (45, 46). During infection, the sgRNA2 accumulates first, followed by the accumulation of the sgRNA1(16).

1.6.5 Secondary translation of CNV RNA

Seondary translation of CNV RNA occurs when translation of newly synthesized genomic or sgRNA occurs. This results in the production of each of the five encoded proteins.

1.6.6 Virus particle assembly

The newly formed progeny (+)ssRNA and the CP assemble to make new virus particles. The site of virus assembly is not known but may occur at or near the site of replication as has been shown for other viruses (47, 48). CNV particles might assemble initially from a nucleating agent consisting of a trimer of C/C dimers as has been suggested for *Turnip crinkle virus* (TCV) (49). Alternatively, a mechanism similar to the *Southern bean mosaic virus* (SBMV) or *Sesbania mosaic virus* (SeMV) may be utilized where assembly initiates from a pentameric cap made up of five A/B dimers (50, 51). Assembly might also require the assistance of a scaffolding protein (scaffolding protein assisted capsid assembly) (52) or specific nucleic acid sequences or structure (nucleic acid assisted capsid assembly) (53). Previous studies in Dr. Rochon's lab have suggested that the R domain of the CNV CP acts as a scaffold during assembly initiation. The R domain along with bound viral RNA assembles to form the T=1 like inner shell. This inner shell then serves as a scaffold upon which further assembly occurs to form the complete CNV T=3 particle (13). Additional viral or cellular factors, including chaperones, have been found to assist in proper folding of the CP of other viruses (54) and contribute towards the formation of intact particles. These interactions would also be expected to prevent premature aggregate formation (52, 54-56). In this thesis, it is shown that the molecular chaperone Hsc70-2 assists in CNV CP folding and that HSP70 homologs also assist in virion assembly.

1.6.7 Movement to adjacent and systemic cells in the infected plant

Finally, the newly formed progeny RNA then moves either to adjacent cells (cell-to cell movement) or the virion enters the vascular system of the plant (systemic movement) for further infection. In cell-to-cell movement, CNV RNA likely moves through the plasmodesmata, junctions connecting the symplast of adjacent plant cells. The means by which the MP of CNV facilitates movement is not known but it may coat viral RNA and elongate it to facilitate its movement through plasmodesmata as has been proposed for *Tobacco mosaic virus* (TMV) (57). It is known that coat protein is not required for CNV cell-to-cell movement, and is also not required for systemic movement, although it does facilitate systemic movement (58). For systemic movement to other plant parts, virus particles likely enter through the phloem and move to distant cells (58). However the means by which particles enter and exit phloem tissue is not known.

1.6.8 Transmission to a new host

As described previously, transmission of CNV in nature to a new host occurs via a specific fungal vector (*O. bornovanus*) present in the soil or water medium (14). This involves a fungal zoospore receptor interaction between specific regions or amino acids in the virus particles and a mannose/fucose containing glycoprotein on the zoospore surface. Further studies have shown that binding of CNV virions to zoospores induces a conformational change resulting in a state similar to “swollen” virus (35, 59). This may facilitate subsequent uncoating in cucumber root cells penetrated by zoospores containing virus particles (29, 60). CNV particles enter the root cells of cucumber plants upon entry of the zoospore and infection ensues (61). One of the

proteins recognized by the CNV particles on zoospore membranes is HSP70 (D. Rochon, unpublished) leading to the speculation that HSP70 assists in CNV swelling upon zoospore attachment.

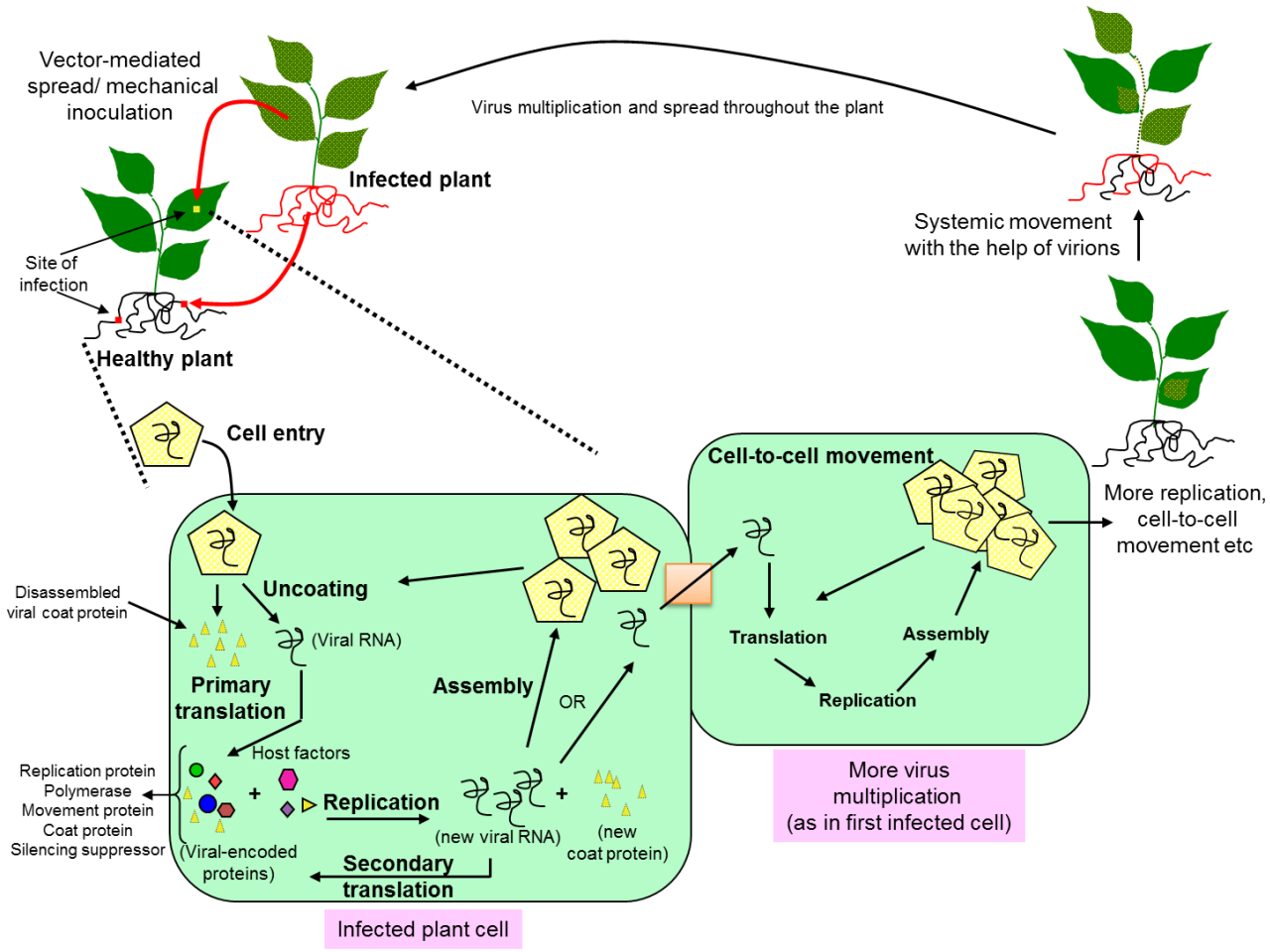

Figure 1.3: Schematic representation of the multiplication cycle of CNV.

For details see Section 1.6

1.7 Research objectives

1. To assess the potential role of HSP70 homologs in CNV particle assembly and disassembly.
2. To assess the potential role of basic amino acid residues of the CNV CP arm in encapsidation of full-length viral RNA, particle assembly and stability.

The overall objective of this thesis was to characterize molecular mechanisms of CNV virion assembly, disassembly and the potential role of HSP70 homologs in this process. Molecular studies on interactions of CP and particles with HSP70 homologs in assembly and disassembly have not been previously conducted in CNV or any other member of the *Tombusvirus* genus. During the course of this research I found that HSP70 homologs play dual roles in particle assembly and disassembly during the multiplication cycle of CNV. So a further objective became to elucidate the additional roles of HSP70 homologs during CNV infection such as in CP stability and accumulation, and CP targeting to chloroplasts as described in Chapters 2 and 3.

In Chapter 4, I have also undertaken a detailed characterization of the role of basic aa residues of the CNV CP arm in encapsidation of viral RNA and virion assembly. During the course of this work I found that removal of all four basic aa residues of a "KGRKPR" sequence in the CP arm lead to encapsidation of host RNA suggesting that the basic residues may be important for selective encapsidation of viral RNA. To my knowledge, the role of basic aa of the CP in imparting selectivity of viral RNA encapsidation over that of cellular RNA have not yet been evaluated in plant viruses.

Additionally, I contributed to a team that studied the induction of retrotransposons by CNV during infection. Induction of heat-inducible retrotransposons by plant viruses has not been

reported yet. In particular, I studied the role of heat shock in induction of retrotransposons showing that heat shock induces the expression of certain specific retrotransposons known to be induced during CNV infection. Hence, an additional objective was added to my thesis and the studies are summarized in Appendix B.

The majority of my thesis research was focused towards studying the role of HSP70 homologs in the multiplication cycle of CNV. In the next section I will first describe heat shock proteins, along with the mechanism of induction *HSP70*. I will also describe the structure and known functions of HSP70 family of proteins along with their mechanism of action.

1.8 Discovery of heat shock proteins

The discovery of heat shock proteins was made in 1962, by Italian geneticist, Ferruccio Ritossa, when a lab worker accidentally boosted the incubation temperature of the larvae salivary glands of the fruit fly, *Drosophila melanogaster* (62). When examining the chromosomes, Ritossa found that temperature shock induced a new set of puffs that indicated enhanced gene transcription of an unknown protein. Twelve years later, Tissieres & Mitchell found that the induction of the puffing pattern coincides with the synthesis of a set of new proteins that are heat inducible (63). The universality of the heat shock response phenomena from bacteria to human was recognized shortly thereafter (64). This discovery eventually led to the identification of heat shock proteins (HSPs) or heat stress proteins (65-67). HSPs are named according to their molecular weight. The heat shock protein 70 family or HSP70 homologs are a family of HSPs having the molecular weight of ~70 kDa. Heat shock 70 kDa protein (Hsp70) and heat shock cognate 70 kDa protein

(Hsc70) are inducible and constitutively expressed homologs of the HSP70 family, respectively. These proteins are one of the most widely studied families of HSPs. Hence, in the next section, I will discuss the structure, mechanism of activation, mode of action as well as functions of HSP70 homologs.

1.9 Structure of HSP70 homologs

HSP70 homologs consist mainly of two domains: namely, the N-terminal ATPase or nucleotide binding domain (NBD) which is 45 kDa and the 24 kDa C-terminal substrate binding domain (SBD) (68). The SBD is further divided into a 15 kDa β-sandwich and a 10 kDa α-helical subdomain. The β-sandwich subdomain constitutes the substrate binding pocket and the α-helical subdomain functions like a lid which opens and closes depending upon the type of nucleotide (ATP- open lid or ADP- closed lid) bound at the NBD (Figure 1.4A).

1.10 Mechanism of activation or induction of *HSP70* family of genes

The induction of *HSP70* is dependent on the activation of specific transcription factors termed heat-shock factors (HSFs) which bind to several *cis*-acting sequences known as heat-shock elements (HSE) in the promoters of the genes encoding *HSP70*s (69, 70). The transcription factor HSF consists of discrete functional domains, including a DNA-binding hydrophobic repeat domain (DBD). The DNA binding domain of each monomeric HSF unit binds to the pentanucleotide unit, 5'-nGAAn-3' (or 5'-nTTCn-3'), in the target DNA. The DBD in HSF binds to the pentanucleotide unit and the typical HSE is composed of three copies of the

pentanucleotide unit and HSF exists as a homotrimer (71-74). As described for *Saccharomyces cerevisiae* (75), there are three different types of HSEs that can interact with HSF. The "perfect-type" (P type) HSE consists of continuous inverted repeats of the pentanucleotide unit (5'-nTTCnnGAAnnTTCn-3' or 5'-nGAAnnTTCnnGAAn-3'), the "gap-type" (G type) contains one gap between the units [5'-nGAAnnTTCn(5bp)nTTCn-3' or 5'-nTTCnnGAAn(5bp)nGAAn-3' or 5'-nGAAn(5bp)nGAAnnTTCn-3' or 5'-nTTCn(5bp)nTTCnnGAAn-3'] and the "step-type" (S type) contains two gaps [5'-nGAAn(5bp)nGAAn(5bp)nGAAn-3' or 5'-nTTCn(5bp)nTTCn(5bp)nTTCn-3'].

1.11 Mechanism of action of the HSP70 family of proteins

1.11.1 The ATPase cycle

The ATPase cycle of HSP70 consists of a low affinity ATP bound state with fast exchange rates for the substrate and a high affinity ADP bound state with low substrate exchange rates. As soon as there is a need for protein folding or protecting the cell from the cytotoxic effects of misfolded or aggregated proteins, the ATPase cycle of the heat shock proteins come into action. HSP70 has a very low intrinsic ATPase activity, but association with the substrates in the substrate binding cleft and the J-domain proteins (JDP) synergistically stimulate the ATPase activity up to several thousand-fold. After ATP hydrolysis, the α-helical subdomain acts as a lid and closes and locks the substrate into the binding pocket (Figure 1.4B) (56, 68).

HSP70s transiently associate with exposed hydrophobic segments of the client via the C-terminal SBD, thereby preventing aggregation and promoting proper folding. Binding of ATP to the HSP70 NBD induces conformational changes in the adjacent SBD, opening up the SBD whereas ATP hydrolysis leads to closure of the pocket and stabilizes the client interaction (76, 77).

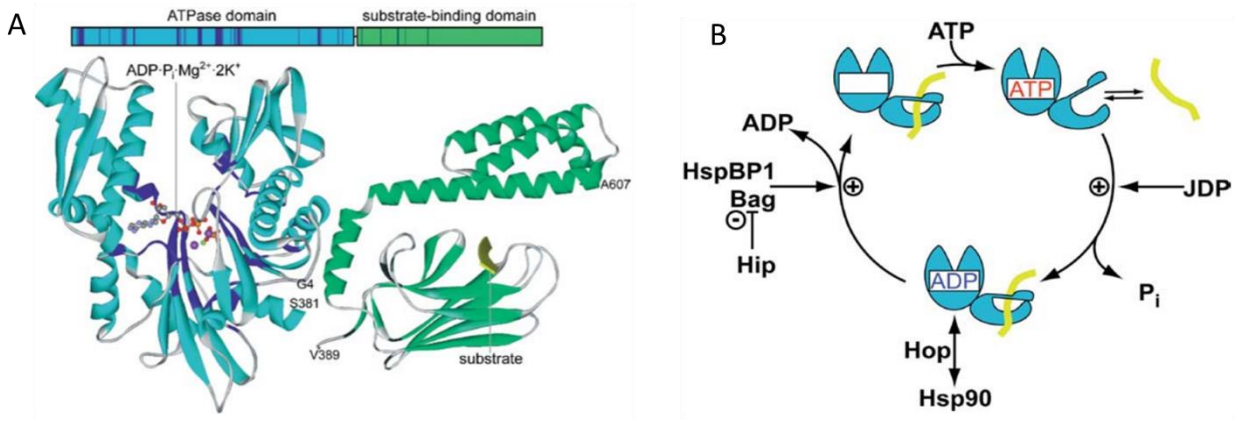

Figure 1.4: Structure and mechanism of function for HSP70 chaperones.

(A) Structure of HSP70 chaperones showing different domains (56); (B) ATPase cycle of HSP70 chaperones and action of some co-chaperones on the ATPase cycle [Reprinted from Recruitment of Hsp70 chaperones: a crucial part of viral survival strategies,153, 1-46, Mayer, M.P.; *Reviews of Physiology, Biochemistry and Pharmacology* (2005) with permission from Springer] (56). For details see Sections 1.9 and 1.11.1 respectively.

1.11.2 Induction of substrate unloading

In order to unload the client protein so that the substrate binding cleft can be emptied for starting a new cycle, nucleotide exchange factors such as GrpE and Bag-1 come into play. GrpE stabilizes the open conformation of the α-helical lid and promotes ADP release whereas Bag-1 stimulates ADP release and stabilizes the open conformation (56, 78).

1.11.3 Nucleotide stabilizing factors

HSP70-interacting protein (Hip) interacts with ATPase domain and stabilizes the ADP state of HSP70 by preventing premature substrate release. It antagonizes the substrate discharging function of Bag-1 for binding to the ATPase domain of HSP70, thereby preventing Bag-1 stimulated nucleotide release.

HSP70 homologs perform various functions as described below in Section 1.12 within a cellular milieu. Hence regulation of the access of HSP70 homologs to their target substrates is essential and is carried out by a group of J-domain proteins called co-chaperones (78). The ATPase cycle of Hsp70 chaperones is controlled by co-chaperones. The co-chaperones not only target HSP70 homologs to their substrate targets but by nucleotide exchange factors also determine the lifetime of HSP70-substrate complex. HSP70-HSP90 organising protein (Hop) stimulates the ATPase activity and interacts via the TPR domain with the EEVD motifs found at the C terminus of HSP70/90 (56, 78). It functions as a co-chaperone to assist and regulate the chaperoning activity of HSP70 or HSP90 chaperones.

1.11.4 Decision making between protein folding and degradation

The carboxyl-terminus of HSP70 interacting protein (CHIP) competes with Hop for binding to the C-terminus of HSP70/90. It acts as an E3-ubiquitin ligase ubiquitinating the bound polypeptide substrates, hence promoting their degradation by the cytosolic proteasome (78).

1.12 Known cellular functions of HSP70

The HSP70 family of proteins have chaperone activity and are involved in signal transduction and quality control functions within a cellular milieu. Hsp70 is activated under stress conditions such as heat, virus infection and oxidative stress (56, 78). Hsc70 is expressed constitutively but can also be induced by environmental stresses such as thermal and pesticide stress (79, 80). It has also been found that Hsp70 and Hsc70 may complement each other in a synergistic manner to preserve cellular integrity during metabolic challenges (81). The primary function of HSP70 family chaperones is to fold unfolded or misfolded proteins by interacting with a stretch of hydrophobic amino acids in the client unfolded proteins and by maintaining proteins in soluble, yet conformationally dynamic states (68, 82). It binds with high affinity to both hydrophobic-aromatic sequences like FYQLALT and hydrophobic-basic sequences like NIVRKKK (83, 84). HSP70 homologs also prevent unfolded proteins from associating with other non-native intermediates thereby preventing the cell from the cytotoxic effects of protein aggregation (78). HSP70s facilitate the recognition of misfolded degradation substrates by the ubiquitin ligation machinery and finally shuttle them to the proteasome (85).

Hsc70s have also been found to play an important role in the disassembly of large macromolecular complexes (56, 78, 86) such as the DNA-replication origin complexes (87) and clathrin coated vesicles (88-91) and are also involved in the inhibition of apoptosis (56, 78). They play an important role in the assembly of large macromolecular protein complexes such as the microtubule cytoskeleton (92), purinosome (93) and steroid receptors (94-98).

Hsp70 or Hsc70 has also been found to play an important role in the chloroplast import of nuclear encoded chloroplast destined preproteins by interacting with transit peptides (containing chloroplast targeting sequences) located near the N-terminus of the preproteins and facilitating their transport to the chloroplast (76, 99). Most chloroplast transit peptides (approximately 82%) have the capacity to bind Hsp70 or Hsc70 (100-102). After navigating through the cytoplasm to chloroplasts, the preproteins encounter the translocon at the outer envelope (TOC; translocon at outer envelope of chloroplast) and inner envelope (TIC; translocon at inner envelope of chloroplast). During or after translocation, the transit peptide is cleaved off by the stromal processing peptidase (SPP) in the stroma (103). The mature proteins are then released and folded in the stroma (76). Stromal Hsp70 has been known to play a role in "reeling in" of the incoming cargo and contributes to the folding, assembly and intraorganellar guidance of the proteins (76). Previous studies have shown that, individual Hsp70 molecules can apply ATP dependent conformational force to protein substrates and by means of entropic pulling can accelerate the local unfolding and pulling of translocating polypeptides into mitochondria (104).

Hsc70 can also protect and reactivate thermally inactivated enzymes (105) and hence it plays a prominent role in acting as a molecular thermometer in acquired cellular thermotolerance and recovery from thermal damage.

Because, of the diverse cellular roles played by HSP70 homologs, they are co-opted by a variety of viruses at several stages of the multiplication cycle (56). In the next section, I will describe why several viruses recruit HSP70 homologs during their multiplication cycle, with an emphasis on the role of HSP70 family of proteins in virus disassembly, replication and assembly.

1.13 Why do viruses recruit HSP70 homologs?

In the course of virus multiplication, a large number of proteins are synthesized in a relatively short period of time, whereby protein folding can become a limiting step. Many viruses therefore recruit cellular chaperones during their multiplication cycle to assist in folding of viral-encoded proteins. Apart from r protein folding, viruses also need to interfere with host cellular processes such as signal transduction, cell cycle regulation and attenuation of apoptosis in order to create a favourable environment for their persistence and to avoid premature cell death. HSP70 chaperones, as central components of the cellular chaperone network are involved in the control of these processes and are frequently recruited by viruses to reprogram the host cell (56). HSP70 chaperones also seem to be involved in avoidance of host defense mechanisms deployed during virus infection. HSP70 homologs have been found to play multiple roles at several stages of the infection of a variety of animal and plant viruses (56).

1.14 Role of HSP70 homologs in virus disassembly

Disassembly is the first and crucial aspect of the virus multiplication cycle which is important for the establishment of infection. Due to the ability of the HSP70 homologs to disassemble stable oligomeric complexes (106), viruses have evolved to recruit these cellular disassembling machines to uncoat their capsids. As described above, Hsc70 is one of the most abundant cytosolic HSP70 isoforms and plays a role in both preventing and reversing protein aggregation and in disassembling protein complexes (78, 86). ssRNA viruses result in a significant financial loss in crops every year (107); thus, they have been studied extensively over many years. Over 75% of all known plant viruses have messenger sense ssRNA genomes (108). Compared to viruses with genomes of ss/dsDNA or dsRNA/negative polarity ssRNA, positive polarity ssRNA viruses can initiate gene expression as soon as the capsid uncoats. Hsc70 homologs have been found to promote the uncoating process of several animal viruses such as *Polyomaviruses*, *Papillomaviruses*, *Reoviruses*, *Adenoviruses*, *Nodaviruses*, *Rotaviruses* and *Nervous necrosis virus* (109-115). A virally encoded HSP70 homolog of *Beet yellows virus* has been hypothesized to play a role in disassembly of the helical capsid (116). During the course of my research, I determined that the HSP70 homolog, Hsc70-2 is bound to CNV virions and plays a role in particle disassembly (described in detail in Chapter 3) (117).

1.15 Role of HSP70 homologs in virus replication

Once the capsid uncoats to release its nucleic acid, it must be protected from host nucleases and the viral RNA must replicate to prompt progeny virion production. Replication in the case of ssRNA viruses involves the formation of the replicase complex that includes association of

virally encoded proteins with certain host factors, as well as targeting to the site of replication. Members of the HSP70 family of proteins have also been found to be involved in the assembly of replicase complex of TBSV and *Red clover necrotic mosaic virus* (RCNMV) (17, 118). They have also been found to increase the replication efficiency of several RNA viruses including TBSV, RCNMV, *Potyviruses, Pepino mosaic virus, Rabies virus* and *Respiratory syncitial virus* (52, 118-121). Hsp70 is found to be associated with the replicase complex, and plays a role in the assembly and insertion of the replicase complex into the peroxisomal membranes, which is the site of replication, during TBSV infection (17, 18, 40). It has also been found to interact with the replicase complex of CNV extracted from CNV infected *N. benthamiana* protoplasts and to promote the replication process in experiments conducted on yeast cells (17, 40). Also, as will be described in Chapter 2, research conducted by me on *N. benthamiana* plants, showed that upregulation of HSP70 homologs positively regulates gRNA accumulation consistent with the role of HSP70 in enhancing CNV replication (122).

1.16 Role of HSP70 homologs in virus assembly

Assembly of the newly replicated viral RNA within the capsid to form a complete metastable virion, which is capable of infecting an uninfected cell is one of the critical steps in the multiplication cycle of viruses. Due to the inherent property of HSP70 family homologs in protein folding and assembly of protein complexes, they have been recruited by some viruses such as *Hantavirus, Polyomavirus, Simian virus 40* (SV40), *Closteroviruses, Enteroviruses, Papillomaviruses and Human immunodeficiency virus I* (HIV I) (123-129) for virus assembly. A virally encoded chaperone promotes the folding of major capsid protein of *African swine fever*

virus (ASFV) (130). Also, as will be described in detail in Chapter 2, I found that HSP70 homologs play an important role in the assembly of virus-like particles (VLPs) formed during agroinfiltration of CP in *N. benthamiana* independent of its role in CP accumulation (122). I speculate that as with VLPs, HSP70 homologs might promote the assembly of CNV virions.

Apart from the role of host factors, such as members of the HSP70 family in virus assembly, there are several other factors which play a prominent role in virus assembly. As CNV is an icosahedral virus, in the following section I will describe the various strategies utilized by icosahedral viruses for particle assembly.

1.17 Major strategies by which icosahedral viruses undergo assembly

Icosahedral viruses comprise a vast group of viruses infecting plants, insects, fungi, bacteria and humans (1). Assembly of the viral genome into spherical virions having icosahedral geometry with the help of CP subunits is an important aspect of the virus multiplication cycle. In the case of plant viruses, assembly is usually important for systemic movement and in some cases for virus movement from cell-to-cell and is also important for a transmission to new hosts, most likely in a ligand-receptor mediated fashion (29, 35, 59, 131). Most plant viruses are non-enveloped and have a positive polarity ssRNA genome. The ssRNA genome could be monopartite (e.g. TMV), bi-partite (e.g., RCNMV) or tri-partite (e.g., *Brome mosaic virus*, BMV). Virion phenotypes include capsids having rigid rods (e.g., *Tobamoviruses*), flexuous rods (e.g., *Potyviruses*), icosahedral shells (e.g., *Cucumoviruses*, *Tombusviruses*, *Nepoviruses*) and bacilliform structures (e.g., *Alfalfa mosaic virus*, AMV) (1). Despite having various virion

phenotypes among different families, the mature virions of a given virus species is often a homogeneous population, suggesting the precision and accuracy of the assembly process. Icosahedral capsids are a feature of roughly half the virus families and the majority of plant viruses have icosahedral symmetry (1). Hence, in this section I will focus on the three major strategies by which icosahedral viruses in general undergo assembly.

1.17.1 Unassisted capsid self-assembly

The simplest icosahedral capsids are self-assembled from 60 identical CP subunits in the same conformation through equivalent sets of interactions (e.g. *Satellite Tobacco necrosis virus*, STNV having T=1 symmetry). On the other hand, capsids having larger geometries that encapsidate a longer genome undergo self-assembly by either allowing the CP subunits to adopt different conformations or by involvement of a molecular switch that leads to a conformational change in the CP to promote CP oligomerization and formation of T=3 particles (55). Molecular switches can include a short CP segment at the N- or C-terminus which is ordered in some CP-CP interactions but disordered at others. Some molecular switches involve other elements sensitive to environmental changes such as divalent cations, protons, water-mediated hydrogen bonds, segments on viral genome or aa on viral proteins (55). For example, in the *Flock house virus* (FHV) T=3 capsid, the conformational switch is provided by the N-terminus of the CP and a capsid-bound RNA duplex (for details see Section 1.19.2). In the case of CNV, proline residues in the arm region of the capsid may promote the ability of the arm to assume the distinct positions required for formation of T=3 particles (60).

1.17.2 Scaffold protein-assisted assembly

Viruses that have a complex quaternary structures such as dsDNA phages and *Herpesviruses* need the assistance of a virally encoded scaffolding protein during assembly (55). Scaffold proteins are also regarded as assembly chaperones by virtue of the role played during the assembly process. Scaffold protein and CP co-assemble into stable, virion precursor structures called procapsids. They transiently participate in the assembly process by protein-protein interaction with CP subunits and are later removed from the mature virions before or during DNA packaging. Their main function is to promote capsid nucleation initiation by increasing the local concentration of CP species via gathering all of the necessary CPs for procapsid formation and by lowering the energy barrier of conformational transition from an assembly incompetent state to an assembly competent state. They also prevent incorporation of non-specific proteins into the capsid and promote the proper conformational switch in the CP subunits so that they are properly positioned at defined positions in the capsid. Some viral or host auxiliary proteins promote the assembly of viral capsids, however, they are not considered to be scaffold proteins as they are not removed from the capsid after particle assembly. In the case of CNV the CP R domain that forms the inner shell acts as a scaffold which facilitates the formation of the virion outer shell (13). Similar to this, the inner capsid in *Reoviruses* acts as a template for the assembly of outer capsid (132). As described in detail in Chapter 2, I speculate that HSP70 homologs might function as a scaffold protein or an auxiliary host factor to promote the assembly of CNV particles (for details see Chapter 2).

1.17.3 Viral nucleic acid-assisted assembly

In the majority of the ssRNA viruses, nucleic acid packaging occurs concomitantly with capsid assembly. Viral RNA is recruited early in the assembly process by CP-RNA interactions, so that no empty virions are formed. This process directly yields nucleic acid containing progeny virions. In the case of CNV, since empty capsids are not found during natural infections, it is believed that assembly of virions is RNA dependent (53).

Viruses do not generally accumulate particles containing cellular RNAs and preferentially encapsulate viral RNA(s) during infection to produce infectious progeny virions. In the next section I will briefly discuss the packaging profile of virus particles.

1.18 Packaging of host RNA by viruses

Although, the predominantly encapsidated RNA species within a population of virions is of viral origin, previous studies have shown that sometimes, authentic virus particles contain cellular RNA, *albeit* at a low level. The first evidence of cellular RNA encapsidation by a plant virus was provided by *Siegel et al.* (1971) (133). The author demonstrated that in standard TMV preparations, a small proportion of pseudovirions are present. These are tobamovirus-like particles that encapsidate host RNAs primarily of chloroplast origin rather than encapsidating viral RNA. It was found that 2-2.5% of the total TMV virion RNA consisted of host RNAs. It was hypothesized that, despite the presence of mechanisms for selective packaging of viral RNAs, a low level of host RNA mis-encapsidation into virions occurred which might reflect the site of particle assembly inside the cell. Studies on FHV showed that about 1% of the total

encapsidated virion RNA is of cellular origin (134). Also, research conducted by *Ghoshal et al.* (2015) in Dr. Rochon's lab, suggests that ~0.1-0.7 % of the total encapsidated RNA in CNV virions consists of host RNA (135). Of the encapsidated RNAs, the majority were chloroplast encoded RNAs. Interestingly, CNV CP targets chloroplasts during infection and so it is possible that chloroplast RNA may be encapsidated within chloroplasts by imported CNV CP (24). Also, nuclear encoded mRNAs corresponding to retrotransposon-like sequences were amongst the most abundantly encapsidated cytoplasmic RNAs. It was postulated by the authors that encapsidation of retrotransposon-like sequences by authentic CNV virions might play an important role in horizontal transmission of new genetic information into a new host that could lead to genome evolution.

1.19 Overview of factors involved in the assembly of plant viruses

Since, assembly of the majority of the plant viruses is primarily believed to dependent on interaction between the CP and viral RNA (1, 53, 136), in this section, I present a general overview of the factors involved in the assembly process of virus particles from CP subunits and viral RNA. This is relevant to Chapter 4 of my thesis where I have found that mutation in an RNA binding site in the CNV CP leads to disproportionate assembly of host RNA rather than viral RNA.

1.19.1 Electrostatic interactions

Electrostatic or ionic interactions play a prominent role in virion assembly; whereby the negatively charged phosphate groups of the RNA molecule interact with the positively charged

side chains of the basic amino acids [lysine (K) and arginine (R)] (1, 137). Divalent cations such as Ca^{2+}, have also been found to stabilize the CP subunit interactions and contribute to the formation of a complete metastable virion at lower pH by bridging the adjacent carboxyl groups of different CP subunits, as observed in members of the genus *Sobemovirus* (138) as well as in *Tombusviruses* and *Carmoviruses* (1). Electrostatic interactions are thought to be sequence-independent as CP can non-specifically encapsidate cellular RNA as determined by *in vitro* assembly assays (139). However, viruses predominantly and preferentially encapsidate their own RNA rather than host RNA during infection. If electrostatic interactions were the only driving force required for assembly of viral RNA into virions, then viral CP would bind to host RNA and encapsidate it non-specifically at a high level. This suggests that in addition to electrostatic interactions, other factors are involved in specific encapsidation of viral RNA into virus particles. For example, the RNA genome itself has been found to contain PSs that promote specific recognition between the viral CP and viral RNA (see Section 1.19.6).

1.19.2 Amino acid sequences on the CP

Viruses have evolved to ensure the encapsidation of their negatively charged genomes. Depending on the type of nucleic acid to be encapsidated, different viruses utilize different strategies for successfully encapsulating the genetic material to form an infectious virion. Among the viruses having DNA genomes, SV40 has been shown to form minichromosomes using positively charged cellular histones (140) and *Adenovirus* have been shown to use a virally encoded basic core protein VII for complexing its DNA (141). Negative polarity RNA viruses (e.g. *Vescicular stomatitis virus*, *Respiratory syncytial virus*) encode nucleocapsid proteins that

bind their RNA through a positively charged cleft (142). However, many positive polarity RNA viruses have a common motif rich in positively charged amino acids in the CP that faces the interior of the virion. This region has been postulated to play an important role in electrostatically interacting with viral RNA and initiating capsid nucleation events (55). An arginine-rich motif (ARM) in the CP of several plant RNA viruses has been shown to play an important role in RNA interaction and genome packaging as described below.

In some positive polarity RNA viruses such as *Cucumber mosaic virus* (CMV), *Cowpea chlorotic mottle virus* (CCMV), SBMV, *Semliki Forest virus*, *Nodavirus* and *Sindbis virus*, an unstructured motif in the CP rich in basic amino acid residues extends into the center of the virions. These regions are largely unresolved in the crystallographic maps, suggesting their potential interaction with viral RNA (143-148). The electrostatic interactions between these positively charged motifs of the CP and viral RNA has additionallybeen postulated to constrain the length the of encapsidated genome (149, 150).

Studies on several viruses such as STMV, *Beet black scorch virus,* BMV, *Ourmia melon virus*, CMV, AMV, RCNMVs, CCMV, SeMV, FHV, HIV, *Macrobrachium rosenbergii nodavirus* and *Melon necrotic spot virus* (MNSV), have shown that a basic aa rich region in the N-terminal portion of the CP plays an important role in virion RNA encapsidation (51, 53, 151-163). Also, previous work in Dr. Rochon's lab by *Reade et al.* (2010) showed that a lysine rich "KGKKGK" sequence in the R domain of the CNV CP plays an important role in encapsidation of full-length viral RNA. Removal of the KGKKGK sequence was found to promote the encapsidation of less than full-length viral RNA, possibly due to the inability of CP mutant to neutralize the negative

charge of the phosphate backbone of full-length RNA (164). In FHV, in addition to the above mentioned positively charged residues at the N-terminus, which helps in the selective packaging of RNA1 (160), the aromatic amino acid phenylalanine at the C-terminus of the CP promotes specific packaging of RNA2, likely via base stacking of the aromatic side chains of phenylalanine with viral RNA (165).

A study on BMV, has shown that the basic aa regions in the N-terminal tail of the CP faces inward into the virion and interacts with virion RNA promoting both assembly and virion stability likely through electrostatic interactions (157). BMV mutants with decreased positive charges packaged lower amounts of RNA whereas mutants with increased positive charges packaged greater amounts of RNAs consisting of truncated and full-length BMV RNA, as well as cellular RNAs up to ~900 nucleotides, without having a significant change in the capsid structure as determined by cryo-EM. These results suggest that the changes in the charge of the capsid could result in changes in the profile of encapsidated RNA species. Also, mutations of specific arginine residues to lysine resulted in defective specific encapsidation of one or more of the four BMV positive-strand RNAs. However, the authors suggested that electrostatic interactions are not the only driving force governing encapsidation in these mutants (157).

Eukaryotic RNA viruses with icosahedral symmetry generally exhibit physical homogeneity among assembled virions *in vivo* for which an optimal CP conformation must be selected. Studies on icosahedral viruses like SeMV and FHV have revealed that near the N- and C-terminus, the CP contains flexible “molecular switches”, the interaction between which determines the morphology of progeny virions (166, 167). Interactions between the N- and C-

termini of the different CP subunits is essential for the formation of CP dimers, the building blocks of *Bromoviruses* (168) and removal of either leads to the formation of polymorphic virions likely due to improper CP-CP interactions (169, 170).

Studies on BMV have shown that specific amino acids on the CP are also involved in maintaining virion structure and stability. Interaction between the N- and C-terminal regions is envisioned to play a crucial role during virus assembly. A lysine rich seven amino acid sequence at the N-terminus of the BMV CP (KAIKAIA) and the related CCMV CP (KAIKAWT) was determined to act as a molecular switch during the assembly process (171). By structural analyses, it was shown that this region of the capsid supports a critical contact (the "clamp") with the C-terminus of 2-fold related subunits that ties the capsomeres together. Hence sequences at both the N- and C-termini play an important role in particle morphology. Mutant viruses, lacking the putative seven amino acid N-terminus molecular switch contained truncated RNA likely due to weak CP-RNA interaction that would make the RNA in the capsid more susceptible to extensive nuclease fragmentation.

The CPs of CCMV and BMV have also been characterized to contain four highly conserved RNA-interacting domains (RID) which have been postulated to contribute towards weak non-specific RNA-protein interactions to promote viral RNA encapsidation and maintain overall stability of virions in synergy with the strong specific interactions provided by the ARM (172). Also, during the course of my research, I found that a highly basic "KGRKPR" sequence in the ε region of the CNV CP arm plays an important role in encapsidation of viral RNA during particle assembly (for details see Chapter 4).

1.19.3 Conformational collapse of vRNA

The genomes of RNA viruses play multiple roles, including acting as a template for both translation of viral proteins and replication to produce multiple copies of RNA. As well, encapsidation of the replicated RNA within the protective CP shell is required for the formation of progeny virions. During the former two processes, the RNAs are not in a compact conformation; however, packaging of virion RNA requires the RNA to be compacted within the restricted space available within the capsid. Studies on MS2 bacteriophage and STNV have suggested a "2-stage cooperative mechanism" for particle assembly (173, 174). According to this model, it is proposed that since the size of RNA to be encapsidated is larger than the space available within a capsid, compaction of RNA is necessary. This is brought about by multiple interactions of different regions on vRNA with CP subunits. The binding of multiple CP subunits with different affinities to sequences or structures distributed throughout the RNA genome mediates rapid condensation of RNA with a 20-30% reduction in the hydrodynamic radii. This multiple RNA-CP interaction forms the assembly initiation complex. The subsequent addition of CP subunits to the nucleating complex in a co-operative manner further collapses the RNA to a radius that can be accommodated in the capsid interior and particle assembly is achieved. The proper distribution and relative positioning of multiple low or high affinity signals on the genome have also been suggested to play an important role in genome condensation and encapsidation during the assembly process (174).

1.19.4 CP-mediated capturing of RNA secondary structures is compatible with capsid geometry

FHV, a *Nodavirus*, is a bipartite (+)ssRNA virus. Both the RNA1 and RNA2 are encapsidated in a single T=3 icosahedral shell. The high-resolution X-ray structure of FHV suggests that ten bp of well-ordered dsRNA is located at each of 30 2-fold axes of the virion resulting in a regular distribution of RNA in the particle interior (175). Using cryo-EM of mutants having different RNA and CP content, it was determined that the encapsidated viral or heterologous RNA was organised as a dodecahedral cage of duplex RNA within the virions that sits directly beneath the protein shell adjacent to the CP (176). The similarity in the tertiary structure of RNA encapsidated in different mutants suggested that, irrespective of the nucleotide sequence and length of RNA, the CP is able to exploit the plasticity of RNA secondary structures, to adopt a conformation that is compatible with the capsid geometry.

1.19.5 Replication coupled encapsidation

For efficient encapsidation of replicating RNA into virions to produce exclusively infectious particles, replication is believed to occur in conjunction with encapsidation in many virus systems, a process referred as replication coupled encapsidation. However, different mechanisms for the specificity of encapsidation have been proposed for different viruses as described below.

1.19.5.1 Physical interaction between CP and the replication complex

One efficient way viruses ensure selective packaging of their own RNA from a pool of cellular RNAs is by interaction of the CP with the replication proteins or essential components of the replication complex. In the case of *Poliovirus* assembly, RNA replication and encapsidation are coupled which is mediated by a direct physical interaction between the replication complex and the CP (177). Moreover, further studies by another group have also shown that RNA is assembled into virions at the site of replication which is governed by protein-protein rather than RNA-protein interactions (178). In this case, encapsidation of RNA does not seem to require an RNA packaging signal (PS) and several attempts to search for a RNA PS have failed (179). However, a direct physical interaction between the capsid protein VP3 and the non-structural protein $2C^{ATPase}$ is sufficient for genome packaging at the site of genome replication. Viral RNA released from the replication complex associates with the pentamers (generated from the protomers that are made up of trimers of mature CP subunits VP0, VP1 and VP3) through their VP3 domains. VP3 interacts with the non-structural protein $2C^{ATPase}$ on the surface of membranous replication complex and hence ensures selective packaging of replicating RNA.

A recent report on STMV shows that the interaction between the N-terminal basic motif of the STMV CP with the helper TMV replicase plays an important role in replication and specific packaging of STMV RNA (151). Also, as will be described further in detail in this thesis, during the course of my research, I found that CNV CP directly or indirectly associates with the auxiliary replicase protein p33. Hence, I speculate that this association might render the specificity of viral RNA encapsidation during particle formation (for more details see Chapter 4).

1.19.5.2 Conformational change in the CP as a result of interaction with the replicase

One of the basic criteria in the assembly process is the formation of capsid building blocks which is primarily initiated by forming CP dimers. Dimer formation takes place when the assembly incompetent capsid proteins are converted to the assembly competent state most likely by a conformational change (55). The conformational change in the CP was proposed to promote the formation of CP dimers and interestingly with an optimal conformation that only recognizes viral RNA for encapsidation (180-182). Studies in BMV have suggested that interaction between the replicase protein p2a with the newly synthesized CP at the cytoplasmic side of the ER, which is the site of BMV replication, induces a conformational change in the CP. This conformational change assymetrically upregulates the formation of (+) strand synthesis over (-) strand.

1.19.5.3 Translation of CP in *cis* from replicating RNA and the microenvironment

The compartment of the cell where replication and assembly of the newly replicated viral RNA into progeny virions takes place plays an important role in the selectivity of the encapsidation process. RNAs that are abundant in a particular microenvironment will largely impact the type of species encapsidated. Also, one of the most efficient ways by which virions can ensure selective packaging of replicating RNA within the CP shell is by exhibiting a direct association of the CP translated in *cis* from the viral genome with the viral RNA. Studies on FHV provide an excellent example. It has been shown that CP translated from the replicating RNA2 specifically encapsidates replicating RNA 2 in *cis* and RNA1 in *trans*, while the CP that is synthesized from non-replicating RNA2 encapsidates relatively higher amounts of cellular RNAs. It was hypothesized that FHV RNA is confined and concentrated to a cellular compartment which is in

the vicinity of mitochondria, which is the site of replication and this compartmentalization contributes to specific genome recognition and encapsidation (183). The authors provided evidence by showing that the N-terminal ARM of FHV targets the CP to the site of replication, i.e., mitochondria (160).

In a separate study, a *Baculovirus* expression system was used to study if uncoupling of viral protein translation from RNA replication affects the nature of encapsidated species. It was found that neither RNA1 nor RNA2 were encapsidated efficiently when the CP was supplied *in trans* from a nonreplicating RNA (183). Also, particles purified from infected cells contained predominantly random cellular RNA, suggesting the importance of spatial coordination of RNA and CP synthesis in genome packaging. An intriguing hypothesis was that replication of RNA2 is essential for the packaging of FHV RNAs because it guarantees that CP is synthesized in a cellular location that permits immediate access to progeny RNA1 and RNA2 (183). Whereas in the case of transcripts made from a nonreplicating system, after exiting the nucleus, the viral RNAs are translated in a separate location distal from the replication site, thereby leading to packaging of cellular RNAs.

In the case of CNV it has been found that the CP when expressed by agroinfiltration encapsidates predominantly host RNA which is consistent with the results described above concerning FHV. However, CNV CP mRNA is also encapsidated, and moreover, it is encapsidated more efficiently than other species analyzed (135). This suggested that CP translated from CP mRNA encapsidates the mRNA in *cis* relatively strongly in comparison to encapsidation of host RNA. However, the TBSV p19 mRNA which is highly similar in sequence to the CNV p20 (86%

identical), is also encapsidated relatively highly efficiently (135). These latter results suggest viral RNAs may contain *cis* acting PSs which promote assembly (see below).

1.19.5.4 Translation of the non-structural protein in *cis* from replicating viral RNA

Due to the high error prone nature of RdRp encoded by RNA viruses, strict *in vivo* mechanisms must exist to prevent the amplification and transmission of defective viral RNAs while promoting the packaging of authentic viral genome among viral quasi species. A common mechanism to specifically encapsidate viral RNAs is the use of PSsin the RNA genome, which are recognized by the viral CP that can be expressed in *trans* from a separate sgRNA molecule such as in the case of BMV and RCNMV (53). A strict *cis* requirement for a viral structural protein in packaging is found in FHV as described above in Sections 1.19.2 and 1.19.5.3, where translation of capsid protein in *cis* directs packaging of replicating FHV genomic RNA by direct association with the RNA from which it is translated (183). Studies on a positive strand *Flavivirus*, *Kunjin*, has demonstrated a very good example for the *cis* requirement of a "non-structural viral protein" translation in genome packaging into virus particles along with viral RNA replication (184). *Kunjin virus* RNA replicates within replication complexes located in virus-induced membranous structures in the cytoplasm called vesicle packets. Translation of the non-structural protein NS3 was shown to be involved in specific packaging of the viral genome. NS3 is a multifunctional protein with enzymatic activities involved in viral polyprotein processing, viral RNA replication and RNA capping. Additionally, NS3's helicase has been shown to be involved in releasing nascent positive-stranded RNA from the replication complex. The 5'-triphosphatase activity of NS3 in conjunction with the methyltransferase activity of

another non-structural protein, NS5, caps the 5' terminus of the released RNA. To support the idea of replication coupled packaging, it was hypothesized that NS3 after being translated from the newly synthesized RNA, remains bound with the RNA and associates with other non-structural proteins or host factors that targets the RNA-NS3 complex to the site of virus assembly containing a high concentration of capsid protein.

1.19.6 Packaging signals

It is believed that viral RNAs contain one or more high affinity sequences or secondary structures that bind the CP subunits or oligomers to participate in capsid nucleation initiation events. These sites are collectively referred as the PS. Possession of these sequences or structures serves to help the CP in discriminating viral RNA from cellular RNA to prevent the "mis-encapsidation" of defective viral or host RNAs. PSs could be single or multiple and can be present on any portion of the genome depending on the type of the virus.

In TCV, the PS is located at the 3' end of the CP ORF as a 28 nt bulged hairpin loop (185). In the case of SBMV, a 28 nt stem-loop structure in the putative RdRp region acts a PS (186). Specific secondary structures at the 5' or 3' UTR could also serve as a PS as found in the case of *Hepatitis B virus* (HBV) (187) and AMV (188), respectively. In a helical plant virus, TMV, the PS is described to be a 51 nt region bearing a stem-loop structure in the MP ORF (189). In RCNMV, a 34 nt stem-loop structure in the RNA2 transactivator region is characterized as a PS (190). FHV uses a 32 nt bulged stem-loop structure in a specific region of defective interfering (DI) RNA derived from RNA2 as a PS (191). The relative position of the PS within the genome

also plays an important role in it's efficiency as a PS as described for *Sindbis virus* (192). Other auxiliary factors such as cellular tRNAs as well as virus-encoded tRNA-like structures at the 3' UTR have been shown to participate in RNA packaging, the latter being the case for BMV (193, 194).

Studies have shown that CCMV, which is a *Bromovirus* like BMV does not have an apparent PS. The CCMV CP can encapsidate heterologous RNA *in vitro* with a packaging efficiency of up to 50% that of virion RNA and the packaged RNA does not bear any apparent sequence similarity with CCMV gRNA (195).

Owing to the limitations associated with a high affinity PS and the relatively high abundance of cellular RNAs over viral RNAs, affinity to a single PS alone might be insufficient to achieve specificity during encapsidation. As such, a co-operative packaging mechanism involving several weak or low affinity RNA-CP interactions is preferred and ensures selection during the assembly process. There is an emerging perception that icosahedral viruses appear to bear multiple PSs, because for such viruses specific binding of CP to PSs throughout the RNA would also help in the compaction of viral RNA to accommodate the RNA within the volume of the virion (174, 196). Viruses such as BMV (197), STNV (198), HIV-1 (199) and *Feline immunodeficiency virus* (FIV) (200) have been shown to have more than one PS. Also, previous work conducted by *K. Ghoshal* in Dr. Rochon's lab suggests the absence of a single high affinity PS on CNV RNA (201). It is possible that like other icosahedral viruses, as described above, CNV RNA has evolved to bear several signals having different affinities towards the CP to promote encapsidation.

1.19.7 Physical size constraint

Assembly is also influenced by the inherent curvature of the capsid that imposes an upper limit on the size and amount of viral genome to be encapsidated. Nucleic acid substantially larger than wild type genome size can't be encapsidated within a single capsid, regardless of the presence of packaging signals. This phenomena has been well studied in TCV which is a 30 nm T=3 icosahedral positive polarity ssRNA virus that encapsulates an approximate a 4 kb genome but not sgRNA. While analyzing the size limits for encapsidated RNA in TCV virions, Qu & Morris (185) observed that virions of TCV isolated from protoplasts coinfected with wild-type TCV and a chimeric construct of the structurally related TBSV and TCV (TBSV-TCV chimera, where the TBSV CP gene was replaced with the TCV CP gene) only contained the 2 kb sgRNA of the chimera but not the larger genomic RNA of 4.6 kb. It was postulated that to meet the criteria of encapsidation within the available volume of the virion interior, two copies of the 2 kb sgRNA (corresponding to 4 kb) are encapsidated in a virion so that the final amount of RNA closely resembles what is encapsidated during WT TCV infections. In a similar coinfection assay performed with a truncated version of the TBSV-TCV chimera having a 4.13 kb genome, packaging the chimeric construct was observed (185). The authors also claimed that the presence of sgRNA in virions, *albeit* at a low level, suggests that assembly of smaller than genome size RNAs does indeed occur. However, the cumulative summation of smaller sized genome must be close to that of WT virus. The evidence for this comes from the observation that, of the two TCV sgRNAs of size 1.7 kb and 1.45 kb, only the smaller one is packaged although both are suggested to contain a packaging signal. It was proposed that possibly three 1.45 kb sgRNA are packaged in a single virion which would then be similar to the size of WT TCV (4.35 kb versus 4 kb). Collectively, these observations suggested that, despite having the required packaging signal,

there is a strict RNA size preference for assembly of complete TCV. Hence, the length of the packaged nucleic acid plays a prominent role in determining virion morphology.

1.19.8 CP-CP interactions in virus assembly

Interaction between the CP and an optimal sized RNA compatible with the interior volume of the capsid has been believed to be a predominant virion assembly determinant. However, in some cases such as *Comoviruses* (e.g. *Cowpea mosaic virus*) and *Tymoviruses* (e.g. *Turnip yellow mosaic virus*), capsids are predominantly stabilized by noncovalent CP-CP interactions (such as the van der Walls force of attraction, hydrophobic interactions, polar interactions, hydrogen bonds, salt bridges, disulphide linkages) and hence capsid shells can be formed in the absence of RNA (1, 53).

1.20 Background, hypothesis and synopsis of Chapters

1.20.1 Chapter 2

Background

Because of the small size of the genome and its limited coding capacity, CNV is dependent on interaction with host cellular components to complete its multiplication cycle. A potential candidate for such processes could be members of the HSP70 family; both due to their abundance and multiple roles in cellular phenomena. Also, previous work in Dr. Rochon's lab has shown that 1-5% of the CP is targeted to chloroplast during infection (24) and as described in

Section 1.12, HSP70 plays an important role in chloroplast targeting of cytoplasmically synthesized preproteins (99).

Hypothesis

In this chapter, I hypothesized that HSP70 is induced during CNV infection. I also hypothesized that the induced HSP70 is recruited by CNV at several stages of the multiplication cycle, such as for CP accumulation, CP solubilisation, chloroplast targeting and particle assembly.

Synopis

I found that CNV co-opts a highly CNV-induced host factor, HSP70, and that HSP70 homologs play multiple roles during several stages of the CNV multiplication cycle. Using Next Generation Sequencing (NGS) and Western blot analyses, respectively, I found that several isoforms of Hsp70 and Hsc70 transcripts are induced to very high levels during CNV infection of *N. benthamiana* and that HSP70 proteins are also induced by at least 10 fold, possibly as a result of the host response to the high levels of CNV proteins that accumulate during infection. Moreover, I have found that CNV co-opts HSP70 family homologs to facilitate several aspects of the CNV infection process such as viral RNA, CP and virus accumulation. Downregulation of HSP70 homologs also interferes with the chloroplast targeting of CNV CP. Since, chloroplasts play an important role in plant defence, targeting of CP to chloroplasts with the help of HSP70 homologs may aid in CNV suppression of host defense responses.

1.20.2 Chapter 3

Background

Virus particles must disassemble and release their nucleic acid in order to establish infection in a cell. Despite the importance of disassembly in the ability of a virus to infect its host, little is known about this process, especially in the case of non-enveloped spherical RNA viruses. HSP70 homologs have previously been shown to play an important role in disassembly of large oligomeric complexes as well as uncoating of several animal viruses as described in Sections 1.12 and 1.14 respectively. Also, in Chapter 2, I found that HSP70 interacts with CNV CP both *in vivo* and *in vitro* and plays multiple roles at several stages of the multiplication cycle. Hence, in Chapter 3, I extended my previous observations and examined a potential role of HSP70 homologs in the CNV disassembly process.

Hypotheis

I hypothesized that HSP70 is bound to CNV virions and that in conjunction with additional cytoplasmic HSP70 homologs promotes the uncoating process of CNV by triggering a conformational change in the capsid.

Synopsis

Using Western blot analysis and mass spectrometry, I found that the HSP70 homolog, Hsc70-2, copurifies with CNV particles. Virus overlay and immunogold labelling assays suggest that

Hsc70-2 is physically bound to virions. Furthermore, trypsin digestion profiles suggest that the bound Hsc70-2 is partially protected by the virus indicating an intimate association with particles. To investigate a possible role of Hsc70-2 in particle disassembly, I showed that particles incubated with Hsp70/Hsc70 antibody produce fewer local lesions compared to prebleed control antibody on *C. quinoa*. In conjunction, CNV virions purified using CsCl and having undetectable amounts of Hsc70-2 produce fewer local lesions. I also showed that plants with elevated levels of HSP70/Hsc70 produce higher numbers of local lesions following CNV inoculation. Finally, incubation of recombinant *N. benthamiana* Hsc70-2 with virus particles in vitro leads to conformational changes or partial disassembly of capsids as determined by TEM and particles are more sensitive to chymotrypsin digestion. Taken together, the data points to an important role of the host factor, Hsc70-2, in CNV disassembly process.

1.20.3 Chapter 4

Background

Encapsidation of viral RNA by CP molecules is a crucial aspect of the virus assembly process. Positively charged amino acids in the CP subunits play an important role in interacting with viral RNA at least in part via electrostatic interactions and hence encapsidation and assembly into a complete virion. The cryo-EM structure of the CNV particle suggests that it consists of two concentric shells with viral RNA sandwiched between the shells (13). Previous work in Dr. Rochon's lab has identified a highly basic "KGKKGK" sequence in the RNA binding domain of the CP that plays an important role in the encapsidation of full-length viral RNA and in particle morphology (62).

Hypothesis

In this chapter I hypothesized that basic residues in the ε region of the CP arm may play a role in particle assembly, stability and encapsidation of full-length viral RNA.

Synopsis

I found that the ε region of the CNV CP arm contains a highly basic "KGRKPR" sequence which in C subunits lines the inner side of the outer shell at the 2-fold axis and coincides with viral RNA. Multiple sequence alignment of this region across several genera in the *Tombusviridae* showed conservation of basic aa residues. Seven different mutants were constructed in the CNV ε region in which the basic residues were mutated to alanine (A) individually, in pairs or in total. Although CP production was affected for each mutant, particle accumulation was affected proportionately more, especially for mutants with two or four aa substitutions, suggesting that the basic aa in the KGRKPR sequence affect particle assembly and accumulation. Double and quadruple "KGRKPR" mutants produced T=1 particles as well as T=3 particles suggesting the importance of "KGRKPR" sequence in determining virion morphology. Significantly more truncated RNA species are encapsidated in double or quadruple mutants suggesting that encapsidation of full-length CNV RNA requires these basic aa residues in the ε region. Interestingly, "KGRKPR" mutants encapsidate a significantly higher proportion of host RNA than WT CNV suggesting that the ε region plays a role in selective encapsidation of viral RNA over host RNA. Taken together, the data presented in this chapter assisted in mapping the RNA binding sites on CNV CP.

Chapter 2: *Cucumber necrosis virus* recruits cellular heat shock protein 70 homologs at several stages of infection[2]

2.1 Introduction

CNV is a positive strand RNA virus in the genus *Tombusvirus*, Family *Tombusviridae* (7). The CNV genome is monopartite and consists of approximately 4.7 kb of positive polarity single-stranded RNA. The genome contains five ORFs which encode five different proteins: the auxiliary replicase factor (p33), the RNA dependent RNA polymerase (RdRp) (p92), the coat protein (CP) (p41), the movement protein (p21) and the silencing suppressor (p20) (Figure 2.2.1A). The UAG stop codon of the p33 ORF is read through to produce the RdRp. p33 and p92 comprise part of the viral replicase which also consists of host components (40). p33 and p92 are translated from gRNA. The CP ORF, being present on an internal region of the genome, is translated from a sgRNA of ~2.1 kb. p21 and p20, which are translated from the overlapping ORFs 4 and 5, are expressed from a second sgRNA of ~0.9 kb (16). p20 is translated following leaky scanning of the p21 AUG codon (20).

The CNV capsid is a T=3 icosahedron that consists of 180 identical CP subunits. The CNV CP has three distinct domains: the "R" domain, which is the N-terminal RNA binding domain that interacts with viral RNA and forms the inner shell; the "S" or shell domain which constitutes the outer shell and the "P" or protruding C-terminal domain, which projects as dimers from the surface of the shell. The "a" or arm region flexibly tethers the R and S domains allowing for the quasi-equivalent subunit interactions required for T=3 icosahedral symmetry (202).

[2] A version of this Chapter has been published in *Journal of Virology*. **Alam, S.B.** and Rochon, D. (2016) *Cucumber necrosis virus* recruits cellular heat shock protein 70 homologs at several stages of infection. J. Virol 90:3302–3317.doi:10.1128/JVI.02833-15.

The arm region can further be divided into the β region which is hydrophobic and the ε region which contains several basic residues. The “S” and the “P” domains are connected by a short flexible hinge, “h”.

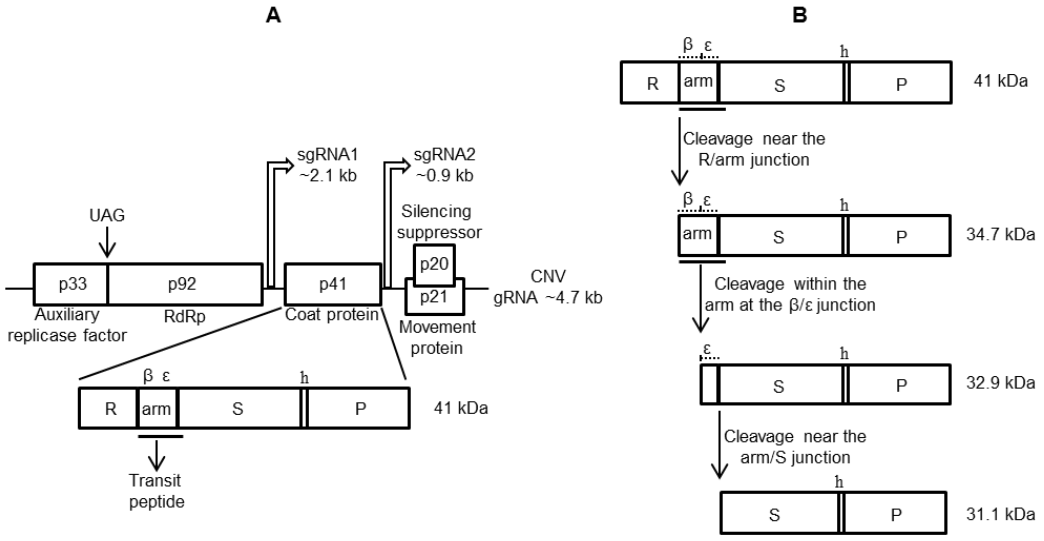

Figure 2.1: Features of CNV CP.

(A) Genome organization of CNV showing the five ORFs and their encoded proteins. The start sites and sizes of sgRNA1 and sgRNA2 relative to gRNA are also shown. The CP ORF is expanded and the three main domains R, S and P along with the arm region (including the β and ε regions) and hinge (h) are shown. The region of the CP that contains the chloroplast transit peptide-like sequence is underlined. (B) Diagrammatic representation of two cleavage events that take place during targeting of the CNV CP to chloroplasts. The first cleavage is near the R/arm junction resulting in a N-terminal truncated CP where the chloroplast transit peptide is at the N-terminus of the protein. The second cleavage is within the arm followed by a third cleavage near the arm/S junction. This cleavage occurs within the stroma likely via the stromal processing peptidase (59).

Plant and animal RNA viruses are agriculturally and medically important viruses. RNA viruses, having small genomes, are highly dependent on their hosts and have evolved to co-opt host components as a part of their multiplication strategy (19, 56, 203). In the course of virus multiplication, a large number of proteins are synthesized in a relatively short period of time, whereby protein folding can become a limiting step. Many viruses therefore recruit cellular chaperones during their multiplication cycle (19, 56, 204).

Heat shock protein 70 (HSP70) family homologs including Hsp70 (heat shock 70 kDa protein) and Hsc70 (heat shock cognate 70 kDa protein) chaperones are central components of the cellular chaperone network and are frequently recruited by viruses (19, 56, 204, 205). Hsp70 is activated under stress conditions such as heat, virus infection and oxidative stress (56, 68, 78, 205-212). Hsc70 is expressed constitutively but can also be induced by environmental stresses such as thermal and pesticide stress as well as virus infection (79, 80, 205, 213, 214). It has also been found that Hsp70 and Hsc70 may complement each other in a synergistic manner to preserve cellular integrity during metabolic challenges (81).

The primary function of HSP70 family chaperones is to fold unfolded or misfolded proteins and maintain proteins in a soluble, yet conformationally dynamic state (68, 78, 82, 215). HSP70 homologs play an important role in the assembly of large macromolecular protein complexes (92-98) including the assembly of viruses such as *Reovirus*, *Hantavirus, Polyomavirus*, SV40, *Closteroviruses*, *Potyvirus*, *Enteroviruses*, *Papillomaviruses* and HIV I (52, 110, 123-129). A virally encoded chaperone have been found to promote the folding of the major capsid protein of ASFV (130). HSP70 homologs have also been found to be involved in the cell-to-cell movement

of *Closteroviruses* and *Tomato yellow leaf curl virus* (TYLCV) (126, 216, 217). Hsc70 has been found to interact with the coat protein and virions of *Pepino mosaic virus* and colocalizes with virions in the phloem of infected plants (213). HSP70s have also been found to be involved in the assembly of the replicase complex of TBSV and RCNMV (17, 118) and positively regulate the replication process of several other RNA viruses including *Potyviruses*, *Pepino mosaic virus*, *Rabies virus*, *Rice stripe virus*, *Tomato yellow leaf curl virus* and *Respiratory syncitial virus* (52, 119-121, 218). Hsp70 is found to be associated with the replicase complex, and plays a role in the insertion of the replicase complex into peroxisomal membranes during TBSV infection (17, 18, 40). It has also been found to interact with the replicase complex of CNV and to promote the replication process (17, 40).

Hsp70 or Hsc70 have both been found to play an important role in the chloroplast import of nuclear encoded cytosolic preproteins by interacting with transit peptides (containing chloroplast targeting sequences) located near the N-terminus of the preproteins (76, 99). Most chloroplast transit peptides (approximately 82%) have the capacity to bind Hsp70 or Hsc70 (100-102). After navigating through the cytoplasm to chloroplasts, the preproteins encounter the translocon at the outer and inner envelope of the chloroplast. During or after translocation, the transit peptide is cleaved off by the stromal processing peptidase (SPP) in the stroma (103) and the mature proteins are then released and folded (76). A stromal HSP70 has also been shown to participate in uptake of preproteins into the chloroplast (219). Previous work in Dr. Rochon's lab has shown that approximately 1-5% of the total CNV CP present in a cell during infection of *Nicotiana benthamiana* is found within chloroplasts (220). The N-terminus of the CP is cleaved near the R/arm junction to yield a protein (34.7 kDa) which is functionally equivalent to a chloroplast

preprotein. This chloroplast preprotein is targeted to chloroplasts followed by a second cleavage within the arm to yield a 32.9kDa species that resides in the chloroplast inter membrane space. Once the 32.9 kDa species enters the stroma, it is further cleaved to a 31.1 kDa product (Figure 2.2.1B) (220). It has been postulated that *N. benthamiana* HSP70 family homologs bind the CP preprotein in the cytoplasm and promote its targeting to chloroplasts (220).

Next generation sequence analysis shows that the mRNAs of several isoforms of Hsp70 and Hsc70 are highly induced during CNV infection and that the proteins of one or both isoforms are also strongly induced. I confirmed that HSP70 homologs play a role in CNV RNA accumulation during infection in both *N. benthamiana* and *Chenopodium quinoa*. I also showed that overexpression of cytosolic Hsc70-2 promotes both CP accumulation and virion assembly and that the presence of Hsc70-2 assists in folding of CNV CP *in vitro*. Additionally, downregulation of HSP70 is associated with decreased chloroplast targeting, suggesting the involvement of HSP70 homologs in transport of CNV CP chloroplast.

2.2 Materials and methods

2.2.1 Transcript inoculation

Approximately 1.5 µg (in 110 µl) of T7 polymerase run-off transcripts of an infectious CNV cDNA clone (pK2/M5) was used to inoculate 3-4 leaves of 4-6 week old *N. benthamiana* as previously described (31). Aliquots of transcript reaction mixtures were routinely examined by agarose gel electrophoresis to check the quality and quantity of transcripts produced.

2.2.2 SDS-PAGE and Western blot analysis

Total leaf protein (TLP) samples were obtained by grinding leaf tissue to a fine powder in liquid nitrogen and mixing 100 mg with 350 µl of 1.4X LDS protein denaturation buffer with sample reducing agent according to the manufacturer's recommended protocol (NuPAGE, Thermo Fisher Scientific). TLP containing sample reducing agent was electrophoresed through NuPAGE 4-12% Bis-Tris gels (Thermo Fisher Scientific), blotted onto polyvinylidine difluoride (PVDF) membranes (Bio-Rad) and probed with either a monoclonal antibody that detects both Hsc70 and Hsp70 (ADI-SPA-820-F, 1mg/ml, Enzo Life Sciences) (referred to as HSP70 antibody hereafter) or a rabbit polyclonal antibody specific to bacterially expressed CNV CP S and P domain sequences (SP antibody). Antigen-antibody complexes were detected with peroxidase labelled goat anti-mouse or anti-rabbit antibodies as appropriate (Sigma-Aldrich).

2.2.3 SYPRO Ruby and Ponceau S staining

TLP samples were subjected to NuPAGE (Thermo Fisher Scientific) followed by staining with SYPRO Ruby protein gel stain (Thermo Fisher Scientific) as recommended by the manufacturer's protocol. Ponceau S staining of PVDF membranes was conducted by immersing blots in staining solution [0.2% Ponceau S (Sigma-Aldrich), 0.5% glacial acetic acid] for 2-3 h followed by several successive washes with distilled water. Ribulose-1,5-bisphosphate carboxylase/oxygenase (Rubisco) was used as the control to standardize the mass of total protein loaded onto the gel.

2.2.4 Transcriptome analysis by next generation sequencing (NGS)

Two to three leaves on 2-3 *N. benthamiana* plants (4-6 weeks old) were inoculated with infectious CNV transcripts as described above. For mock inoculations, plants of the same age and leaves at identical developmental stages were rubbed with 10 mM sodium phosphate buffer, pH 7.0 following dusting of leaves with abrasive carborundum. At 3 dpi, both mock and CNV infected leaf tissue were collected and ground to a fine powder in liquid nitrogen. Total leaf RNA (TLR) was extracted from 100 mg of ground material using the RNeasy Plant Mini Kit (Qiagen) according to the manufacturer's instructions which included DNase I on-column treatment, to remove contaminating DNA. rRNA was removed from TLR using an rRNA depletion step (Applied Biological Materials, Cat. No. IR16002) and then subjected to NGS analysis using the Illumina Platform (Applied Biological Materials).

Following quality control analyses and trimming of sequences, reads from CNV infected leaf tissue were mapped to the CNV genomic RNA sequence (NCBI accession number M25270) and unmapped reads were collected. Residual rRNA and tRNA reads from CNV infected and mock infected leaves were mapped to *N. tabacum* cytoplasmic (NCBI accession numbers AF479172 and AJ236016), mitochondrial (NCBI accession number BA000042) and chloroplast rRNAs (NCBI accession number Z00044), as well as the corresponding tRNAs of *Solanum tuberosum* (http://plantrna.ibmp.cnrs.fr) (221). Unmapped reads were collected for further analysis using the CLC Genomics Workbench v7.5. Reads were mapped to the *N. benthamiana* transcriptome (*N. benthamiana* v5 transcriptome, http://sydney.edu.au/science/molecular_bioscience/sites/benthamiana/) (222). Approximately 10 million and two million reads were obtained from mock and CNV infected leaves respectively.

Sequences that mapped to the *N. benthamiana* transcriptome were identified based on the annotations in the downloaded *N. benthamiana* transcriptome. Reads corresponding to *N. benthamiana* genes annotated as "heat shock 70 kDa protein" or "heat shock cognate 70 kDa protein" (all isoforms including those annotated as "probable" or "similar to", excluding mitochondrial or chloroplast isoforms) were compiled. The accuracy of all the annotations was checked by BLAST analysis against the NCBI database and adjusted accordingly. Reads were converted to reads per kilobase per million (RPKM) and a heat map from the $\log_2$ transformed values was constructed for visualization of data. Parameters used for creating the heat map, using the CLC Genomics Workbench v7.5, utilizing the hierarchical clustering feature under the clustering tool, were as follows: Euclidean distance was selected as a measure of the distance and average linkage was selected as a cluster-linkage criterion.

2.2.5 Heat shock of *Chenopodium quinoa*

Chenopodium quinoa (a CNV local lesion host) plants of identical age were heat-shocked (HS) at 48℃ for 30 min and allowed to recover for 2 h at 26℃ as described for HS treatment of *Arabidopsis thaliana* (223). Untreated plants of the same age were kept at 26℃. After recovery, leaves at comparable positions in heat-treated or untreated plants were rubbed with carborundum and then immediately inoculated with 4 ng of CNV particles (10 ul). Four to six leaves per plant were inoculated and 2-3 plants were used per treatment. Samples were collected at time points indicated in the figure legend (Figure 2.4).

For local lesion assays, 10 ul of CNV particles (0.004 ng/ul) were used to inoculate heat-shocked and untreated plants of identical age. Comparable leaves with respect to developmental position on the plant (12-20 leaves per treatment) were analyzed for the size of lesions using ImageJ software (http://imagej.nih.gov/ij/) at 7 dpi. Photographs were taken at 7 dpi (Nikon Camera Control Pro 2 version 2.14.0). GraphPad software was used to evaluate statistical differences between the size of local lesions in heat-shocked and untreated plants using a Student's t-test. Probability values (*p*) less than 0.05 were considered as indicating statistically significant differences.

2.2.6 Production and purification of CNV VLPs

N. benthamiana plants were agroinfiltrated with pCNVCPpBin(+) which is a binary vector that expresses the CNV CP, as described previously (135). Agroinfiltration was performed in the presence of pNbHsc70-2/pBin(+) which encodes *N. benthamiana* Hsc70-2 (see below) or pGFP/pBin(+) which expresses GFP as a control. I also included pTBSVp19/pBin(+) to express the silencing suppressor TBSV p19 (224) to increase protein levels in co-agroinfiltrated plants. The OD_{600nm} of cultures used for agroinfiltration was 1.0 for each construct. VLPs were purified from approximately 5 to 10 g of tissue using a previously described protocol (21, 225) with some modifications. Agroinfiltrated leaf material was ground in liquid nitrogen and added to at least 5 volumes of 100 mM NaOAc pH 5.0 containing 20 mM β-mercaptoethanol. The slurry was gently rotated at 4°C for at least 1 h and then spun at 8000 x g for 15 min at 4°C to remove plant debris. The supernatant was passed through twolayers of Miracloth (Calbiochem) and the solution was adjusted to 8% polyethylene glycol (PEG8000, Sigma-Aldrich) and incubated for at

least 2 h at 4°C with constant stirring. The virus was pelleted at 10,000 x g for 20 min at 4°C then resuspended in 300-600 µl of 10 mM NaOAc, pH 5.0, depending on size of the pellet. The virus was subjected to constant rotation at 4°C overnight, and then centrifuged again at 15,000 x g for 20 min at 4°C. The supernatant (containing virions) was collected and stored at 4°C until further use.

2.2.7 Virus purification

A miniprep procedure was employed to purify CNV particles (225) for comparative studies in Hsp70 or Hsc70 upregulation and downregulation experiments. Virus concentration was determined by co-electrophoresis of virus particles with highly purified CNV particles of known concentration extracted by a differential centrifugation technique as described previously (30). The concentration of the highly purified virus particles was determined spectrophotometrically (absorbance at 260 nm of a 1 mg/ml suspension of CNV is 4.5).

2.2.8 Agarose gel electrophoresis of purified particles

Virus particles were electrophoresed through 1% (w/v) agarose gels in TB buffer (45 mM Tris, 45 mM borate, pH 8.3) as described previously (30). Virions were stained with ethidium bromide (EtBr) in the presence of TB buffer containing 1 mM EDTA and photographed under ultraviolet illumination (Gel Doc, Alpha Innotech Corporation) (59). Electrophoresis of VLPs was conducted by using 2% (w/v) agarose gels in TB buffer for 2 h as described previously (21) followed by ethidium bromide and SYPRO Ruby staining to visualize ribonucleoprotein

complexes. Known concentrations of CNV particles (as determined by spectrophotometry, see above) were used as mass standards.

2.2.9 TLR extraction and electrophoresis

Two to three leaves from two plants were ground in liquid nitrogen to a fine powder and 100 mg was used for RNA extraction using phenol/chloroform as described previously (202). RNA to be used for droplet digital PCR (ddPCR) was purified as described above using an RNeasy Plant Mini Kit which included DNase I treatment. RNA was analyzed by electrophoresis through 1% agarose gels buffered in 0.5 X TBE (45 mM Tris, 45 mM boric acid, 1 mM EDTA, pH 8.0) and visualized by staining with EtBr as previously described (30).

2.2.10 ddPCR

Reverse transcription polymerase chain reaction (RT-PCR) was conducted using 250 ng of purified total leaf RNA using Superscript III enzyme (Thermo Fisher Scientific). Gene specific reverse primers (see Table 2.1) for either CNV RNA (NCBI accession number M25270) i.e. CNV386R corresponding to the reverse complement of CNV nts 924-945 or *N. tabacum* cytoplasmic 18S rRNA (NCBI accession number AJ236016) i.e. 18S1R corresponding to the reverse complement of nts 1652-1673 were used in the reverse transcription reaction according to the manufacture's recommended conditions. A combination of primers CNV387F, corresponding to CNV nts 749-769, and CNV388R corresponding to the reverse complement of CNV nts 846-868 was used to amplify CNV cDNA. 18S rRNA primers, 18S2F corresponding to

nts 924-945 and 18S3R corresponding to the reverse complement of nts 1117-1135 were used to amplify 18S rRNA cDNA. A pilot experiment was conducted to determine the optimal conditions for quantitative assessment of CNV RNA and 18S rRNA levels. ddPCR was conducted and the data were analyzed according to the manufacturer's (Bio-Rad, QX200^{TM} ddPCR^{TM}) protocol.

2.2.11 Cloning of pNbHsc70-2 cDNA and construction of pNbHsc70-2/pBin(+) and pNbHsc70-2/GFP/pBin(+)

cDNA clones of the complete coding region of *N. benthamiana* Hsc70-2 RNA were produced using Gibson assembly (226). Four to six week old *N. benthamiana* plants were heat-shocked at 42℃ for2h as described (205) and TLR was extracted using the RNeasy Plant Mini Kit. First strand cDNA synthesis was conducted using the reverse primer GA2R (see Table 2.1) which corresponds to the 3' terminal region of *N. tabacum* Hsp70 ORF (NCBI accession number AY253326) according to the manufacturer's recommended conditions (Thermoscript, Thermo Fisher Scientific). The underlined region represents the overlapping region complementary to the intermediate cloning vector pBBI525 and the remaining sequences correspond to the complement of the 3' terminal 23 nts of the *N. tabacum* Hsp70 ORF including the stop codon (shown in italics, Table 2.1).

Hsp70 cDNA was amplified using a degenerate forward primer, GA1F, and GA2R as reverse primer. GA1F contains pBBI525 overhangs (indicated as underlined) and includes an ATG initiator codon (shown in bold as well as italics, Table 2.1). The degenerate primer was designed based on an alignment of *N. tabacum* Hsp70 sequences (NCBI accession numbers AY253326,

AB689673 and AY372071) and *Solanum lycopersicum* Hsp70 (NCBI accession number FR828679). (It is noted that although the *N. tabacum* genes were indicated as being Hsp70 in the NCBI data base, subsequent BLAST searches showed that they are more closely related to Hsc70).

pBBI525 was amplified using primer pBBI525F corresponding to nts 800-820 and primer pBBI525R which corresponds to the reverse complement of pBBI525 nts 776-797. Gibson assembly of the amplified Hsp70 cDNA and pBBI525 fragments was conducted using the Gibson Assembly Cloning Kit (New England Biolabs) as per the manufacture's recommendations. The Hsp70 region of the resulting clone pNbHsp70/pBBI525 was sequenced and found to be 99% identical to *N. benthamiana* Hsc70-2 (Nbv5tr6412958) (the sequence is available through the University of Sydney *N. benthamiana* database; http://sydney.edu.au/science/molecular_bioscience/sites/benthamiana/index.php) (referred to as NbHsc70-2, see Appendix A.2 for complete nucleotide sequence of the clone). The resulting construct, pNbHsc70-2/pBBI525, was digested with SmaI, HindIII and BglI and the 2.9 kb fragment, containing the duplicate 35S promoter, the Hsc70-2 insert and the NOS terminator, was cloned into SmaI, HindIII digested pBin(+). The sequenced pNbHsc70-2/pBin(+) construct was transformed into *Agrobacterium tumefaciens* strain GV3101/c58c1 (PMP90) and used for agroinfiltration of *N. benthamiana* leaves as described below.

The Hsc70-2 GFP fusion construct, pNbHsc70-2/GFP/pBin(+) was constructed by Gibson assembly technology by performing PCR on pNbHsc70-2/pBBI525 using the forward primer GA11F and the reverse primer GA12R (see Table 2.1). The GFP ORF was amplified from an

existing plasmid using the forward primer GA13F and reverse primer GA14R. The Gibson assembly reaction of the resulting fragments was conducted as per the manufacture's recommendations. After confirmation by sequencing, the resulting clone pNbHsc70-2/GFP/pBBI525 was digested with SmaI, HindIII and BglI. The 3.3 kb fragment containing the duplicate 35S promoter, the Hsc70-2/GFP insert and the NOS terminator, was cloned into SmaI and HindIII digested pBin(+). The sequenced pNbHsc70-2/GFP/pBin(+) construct was transformed into *A. tumefaciens* strain GV3101/c58c1 (PMP90) and used for agroinfiltration of *N. benthamiana* leaves as described below.

2.2.12 Cloning and purification of bacterially expressed *N. benthamiana* Hsc70-2 [pNbHsc70-2/His_7/pET24D(+)]

N. benthamiana Hsc70-2 was cloned into a bacterial expression vector pET24D(+) (Novagen) with 7X His tags at the C-terminus (NbHsc70-2/His_7) using the Gibson assembly cloning strategy. pET24D(+) was amplified using the forward primer GA15F, corresponding to pET24D(+) nts 168 to 203 and the reverse primer GA16R corresponding to pET24D(+) nucleotides 43 to 87 (see Table 2.1). Hsc70-2 was amplified from pHsc70-2/pBBI525 with pET24D(+) overhangs using the forward primer GA17F and the reverse primer GA18R.

After confirmation of the clone through sequencing, the DNA was transformed into *E.coli* BL21 RIL cells (Thermo Fisher Scientific). Isopropylthio-β-galactoside (IPTG) (Thermo Fisher Scientific) (1 mM) was used to induce 500 ml of log phase (OD_{600nm} = 0.6-0.8) bacterial culture. NbHsc70-2/His_7 was purified under denaturing conditions from the total (soluble and insoluble) lysate using TALON Superflow metal affinity resin (Clontech) using methods recommended by

the manufacturer. The purified recombinant protein was concentrated using 2 ml centrifuge filters (Amicon) with a 50 kDa nominal molecular weight limit Centricon filter (Millipore) and quantified by running several dilutions on a SDS-PAGE using bovine Hsc70/Hsp73 (ADI-SPP-751-D, Enzo Life Sciences) (referred to as bovine Hsc70) as mass standards. The purified protein was stored at 4℃ in the presence of 1X cOmplete™ EDTA-free Protease Inhibitor (Roche).

2.2.13 Agroinfiltration

For transient gene expression in *N. benthamiana*, agroinfiltration was performed as described previously (220).

2.2.14 *In vitro* CP solubilisation assay

100 µg of purified CNV particles were dissociated in 300 µl disassembly buffer [5.4 M guanidine-HCl, 270 mM NaCl, 45 mM $NaPO_4$, pH 7.0] containing 80 units of RNaseOut (Thermo Fisher Scientific), 1 mM DTT and 1X cOmplete™ EDTA-free Protease Inhibitor (Roche). The reaction was incubated at room temperature (RT) for 30 min then placed into a 3.5 kDa molecular weight cut off dialysis cassette (Thermo Fisher Scientific). A step-wise dialysis was performed against guanidine-HCl at concentration of 4 M, 3 M and 2 M each in buffer A (50 mM $NaPO_4$, 300 mM NaCl, pH 7.0) for at least 1 h at 4℃.

Solution was removed from the dialysis bag and mixed with either 100 ul (200 ug) of purified NbHsc70-2/His_7 in buffer A or 100 ul (200 ug) Bovine serum albumin (BSA) in buffer A or with

100 µl of buffer A only. The mixtures were then transferred to another dialysis cassette and dialyzed against successively against 1 M, 0.5 M and 0 M guanidine-HCl in Hsc70-2 binding buffer (10 mM Tris-HCl, pH 7.0, 5 mM $MgCl_2$, 5 mM $CaCl_2$, 50 mM KCl, 1 mM DTT, and 1 mM ATP) containing 1X cOmplete™ EDTA-free Protease Inhibitor at least for 1 h. A further dialysis was performed for 2 h at 4℃ as described above in the Hsc70-2 binding buffer.

The solution was then taken out of the dialysis bags and allowed to stand overnight at 4℃. The solutions were removed and equal aliquots of each mixture were centrifuged at 10,000 x g for 2 min at 4℃. The supernatant was saved and adjusted to 1X LDS buffer and the pellet was resuspended in 1X LDS/6 M urea in a volume equivalent to that of the supernatant. For analysis, equal volumes of the pellets and supernatants were subjected to Western blot analysis using the CNV antibody SP.

2.2.15 Quercetin treatment

A 100 mM quercetin (Sigma-Aldrich) stock solution was prepared in 100% DMSO (17). Four to six week old *N. benthamiana* plants were infiltrated with a 1 mM solution of quercetin (diluted from the stock solution in 10 mM sodium carbonate buffer, (Na_2CO_3) pH 9.6. Plants were mock infiltrated with an equivalent amount of DMSO (1%) in 10 mM Na_2CO_3 buffer, pH 9.6. At 10 min post-infiltration, the leaves were patted dry, dusted with carborundum and inoculated with 5 ng of WT CNV particles in 25 mM KPO_4 buffer, pH 6.8.

2.2.16 Co-immunoprecipitation

Protein G Sepharose beads (Protein G Sepharose 4 Fast Flow, GE Healthcare) were bound to CNV polyclonal or prebleed antiserum and cross-linked by incubating the beads with 1X PBS containing 0.05% glutaraldehyde (Sigma-Aldrich) for 2 h at RT. The beads were washed free of non-cross-linked IgG using 0.1 M glycine, pH 2.7. Beads were washed immediately; once with 10 mM Tris HCl, pH 9.0 and twice with 20 mM $NaPO_4$, pH 7.0. The antibody conjugated resin was stored at 4℃ overnight.

Four to six week old *N. benthamiana* plants were co-agroinfiltrated either with pCNVCPpBin(+) plus pTBSVp19/pBin(+) or empty vector (EV) plus pTBSVp19/pBin(+). Atfour days post agroinfiltration (dpai), approximately 8-10 g of leaf material was collected and homogenized in 1X homogenization buffer [(50 mM HEPES, 75 mM NaCl, 10 mM EDTA, 5 mM DTT, pH 7.3 and 1X EDTA-free cOmplete™ Protease Inhibitor Cocktail (Roche)]. The homogenate was filtered through two layers of Miracloth and two layers of cheese cloth. The filtrate was incubated with antibody conjugated beads (as described above) in 1X homogenization buffer containing 0.1% Triton X100 for 1 h at 4℃. The beads were washed 7X times with wash buffer [50 mM HEPES, 125 mM NaCl, 10 mM EDTA, 5 mM DTT, pH 7.3 and 1X EDTA-free cOmplete™ Protease Inhibitor Cocktail (Roche)] before elution with 1 ml of hot protein denaturation buffer (1X LDS at 70℃, Thermo Fisher Scientific). Equal volumes of eluent from CNV polyclonal antibody bound beads from both samples were analyzed by Western blot analysis using HSP70 antibody.

2.2.17 Mass spectrometry

Co-immunoprecipitated samples were analyzed by mass spectrometry using the University of British Columbia's Center for High-Throughput Biology. Formaldehyde isotopologues were used to differentially label the control sample [EV and pTBSVp19/pBin(+)] and the experimental sample [pCNVCPpBin(+) and pTBSV p19/pBin(+)]. Equal volumes of the differentially labelled control and experimental samples were pooled and electrophoresed into an SDS PAGE for 4 mm and the single unresolved band was excised from the gel and digested with trypsin followed by liquid chromatography-tandem mass spectrometry (LC-MS/MS) analysis. Predicted peptides were blasted against the SWISS-PROT database (http://web.expasy.org/docs/swiss-prot_guideline.html).

2.2.18 Confocal microscopy

Four to six week old *N. benthamiana* plants were co-agroinfiltrated with pNbHsc70-2/GFP/pBin(+) and pTBSVp19/pBin(+) or with pGFP/pBin(+) and pTBSVp19/pBin(+) using cultures adjusted to OD_{600nm} =1.0. Leaf samples were analyzed at 3 dpai using a Leica TCS SP2-AOBS microscope as described previously (32).

2.2.19 Temperature sensitivity assay

CNV virions (600 ng) were incubated with Hsc70 binding buffer [10 mM Tris-HCl, pH 7.5, 50 mM potassium chloride (KCl), 5 mM magnesium chloride ($MgCl_2$), 1mM dithiothreitol (DTT), 1

mM adenosine triphosphate (ATP)], BSA or NbHsc70-2/His_7 in binding buffer in the presence of 1X cOmplete EDTA-free protease inhibitor as previously established for Hsc70 (227, 228) with some modifications. The mixture was incubated at 25℃. After a 3.5 h incubation period, the reaction mixture was subjected to increasing temperatures (25°C-75°C) for 30 min followed by agarose gel electrophoresis through a 1% agarose gel buffered in TB for 1 h. The gel was stained with EtBr to stain virion RNA.

Table 2.1: Oligonucleotides used for RT-PCR, PCR and ddPCR

Primer name[a]	Sequence from 5' to 3' direction[b]	Description of use[c]
CNV386R	ATGACATCCCTGTCAACATACC	3' primer used in the FS cDNA synthesis of CNV gRNA
CNV387F	ACTGGCAGTAGGATGACAAAG	5' primer to amplify p33 region of CNV gRNA in combination with CNV388R
CNV388R	CTCAGGAGTGTTCTTCAGGTAAC	3' primer to amplify p33 region of CNV gRNA in combination with CNV387F
18S1R	CGGATCATTCAATCGGTAGGAG	3' primer used in the FS cDNA synthesis of 18S rRNA
18S2F	GAAAGACGAACAACTGCGAAAG	5' primer to amplify 18S rRNA in combination with 18S3R
18S3R	TTCAGCCTTGCGACCATAC	3' primer to amplify 18S rRNA in combination with 18S2F
GA1F	CTTTCAAATACTTCCACC***ATG***GCM(A,C)GGAAAAGGW(A,T)GAAGGW(A,T)CC	5' primer to amplify *N. benthamiana* Hsc70-2 ORF in combination with GA2R
GA2R	ACGATCGGGGATCCGTCTAGA*TTA*GTCGACCTCCTCAATCTTGG	3' primer to amplify *N. benthamiana* Hsc70-2 ORF in combination with GA 1-F. Also used as the 3' primer in the FS cDNA synthesis of Hsc70-2
pBBI525F	TCTAGACGGATCCCCGATCGT	5' primer to amplify pBBI525 in combination with pBBI525R
pBBI525R	CCATGGTGGAAGTATTTGAAAG	3' primer to amplify pBBI525 in combination with pBBI525F
GA11F	*TAA*TCTAGACGGATCCCCGATCG3	5' primer to amplify Hsc70-2/pBBI525 in combination with GA12R
GA12R	GTCGACCTCCTCAATCTTGGGACC3	3' primer to amplify Hsc70-2/pBBI525 in combination with GA11F
GA13F	GTGCAGGTCCCAAGATTGAGGAGGTCGACGTGAGCAAG	5' primer to amplify GFP ORF in combination with GA14R
GA14R	CGATCGGGGATCCGTCTAGATTACTTGTACAGCTCGTCC	3' primer to amplify GFP ORF in combination with GA13F
GA15F	CACCACCACCACCACCACTGAGATCCGGCTGCTAAC	5' primer to amplify pET24D(+) in combination with GA16R
GA16R	GGTATATCTCCTTCTTAAAGTTAAACAAAATTATTTCTAGAGGGG	3' primer to amplify pET24D(+) in combination with GA15F
GA17F	GTTTAACTTTAAGAAGGAGATATACC***ATG***GCAGGAAAAGGAGAAGGTCC	5' primer to amplify Hsc70-2 in combination with GA18R
GA18R	GGATCTCAGTGGTGGTGGTGGTGGTCGACCTCCTC	3' primer to amplify Hsc70-2 in combination with GA17F

[a] F= forward primer, R=reverse primer.

[b] = bold italicized sequence (ATG) represent the start codon; normal italicized sequence (TAA) represent the stop codon; underlined sequences represent the overlapping regions to amplify the insert using the Gibson assembly method.

[c] FS= first strand cDNA.

2.3 Results

2.3.1 Heat shock protein 70 (HSP70) family proteins are induced during CNV infection

Since Hsp70 and Hsc70 family proteins have been found to have important roles in many different aspects of the infection cycle of several animal and plant viruses (56), I wished to investigate if plant HSP70 family homologs play a role in CNV infection. To initiate these studies, I conducted Western blot analysis using an antibody that binds both Hsp70 and Hsc70 (HSP70 antibody). CNV inoculated *N. benthamiana* leaves (4-6 leaves) were collected daily from 1-6 dpi along with systemically infected leaves at 6 dpi and equal volumes of total leaf protein were blotted and probed with HSP70 antibody. HSP70 protein levels were found to increase significantly during the course of CNV infection in *N. benthamiana* (Figure 2.2), where an approximate 10 fold increase occurred over the six day time period analyzed.

However, due to the nature of the antibody, which binds both Hsp70 and Hsc70 homologous, I was unable to conclude which isoform was induced. It is to be noted here that the increase in HSP70 protein level parallels the increase in CNV CP (Figure 2.2, compare first panel with the middle panel). However induction of HSP70 was not specific to expression of CP or to any other particular viral protein (S.B. Alam, unpublished observations).

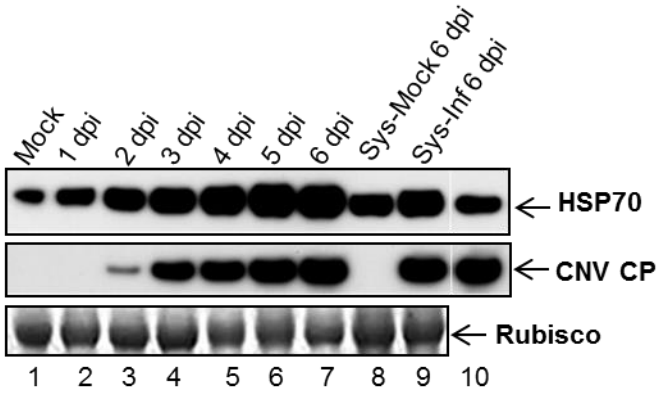

Figure 2.2: HSP70 is induced during CNV infection.

Western blot analysis of *N. benthamiana* plants infected with CNV. *N. benthamiana* plants were either mock inoculated or inoculated with CNV transcripts and infection was allowed to proceed for six days. Three leaves each from two inoculated plants were collected daily from 1-6 dpi and ground in liquid nitrogen. Samples of systemically infected leaves (Sys-Inf) along with the corresponding leaves from a mock inoculated plant (Sys-Mock) at 6 dpi were also removed and ground in liquid nitrogen. One hundred mg of ground material was then added to 350 µl of 1.4X LDS protein denaturation buffer. Equal volumes were loaded onto duplicate NuPAGE gels and following electrophoresis, the gels were blotted. An antibody that reacts to both Hsc70 and Hsp70 (HSP70 antibody) was used in the upper blot and a CNV CP antibody (SP) was used in the lower blot. Bovine Hsc70 was used as a positive control in the upper blot (lane 10) and CNV CP as a control in the lower blot (lane 10) as indicated. The bottom panel is the Ponceau S stained blot showing Rubisco as a loading control. The experiment was conducted three times and representative results are shown.

2.3.2 Both Hsp70 and Hsc70 mRNA levels increase during CNV infection

To assess which isoform of the HSP70 family is induced during CNV infection, I performed next generation sequence analyses on mock and CNV infected TLR obtained from leaves at 3 dpi and mapped the reads to the *N. benthamiana* transcriptome. Reads specific to Hsp70 and Hsc70 homologs were compiled and $\log_2$ transformed RPKM values were utilized for constructing a heat map to analyze differential expression of HSP70 family genes in CNV compared to mock inoculated samples.

It can be seen in the heat map in Figure 2.3A that several different Hsc70 and Hsp70 isoforms are induced in CNV infected plants compared to mock inoculated plants. To examine the level of induction, the ratio of the RPKM value of HSP70 homolog mRNAs in CNV infected plants versus mock inoculated plants was determined and the ranked values are shown in Appendix A.1 and summarized in Figure 2.3B. It is noted that some of the isoforms are strongly induced (≥ 100 fold), some are moderately induced (>4.5-100 fold) while others are only mildly induced (< 4.5 fold). The most highly induced homologs include Hsc70, Hsc-70-1, Hsc70-2, Hsp70 and Hsp70-5. The moderately induced group mainly consists of Hsc70-2, Hsp70, Hsp70-15, Hsp70-8 and Hsp70-18 isoforms. Those that are more mildly induced include mainly Hsp70-16, Hsp70-17 and Hsp70-15 which as stated above also has isoforms that falls into the moderately induced group (For details see Appendix A.1). Figure 2.3C shows a tabular representation of different Hsp70 and Hsc70 isoforms which are maximally induced (>1000 fold) during CNV infection. The most predominantly induced isoforms are Hsc70 followed by Hsc70-5 (~4,000-5,500 fold induction) and then mostly Hsp70 and Hsp70-5 (~1,000-4,000 fold induction) (for details see Appendix A.1).

HSP70 family homologs have been previously shown to be induced by several animal and plant viruses (208, 209, 214, 229, 230). But, it is interesting that Hsc70 is strongly induced as it is generally believed that Hsp70 is the major inducible isoform. However, cases where Hsc70 can be induced such as from heat shock, ethanol treatment, virus infection or pesticide toxicity have been described but such cases are not prominent in the literature (80, 214, 231-233). Hsc70 isoforms have been found to be induced during *Baculovirus* infection but only very modestly (234). Hsc70 is induced in *White spot syndrome virus* infection as high as 40 fold and has been suggested to assist in the prevention of apoptosis induced by virus infection (235). Infection of *Pseudomonas syringae pv. tomato DC3000* on *A. thaliana* leads to an induction of Hsc70-2 and Hsc70-4 isoforms (236). In the case of *Turnip mosaic virus* (TuMV) and TCV it has been suggested that the induction of Hsc70 may be related to a process analogous to the unfolded protein response in reaction to the high level of protein that accumulates during virus infection (214).

From the results shown above, I postulated that CNV may have evolved to co-opt the induced Hsp70 or Hsc70 isoforms for one or more aspects of its multiplication cycle such as replication, CP accumulation, chloroplast targeting or particle assembly during infection.

B

Induction level	CNV to mock ratio	Major HSP70 isoform
Strong	≥ 100 fold	Hsc70, Hsp70-5, Hsp70, Hsc70-1, Hsc70-2
Moderate	> 4.5-100	Hsc70-2, Hsp70, Hsp70-15, Hsp70-8, Hsp70-18
Mild	< 4.5 fold	Hsp70-15, Hsp70-16, Hsp70-17

C

HSP70 homolog transcript ID	Description	CNV infected expression values (RPKM)	Mock expression values (RPKM)	CNV to mock ratio
Nbv5tr6313114	Heat shock cognate 70 kDa protein (similar to)	218.0	0.04	5491.0
Nbv5tr6313115	Heat shock cognate 70 kDa protein (similar to)	183.4	0.04	4293.1
Nbv5tr6237742	Heat shock cognate 70 kDa protein (similar to)	270.9	0.07	4049.9
Nbv5tr6262864	Heat shock 70 kDa protein 5 (probable)	192.6	0.05	4018.7
Nbv5tr6217195	Heat shock 70 kDa protein (probable)	44.4	0.01	3526.5
Nbv5tr6340970	Heat shock cognate 70 kDa protein (similar to)	203.9	0.06	3275.0
Nbv5tr6248470	Heat shock 70 kDa protein (probable)	113.4	0.04	2913.9
Nbv5tr6274820	Heat shock 70 kDa protein 5 (probable)	95.8	0.03	2740.5
Nbv5tr6411059	Heat shock 70 kDa protein 5 (probable)	49.0	0.02	2658.9
Nbv5tr6263838	Heat shock 70 kDa protein (probable)	59.3	0.03	2269.4
Nbv5tr6343294	Heat shock 70 kDa protein (probable)	25.9	0.01	1931.2
Nbv5tr6239778	Heat shock 70 kDa protein 5 (probable)	113.1	0.07	1548.0
Nbv5tr6263036	Heat shock 70 kDa protein (probable)	75.9	0.05	1534.7
Nbv5tr6315459	Heat shock 70 kDa protein (probable)	47.4	0.03	1483.4
Nbv5tr6228252	Heat shock 70 kDa protein (probable)	293.5	0.23	1286.9
Nbv5tr6240566	Heat shock 70 kDa protein (probable)	76.6	0.07	1174.0

Figure 2.3: Hsc70 and Hsp70 mRNA isoforms are highly induced during CNV infection.

(A) Heat map corresponding to HSP70 mRNA homologs differentially expressed in mock inoculated versus CNV infected plants at 3 dpi. The reads per kilobase per million (RPKM) values for individual transcripts were determined and the heat map was constructed from the $\log_2$ transformed RPKM values. RPKM values that were 0 were converted to 0.001 in order to obtain $\log_2$ values. (B) Tabular summary of different isoforms of Hsc70 and Hsp70 that are induced at

different levels based on original RPKM expression values. (C) Tabular representation of different Hsc70 and Hsp70 isoforms that are induced greater than 1000 fold. The level of induction in B and C was measured by dividing the RPKM values obtained for a given transcript ID in CNV infected leaves by that obtained in mock inoculated leaves. Appendix A.1 shows the RPKM values for all identified HSP70 homologs along with the level of induction. Note thatfour of the HSP70 homolog transcript IDs have RPKM values that equal zero and therefore the level of induction could not be calculated with certainty. These data were therefore omitted from B and C.

2.3.3 Increased levels of Hsp70 and/or Hsc70 in CNV infected plants is associated with enhanced CNV gRNA, CP and virion accumulation

To determine if increased levels of Hsp70 enhance CNV accumulation I heat-shocked the CNV local lesion host *C. quinoa* for 30 min at 48℃ and then allowed plants to recover 2 h prior to CNV inoculation. I confirmed that Hsp70 is significantly induced 2 h post heat shock treatment and remains at elevated levels for at least three days (Figure 2.4A, lanes 5-8). To assess if CNV multiplication is increased in plants containing elevated levels of Hsp70 I inoculated both heat-shocked and untreated plants with CNV, 2 h post treatment and analyzed leaf samples for the levels of viral gRNA at 3 dpi. Figure 2.4B, panel i, lane 2, shows that total leaf RNA of heat-shocked plants contained CNV gRNA as determined by agarose gel electrophoresis and EtBr staining, whereas untreated plants contained little or no detectable CNV gRNA (Figure 2.4B, panel i, lane 1). This observation is consistent with the notion that Hsp70 increases the ability of CNV to replicate in plants as has been shown previously (17, 40). Enhanced gRNA accumulation was further confirmed and quantified using ddPCR (Figure 2.4B, panel ii), where I found that heat-shocked plants accumulated approximately five fold more CNV gRNA than untreated plants.

Furthermore, CP levels in total leaf protein extracts as determined by Western blot analysis of equal volumes of denatured protein from equal masses of tissue showed that heat-shocked plants contained significantly higher levels of CNV CP than untreated plants (Figure 2.4C, compare lanes 2 and 1, respectively).

Virion accumulation was also greater in heat-shocked versus untreated plants as determined by agarose gel electrophoresis of equal volumes of virions isolated from equal masses of infected leaf tissue (Figure 2.4D, compare lanes 2 and 1, respectively). The increased levels of CP and virions is consistent with my finding that viral RNA levels are increased in plants with elevated levels of Hsp70. Figure 2.4E confirms that levels of HSP70 are increased in *C. quinoa* plants that were heat-shocked and then inoculated with CNV. It is noted that it has been reported that Hsc70 can also be induced by heat shock treatment (80, 214, 232) so the observed increase in CNV multiplication may also be related to Hsc70 induction.

I also examined the phenotype of lesions produced on heat-shocked *C. quinoa* plants inoculated with CNV versus untreated CNV inoculated plants. It can be seen in Figure 2.4F, panel i that heat-shocked leaves on average contained larger lesions than untreated leaves. At 7 dpi, I measured the size of the lesions and conducted a Student's t-test which showed that lesions formed in heat-shocked plants are significantly larger than those of untreated plants (0.048 mm^2 vs. 0.014 mm^2 on average respectively; $p<0.05$) (Figure 2.4F, panel ii). The increase in diameter of the lesions could reflect increased replication and accumulation of CNV resulting in increased movement. It is also possible that heat-shocked plants support greater cell-to-cell movement of CNV as has been reported previously for other viruses (126, 204, 213). Additionally, heat-shocked plants might display compromised resistance to CNV allowing for increased spread. The larger lesion size could indicate that less apoptosis is occurring in heat-shocked plants resulting in a greater capacity for viral multiplication and spread. For example, Hsp70 induction has been shown to be associated with decreased apoptosis (235, 237-239), however there are a

few reports in the literature that suggest that Hsp70 might positively regulate apoptosis (223, 236, 240, 241). The basis for increased lesion size remains to be determined.

I also heat-shocked *N. benthamiana* plants at 48℃. However, HSP70 levels had actually declined following a 2 hour recovery period. When inoculated plants were examined for levels of viral RNA, CP and virions, little or no increase was observed (S.B. Alam, unpublished observations). I therefore lowered the temperature used for heat shock to 42℃ for 2 h as previously described (205) where I found an approximate two-fold increase in HSP70 levels. However, no consistent increase in the levels of CNV virion RNA, CP or virions was observed likely due to the low level of induction of HSP70 (S.B. Alam, data not shown).

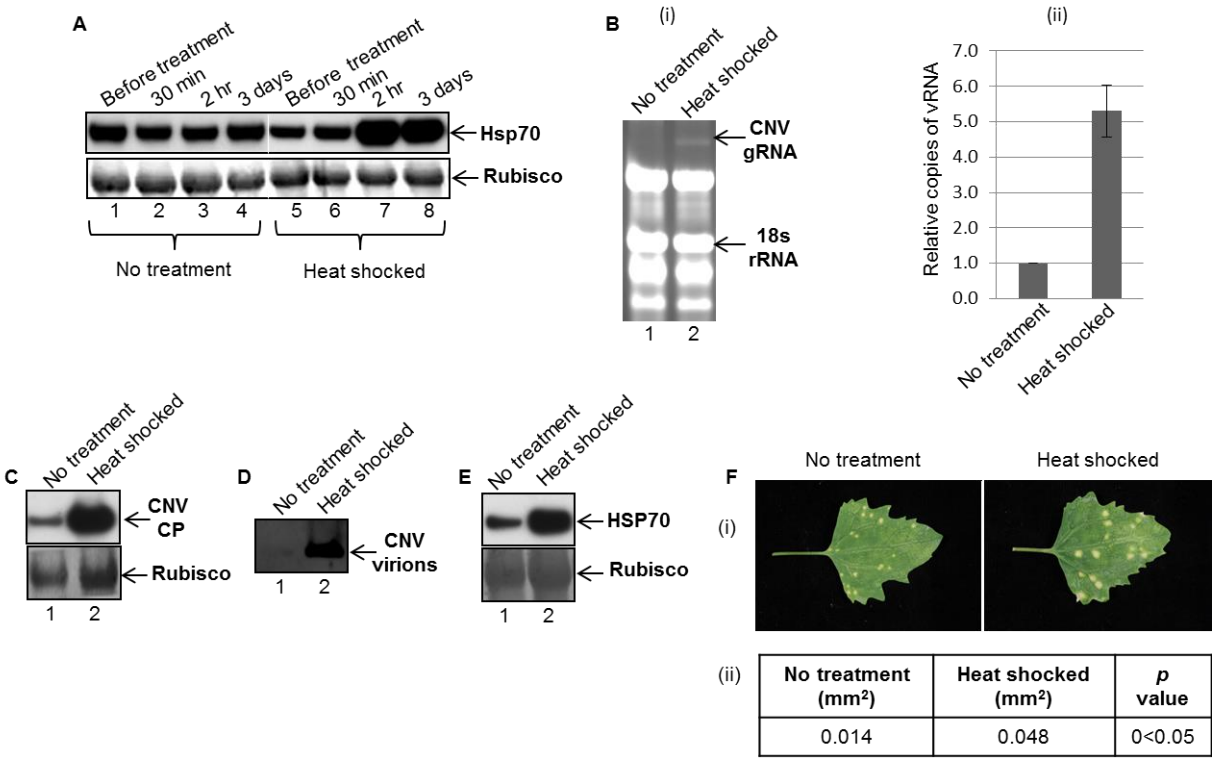

Figure 2.4: Increased levels of Hsp70 and/or Hsc70 in CNV infected plants is associated with enhanced CNV gRNA, CP and virion accumulation.

(A) Western blot analysis showing the levels of Hsp70 in *C. quinoa* either not treated or heat-shocked. Total leaf protein samples were obtained from leaves collected before treatment and at 30 min, 2 h and 3 days post heat shock. Three leaves from two plants were combined and ground to a fine powder with liquid nitrogen and 100 mg of tissue was placed in 350 µl of LDS denaturation buffer. Equal volumes were electrophoresed, blotted and then probed with HSP70 antibody. The blot was stained with Ponceau S and Rubisco was used as loading control. (B, C, D) *C. quinoa* plants were either subjected to no treatment or heat-shocked as indicated and then 2h post treatment each leaf was inoculated with 4 ng of CNV particles. At 3 dpi three leaves from two plants were combined and ground with liquid nitrogen as described above. Total leaf RNA (B) and total leaf protein (C) was obtained from 100 mg of ground tissue and virions (D) were obtained from the remaining tissue. RNA from each treatment was resuspended in an equal volume and equal volumes were electrophoresed through a 1% agarose gel and stained with ethidium bromide [(B) i]. 18S rRNA was used as a loading standard. [(B) ii] The amount of gRNA present in untreated (no treatment) and heat-shocked plants was quantified using ddPCR using primers specific to the CNV p33 ORF and using 18S rRNA as a standard. The relative amounts of CNV gRNA are shown in the bar graph. (C) Total leaf protein was placed in 350 µl of LDS denaturation buffer as described above and equal volumes were electrophoresed, blotted and probed with CNV CP antibody SP. Rubisco was used as a loading standard and the blot was stained with Ponceau S. (D) Virions were resuspended in 40 µl of NaOAc buffer, pH 5.0 at 160 µl/gram of tissue and equal volumes were electrophoresed through a 1% agarose gel and stained with ethidium bromide. (E) Western blot showing the levels of HSP70 at 3 dpi in untreated and heat-shocked CNV inoculated plants using samples prepared as in C. (F) *C. quinoa* plants were

either subjected to no treatment or to heat shock as indicated and 2 hours post treatment leaves were inoculated with CNV using 0.04 ng/leaf. (i) Photographs of inoculated leaves were taken at 7 dpi. (ii) The average area of the lesion was calculated using ImageJ software (http://imagej.nih.gov/ij/) followed by a statistical t-test. All experiments were conducted at least three times and representative results are shown.

2.3.4 Downregulation of Hsp70 or Hsc70 in CNV infected plants is associated with decreased CNV gRNA, CP and virions

To assess the effects of Hsp70 downregulation, I used a commercially available chemical inhibitor quercetin, previously described in the analysis of the role of Hsp70 in TBSV replication (17). As seen for TBSV, I found that quercetin treated *N. benthamiana* plants contained lower levels of CNV gRNA (Figure 2.5A) and that the CP (Figure 2.5B) and virion (Figure 2.5C) levels were also lower.

Since quercetin blocks Hsp70 synthesis only transiently and normal levels of Hsp70 are reached after an initial delay of 3-4 hrs (242), I wished to utilize an additional method for assessing the effect of downregulation of Hsp70 on CNV multiplication. To do this I attempted to clone *N. benthamiana* Hsp70 mRNA using primers designed against *N. tabacum* Hsp70 mRNAs for use in silencing assays. My only resulting clones were derived from Hsc70-2 mRNA. Subsequent to this I found that the Hsp70 cDNA sequences used to design primers actually corresponded to Hsc70-2 sequences due to inadvertent mis-annotation in the NCBI database. I nevertheless proceeded and cloned Hsc70-2 sequence into the *A. tumefaciens* binary vector pBin(+) resulting in the construct pNbHsc70-2/pBin(+) (Figure 2.5D, panel i, upper construct).

To confirm the cytoplasmic localization of the cloned Hsc70-2 sequence, I fused GFP to the pNbHsc70-2/pBin(+) clone at the C-terminus resulting in the clone pNbHsc70-2/GFP/pBin(+) (Figure 2.5D, panel i, lower construct). Four to six week old *N. benthamiana* plants were agroinfiltrated with pNbHsc70-2/GFP/pBin(+) in the presence of TBSV p19 and the leaves were analysed using confocal microscopy. Figure 2.5D, panel ii, part a shows that NbHsc70-2 is

cytoplasmic in nature as indicated by the green fluorescent signal in the cytoplasm surrounding chloroplasts in mesophyll cells. Such results were similar to those observed in pGFP/pBin(+) agroinfiltrated plants (Figure 2.5D, panel ii, part b). Hence it can be concluded that the cloned *N. benthamiana* Hsc70-2 is a cytoplasmic isoform.

I next agroinfiltrated plants with pNbHsc70-2/pBin(+) to silence Hsc70 followed by inoculation with CNV. Figure 2.5E shows a Western blot of equal amounts of total leaf protein from the EV control and pNbHsc70-2/pBin(+) infiltrated, CNV inoculated plants at 3 dpi, probed with HSP70 antibody. It can be seen that no detectable signal was observed indicating that Hsc70 was silenced. Also, since the antibody binds both Hsc70 and Hsp70 and no signal was obtained it is possible that Hsp70 was also silenced in this experiment. I then assessed the levels of CNV gRNA in silenced plants by examining total leaf RNA extracts by agarose gel electrophoresis. It can be seen in Figure 2.5F, that levels of CNV gRNA are strongly reduced in silenced plants compared to the EV control indicating that Hsc70 and/or Hsp70 is required for CNV gRNA accumulation, which is consistent with the previously published report (17) where it was shown using virus-induced gene silencing (VIGs) that Hsp70 downregulation resulted in decreased accumulation of CNV gRNA. Silencing of Hsc70 and/or Hsp70 also resulted in decreased CP levels (Figure 2.5G) as well as decreased virion accumulation (Figure 2.5H) consistent with the decreased gRNA accumulation observed in Figure 2.5F. The results of these experiments are consistent with those using quercetin for downregulation of HSP70 and thus provide further support for the involvement of HSP70 homologs in the enhancement of CNV gRNA accumulation and CP and virion accumulation as described below.

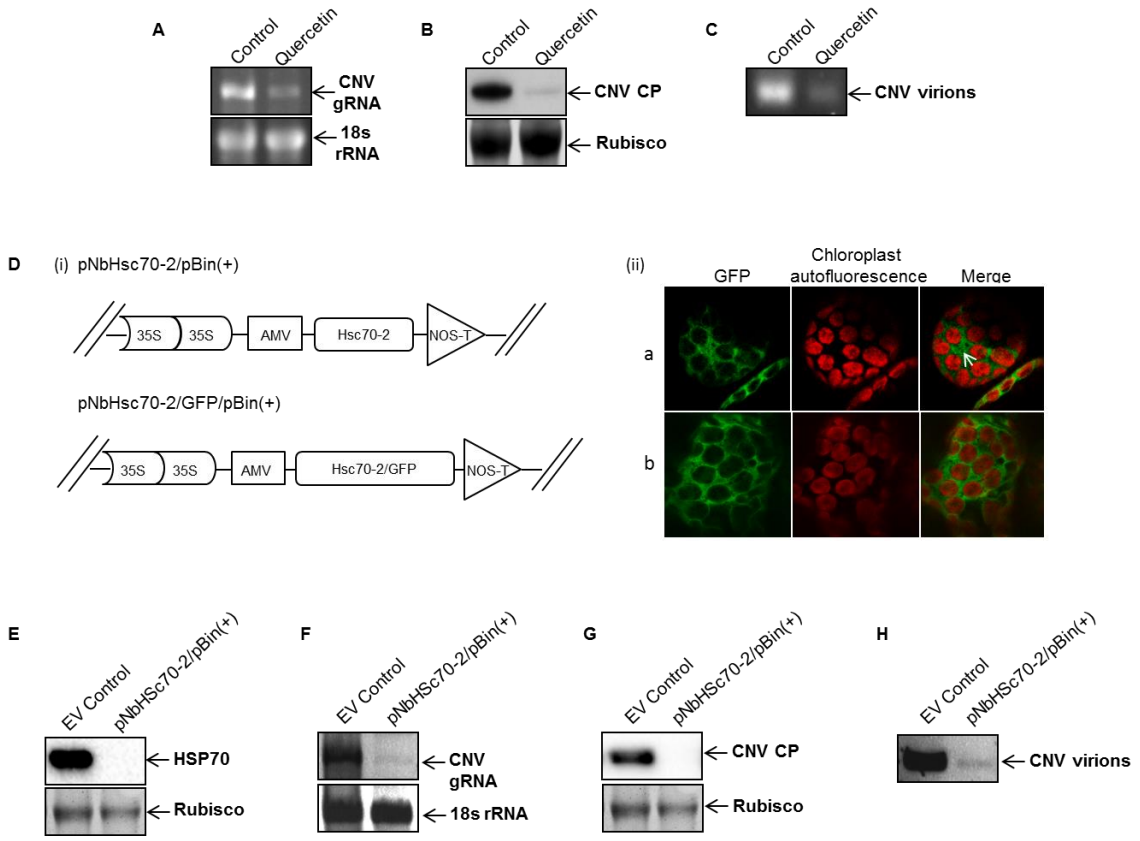

Figure 2.5: Downregulation of Hsp70 or Hsc70-2 in CNV infected plants is associated with decreased CNV gRNA, CP and virions.

Downregulation of Hsp70 using quercetin. (A) RNA, (B) CP and (C) virion accumulation in *N. benthamiana* plants at 3 dpi in which Hsp70 was down-regulated by infiltrating leaves with 1 mM quercetin in 1% DMSO and 10 mM sodium carbonate buffer pH 9.6, for 10 min prior to inoculation. Control plants were infiltrated with 10 mM sodium carbonate buffer containing 1% DMSO. See Figure 2.4 for details on sample preparation and analysis. (D) (i) Schematic representation of pNbHsc70-2/pBin(+) and pNbHSc70-2/GFP/pBin(+). The dual *Cauliflower mosaic virus* 35S promoter is shown, along with the AMV translation enhancer and the nopaline synthase transcription terminator (NOS-T). (ii) (a) *N. benthamiana* plants were agroinfiltrated with pNbHsc70-2/GFP/pBin(+) in the presence of pTBSVp19/pBin(+) and at 3 dpai analyzed by confocal microscopy. (b) A similar experiment was conducted using pGFP/pBin(+) and pTBSVp19/pBin(+). The first panel shows GFP fluorescence (green), the second panel chloroplast autofluorescence (red) and the third panel a digitally merged image of the first and second panels. (E) Plants were agroinfiltrated with either EV control (OD_{600nm}=0.5) as a control or pNbHsc70-2/pBin(+) (OD_{600nm}=0.5). At 3 dpai three pre-infiltrated leaves from two plants were inoculated with 50 ng of CNV particles. At 3 dpi leaves were collected, ground with liquid nitrogen and levels of HSP70 (E), CNV gRNA (F), CP (G) and virions (H) were analyzed by Western blot analyses (E, G) or agarose gel electrophoresis (F, H) as described in Figure 2.4. All experiments were conducted at least three times and representative results are shown.

2.3.5 Overexpression of Hsc70-2 is associated with increased CNV CP accumulation and VLP assembly

It cannot be determined from the above described experiments if HSP70 levels can affect levels of CP and virion accumulation independently of the effect on viral RNA accumulation. To assess the possibility that Hsc70-2 plays a direct role in CNV CP accumulation, I first tested whether *N. benthamiana* Hsc70-2 could be overexpressed in *N. benthamiana* by co-agroinfiltration of pNbHsc70-2/pBin(+) with TBSV p19 (224). The results (Figure 2.6A) show that NbHsc70-2 is highly overexpressed by 3 dpai.

To determine the effects of NbHsc70-2 overexpression on CP levels, I co-agroinfiltrated pCNVCPpBin(+) with either pNbHsc70-2/pBin(+) plus pTBSVp19/pBin(+) or the control pGFP/pBin(+) plus pTBSVp19/pBin(+) and analyzed the levels of CP over a six day time period. I found that more full-length CP accumulates in pCNVCPpBin(+) agroinfiltrated plants co-agroinfiltrated with pNbHsc70-2/pBin(+) than with pGFP/pBin(+) (Figure 2.6B). I also observed an increase in the levels of the chloroplast localized 32.9 kDa CP cleavage product as well as a slight increase in the levels of the second chloroplast localized 31.1 kDa species. These CP species arise during chloroplast targeting and stromal uptake of the CNV CP (243) (Figure 2.2.1B) and would be expected to rise should full-length CNV CP levels rise. Taken together, the results suggest that the presence of NbHsc70-2 in agroinfiltrated plants increases accumulation of the CP independent of its role in increasing accumulation of viral RNA. It is to be noted here that during WT CNV infection the majority of the full-length CP (41 kDa) is assembled into virions and only about 1-5% of the CP is targeted to chloroplasts resulting in a low proportion of cleaved CP species (32.9 kDa and 31.1 kDa) (24). However, during argoinfiltration of plants

with CP, the majority of the CP is unassembled likely due to the absence of a replicating viral RNA that might contain PSs for encapsidation and concurrent particle assembly (see Section 1.19.6). Hence the majority of the unassembled full-length CP is targeted to chloroplasts followed by cleavage during orgenellar uptake to yield a relatively greater proportion of CP cleavage products (135).

The observed increase in the level of CP could conceivably arise as a result of HSP70 directly conferring stability to the CP or as described below, it could also result from HSP70 playing a role in particle assembly, which would indirectly increase the stability of the CP. To assess the latter possibility, I analyzed the level of VLPs that accumulated in the above described experiment at 6 dpai. We have recently found that pCNVCPpBin(+) agroinfiltrated plants accumulate VLPs that harbor host RNA (135). The particles consist of both T=3 and T=1 icosahedra as well as intermediate sized (IS) spherical particles of unknown icosahedral symmetry (Rochon Lab, unpublished observations).

Figure 2.6C shows that at 6 dpai there is a clear increase in the level of VLPs in pCNVCPpBin(+) and pHsc70/pBin(+) co-infiltrated plants as determined by agarose gel electrophoresis of purified VLPs from the experiment conducted in Figure 2.6B. Densitometric analyses of CP species as well as VLP bands were conducted (Figure 2.6D). In the experiment shown, an approximate increase of ~3.5 fold was found in the case of VLPs whereas the increase in the level of CP subunit at 6 dpai in Figure 2.6B was determined to only be ~1.4 fold. Together, these observations suggests that Hsc70-2 not only contributes to increased CNV CP accumulation but that CNV particle assembly is also increased since there is a proportionately

greater increase in VLP levels as compared to CP subunit levels. In an independent experiment similar results were obtained (Figure 2.6D); i.e., CP accumulation was found to increase by ~1.7 fold whereas VLP accumulation increased by ~4.2 fold.

I therefore conclude that Hsc70-2 assists in both CP subunit accumulation independent of its effect on viral RNA accumulation and increased VLP production independent of its effect on CP subunit accumulation. As stated in the Introduction, HSP70 homologs have been found to be involved in the assembly of some viruses such as *Hantavirus*, *Polyomavirus*, SV40, *Closteroviruses*, *Enteroviruses*, *Papillomaviruses* and HIV I (123-129) and the folding of the major capsid protein of ASFV is mediated by a chaperone (130, 216). This is the first report of an HSP70 homolog being involved in the assembly of an icosahedral plant virus.

It is interesting that CNV CP is targeted to chloroplasts with the aid of HSP70 homologs (see below). In previous studies we have shown that the CP utilizes molecular mimicry to enable chloroplast targeting as the CP arm region is sufficient for targeting GFP to chloroplasts (220). It is possible that the molecular mimicry evolved, at least in part, to enable CP interaction with HSP70 homologs in order to facilitate the CNV particle assembly process. Further studies are required to ascertain a role of HSP70 homologs in the CNV assembly process.

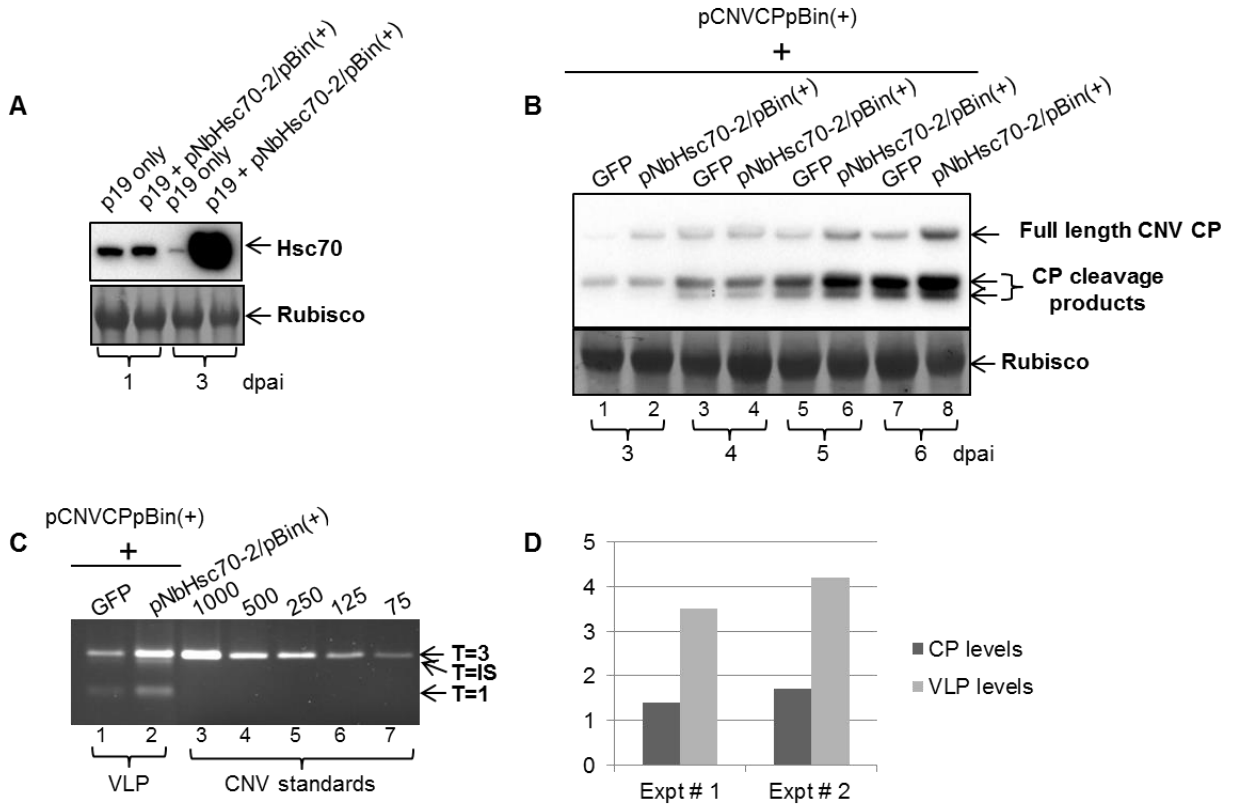

Figure 2.6: Overexpression of Hsc70-2 via agroinfiltration increases both CNV CP and VLP accumulation.

(A) Western blot analysis of *N. benthamiana* leaves co-agroinfiltrated with pNbHsc70-2/pBin(+) and pTBSVp19/pBin(+) (p19) (each at OD_{600nm}=0.5) at 1 and 3 dpai as indicated using a HSP70 antibody (upper panel). A Ponceau S stained image of the blot showing levels of Rubisco used as a loading control is present in the lower panel. (B) Western blot analysis of a time course (from 3-6 dpai) of pCNVCPpBin(+) co-agroinfiltrated with pGFPpBin(+) (GFP) or pNbHsc70-2/pBin(+) both in the presence of co-agroinfiltrated pTBSVp19/pBin(+) (p19). An OD_{600nm}=1.0 was used for each construct for agroinfiltration. A Ponceau S stained image of the blot showing levels of Rubisco used as a loading control is present in the lower panel. (C) EtBr stained agarose gel of VLPs extracted from *N. benthamiana* plants at 6 dpai which were agroinfiltrated with pCNVCPpBin(+) and either pGFPpBin(+) (GFP) or pNbHsc70-2/pBin(+) both in the presence of pTBSVp19/pBin(+) (p19). VLP preparations (lanes 1 and 2) contained T=3, T=IS (intermediate sized) and T=1 particles whereas WT CNV from infected leaves (lanes 3-7) contained T=3 particles as indicated. (D) Graphical representation of densitometric analyses of the relative increase in CP at 6 dpai (as in B, lanes 7 and 8) and VLP levels at 6 dpai (as in C, lanes 1 and 2). The level of CP or VLP in the presence of Hsc70-2 was determined compared to that of CP and VLP in the presence of GFP.

2.3.6 Hsc70-2 co-immunoprecipitates with CNV CP

To confirm that an interaction occurs between CNV CP and HSP70 family homologs, I agroinfiltrated plants with pCNVCPpBin(+) and immunoprecipitated these leaf extracts or EV infiltrated leaf extracts with a CNV polyclonal antibody. Figure 2.7A shows a Western blot of the co-immunoprecipitate probed with an HSP70 antibody. It can be seen in Figure 2.7A (lane 6) that the HSP70 antibody binds strongly to a 70 kDa protein in co-immunoprecipitates of pCNVCPpBin(+) infiltrated plants but only a low level of binding is present in that of EV infiltrated plants (Figure 2.7A, lane 3). Such binding was only apparent following a longer exposure of the blot (longer exposure not shown). The presence of the strong signal in pCNVCPpBin(+) infiltrated plants suggests that CNV CP binds HSP70 homologs in plants. The faint signal in EV infiltrated plants may be due to the presence of some HSP70 antibody in the CNV polyclonal antibody; since I have found a low level of Hsc70-2 in CNV particle preparations (see Chapter 3).

To confirm the presence of a HSP70 family homolog(s), the co-immunoprecipitated proteins were analysed by mass spectrometry. In total, five peptides were detected that were 100% identical to *N. benthamiana* Hsc70-2 (Gene ID no. Nbv5tr6412958) (Figure 2.7B) in the *N. benthamiana* database available through the University of Sydney, AU (http://sydney.edu.au/science/molecular_bioscience/sites/benthamiana/index.php).

These results indicate that CNV CP interacts with Hsc70-2 either directly or indirectly in plants. In addition, the data suggest that CP interacts predominantly with Hsc70-2 rather than Hsp70. My finding that CNV CP co-immunoprecipitates with Hsc70-2 suggests that these two proteins

interact either directly or indirectly in plants and is consistent with my findings that Hsc70-2 can assist in CNV CP and VLP accumulation.

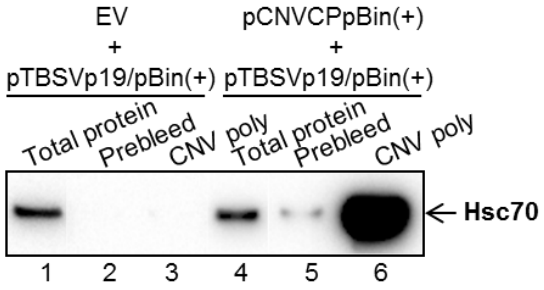

A

	Exp#1	Exp#2
Score:	387	206
Peptide:		
1. RTTPSYVGFTDSERL	X	X
2. KDAGVISGLNVMRI	X	X
3. KNALENYAYNMRN	X	X
4. KNQVAMNPINTVFDAKR	X	X
5. KSTVHDVVLVGGSTRI	X	-

B

Figure 2.7: Hsc70-2 co-immunoprecipitates with CNV CP.

(A) Western blot analysis of leaves agroinfiltrated with EV plus pTBSVp19/pBin(+) or pCNVCPpBin(+) plus pTBSVp19/pBin(+). Leaf extracts at 4 dpai were incubated with CNV pre-bleed antiserum (lanes 2 and 5) or CNV polyclonal antiserum (lanes 3 and 6) previously bound to Protein G sepharose beads. After washing extensively, CP was eluted and equal amounts of the co-immunoprecipitates were analyzed by Western blotting using HSP70 antibody. Lanes 1 and 4 show total protein from EV plus pTBSVp19/pBin(+) or pCNVCPpBin(+) plus pTBSVp19/pBin(+) agroinfiltrated leaf extracts, respectively. Note that in an independent experiment a weak signal was observed in the co-immunoprecipitate of CNV polyclonal antibody and EV plus pTBSVp19/pBin(+) leaf extracts. This is likely due to the fact that the CNV virions used to make the polyclonal antibody contain low levels of Hsc70-2 (see Chapter 3). (B) Figure showing the five Hsc70-2 peptides obtained from mass spectrometric analysis of two independent co-immunoprecipitation experiments. The score for each experiment is shown based on a MASCOT search that identified these peptides in *Solanum lycopersicum*. X indicates the presence of the peptide in the mass spectrometric analysis. A BLAST analysis of the five peptides in the taxid *Nicotianoideae* identified four proteins that showed 100% identity to all five peptides with the accession numbers AAP04522, AAR17080, XP009620324.1 and XP009777579.1 All four proteins are most similar to Hsc70-2 like proteins as determined by BLAST analysis of each of the proteins against the taxid *Nicotianoideae*. The nucleotide sequences of these genes are most similar (96%) to *N. benthamiana* Hsc70-2 (Nbv5tr6412958; University of Sydney, Au; http://sydney.edu.au/science/molecular_bioscience/benthamiana).

2.3.7 *N. benthamiana* Hsc70-2 prevents aggregation of CNV CP *in vitro*

HSP70 family homologs are known to have a prominent role in protein folding as well as preventing the formation of aggregates (68, 77, 78). To determine if *N. benthamiana* Hsc70-2 assists in folding of CNV CP *in vitro*, I cloned *N. benthamiana* Hsc70-2 into the bacterial expression vector pET24D(+) [construct pNbHsc70-2/His_7/pET24D(+)]. I then purified the expressed protein (NbHsc70-2/His_7) and tested its ability to facilitate solubilisation of CNV CP using an *in vitro* solubilisation assay.

To do this, I first denatured CNV CP by incubating virions in the presence of 5.4 M guanidine-HCl and then successively lower concentrations of guanidine-HCl until 2M guanidine levels were reached. NbHsc70-2/His_7, BSA or buffer was added to the CP and step wise dialysis was conducted in Hsc70-2 binding buffer. Following overnight incubation in binding buffer without guanidine the dialysate was removed and centrifuged at 10,000 x g for 2 min to precipitate any insoluble protein. The pellet was resuspended in a volume equal to that of the supernatant.

Equal volumes of supernatant and pellet were electrophoresed under denaturing conditions and blotted using a CNV CP SP antibody to compare levels of the CNV CP in the pellet (insoluble) and supernatant (soluble) fractions. It can be seen that in the presence of NbHsc70-2/His_7 some protein is present in the supernatant (soluble) fraction (Figure 2.8, lane 2), however protein was not detectable in the supernatant fraction when NbHsc70-2/His_7 was not added or when BSA was added (Figure 2.8, lanes 1 and 3, respectively). This observation suggests that NbHsc70-2 can bind and assist in folding and/or in preventing the development of insoluble CNV CP aggregates. These results are consistent with previous reports where it was found that

overexpression of Hsp70 can increase the solubility and expression of recombinant proteins in bacterial and insect cells (244, 245). It is therefore possible that in plants, Hsc70-2 assists in the accumulation of CNV CP as described in Figure 2.6B via preventing its aggregation and consequent degradation by the ubiquitin proteasome degradation pathway (246).

Attempts were made to determine if NbHsc70-2 could also assist in the *in vitro* assembly of CNV particles, however, particles were not observed in the presence or absence of NbHsc70-2, possibly due to the low level of soluble protein produced in my *in vitro* system. Further optimization of *in vitro* assembly conditions may assist in resolving whether Hsc70-2 can assist in CNV assembly *in vitro*.

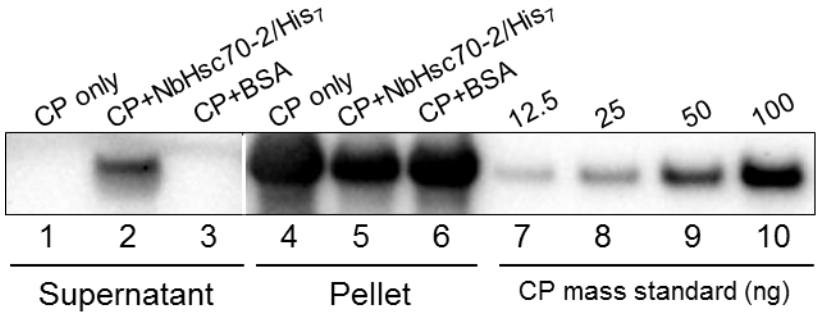

Figure 2.8: Hsc70-2 assists in solublization of CNV CP.

One hundred µg of CNV particles were denatured in 5.4 M guanidine-HCl and then dialyzed at successively lower concentrations and finally in 2 M guanidine-HCl. Either 200 µg of bacterially expressed *N. benthamiana* Hsc70-2 (NbHsc70-2/His_7) or BSA or an equal volume of buffer was added to dialysates. The mixtures were successively dialyzed against lower concentrations of guanidine-HCl in Hsc70-2 binding buffer and then finally in binding buffer only for 2 h. Mixtures were then allowed to stand overnight at 4°C and centrifuged at 10,000 x g for 2 min. The pellet (corresponding to insoluble protein) was resuspended in 1X LDS buffer containing 6 M urea equivalent to the volume of the supernatant (resuspended in a final concentration of 1X LDS). Equal volumes of the pellet and supernatant fractions were analyzed by denaturing gel electrophoresis and Western blot analysis using CNV CP antibody SP. Lanes 1-3 correspond to the supernatant fraction whereas lanes 4-6 correspond to the resuspended pellet. Lanes 7-10 contain the indicated amounts (in ng) of CNV CP used as a mass and size standard. The experiment was conducted three times and representative results are shown.

2.3.8 HSP70 facilitates targeting of CNV CP to chloroplasts

One of the well characterized functions of HSP70 family homologs is to facilitate the chloroplast import of cytoplasmically synthesized cellular chloroplast preproteins (99, 247). Previous work in Dr. Rochon's lab has shown that CNV CP efficiently targets chloroplasts and that approximately 1-5% of the CP is present in chloroplasts as cleaved proteins of 32.9 kDa and 31.1 kDa (220). To determine if targeting of CNV CP to chloroplasts occurs with the aid of a HSP70 family homolog(s), I conducted silencing experiments through agroinfiltration with pNbHsc70-2/pBin(+) (as in Figure 2.5E) and then inoculated the silenced plants with CNV. Western blot analysis of total leaf protein at 4 dpi showed that the two typical chloroplast cleavage products (32.9 kDa and 31.1 kDa), were not detectable in silenced plants when equal amounts of full-length CP were loaded onto the gel (Figure 2.10, lane 3), whereas these two proteins were readily detected in CNV infected uninfiltrated plants and plants infiltrated with EV (Figure 2.10, lanes 1 and 2, respectively). I therefore conclude that *N. benthamiana* HSP70 homologs play a role in targeting CNV CP to chloroplasts during infection.

It is also known that stromal Hsp70 acts as a molecular motor facilitating uptake of chloroplast preproteins into to chloroplast stroma (219). However, little nucleotide sequence identity exists between this nuclear encoded protein and Hsc70-2 (approximately 66% overall and only 1 region of extended nucleotide sequence identity of only 20 nucleotides; data not shown) so the observed decrease in chloroplast targeting of the CNV CP is likely due to the role of the cytoplasmic HSP70 homologs in chloroplast targeting.

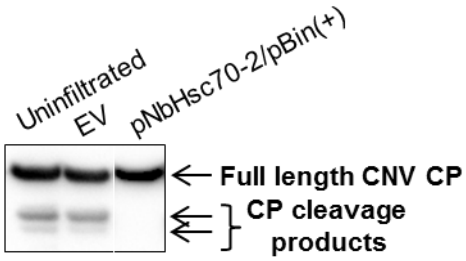

Figure 2.9: Downregulation of HSP70 interferes with chloroplast targeting of the CNV CP in *N. benthamiana*.

Western blot analysis of total leaf extracts from plants that were agroinfiltrated with EV (OD_{600nm}=0.5) or pNbHsc70-2/pBin(+), (OD_{600nm}=0.5). At 3 dpai, leaves were inoculated with 100 ng of CNV particles along with a control plant which was not infiltrated prior to inoculation (uninfiltrated control). Total protein extracts were analyzed at 4 dpi by running equal amounts of the full length CP. (Note this corresponded to a 4X greater mass of total protein in the pNbHsc70-2/pBin(+) infiltrated sample due to the lowered accumulation of CNV CP in silenced plants as well as a longer exposure of the blot). The lower two arrows on the right point to CNV CP chloroplast cleavage products that are present in uninfiltrated and EV infiltrated plants but not apparent in silenced plants. HSP70 downregulation was confirmed by Western blot analysis as in Figure 2.5E. The experiment was conducted three times and representative results are shown.

2.4 Discussion

In summary, the studies described here provide evidence that HSP70 homologs increase dramatically during infection and that they play multiple roles during CNV infection including the accumulation of CNV gRNA, CP and VLP as well as CNV CP targeting to chloroplasts. I also showed that Hsc70-2 contributes to the solubility of CNV CP and that it is associated with CNV CP either directly or indirectly in plants (also see Section 5.1). HSP70 homologs are central to the cellular protein quality control system and viruses have often been found to utilize them for performing various functions (see Introduction). I have found that during CNV infection, the induction of HSP70 protein levels increase as the levels of viral CP increase (Figure 2.2). It is most probable, however, that other CNV proteins also accumulate to high levels during infection so HSP70 induction is not likely specifically due to increased CP levels. As reported for TuMV and TCV(214), HSP70 induction was not specific to the expression of any one CNV protein (S.B. Alam, unpublished observations).

With respect to HSP70 transcript levels, transcriptome analysis of CNV infected *N. benthamiana* showed that different isoforms of Hsc70 and Hsp70 are induced at very high levels during CNV infection (Figure 2.3). I hypothesize that HSP70 family homologs are induced during CNV infection likely as a result of the high levels of viral proteins that are produced during infection and then are co-opted by the virus at various stages of the infection cycle due to its multiple functions and its abundance inside cells.

Previous studies have shown that several disease-causing plant viruses such as TMV, BMV, *Tobacco rattle virus* (TRV) and CMV can confer drought or cold tolerance to their hosts (248).

In addition, several plant viruses are known to induce HSP70 homologs, including TMV and CMV (214). Hence, it is possible that induction of heat shock proteins by CNV and other plant viruses confers heat tolerance to their hosts in natural environments. The viruses may thereby act as beneficial viruses in this regard (248) (also see Section 5.6 and 5.7).

With regard to CNV CP accumulation, I found that Hsc70-2 interacts with CP both *in vivo* (Figure 2.7) and *in vitro* (Figure 2.8 and 2.9) and is involved in increasing the accumulation of CP (Figure 2.6B). The greater accumulation of CP in infected plants can be correlated with a role of Hsp70 in increasing the local concentration of CP either by preventing its aggregation and consequent proteasomal degradation and/or by promoting assembly. I have found that NbHsc70-2 promotes the solubilisation of CP in an *in vitro* solubilisation assay, which is consistent with the role of Hsc70 in preventing the accumulation of denatured protein aggregates (246). I have also found that NbHsc70-2 also independently promotes assembly of CNV VLPs.

In this chapter I show by co-immunoprecipitation analysis that Hsc70-2 is associated with CP in cells (Figure 2.7) and that Hsc70-2 assists in CNV virion accumulation (Figure 2.6C & D). I have also observed that Hsc70-2 is associated with virions (see Chapter 3). Thus, Hsc70-2 may serve as a central control mechanism for regulating the accumulation of virions as well as their disassembly for establishing new infections.

The synthesis of artificial protein cages for drug delivery is a rapidly developing area of nanobiotechnology and material science (249). Natural proteins can be versatile building blocks for oligomeric, self-assembling structures, however development of protein based cages with

specific geometries can be challenging (250). As such, the ability of NbHsc70-2 to assist in the formation of CNV capsids may be useful for the development of protein cages for drug delivery.

Viruses completely rely on their hosts and can only multiply in living cells. Hosts, in turn, have evolved several defense responses against infecting viruses. The defense response in the case of plant viruses often tends to restrict the virus to infection foci by triggering a hypersensitive response or programmed cell death, resulting in development of local lesions or localized necrosis (251). Viruses, in turn, have evolved to counteract the defense response to ensure their continued ability to multiply. Recent work in Dr. Rochon's lab has shown that the ability of CNV CP to enter chloroplasts during infection can lead to attenuation of hypersensitive (HR)-like necrotic symptoms (S.B. Alam, unpublished observations). In this chapter, I show that NbHsc70-2 assists in targeting of CNV CP to chloroplasts (Figure 2.9) and that overexpression of Hsp70 can result in larger lesions (Figure 2.4F). Hence, it is possible that CNV has evolved to co-opt HSP70 for chloroplast targeting of CP, to attenuate symptoms, and in order to create a more favourable environment for CNV multiplication.

Previously it has been reported that cytosolic Hsp70 (Ssa1/2p) is associated with the replicase complex of CNV (40). Replication is believed to occur in conjunction with encapsidation in many virus systems such as *Poliovirus,* BMV, FHV (47, 177, 181). As mentioned above, my results suggest that there is an interaction between CNV CP and Hsc70-2. Hence, it might be possible that CNV recruits HSP70 associated with the replicase complex for promoting assembly.

Chapter 3: Evidence that Hsc70 is associated with *Cucumber necrosis virus* and plays a role in particle disassembly[3]

3.1 Introduction

Non-enveloped viruses are made up of a nucleic acid genome and a protein coat that plays an essential role in protection of the genome from nuclease attack in host cells. The nucleic acid is enclosed in the capsid which is composed of repeating virus-encoded polypeptide units stabilized by divalent cations, cementing proteins or disulphide bonds (252). The stable proteinaceous coat must be at least partially shed in order to release the encapsidated genome into the host cell to initiate an infection. The metastability associated with viruses allows structural rearrangements within capsids (55, 252) and is also important to prevent premature disassembly of capsids, which will not only expose the genome to host nucleases but will also compromise the targeting of the genome to its site of replication.

Enveloped viruses mostly enter and uncoat by membrane fusion followed by receptor mediated endocytosis (253). On the other hand, non-enveloped viruses mainly disassemble by initiating a conformational change in their capsids either by using a receptor, mechanical or chemical cues or via co-translational disassembly (36, 252, 254, 255). Structural transformations of viral capsids are also triggered through interaction with chaperones such as members of the heat shock protein 70 (HSP70) family including the constitutively expressed isoform Hsc70 (heat shock cognate 70 kDa protein) and the stress inducible isoform Hsp70 (heat shock 70 kDa protein) (78,

[3] A version of this Chapter has been published in *Journal of Virology* as a Spotlight Article. **Alam, S.B.** and Rochon, D. (2017) Evidence that Hsc70 is associated with *Cucumber necrosis virus* and plays a role in particle disassembly. J. Virol 91:e01555-16.https://doi.org/10.1128/JVI.01555-16.

254). Although constitutively expressed, Hsc70 can also be induced under specific conditions (80, 256) and can synergistically complement the functions of Hsp70 to preserve cellular integrity during metabolic challenges (81).

Hsc70 is one of the most abundant cytosolic HSP70 isoforms and has many distinct functions, both in preventing or reversing protein aggregation and in disassembling protein complexes (78, 86). Hsc70s have been found to play an important role in the disassembly of large macromolecular complexes (56, 78, 86) such as the DNA-replication origin complexes (87) and clathrin coated vesicles (88-91). Recent studies have revealed that Hsc70 functions by trapping the conformational fluctuations in the clathrin lattice causing local strains to accumulate (91). This destabilizes the lattice causing it to disintegrate in the cytoplasm.

Due to the ability of Hsc70 homologs to disaggregate stable oligomeric complexes (106), viruses have evolved to recruit these cellular disassembling machines to uncoat their capsids for the establishment of infection. Hsc70 homologs have been found to promote the uncoating process of several animal viruses such as *Polyomaviruses*, *Papillomaviruses*, *Reoviruses*, *Adenoviruses*, *Nodaviruses*, *Rotaviruses* and *Nervous necrosis virus* (109-115). However, there are no reports regarding the involvement of cellular Hsc70 in the disassembly of plant viruses although the virally encoded HSP70 homolog of *Beet yellows virus* has been hypothesized to play a role in disassembly of the helical capsid (116). I wished to determine if *N. benthamiana* HSP70 family homologs play a role in the disassembly of the plant virus CNV. This would extend my previous observation that HSP70 homologs play multiple roles in the CNV multiplication cycle (122).

CNV is a non-enveloped (+)ssRNA virus that belongs to the *Tombusvirus* genus in the *Tombusviridae* family (7). The CNV capsid is a T=3 icosahedron having a diameter of 34 nm and consists of 180 identical copies of a 41 kDa coat protein (CP), that encapsidates a 4.7 kb monopartite RNA molecule. Each of the CP subunits folds into three major domains: an RNA binding domain (R); the shell domain (S) and the protruding domain (P). The P and the S domains are connected by a short hinge, "h" region while the "a" or arm region flexibly tethers the R and S domains, both allowing for T=3 icosahedral symmetry and quasi-equivalent subunit interactions (13, 14).

To meet the requirements of quasi-equivalence, the CP adopts three different conformations (A, B and C). The arms are disordered in the A and B subunits while C subunits are characterized by ordered arms that extend to form the β-annulus at the particle 3-fold axis (13, 14). In analogy to TBSV, Ca^{2+} ions stabilize the interactions between adjacent A, B and C subunits in the shell domain by bringing together aspartate residues at the particle quasi 3-fold axis (Q3) (26, 257). The isoelectric point of the CNV virion is pH 5.2; hence the particles are stable at acidic pH. However, particles expand above pH 7, this being enhanced in the presence of a Ca^{2+} chelator (59, 257). The internally located R domain and arm region externalize during particle expansion and a hole is created at the particle Q3 axis (257) which is believed to allow for exit of virion RNA (37, 258). The expanded state of CNV as well as that of other members of the *Tombusviridae* is believed to represent an uncoating intermediate (13, 37, 259).

CNV particles are transmitted in nature through the recognition of specific amino acids in the shell and the protruding domains of the CP by glycoprotein receptors present on the surface of

zoospores of the fungus *Olpidium bornovanus* (29, 30). Receptor binding initiates a conformational change that is essential for vector transmission (29, 35, 59, 60). CNV particles have been found to interact with Hsp70 of fungal zoospores as determined by Western blot analysis and virus overlay assays (Rochon lab, unpublished observations). It is possible that the Hsp70 associated with the vector zoospores is responsible for bringing about the conformational change required for cellular entry of CNV particles as has been reported for *Rotavirus* entry into cells (111). This, and my recent finding that HSP70 homologs play multiple roles in the CNV infection cycle (122), raised the possibility of the involvement of plant Hsp70 or Hsc70 homologs in the disassembly of CNV.

Here I report several observations that suggest that CNV particles co-opt Hsc70-2 and/or Hsp70 for uncoating. CNV particle preparations were found to contain Hsc70 which is associated with virions as determined by its comigration with CNV particles in an agarose gel and by immunogold labelling of CNV particles using an HSP70 antibody. The bound Hsc70-2 is intimately associated with CNV particles as it is relatively resistant to trypsin digestion. Heat-shocked plants that express HSP70 at a high level or plants overexpressing Hsc70-2 produce a significantly higher number of local lesions when inoculated with CNV particles than do untreated plants. This is not observed when such treated plants are inoculated with viral RNA suggesting that the increased numbers of local lesions are due to increased viral disassembly rather than an increase in the efficiency of some other aspect of the initiation of infection. In addition, CNV particles incubated with Hsc70 partially disassemble or are conformationally altered and are more sensitive to chymotrypsin digestion. Taken together, my data strongly supports that CNV co-opts cellular Hsc70 for disassembly.

3.2 Materials and methods

3.2.1 Virus purification

Approximately 1.5 µg (in 110 µl) of T7 polymerase run-off transcripts of an infectious WT CNV cDNA clone (pK2/M5) was used to inoculate 3-4 leaves of 4-6 week old *Nicotiana benthamiana* as previously described (31). At five dpi infected leaves were collected and macerated in 100 ml of 25 mM potassium phosphate (KPO_4) buffer, pH 6.8 and used for inoculation using carborundum as an abrasive and a sterile sponge. For mock inoculation 3-4 leaves of 4-6 week old healthy *N. benthamiana* were ground as described above and the sap was used for inoculation.

At 6 dpi, approximately 60-100 g of mock or infected leaf tissue was collected and homogenised in a blender using at least five volumes of 100 mM NaOAc, pH 5.0 containing 10 mM β-mercaptoethanol. The homogenate was filtered through two layers of Miracloth (Calbiochem) and the filtrate was gently rotated at 4°C for at least 1 h and then spun at 8000 x g for 15 min at 4°C to remove plant debris. The solution was adjusted to 8% polyethylene glycol (PEG8000; Sigma-Aldrich) and incubated for at least 2 h at 4°C with constant stirring. The virus was pelleted at 8,000 x g for 20 min at 4°C and then resuspended in 10 ml of 10 mM NaOAc, pH 5.0. The suspension was gently rotated at 4°C overnight, and then subjected to centrifugation at 8,000 x g for 20 min at 4°C.

The supernatant (containing virions) was transferred to polycarbonate tubes (Beckman centrifuge tubes, PC 26.3 ml) and then subjected to ultracentrifugation (Beckman® L8-70M Ultracentrifuge)

at 40,000 x rpm for 4 h at 4°C in a Beckman Type 50.2 Ti rotor. The supernatant was discarded and the pellet was resuspended in 500-1000 µl of 10 mM NaOAc, pH 5.0. The suspension was gently rotated at 4°C overnight, and then centrifuged again at 20,000 x g for 15 min at 4°C. The supernatant (containing virions) was collected and stored at 4°C until further use. Virus concentration was determined spectrophotometrically (absorbance at 260 nm of a 1 mg/ml suspension of CNV is 4.5). CsCl purification of CNV was performed as previously described (14).

3.2.2 SDS-PAGE and Western blot analysis

Protein samples used for electrophoresis were prepared as described previously (122). Samples were electrophoresed through NuPAGE 4-12% Bis-Tris gels (Thermo Fisher Scientific), blotted onto PVDF membranes (Bio-Rad) and probed with either a monoclonal antibody that detects both Hsc70 and Hsp70 (ADI-SPA-820-F, 1mg/ml, Enzo Life Sciences) (hereafter referred to as HSP70 antibody), a rabbit polyclonal antibody specific to bacterially expressed CNV S and P domain sequences (SP antibody) or R and arm domains (RAD antibody) or a rabbit polyclonal antibody raised against CNV particles (CNV polyclonal antibody). Antigen-antibody complexes were detected with peroxidase labelled goat anti-mouse or goat anti-rabbit antibodies as appropriate (Sigma).

3.2.3 Ponceau S staining

Ponceau S (Sigma-Aldrich) staining of blots was conducted as described previously (122). CNV CP or ribulose-1,5-bisphosphate carboxylase/oxygenase (Rubisco) was used as the loading control to standardize the mass of total protein loaded onto the gel prior to blotting.

3.2.4 Mass spectrometry

Two independent virus purification experiments were performed from equal amounts of CNV and mock inoculated leaf tissue using the differential centrifugation technique described above. Preparations were resuspended in identical volumes and equal amounts of the two samples (mock and CNV infected) were analyzed for the presence of Hsc70-2 by mass spectrometry using the Proteomics Core Facility at the University of British Columbia Center for High-Throughput Biology. Samples were subjected to denaturing gel electrophoresis and bands greater and less than the size of CNV CP (41 kDa) were extracted, digested with trypsin and then differentially labeled with formaldehyde isotopologues. Samples were pooled and subjected to liquid chromatography-tandem mass spectrometry (LC-MS/MS) analysis. MASCOT was used to identify peptides using the Swiss-Prot database (260).

3.2.5 Purification of bacterially expressed *N. benthamiana* Hsc70-2 [pNbHsc70-2/His_7]

The previously described *N. benthamiana* Hsc70-2 cloned into a bacterial expression vector pET24D(+) with a 7X His tag (122) was purified using the TALON Superflow Metal Affinity Resin (Clontech Laboratories) as recommended by the manufacturer. Isopropylthio-β-galactoside

(IPTG) (1 mM) (Thermo Fisher Scientific) was used to induce 1000 ml of log phase (OD_{600} = 0.6-0.8) bacterial culture. Hsc70-2 was purified under denaturing conditions from the total (soluble and insoluble) lysate as described previously (122). The purified recombinant protein (NbHsc70-2/His_7) was concentrated using an Amicon Ultra-2ml Centrifugal Filter with a 50 kDa nominal molecular weight limit, and quantified by running several dilutions on a SDS-PAGE gel with bovine Hsc70 (ADI-SPP-751-D, Enzo Life Sciences) as the mass standard. The purified protein was stored at 4℃.

3.2.6 Quantification of Hsc70-2 present in CNV virion preparations

Increasing amounts (from 2.5 µg-40 µg) of purified virus particles were mixed with protein denaturation buffer (LDS; Thermo Fisher Scientific) in the presence of sample reducing agent. The mixture was heated at 70°C for 10 min and subjected to denaturing acrylamide gel electrophoresis followed by Western blot analysis as described above. Several dilutions of NbHsc70-2/His_7 (from 0.625 ng-10 ng) were also electrophoresed for quantifying the amount of Hsc70-2 present in virion preparations. For detection of Hsc70-2, HSP70 antibody was used at 1/2000 dilution (1 mg/ml stock). Antigen antibody complex was detected using a goat anti-mouse antibody (Sigma). The amount of Hsc70-2 present in virion preparations was determined by densitometric analysis utilizing Image Lab™ Software Version 5.1 (Bio-Rad Laboratories). Two independent Western blot analyses at two different concentrations (20 µg and 40 µg) of virus were conducted followed by quantification as above and an average was taken to estimate the mass of *N. benthamiana* Hsc70-2 present in CNV virion preparations.

3.2.7 Agarose gel electrophoresis of purified particles followed by Western blot analysis

Twenty μg of purified virus particles from two independent purifications were electrophoresed through 1% (w/v) agarose gels in TB buffer (45 mM Tris, 45 mM boric acid, pH 8.3) as described previously (30). 100 ng of bovine Hsc70/Hsp73 (ADI-SPP-751-D, Enzo Life Sciences; referred as bovine Hsc70 in the text) and human Hsp70/Hsp72 (ADI-NSP-555-D, Enzo Life Sciences; referred as human Hsp70 in the text) were also loaded onto the gel as controls. The particles were stained with EtBr as described previously (122). After visualization, electrophoresed particles and proteins were blotted onto PVDF membranes in TB buffer using capillary transfer (261).

After overnight transfer, the membrane was divided into two halves and each of the two blots were blocked with 5% skim milk in 1X TBS (Tris-buffered saline; 50 mM Tris-HCl pH 7.5, 150 mM NaCl, 2.5 mM KCl) containing 0.4% Triton-X 100 for 1 h at RT. After blocking, one of the membranes was probed with a CNV polyclonal antibody while the other was incubated with HSP70 antibody. Antigen-antibody complexes were detected using peroxidase labelled goat anti-rabbit or goat anti-mouse antibody (Sigma) for detecting CNV particles and HSP70 respectively. The Amersham™ ECL™ Prime Western Blotting Detection Reagent (GE Healthcare Life Sciences) was used for detection of bound antibodies.

3.2.8 Virus overlay assay

Ten μg of recombinant human Hsp70, bovine Hsc70 or BSA (Sigma) were mixed with the protein denaturation LDS buffer (Thermo Fisher Scientific) and electrophoresed along with CNV

CP mass standards through a NuPAGE 12% Bis-Tris gel using MOPS buffer (Thermo Fisher Scientific). The proteins were transferred to a nitrocellulose membrane (0.45 μm pore size; Bio-Rad) and allowed to renature overnight at 4℃ in the presence of 4% BSA in 1X PBS as described previously (29). After overnight incubation with BSA, the membrane was washed 3X times with 1X PBS and then blocked with 1X PBS containing 5% skim milk for 1 h at RT. After being washed three times with 1X PBS, the membrane was incubated with 100 μg of CNV particles in 10 ml of sodium phosphate ($NaPO_4$) buffer pH 7.6 for 3 h at RT. The membrane was then washed and probed with a CNV CP specific antibody (SP).

3.2.9 Immunogold labelling assay

1 μg of CNV virions (in 10 μl) were adsorbed onto Formvar-carbon coated nickel grids for 15 min. The solution was gently removed with Whatman filter paper 1 and then placed on 50 μl drops of blocking agent (1% BSA-1X PBS) for 10 min. Excess blocking agent was removed as above and grids were placed on 10 ul drops of either HSP70 antibody ($1/5^{th}$ dilution of a 1 mg/ml stock) or no antibody (negative control) in 1% BSA-1X PBS. After an overnight incubation at 4°C, the grids were washed three times in 50 μl drops of 1X PBS, 5 min each at RT. Grids were then incubated with 4 nm Colloidal Gold-AffiniPure Goat Anti-Mouse IgG (H+L) (Jackson ImmunoResearch Laboratories, Inc) at $1/20^{th}$ dilution in 1% BSA-1X PBS (10 μl) for 1 h at RT. The grids were washed again in 1X PBS as described above followed by four additional washes in distilled water (10 μl), 1 min each. The grids were then stained with 2% uranyl acetate for 30 sec and analysed by TEM using a Hitachi H-7100 TEM. The images were captured at 100 kV at a magnification of 80,000X using an ORIUS^{TM} CCD Camera.

3.2.10 Trypsin digestion of CNV preparations

Forty µg of virus particles (in 5 ul 10 mM $NaPO_4$ buffer, pH 7.6) were subjected to different concentrations of trypsin (Sigma) at RT as described in the legend to Figure 3.5 for 30 min as described previously with some modifications (37, 59). The reactions were stopped by adding LDS sample buffer (Thermo Fisher Scientific) (to a final concentration of 1X LDS buffer) containing sample reducing agent and 5X cOmplete Protease Inhibitor (Roche) and heating the samples at 70℃ for 10 min. The samples were electrophoresed through a 4-12% Bis-Tris NuPAGE gel and analysed by Western blot analysis using either HSP70 antibody or a mixture of CNV CP antibodies SP and RAD. Control reactions included 6.5 ng of NbHsc70-2/His_7 (the approximate amount associated with 40 µg of CNV particles as determined in Figure 3.1) alone or in conjunction with 40 µg of BSA and treated with trypsin as described above. In a further control 6.5 ng of NbHsc70-2/His_7 was incubated with an equivalent amount of extract of "virus" obtained from mock inoculated leaf tissue (followed by trypsin digestion as described above) in order to rule out the possibility that components in the CNV virion extract interfere with the trypsin digestion assay.

3.2.11 Local lesion analysis following incubation with HSP70 antibody

CNV virions (400 pg) were incubated with an equivalent mass of either HSP70 antibody or prebleed IgG antibody in 25 mM potassium phosphate (KPO_4) buffer, pH 6.8 at 37℃ for 1 h in a 10 µl reaction volume. After incubation, the volume was increased to 100 µl with 25 mM KPO_4, pH 6.8 and 10 µl (containing 40 pg of virions) was used to inoculate *Chenopodium quinoa*, a CNV local lesion host. Three to 5plants of the same age and 3-4 leaves at identical

developmental positions were rubbed with carborundum and then immediately inoculated. Lesions were counted at 4-7 dpi. The number of leaves counted (n) for each experimental set is given in the figure legend. A Student's t-test using GraphPad (GraphPad Software, Inc.) was conducted to determine if statistically significant differences existed between the two treatments. *p* values less than 0.05 were considered to indicate statistically significant differences.

3.2.12 Local lesion assay on *N. benthamiana* expressing Hsc70-2

N. benthamiana Hsc70-2 cloned into a binary vector pBin(+) as previously described [pNbHsc70-2/pBin(+)] (122), was used for agroinfiltration of *N. benthamiana*. Two leaves at identical developmental positions, each from 3-8 *N. benthamiana* plants (4-6 weeks old) were agroinfiltrated with either empty pBin(+) vector (EV) or pNbHsc70-2/pBin(+). To ascertain that the levels of Hsc70-2 increased in agroinfiltrated leaves, TLP samples were collected as described previously (122) at the indicated time points in the figure legends and subjected to Western blot analysis using HSP70 antibody. For local lesion assays, *N. benthamiana* plants were agroinfiltrated and at 3 dpai, leaves were inoculated with 100 ng of CNV particles. Lesions were counted at 4-6 dpi. The number of leaves counted (n) for each experimental set is given in the figure legend. A Student's t-test was conducted to determine if differences between treatments were statistically significant using GraphPad software. *p* values less than 0.05 were considered to be statistically significant.

3.2.13 Local lesion assays on heat-shocked *C. quinoa*

The CNV local lesion host *C. quinoa* was heat-shocked (HS) at 48℃ for 30 min followed by a 2 h recovery period at 26℃ as has been described for *Arabidopsis thaliana* (223). Untreated plants (no treatment) of the same age were kept at 26℃. Western blot analysis was utilized to confirm induction of HSP70. As a means for estimating the disassembly efficiency of CNV, *C. quinoa* plants of identical age were either heat-shocked (HS) or not heat-shocked (untreated) as described above. At 2 h post treatment, 3-4 leaves each from 3-7 plants at identical developmental positions in HS or untreated plants were rubbed with carborundum and then inoculated with CNV.

A pilot experiment was conducted to assess the concentration range in which the number of local lesions produced by CNV virions or virion RNA was linearly proportional to the inoculum concentration as described previously (220). A concentration of 40 pg virus/leaf or 1 ng virion RNA/leaf were used for virus or virion RNA inoculations, respectively, on HS or untreated plants. Four to six leaves per plant were inoculated on 3-5 plants per experiment. Lesions were counted at 5-7 dpi. The number of leaves counted (n) for each experimental set is given in the figure legend. A swas used to evaluate statistical differences between the number of local lesions in HS and untreated plants. *p* values less than 0.05 were considered as indicating statistically significant differences.

3.2.14 *In vitro* CNV/Hsc70-2 binding assay

CNV particles (600 ng) were treated with Hsc70 binding buffer or with 1800 ng BSA (Sigma) or 1800 ng NbHsc70-2/His_7 under binding conditions [10 mM Tris-HCl, pH 7.5, 50 mM potassium chloride (KCl), 5 mM magnesium chloride ($MgCl_2$), 1mM dithiothreitol (DTT), 1 mM adenosine triphosphate (ATP)] in the presence of 1X cOmplete EDTA-free protease inhibitor as previously established for Hsc70 (227, 228) with some modifications. The mixture was incubated at 25℃ for 3.5 h. The particles were then adsorbed onto Formvar-carbon coated copper grids for 10 min followed by negative staining with 2% uranyl acetate for 30 sec. Images were taken at 100 kV and 80,000X as described above. (22).

3.2.15 Chymotrypsin sensitivity assay

In vitro binding assays were performed as described above except no protease inhibitor was added in the reaction mixture. After incubating for 3.5 h at 25℃, 10 ng of chymotrypsin (Sigma) was added to the reaction tube and samples were collected at different times from 2 to 64 min as indicated in the figure legend (Figure 3.9C) and mixed with the reaction stop buffer [containing LDS with 5X cOmplete Protease Inhibitor (Roche) and sample reducing agent]. A control representative sample was collected from each tube, i.e., virus treated with binding buffer only, virus treated with BSA or NbHsc70-2/His_7 at 0 min before the addition of chymotrypsin and processed similarly. The collected samples were heated at 70℃ for 10 min followed by SDS-PAGE and Western blot analyses. A CNV CP antibody RAD (see above) was utilised for the detection of CP.

3.3 Results

3.3.1 Hsc70-2 is present in CNV particle preparations

I have previously found that HSP70 homologs play multiple roles in the CNV infection cycle and that Hsc70-2 co-immunoprecipitates with CNV CP (122). This prompted us to determine if Hsc70-2 is present in CNV particle preparations. To do this, I purified CNV particles from equal masses of mock or CNV inoculated *N. benthamiana* leaf material using PEG precipitation followed by differential centrifugation (see Materials and methods). After resuspending the pellets in equal volumes I conducted Western blot analyses using equal volumes of purified material and a monoclonal antibody that detects both Hsp70 and Hsc70 (HSP70 antibody). Figure 3.1A shows that HSP70 can be readily detected in virion preparations extracted from CNV infected plants (lane 2) when a high amount (40 µg) of denatured CNV particles is loaded onto the gel. However, no HSP70 signal was detected when an equal volume of material obtained from a mock virion preparation (lane 1) was loaded on the gel suggesting that HSP70 co-purifies with CNV virions.

HSP70 was also detected in virion preparations extracted from CNV infected plants using a miniprep procedure (225) or following sucrose density gradient purification (21) (S.B. Alam, unpublished observations). However, when virus purification from CNV infected plants was performed under stringent conditions using cesium chloride (CsCl) gradient (14) (note CsCl was removed from virion preparations by dialysis), HSP70 was not detectable. Figure 3.1B shows that when equal amount of virions extracted either by differential centrifugation (lanes 1-3) or CsCl gradients (lanes 4-6) were subjected to SDS-PAGE followed by Western blot analyses,

HSP70 was not detectable in the latter suggesting that HSP70 may not be firmly attached to CNV virions. This is consistent with my observation that levels of HSP70 in CNV preparations decline after long term storage of the virus (S.B. Alam, unpublished observations), possibly due to release from virions and/or degradation.

To determine which isoform of the HSP70 protein family is present in purified CNV virion preparations, mass spectrometry was conducted in two independent experiments. In each experiment equal volumes of material obtained from equal masses of mock and CNV inoculated leaf material were subjected to CNV purification procedures. In total, five Hsc70 peptides were specifically identified in CNV virion preparations, each showing 100% identity to the deduced amino acid sequence of *N. benthamiana* Hsc70-2 [(Gene ID Nbv5tr6412958) in the *N. benthamiana* database available through the University of Sydney, AU (http://benthgenome.qut.edu.au/)] (Figure 3.1C). These peptides were not detected in preparations purified in a similar manner from equal masses of mock inoculated leaves which indicates that Hsc70-2 co-purifies with CNV virions possibly due to an interaction between the virion and Hsc70-2.

To quantify the amount of Hsc70-2 present in CNV preparations, I purified bacterially expressed recombinant *N. benthamiana* Hsc70-2 containing seven C-terminal histidine (His) residues (NbHsc70-2/His_7) (Figure 3.1D) as described previously (122). Increasing masses of CNV particles along with several different dilutions of recombinant NbHsc70-2/His_7 were electrophoresed through a SDS-PAGE gel and then Western blot analysis was conducted using a HSP70 antibody (which detects both Hsp70 and Hsc70) (Figure 3.1E). From these experiments, I

estimate that approximately 5.7 ng of *N. benthamiana* Hsc70-2 is present in 40 µg of CNV which corresponds to approximately 18 molecules of Hsc70-2 per 1000 CNV particles. In an independent experiment a value of approximately 11 molecules of Hsc70-2 per 1000 virions was calculated. Taken together, the results strongly suggest that *N. benthamiana* Hsc70-2 is present in CNV virion preparations.

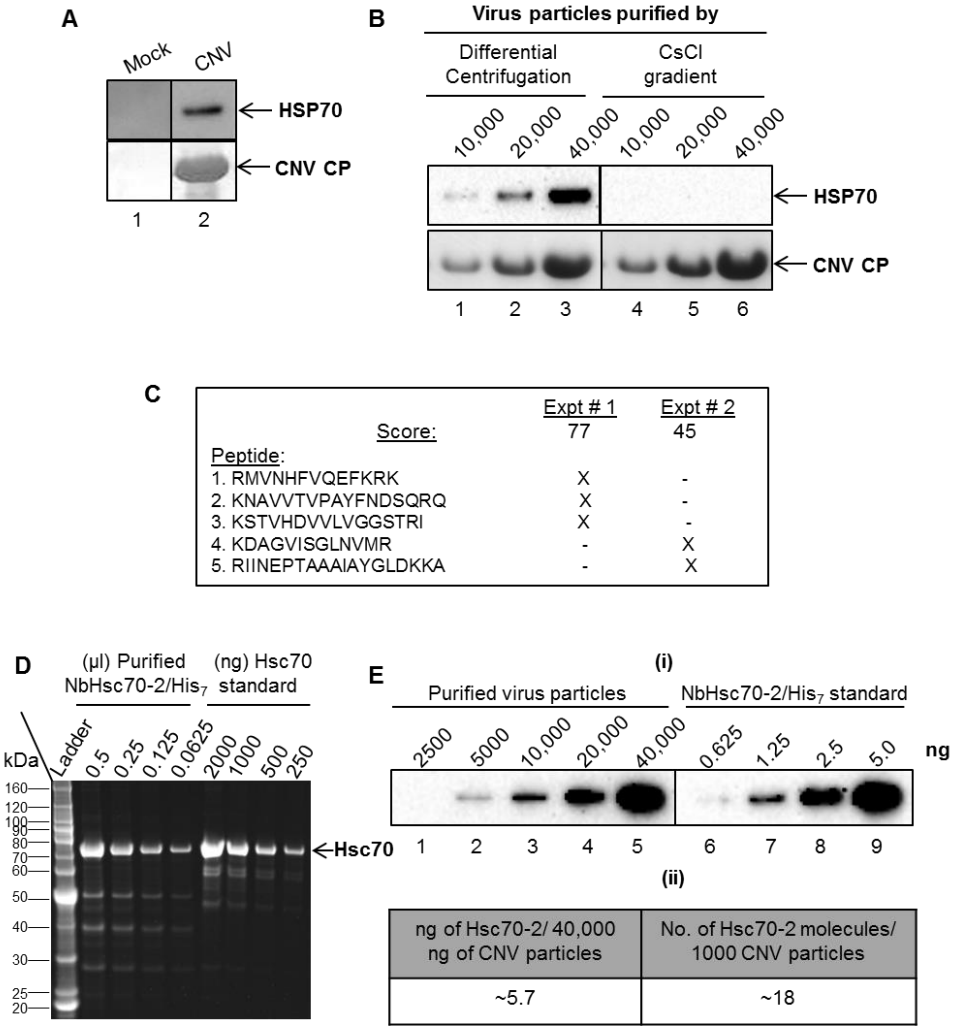

Figure 3.1: Hsc70-2 is present in CNV virion preparations.

(A) Western blot analysis of CNV virion preparations. Virion extraction was from equal masses of mock (lane 1) and CNV (lane 2) inoculated leaves. Pellets were resuspended in an equal volume of 10 mM sodium acetate, pH 5.8 and equal volumes of material (40,000 ng of CNV) were loaded onto a denaturing NuPAGE gel followed by blotting to PVDF membranes. The upper panel was probed with an antibody that reacts to both Hsp70 and Hsc70 (hereafter referred to as HSP70 antibody) and the lower panel was stained with Ponceau S to visualize CNV CP. (B) 10,000, 20,000 and 40,000 ng of CNV virions extracted either by differential centrifugation (lanes 1-3) or CsCl gradient centrifugation (lanes 4-6) were subjected to SDS-PAGE followed by Western blot analyses. The upper panel is a Western blot probed with an HSP70 antibody and the lower panel is the blot stained with Ponceau S to visualize CNV CP. (C) Summary of Hsc70-2 peptides detected by mass spectrometric analysis of proteins present in two independently purified CNV virion preparations (Expt #1 and Expt #2, respectively). The score for each experiment is shown based on a MASCOT search. X indicates the presence of the peptide in the mass spectrometric analysis. A BLAST analysis of the five detected peptides in the taxid

Nicotianoideae identified three proteins that showed 100% identity to all five peptides (accession numbers AAP04522, AAR17080 and XP009620324.1). All three proteins were most similar to Hsc70-2 like proteins as determined by BLAST analysis. The nucleotide sequences of these genes are most similar (95-96%) to *N. benthamiana* Hsc70-2 (Nbv5tr6412958; University of Sydney, Au; http://benthgenome.qut.edu.au/). These peptides were not detected in mock virus preparations extracted in a similar manner from the same amount of leaf tissue used to extract virions. (D) Denaturing gel electrophoresis of several dilutions (shown as µl) of recombinant *N. benthamiana* Hsc70-2/His_7 protein purified from bacterial cells using a TALON metal affinity matrix (Clontech). Bovine Hsc70 was used as the mass and size standard (shown in ng). The first lane shows a protein molecular mass standard (ladder) in kDa. (E) Estimate of amount of Hsc70-2 present in CNV virion preparations. Panel (i) shows a Western blot of CNV virion preparations probed with an HSP70 antibody. CNV particles (2,500, 5000, 10,000, 20,000 and 40,000 ng, as indicated) were electrophoresed under denaturing conditions and blotted to PVDF membranes prior to incubating with antibody. Dilutions of bacterially expressed *N. benthamiana* Hsc70-2/His_7 (0.625, 1.25, 2.5 and 5.0 ng) probed with HSP70 antibody were used to estimate the amount of Hsc70-2 present in CNV virion preparations. The amount of Hsc70-2 present in virion preparation was determined by densitometry using Image Lab™ software version 5.1 (Bio-Rad) and the results are summarized in panel (ii). In an independent experiment, I found approximately 3.5 ng of Hsc70-2/His7 per 40 µg of virus (i.e., approximately 11 molecules of Hsc70-2 in 1000 CNV particles).

I also assessed whether another member of the *Tombusviridae* family, the *Aureusvirus*, *Cucumber leaf spot virus* (CLSV) is associated with HSP70 using differential cenrifugation as described above. Figure 3.2 shows that CLSV is associated with HSP70 (panel i) and that approximately 4.5 ng, per 40,000 ng of CLSV is present (panel ii) which is similar to that observed with CNV. This observation shows that another virus in the *Tombusviridae* family is associated with HSP70 homologs reinforcing the notion that this association has biological significance.

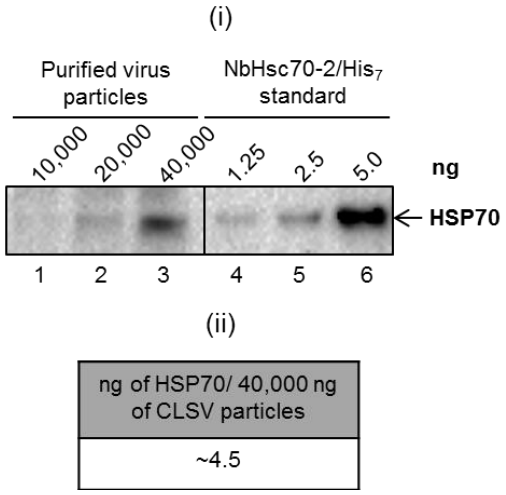

Figure 3.2: HSP70 co-purifies with CLSV.

Panel (i) Western blot of CLSV virion preparations (extracted by differential centrifugation as described for CNV) probed with an HSP70 antibody. CLSV particles (10,000, 20,000 and 40,000 ng, as indicated) were electrophoresed under denaturing conditions and blotted to PVDF membranes prior to incubating with antibody. Dilutions of *N. benthamiana* Hsc70-2/His_7 (1.25, 2.5 and 5.0 ng) probed with HSP70 antibody were used to estimate the amount of Hsc70-2 present in CLSV virion preparations. The amount of Hsc70-2 present in virion preparation was determined by densitometry using Image Lab™ software version 5.1 (Bio-Rad) and the results are summarized in panel ii.

3.3.2 CNV particles bind Hsc70 *in vitro*

To determine if CNV particles can bind HSP70 homologs *in vitro* I performed a virus overlay assay as described previously (29). Ten µg of recombinant Hsc70 (bovine), Hsp70 (human) and BSA as a negative control along with CNV CP controls were subjected to SDS-PAGE and blotted onto a nitrocellulose membrane. The proteins were allowed to renature *in situ* overnight. The membrane was then incubated with CNV particles for 3 h, washed and then probed with a CNV CP specific antibody. As shown in Fig 3.3A, the antibody bound to protein in the lane loaded with Hsc70 but not in the lanes containing Hsp70 or BSA suggesting that CNV virions can bind Hsc70 *in vitro*. This reinforces my finding that Hsc70 can interact with and therefore co-purify with CNV during virus extraction. It is to be noted that ATP was not included in these experiments. However, the recombinant bovine Hsc70 and human Hsp70 might contain some residual ATP molecules co-purified during the extraction procedure as suggested by the manufacturer (Enzo Life Sciences).

3.3.3 Hsc70-2 is bound to virions in purified CNV preparations

To determine if Hsc70-2 is bound to CNV virions in purified particle preparations, 20 µg of CNV particles from two independent purifications were electrophoresed through 1% (w/v) agarose gels. Recombinant Hsp70 and Hsc70 were also loaded on the gel. Proteins were blotted to PVDF membranes followed by Western blot analyses using a HSP70 (Figure 3.3B, panel i) or CNV polyclonal antibody (Figure 3.3B, panel ii). It can be seen that a signal was obtained using the HSP70 antibody and that this signal is present at a position on the blot that is similar to that of CNV particles probed with a CNV polyclonal antibody (compare blots in Figure 3.3B, panel i,

lanes 3, 4 with Figure 3.3B, panel ii, lanes 1, 2). Such binding was not apparent at a similar position in the lanes containing purified Hsp70 and Hsc70 (Figure 3.3B, panel i, lanes 1, 2 respectively) showing that the signal to CNV particles is not due to fortuitous comigration of CNV particles with free HSP70 homologs. These results indicate that Hsc70-2 detected by mass spectrometry in CNV preparations is bound to virions.

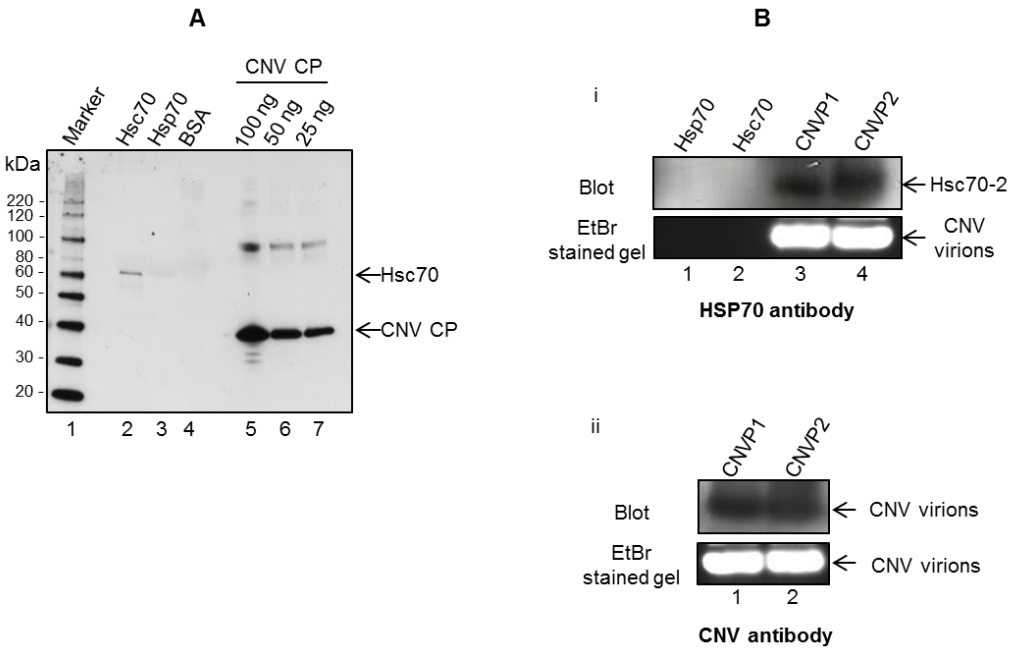

Figure 3.3: Purified CNV particles bind to Hsc70 *in vitro and in vivo*.

(A) Virus overlay assay showing that CNV particles bind to Hsc70 *in vitro*. Equal masses (10 µg) of bovine Hsc70, human Hsp70 and BSA as a negative control along with CNV CP standards (100, 50 and 25 ng, as indicated) were subjected to SDS PAGE. The proteins were blotted to a nitrocellulose membrane and allowed to renature overnight. The membrane was then incubated with CNV particles, washed and then probed with a CNV CP specific antibody. The first lane shows a protein molecular size marker with sizes of protein bands indicated to the left of the blot. Note: recombinant *N. benthamiana* Hsc70-2 was not available at the time when these experiments were conducted and hencewas not used for this experiment. However, preliminary experiments conducted with recombinant *N. benthamiana* Hsc70-2 do suggest that CNV particles bind Hsc70-2 *in vitro*. (B) HSP70 antibody binds to CNV particles subjected to agarose gel electrophoresis suggesting a physical interaction between Hsc70and CNV particles *in vivo*. 20 µg of two independently purified CNV particle preparations (CNVP1 and CNVP2) were electrophoresed through 1% agarose gel (panels i and ii), blotted and either probed with a HSP70 antibody (i) or a CNV antibody made to bacterially expressed S and P domains of the CP (ii) as a positive control. The upper panel shows the blots and the lower panel shows the ethidium bromide (EtBr) stained gels. In (i) 100 ng of human Hsp70 and bovine Hsc70 were also included in the gel to rule out the possibility that these proteins might co-migrate with CNV particles and thus artifactually indicate that CNV particles are bound to Hsc70.

3.3.4 Hsc70-2 is associated with CNV virions as determined by immunogold labelling

The results shown so far provide evidence that *N. benthamiana* Hsc70-2 is bound to CNV virions. To more directly assess this I performed immunogold labelling experiments. One µg of CNV particles was adsorbed onto Formvar/carbon coated nickel grids followed by incubation with HSP70 antibody. After washing, the grids were incubated with a goat anti-mouse secondary antibody conjugated to 4 nm colloidal gold particles to label Hsc70-2 molecules present in CNV virion preparations. After gold labelling the virus particles were negatively stained and analysed by TEM. A control experiment was performed in a similar manner except no primary antibody was used.

Figure 3.4A shows that CNV virions are labelled with gold as indicated by the white arrows. From three independent experiments it was found that, when labelled, the majority of the virions are labelled with 1(~53%) or 2(~19%) gold particles (representative images shown in Figure 3.4A). The remaining virus particles were labelled with three (~8.8%), four (~5.8%), five (~7.3%) or >5 (~5.8%) gold particles (S.B. Alam, data not shown). These data indicate that Hsc70-2 is bound to CNV particles and that some particles are bound to more than 1 Hsc70-2 molecule.

To assess if binding to CNV particles is specific, 100 random TEM images were taken of both the experimental samples and the control (no primary antibody) prepared as described above. The total numbers of virions, as well as the number of labelled virions were counted and the percentage of virions bound to gold was determined and is shown graphically in Figure 3.4B. As can be seen, approximately 20 times more particles are gold labelled in the experimental sample,

compared to the control sample. These observations suggest that in the experimental treatment gold labelled antibody is predominantly bound to CNV particles containing Hsc70-2 rather than being randomly distributed on the grid. Moreover, the bound Hsc70-2 is accessible to antibody suggesting that the Hsc70-2 epitope is on the particle surface rather than being present within virions.

It is also noted that about 4.5% of CNV particles were bound to gold which extrapolates to approximately 70 particles of gold per 1000 CNV particles given that many of the labelled virions contain more than 1 bound antibody (see above) (Figure 3.4B). This ratio of Hsc70-2 particles to CNV particles is slightly higher than but similar to that observed using Western blot analyses which suggested that approximately 11-18 molecules of Hsc70-2 are present in 1000 CNV particles (Figure 3.1E). Taken together, the presented data strongly supports that a subset of CNV particles are bound to Hsc70-2 with approximately 1.1 to 7% of the particles being bound as determined by Western blot analysis and immunogold labelling. The reason for the low level of Hsc70-2 binding to CNV virions is not known currently and needs further investigation. However, it is possible that greater numbers of CNV virions are associated with HSP70 homologs in infected plants and the virion bound HSP70 molecules become extracted from the particles during the virion purification procedure. On the other hand it is also possible that HSP70 homologs only transiently associate with CNV virions.

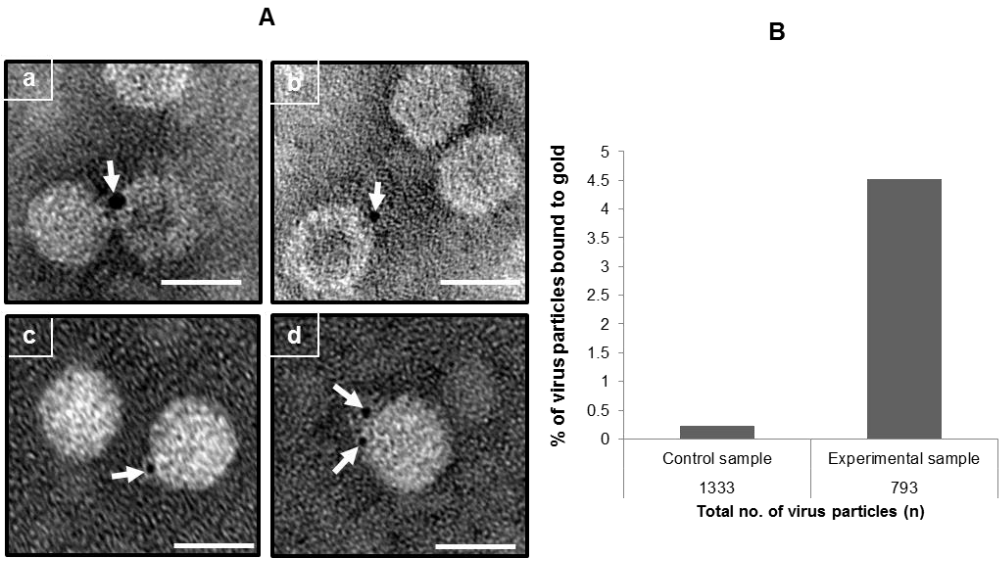

Figure 3.4: Immunogold labelling experiment showing that purified CNV particles are bound to Hsc70.

(A) 1 µg of purified CNV particles were adsorbed onto Formvar carbon coated nickel grids followed by incubation with 1% BSA-1XPBS as blocking agent. The grids were then incubated with HSP70 antibody at 4°C overnight. After incubation the grids were washed and treated for 1 h at RT with a goat anti-mouse antibody conjugated to 4 nm gold particles in 1% BSA-1XPBS. After washing, virus particles were negatively stained with 2% uranyl acetate. A negative control experiment was performed in a similar fashion except the particles were incubated with buffer instead of the primary antibody. The grids were analysed by TEM at 100 kV and the images were taken at 80,000X. Panels a, b and c show virus particles bound to 1 gold particle as shown by the white arrow and panel d shows a virus particle bound to two gold particles. The scale bar represents 34 nm. The experiment was repeated three times. (B) A graphical representation of the percentage of virus particles bound to gold in the control (without primary antibody) and experimental (with primary antibody) samples is shown. Immunogold labelling was conducted as described in (A) and 100 randomly selected fields were photographed for subsequent analysis. The total numbers of virus particles were counted in the control (1,333) and experimental (793) samples along with the number of particles bound to gold.

3.3.5 The Hsc70-2 bound to CNV in purified virion preparations is partially protected from trypsin digestion

Previous work from other labs has shown that HSP70 homologs can be incorporated into the interior of *Lentivirus* virions (262). However, my immunogold labelling results indicate that Hsc70-2 is at least partially present on the surface of CNV particles. To further assess if the bound Hsc70-2 is exposed or partially exposed on the exterior of CNV virions I performed a trypsin digestion assay. CNV virions (40 ug) were treated with increasing amounts of trypsin and the presence of Hsc70-2 was assessed by Western blot analyses (Figure 3.5). HSP70 antibody was used in the blot in panel a, and CNV CP antibodies SP and RAD were utilised in panel b**.**

It can be seen in Figure 3.5, panel a, that Hsc70-2 is sensitive to trypsin since levels decline noticeably when 4 ng of trypsin are used (Figure 3.5, panel a, lane 5) and no Hsc70-2 is apparent when approximately 40,000 ng of trypsin are used (Figure 3.5, panel a, lane 8). This indicates that Hsc70-2 is at least partially exposed on the particle surface rather than being present entirely within virions consistent with the results of immunogold labelling experiments. Also, while levels of Hsc70-2 start to degrade partially at 4 ng of trypsin, the CP in virions is still intact (Figure 3.5, panel b, lane 5). However, Hsc70-2 is efficiently degraded only when the virions start to degrade (Figure 3.5, compare lanes 7-9 in panels a and b) suggesting that although Hsc70-2 is exposed on the exterior of CNV it is partially protected by virions.

The conclusion that CNV virions partially protect Hsc70-2 from trypsin degradation is reinforced by the observation that free bacterially expressed NbHsc70-2/His_7 is susceptible to digestion with significantly lesser amounts of trypsin. For example, free NbHsc70-2/His_7 is completely

digested using 4 ng of trypsin (Figure 3.5, panel c, lane 5) whereas Hsc70-2 present in CNV preparations requires approximately 40,000 ng of trypsin for complete digestion (Figure 3.5, panel a, lane 9). However, it is possible that the decreased sensitivity of CNV bound Hsc70-2 to trypsin could simply be due to the presence of a high amount of CNV particles in the digestion mixture in panel a, which could competitively protect the Hsc70-2 from degradation. To rule out this possibility NbHsc70-2/His_7 was incubated with 40 µg of BSA (which is equivalent to the amount of CNV particles used in panel a) followed by trypsin digestion. It can be seen in Figure 3.5 panel e, that the presence of BSA does partially interfere with digestion of NbHsc70-2/His_7 as would be expected. However, unlike that of Hsc70-2 in CNV virions only 10 fold more trypsin (rather than the 1000 fold seen with CNV virions in panel a) was required to completely digest NbHsc70-2/His_7 in the presence of BSA. Thus, these data indicate that the reduced digestion of Hsc70-2 observed in the presence of CNV is due to partial protection by CNV virions.

In order to rule out the possibility that components of the CNV virus preparation interfere with trypsin sensitivity of CNV bound Hsc70-2 seen in panel a, I incubated NbHsc70-2/His_7 with the same volume of "virus" extracted from an equivalent mass of mock inoculated leaves that was used for CNV extraction from infected leaves in panel a (Figure 3.5, panel d). I found that the trypsin digestion pattern of NbHsc70-2/His_7 in the presence of the mock "virus" preparation was similar to that of free NbHsc70-2/His_7 (compare Figure 3.5, panels c and d). This observation reinforces my hypothesis that CNV particles partially protect the bound Hsc70-2 from trypsin digestion and that this protection is not due to interference by components of the virus preparation. The implied intimate interaction between CNV particles and Hsc70-2 suggests that

bound Hsc70-2 may be involved in some aspect of the establishment of infection such as disassembly or that it may assist in CNV particle stability.

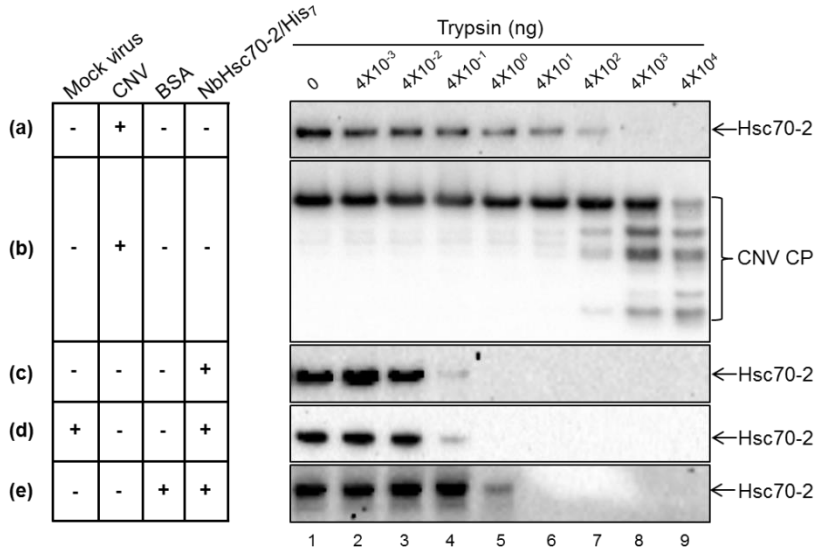

Figure 3.5: The Hsc70-2 bound to virions is partially protected from protease digestion.

Panels a and b. A trypsin protection assay was performed by incubating 40 µg of purified CNV virions with increasing amounts of trypsin (0 to 4 X 10^4 ng, as indicated) at RT for 30 min. Samples were then electrophoresed through a NuPAGE gel, blotted, and then probed with either a HSP70 antibody (panel a) or a mixture of two CNV CP antibodies that react to the CNV R and arm domains (RAD) or shell and protruding domains (SP) (panel b). In panel c, a similar experiment was performed using 6.5 ng of recombinant NbHsc70-2/His_7 (which corresponds to the approximate amount present in 40 µg of CNV virions) to compare the trypsin sensitivity of free Hsc70-2 with that of Hsc70-2 present in CNV virion preparations (panel a). In panel (d), 6.5 ng of NbHsc70-2/His_7 was mixed with mock virus extracted from a mass of leaf material equal to that used for CNV in panel (a), to determine if components of the virus preparation interfere with trypsin sensitivity of Hsc70-2. In panel (e), 6.5 ng of recombinant NbHsc70-2/His_7 was mixed with 40 µg of BSA prior to trypsin treatment. The blots in panels (c), (d) and (e) were each probed with HSP70 antibody under conditions identical to that in panel (a). Note that trypsin treated CNV has numerous degradation products (shown by brackets in panel b). Blots in panels (a) and (c-e) were each exposed for 39 min.

3.3.6 HSP70 antibody incubated virus particles or CsCl purified CNV virions having undetectable amounts of HSP70 produce a reduced number of local lesions on *C. quinoa*

Local lesion assays provide a means for measuring infection by virus particles or viral RNA inocula where each lesion is believed to result from a single particle (or single uncoating event) or a single infectious RNA molecule (263). Viral RNA replicates in the inoculated cell, and in the case of CNV, newly replicated viral RNA (rather than virions) moves to adjacent cells where replication is established once again, with further viral RNA cell-to-cell movement eventually resulting in the formation of a visible local lesion (Figure 3.6A).

To assess the possibility that the Hsc70-2 associated with CNV particles assists in disassembly during the establishment of infection, I incubated CNV particles with HSP70 antibody or with control prebleed antibody and then conducted a local lesion assay using the local lesion host *C. quinoa*. For this experiment, 400 pg of virus particles (~0.04 fmoles), were incubated with HSP70 antibody (~6 fmoles) at 37℃ for 1 h to bind the Hsc70-2 molecules associated with particles. An equivalent amount of prebleed antibody was used in control experiments in place of HSP70 antibody. After incubation, 40 pg of virions were used to inoculate *C. quinoa* leaves and the average number of local lesions per leaf was determined followed by conducting a Student's t-test. Figure 3.6B shows that in four independent experiments, significantly lower numbers of local lesions per leaf were obtained using virions incubated with HSP70 antibody versus virions incubated with prebleed antibody. These observations are consistent with the notion that the Hsc70-2 present in virion preparation plays a role in the establishment of CNV infection, possibly by enhancing disassembly in inoculated cells.

Also, I wished to determine if particles extracted via differential centrifugation which have detectable amounts of HSP70 (Figure 3.1B) would produce a greater number of local lesions on *C. quinoa* than CsCl purified virions which have undetectable amounts of HSP70. Therefore, equal amounts of virions (40 pg) extracted by differential centrifugation (DC CNV) or by CsCl gradients (CsCl CNV) were inoculated onto *C. quinoa* leaves. Figure 3.6C shows that in three independent experiments, significantly greater numbers of local lesions were observed in DC CNV virions in comparison to CsCl purified CNV virions. These results suggest that Hsc70-2 bound to virions plays an important role in the establishment of infection possibly via enhancing disassembly in inoculated cells.

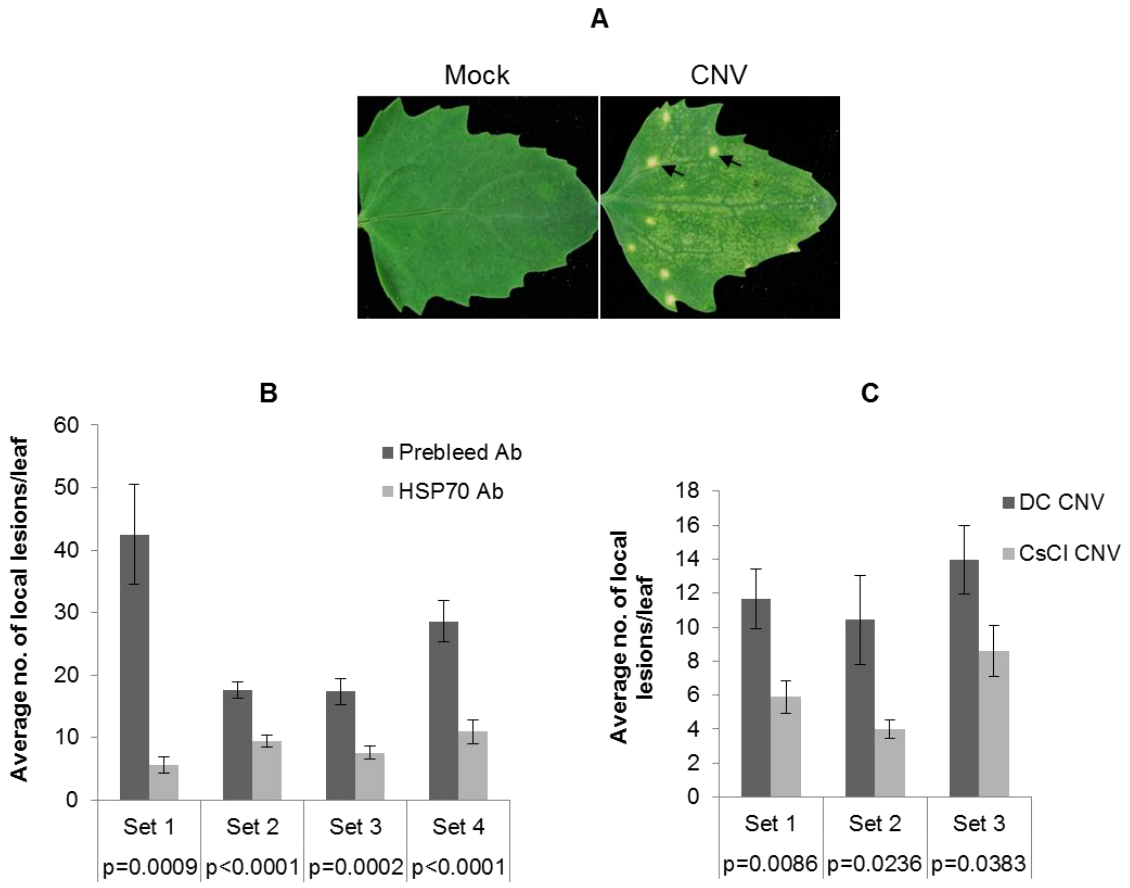

Figure 3.6: CNV particles incubated with HSP70 antibody or having undetectable amounts of HSP70 produce fewer local lesions on the local lesion host *Chenopodium quinoa.*

(A) Locals lesions produced on *C. quinoa* leaves following inoculation with CNV virions. The leaf in the left panel was mock inoculated with buffer only and the leaf in the right panel was inoculated with CNV virions. Arrows point to the local necrotic lesions observed at 5 dpi. (B) CNV particles (400 pg) were incubated with an equal mass of prebleed IgG or HSP70 antibody at 37°C for 1 h and then 40 pg of virus was used to inoculate individual *C. quinoa* leaves. The numbers of local lesions per leaf were counted at 5 dpi. A graphical representation of the average number of local lesions per leaf obtained from four independent experiments (set 1, n= 8; set 2, n=10; set 3, n=20; set 4, n=23) is shown. (C) Graphical representation of three independent local lesion assays (set 1, n=22; set 2, n=14; set 3, n=22) showing average no. of local lesions/leaf on *C. quinoa* plants inoculated with 40 pg/ leaf of CNV virions extracted either by differential centrifugation (DC CNV) or CsCl gradient (CsCl. CNV). The lesions were counted on 5 dpi. The *p* values for each experimental set as determined by a Student's t-test are shown and indicate that the differences are statistically significant (i.e. $p<0.05$). The standard error is shown by the brackets above the bars. "n" represents the number of leaves counted for each treatment in an experimental set.

3.3.7 Overexpression of Hsc70-2 or Hsp70 leads to enhanced CNV disassembly efficiency

To further examine the possibility that *N. benthamiana* Hsc70-2 may play a role in CNV disassembly during the establishment of infection, I agroinfiltrated plants with either Hsc70-2 cloned as previously described into the binary vector pBin(+) [pNbHsc70-2/pBin(+)] (115) or with empty pBin(+) (EV) as a control (122). I then inoculated infiltrated leaves with CNV to determine if overexpression of Hsc70-2 would lead to enhanced local lesion production. To confirm that Hsc70-2 was overexpressed, total leaf protein samples were collected at 1 and 3 dpai and analysed through Western blot analysis using a HSP70 antibody. I observed that plants agroinfiltrated with pNbHsc70-2/pBin(+) contained significantly elevated levels of Hsc70-2 at 3 dpai compared to the EV control (Figure 3.7A, compare lanes 3 and 4). I therefore inoculated agroinfiltrated leaves at 3 dpai, when the expression levels of Hsc70-2 was high, with 100 ng of CNV and then counted the number of local lesions at 4-6 dpi. Four independent experiments were conducted and in each experiment, plants overexpressing Hsc70-2 were found to develop significantly ($p<0.05$) greater numbers of local lesions compared to EV infiltrated plants (Figure 3.7B). I suggest that overexpression of *N. benthamiana* Hsc70-2 leads to enhanced disassembly efficiency of CNV leading to a greater number of local lesions.

It is noted here that CNV does not normally produce discrete, countable, local lesions on inoculated leaves of *N. benthamiana*, rather the lesions are broad and spreading (Rochon Lab, unpublished observations). However, I have found that discrete lesions are produced when plants are agroinfiltrated (Figure 3.7C). This is likely due to the combined immune response of *N. benthamiana* to CNV infection and the pattern triggered immunity induced by *A. tumefaciens* (264).

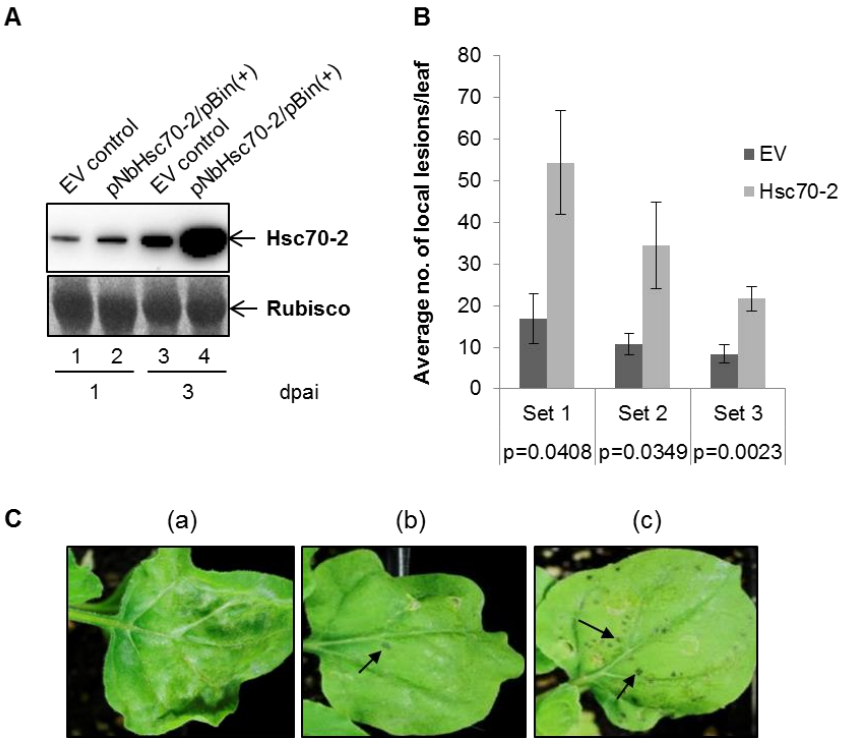

Figure 3.7: *N. benthamiana* leaves agroinfiltrated with Hsc70-2 show an increase in the number of local lesions produced by CNV in comparison to plants agroinfiltrated with EV.

(A) Western blot analysis of leaf extracts from *N. benthamiana* plants agroinfiltrated with EV or pNbHsc70-2/pBin(+) at 1 and 3 dpai showing overexpression of Hsc70-2. Two to three leaves from two plants were collected, ground in liquid nitrogen and 100 mg of the ground leaf material was added to 350 µl of LDS protein extraction buffer. Equal volumes were electrophoresed using SDS-PAGE and probed with a HSP70 specific antibody. A Ponceau S stained image of the blot showing levels of Rubisco used as a loading control is present in the lower panel. (B) Local lesion assay on *N. benthamiana* plants that were agroinfiltrated with EV or pNbHsc70-2/pBin(+) as indicated and then three days later were inoculated with 100 ng of CNV virions. Note that at the time plants are inoculated the levels of NbHsc70-2 are elevated [see A (compare lanes 3 and 4)]. Graphical representation of the average number of local lesions per leaf on EV or Hsc70-2 agroinfiltrated plants from three independent local lesion assays (set 1, n=6; set 2, n=8; set 3, n=16). The *p* values for each experimental set as determined by a Student's t-test are shown in the figure and indicate that the differences are statistically significant (i.e. $p<0.05$). The standard error is shown by the brackets above the bars. "n" represents the number of leaves counted for each treatment in an experimental set. (C) *N. benthamiana* leaves were agroinfiltrated and inoculated as in B. Panel a represents a leaf inoculated with 100 ng of CNV particles showing chlorosis at 3 dpi which leads to a typical spreading necrosis by 5-6 dpi (Rochon Lab, data not shown). Panel b represents an image of a leaf at 3dpi agroinfiltrated with EV and inoculated with CNV and panel c represents the image of a 3 dpi leaf agroinfiltrated with pNbHsc70-2/pBin(+) and inoculated with CNV. Note that inoculation of CNV on agroinfiltrated *N. benthamiana* produces contained rather than spreading local lesions as shown by the arrow in panel b and c.

I also wished to determine if overexpression of HSP70 homologs would lead to increased disassembly efficiency in the CNV local lesion host *C. quinoa*. Since *C. quinoa* is a poor host for transient protein expression via agroinfiltration (Rochon Lab, unpublished findings), I utilized heat shock treatment to increase the levels of HSP70 homologs. Previously I have found that *C. quinoa* plants heat-shocked at 48℃ for 30 min followed by a 2 h recovery period leads to overexpression of Hsp70 and possibly Hsc70 at 2 h post heat treatment and that high levels of expression remains for up to 3 days post heat shock (122). Hence, I inoculated the heat-shocked (HS) or non-heat-shocked (N) plants 2 h post treatment with 40 pg of CNV particles and examined the number of local lesions produced per leaf in both sets of plants. Figure 3.8A shows a graphical representation of the average number of local lesions per leaf on HS and N plants. Four independent experiments were conducted and in each experiment it was shown that HS plants developed a significantly ($p<0.05$) greater number of local lesions per leaf than N plants suggesting that Hsc70 and/or Hsp70 may enhance CNV disassembly efficiency.

To distinguish between greater disassembly efficiency and the possibility that heat-shocked plants might simply support CNV replication and accumulation to a higher level as reported (17, 122), I conducted a similar local lesion analysis with CNV virion RNA as the inoculum. I found that in five independent experiments that the average number of local lesions/leaf between the HS and N plants were not statistically significant ($p>0.05$) (Figure 3.8B), suggesting that the greater number of local lesions found in heat-shocked plants using CNV particles could be due to enhanced disassembly efficiency of CNV virions rather than increased capacity of heat-shocked *C. quinoa* plants to support CNV infection. My results are therefore consistent with the hypothesis that HSP70 homologs assist in the CNV uncoating process.

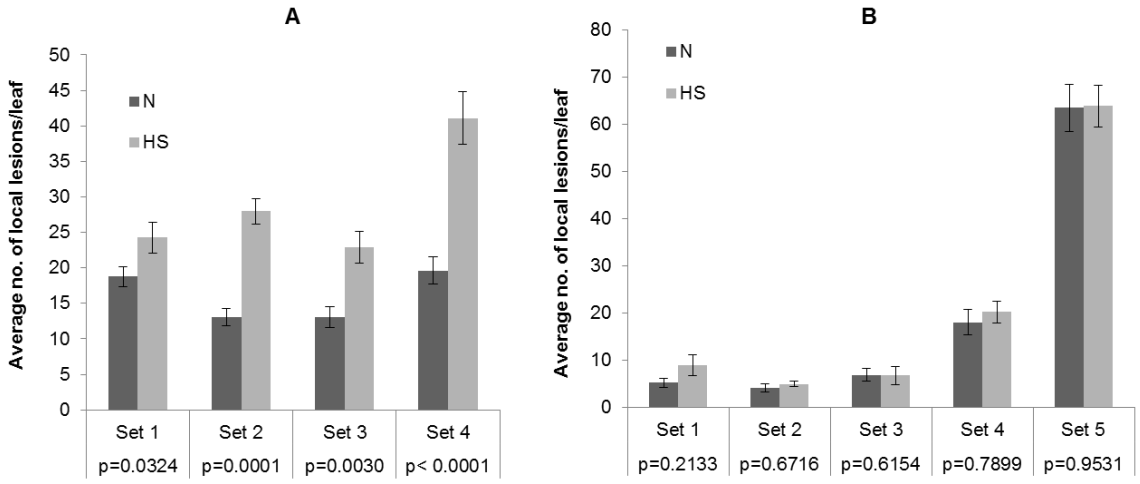

Figure 3.8: Heat-shocked *C. quinoa leaves* show an increase in the number of local lesions in comparison to untreated plants when virions are used as inoculum but not when virion RNA is used.

(A) Graphical representation of the average number of local lesions per leaf on heat-shocked (HS) and non-heat-shocked (N) *C. quinoa* plants from four independent local lesion assays (set 1, n=20; set 2, n=38, set 3, n=27; set 4, n=19) using virions as inoculum (40 pg/leaf). The *p* values for each experimental set as determined by a Student's t-test are shown in the figure and indicate that the differences are statistically significant (i.e. $p<0.05$). (B) Graphical representation of five independent local lesion assays (set 1, n=12; set 2, n=15; set 3, n=17; set 4, n=18; set 5, n=32) conducted as in (A), except virion RNA (1 ng/leaf) was used as an inoculum. Note that *p* values are greater than 0.05 indicating that the differences in local lesion numbers are not statistically significant. "n" represents the number of leaves counted for each treatment in an experimental set.

3.3.8 Incubation of virus particles with *N. benthamiana* Hsc70-2 at pH 7.5 leads to partial disassembly and/or conformational change of CNV virions

Studies have shown that Hsc70 can initiate the disassembly of oligomeric protein complexes (106). Also as described above, Hsp70 and Hsc70 have been found to have roles in inducing conformational change in viral capsids which is then followed by entry and uncoating in cells (111, 265). I hypothesized that Hsc70-2 induces a conformational change in CNV capsids which may contribute to disassembly of particles in the cytoplasm. To assess this, I performed an *in vitro* binding assay using 600 ng of CNV particles and 1800 ng of NbHsc70-2/His_7 or recombinant BSA as a control under optimised Hsc70-2 binding conditions at pH 7.5 in the presence of 1X EDTA free protease inhibitor (see Materials and methods). After incubation for 3.5 h, the particles were stained with 2% uranyl acetate and analyzed by TEM. It can be seen in Figure 3.9A that incubation of virus particles with NbHsc70-2/His_7 results in conformationally altered or partially dissociated virions (shown by the white arrowheads in panels c-h) which was not observed following incubation of particles in binding buffer (panel a). In some cases it appeared that viral RNA could be seen extruding from particles or perhaps instead that "strings" of CP subunits were found associated with particles (shown by black arrows in panel d and h). These findings are consistent with the hypothesis that *N. benthamiana* Hsc70-2 plays a role in the disassembly of CNV particles at pH 7.5.

To further assess the validity of the observed phenomena, an *in vitro* binding assay was performed as described above and 100 random images were photographed. The total number of CNV particles was counted along with the number of virions that were conformationally altered or partially disassembled. Figure 3.9B shows that an approximate 11 fold increase was found in

the percentage of conformationally altered or partially disassembled virions when CNV was incubated with NbHsc70-2/His_7 (7.5%) compared to the BSA control (0.69%). These results are consistent with my hypothesis that Hsc70-2 may play a role in CNV disassembly in inoculated cells.

To further ascertain that some virions undergo structural changes in the presence of exogenously added NbHsc70-2/His_7, chymotrypsin digestion assays on virions incubated in the presence or absence of *N. benthamiana* Hsc70-2 were conducted. It can be seen in Figure 3.9C; lanes 13-18 that a low proportion of CP associated with CNV virions were digested by chymotrypsin, whereas buffer or BSA treated virions were insensitive to chymotrypsin (Figure 3.9C, lanes 1 to 12). The sensitivity of Hsc70-2 treated CNV particles to chymotrypsin suggests that Hsc70-2 induces a conformational change in particles rendering them susceptible to protease treatment. I also noted that only a low level of digestion by chymotrypsin is observed. This could be due to inefficient binding of Hsc70-2 to CNV particles in the *in vitro* assay used, as was observed in TEM analysis of Hsc70-2 treated CNV (see above), and a resulting low level of conformational change and thus chymotrypsin sensitivity.

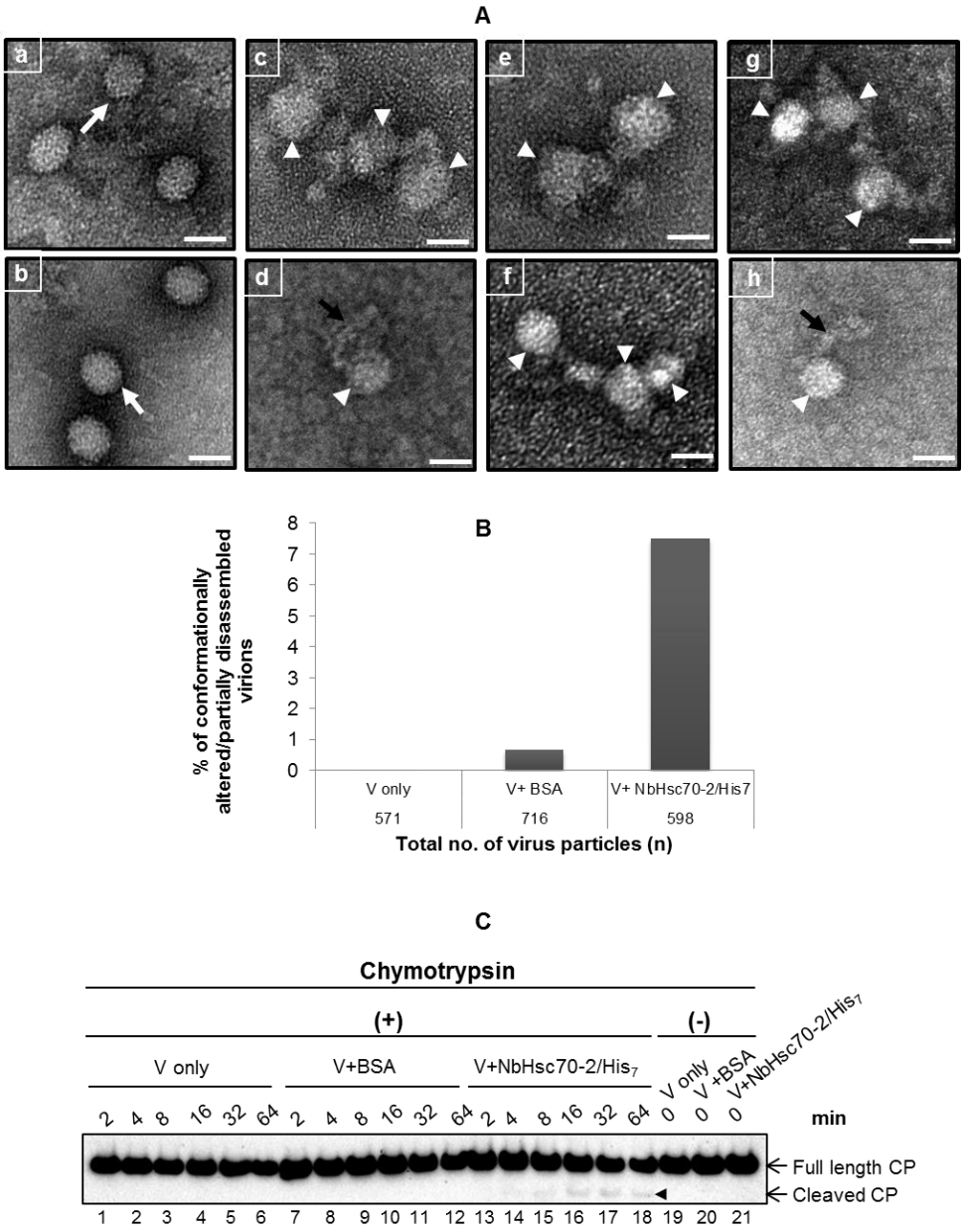

Figure 3.9: Incubation of CNV with NbHsc70-2/His$_7$ at pH 7.5 leads to partial disassembly of virions.

(A) 600 ng of CNV virions were incubated with NbHsc70-2/His$_7$ binding buffer (a),1800 ng of BSA (b) or 1800 ng of NbHsc70-2/His$_7$ (c-h) under optimised binding conditions at pH 7.5 in the presence of 1X EDTA free protease inhibitor for 3.5 h. Particles were adsorbed to Formvar coated nickel grids and subjected to negative staining with 2% uranyl acetate. Intact virus particles are shown by white arrows in panels (a) and (b). The partially disassembled virions are shown by white arrow heads (c-h). The black arrow possibly represents viral RNA extruding from a partially disassembled virion or coat protein subunits (d and h). The scale bar represents 34 nm. The experiment was repeated three times and representative results are shown. (B) A

graphical representation of the percentage of conformationally altered or partially disassembled virions in samples prepared as in (A) is shown. 100 fields were randomly selected and photographed for subsequent analysis. The total number of virus particles were counted in the controls, [either virus treated with NbHsc70-2/His_7 binding buffer (V only; n=571) or virus treated with BSA (V+BSA; n=716)] or the experimental sample (virus treated with NbHsc70-2/His_7 (V+Hsc70; n=598)], along with the number of particles that were conformationally altered or partially dissassembled. An approximate 11 fold increase in the percentage of conformationally altered/partially disassembled virions was observed in V+Hsc70-2 compared to V+BSA samples. Approximately 7.5 % of CNV virions were found to be conformationally altered or partially disassembled in the presence of NbHsc70-2/His_7. (C) 600 ng of virions were treated with binding buffer only (Lanes 1-6), BSA (Lanes 7-12) or NbHsc70-2/His_7 (Lanes 13-18) as in (A), but in the absence of any protease inhibitor. After an incubation of 3.5 h, the virions were treated with 10 ng of chymotrypsin at RT and equal volume of samples were collected and mixed with the reaction stop buffer at indicated time points followed by SDS-PAGE and Western blot analyses using the CNV CP antibody RAD. An equal amount of samples from each treatment were collected and processed as described above before the addition of chymotrypsin (lanes 19-21). The chymotrypsin cleavage products in V+NbHsc70-2/His7 samples are shown by the arrowhead.

3.4 Discussion

Little is known about the means by which non-enveloped virus particles disassemble to establish infection in a host. I provide evidence that Hsc70-2 is associated with CNV particles and that Hsc70-2 and/or HSP70 homologs can assist in the CNV disassembly process. Previous work has demonstrated that HSP70 homologs are highly upregulated during CNV infection and that they contribute to multiple aspects of the CNV infection process such as accumulation of viral RNA, and CP, VLP assembly and targeting of CNV CP to chloroplasts (122). HSP70 homologs have been found to promote the uncoating of several animal icosahedral viruses such as *Rotaviruses*, *Polyomaviruses*, *Reoviruses* and *Papillomaviruses* (109-111, 265). My studies show for the first time that a plant HSP70 homolog, Hsc70-2, may be involved in the disassembly of an icosahedral plant virus, CNV.

Hsc70 and Hsp70 are molecular chaperones that play important roles in protein folding and preventing aggregate formation (78). They also have been found to promote the disassembly of macromolecular complexes such as clathrin coated vesicles (88-90). Studies have shown that Hsc70 not only uncoats clathrin, but also primes it to reform clathrin coated pits (266). Studies on *Human polyomavirus* suggests that Hsp70 also plays dual roles during virus infection by facilitating both capsid assembly (267) and disassembly (109). Recently I have found that Hsc70-2 plays a role in the assembly of virus-like particles that accumulate during agroinfiltration of plants with CNV CP (122). My observation that Hsc70-2 is likely involved in the uncoating of CNV capsids is consistent with the notion that Hsc70-2 might be involved in both CNV assembly and disassembly as in *Polyoma* and *Papillomaviruses* (109, 267)

As shown in Figure 3.1, Hsc70-2 co-purifies with CNV suggesting an association between CNV particles and Hsc70-2. Virus overlay assays (Figure 3.3A) show that CNV particles can bind bovine Hsc70. Moreover, Figure 3.3B shows that CNV particles remain associated with Hsc70-2 following agarose gel electrophoresis reinforcing the notion that Hsc70-2 is physically bound to CNV particles. Immunogold labeling experiments provide further evidence that Hsc70-2 is bound to particles with the majority of particles containing one or two bound Hsc70-2 molecules (Figure 3.4). The nature of the association between CNV particles and Hsc70-2 was examined using trypsin sensitivity assays and it was found that Hsc70-2 present in CNV preparations is less sensitive to trypsin treatment than "free" Hsc70-2, requiring between 1,000-10,000 fold more trypsin for complete digestion (Figure 3.5). This suggests that Hsc70-2 is intimately associated with CNV particles.

I have also examined whether CLSV is associated with HSP70 homologs and found that approximately 4.5 ng of HSP70 per 40,000 ng of CLSV is present (Figure 3.2). This is similar to the level of Hsc70-2 detected in CNV preparations (3.5-5.7 ng/40,000 ng of CNV; Figure 3.1). Additionally, in a preliminary experiment I have found that *N. benthamiana* plants agroinfiltrated with Hsc70-2 and inoculated with CLSV as described for CNV; develop visibly greater numbers of local lesions (S.B. Alam, unpublished observations). The finding that CLSV is associated with HSP70 homologs suggests that other members of the *Tombusviridae* may similarly be associated with HSP70. Further experiments are required to ascertain this possibility and its significance to the disassembly process.

Although my data shows that Hsc70-2 is intimately associated with CNV virions, I do not know the details of its association from a structural point of view. However, in analogy to the maturation protein of MS2 bacteriophage, which replaces 1 CP dimer in the T=3 structure, it is possible that Hsc70-2 (~70 kDa) may a replace a CNV CP dimer (~82 kDa).

How then does Hsc70-2 become associated with CNV particles? HSP70 homologs are known to require a short region of hydrophobic residues flanked by basic amino acids for efficient binding of substrates (56, 268, 269). Interestingly, the 18 aa β region of the CNV CP arm is highly hydrophobic and this is flanked by highly basic regions in the adjacent R domain and ε region of the arm. It is possible that this represents the site of interaction of Hsc70-2. This is a likely possibility since it is known that the CNV arm region acts as a transit peptide targeting CNV CP to chloroplasts (220) and many transit peptides are believed to interact with HSP70 homologs (100-102). Moreover, I have shown that HSP70 homologs are required for CNV entry into chloroplasts and that Hsc70-2 increases the accumulation of CNV virus-like particles (122). In addition, I have found that Hsc70-2 interacts with CNV CP *in vivo* (122).

I propose that Hsc70-2 bound to the CNV arm region of the CP becomes associated with CNV particles during virion assembly. Alternatively, Hsc70-2 may associate with the arm region following assembly during the CNV breathing process when the arm becomes externalized. Consistent with these suggestions, I have found that mutant CNV particles that lack the β region of the arm do not associate with HSP70 homologs to a detectable level as determined by Western blot analysis (S.B. Alam, unpublished observations). Additionally, unlike WT CNV, mutant virions do not produce a significantly greater number of local lesions on heat-shocked versus

non-heat-shocked *C. quinoa* (S.B. Alam, unpublished observations). Further experiments are required to address the site on CNV CP or particles where Hsc70-2 is bound and how Hsc70-2 becomes associated with virions.

In Figure 3.6B and 3.6C respectively, I found that CNV particles incubated with HSP70 antibody or CsCl purified virions having undetectable amounts of HSP70 produce fewer local lesions on *C. quinoa*. This finding suggests that the Hsc70-2 associated with CNV particles enhances the establishment of infection. This could be due to a role for Hsc70-2 in initiating virus disassembly. On the other hand, it is known that HSP70 homologs play a role in the formation of the replication complex of CNV and TBSV (18, 40). Therefore, it is possible that the associated Hsc70-2 assists in establishing infection by providing a source of Hsc70 for replication complex formation. It is also noted that, since CsCl purified virions produce local lesions on *C. quinoa,* it is possible that virion preparations might contain a very low level of Hsc70-2 which is beyond the capacity of detection by Western blot analyses. Alternatively, Hsc70-2 may enhance infectivity of CNV virions but may not be essential. Enhancement of infection could be due to a role in facilitating disassembly or perhaps by supplying the HSP70 homolog required for formation of the initial replication complex.

It is possible that many CNV virions may not be able to efficiently establish an infection in a susceptible host due to the absence of Hsc70-2 in the particle. This is consistent with the great number of virions required to establish an infection. For example, in *C. quinoa,* 40 pg of virus (~2.7 X 10^6 molecules) produces an average of only approximately 20-40 local lesions. Although numerous factors certainly play a role in the ability of a particle to establish an

infection, it is possible that the association of Hsc70-2 with CNV may comprise one contribution to the establishment of infection.

To assess my hypothesis that Hsc70-2 assists CNV in disassembly I examined particles incubated with an excess of bacterially expressed Hsc70-2 by TEM analysis and found that approximately 7.5% of treated virions showed observable changes in morphology (see Figure 3.9B), I also examined Hsc70-2 treated particles for conformational changes by conducting chymotrypsin sensitivity assays where I found that a small proportion of the CP of these particles becomes accessible to chymotrypsin treatment. Together, these observations suggest that exogenously added Hsc70-2 changes the conformation of CNV particles, consistent with a role in virus disassembly.

I noted that only a small proportion of CNV particles are altered following incubation with bacterially expressed Hsc70-2 (Figure 3.9B). One likely explanation for this is that HSP70 homologs are known to have a lower affinity for natively folded polypeptides than for misfolded or alternatively folded polypeptides (86). Also, the *in vitro* reaction conditions likely do not sufficiently mimic the complex intracellular environment where CNV disassembly occurs.

I conducted local lesion assays using either CNV virions (Figure 3.8A) or CNV RNA (Figure 3.8B) on heat-shocked *C. quinoa* to distinguish between the possibilities that HSP70 homologs assist in CNV disassembly versus assisting in some other aspect of the initiation of infection, such as supplying HSP70 homologs needed for formation of the replication complex. I found that although the number of local lesions did not change in heat-shocked versus non-heat-

shocked plants when viral RNA was used as the inoculum, that the number of local lesions was significantly higher when virions were used as inoculum. This reinforces my conclusion that HSP70 homologs, or more specifically Hsc70-2, assists in the efficiency of the establishment of infection by assisting in particle disassembly. This finding also suggests that cytoplasmic HSP70 homologs may further assist in CNV disassembly beyond that which is facilitated by CNV bound Hsc70-2.

Conformational change of viral capsids during cellular entry and uncoating has been suggested or documented for several animal and plant viruses including *Human rhinovirus 2*, *Poliovirus*, *BK polyomavirus*, TBSV, TMV, TCV, *Carnation mottle virus* (CarMV), SBMV, *Turnip yellow mosaic virus*, BMV, CCMV, AMV, RCNMV and FHV (36, 37, 255, 270-274). In the case of TBSV, TCV, RCNMV and SBMV it has been suggested that particles swell in the higher pH, low calcium environment of the cytoplasm leaving a hole at the particle 3-fold axis where the RNA can exit (37, 258, 259, 275-277). Additionally, for AMV, TMV, TCV, CCMV, FHV and BMV (36, 37, 255, 273) it has been suggested that the particles undergo co-translational disassembly whereupon the exposed virion RNA of partially disassembled particles binds ribosomes and subsequent translation assists in further uncoating of particles. I also noted that following numerous attempts to observe co-translational disassembly of CNV in wheat germ extracts and rabbit reticulocyte lysates, translation products were not observed even when particles were swollen prior to addition to the cell free translation systems or when particles were pretreated with Hsc70-2 (S.B. Alam, unpublished observations). Thus it is possible that CNV differs from other similar non-enveloped viruses and TMV in that disassembly does not occur

co-translationally. Alternatively, it may be that the cell-free systems are lacking the components normally present in a cell that are required for co-translational disassembly of CNV.

The data described in this chapter supports the notion that CNV CP can co-opt HSP70 homologs for virion disassembly. Like most spherical viruses, CNV persists in a metastable state where it can exist in two distinct conformations: a compact closed state and relaxed (expanded) open conformation (13, 37, 55, 257, 258). Virions can undergo a breathing phenomenon during which it moves from a closed to an open conformation. These two states of the particle could be influenced by conditions within the host cell such as high pH or low calcium ions, where the particle would be in the expanded conformation. In analogy to TBSV, the R and arm region wholly or partially externalize during particle expansion and an opening is created at the particle quasi three-fold axis (26). It is possible that the viral RNA comes out of the hole from the three-fold axis that is created during particle swelling as has been suggested for *Carnation mottle virus* and other viruses (258). It is possible that CNV bound Hsc70-2 assists in this breathing phenomenon, promoting expansion under favourable cytoplasmic conditions such as elevated pH and low calcium. Experiments were conducted in which CNV particles were incubated with Hsc70-2 at pH 7.5 and then analyzed for a change in conformation by agarose gel electrophoresis, a procedure that can readily identify swollen CNV particles (59); however, no difference could be discerned using this method possibly due to a low number of particles that may be affected by Hsc70-2 as deduced from the TEM and chymotrypsin experiments conducted in Figure 3.9.

I provide the following hypothetical model for CNV virion disassembly facilitated by Hsc70-2 (For more details see Chapter 5, Section 5.2.1). According to this model, CNV acquires Hsc70-2 during the assembly process possibly due to Hsc70-2 interaction with the transit peptide-like region of the arm of the CNV CP. The disassembly process is facilitated by the bound Hsc70-2 along with the high pH environment of the cytoplasm resulting in CNV expansion which creates an opening in the particle at the quasi three-fold axis. As the arm and R domains externalize through this opening, virion RNA may be concomitantly externalized. Recently, we have shown that the R domain of CNV contains a highly basic KGKKGK region which likely binds viral RNA within the capsid (164). Also, the arm domain contains a KGRKPR region which may similarly bind virion RNA (see Chapter 4). Thus it seems possible that RNA bound to these basic sequences may exit the virion in association with R and arm domain externalization. The RNA may then be accessible for translation of the p33 and p92 ORFs, which encode the auxiliary replicase protein and RNA dependent RNA polymerase, respectively. As we have found that CNV produces a greater number of local lesions on plants overexpressing HSP70 homologs (Figures 3.6 and 3.7), it is possible that cytoplasmic HSP70 homologs may further assist in CNV disassembly beyond that facilitated by the virion associated Hsc70-2. This may allow for a more complete disassembly and release of viral RNA which may be required to "untangle" the partially disassembled virion. Finally, it is possible that the Hsc70-2 associated with the particle or the sequestered HSP70 homologs may assist in the formation of the replication complex.

In summary, I have provided evidence that CNV particles are associated with Hsc70-2 and that this association may contribute to particle disassembly. I believe this finding may provide

fruitful insight into the multifaceted aspects of the disassembly process of other non-enveloped viruses as well.

Chapter 4: Evidence for the role of basic amino acids in the coat protein arm region of *Cucumber necrosis virus* in particle assembly and selective encapsidation of viral RNA over host RNA[4]

4.1 Introduction

Virion assembly is one of the most important steps in the virus multiplication cycle. In the case of small icosahedral RNA viruses the most commonly occurring form of virion assembly is nucleic acid-assisted capsid assembly where packaging of viral nucleic acid occurs concomitantly with capsid formation. More rarely, formation of capsid structures occurs which is followed by filling of the capsid with previously synthesized viral RNA (53, 55). The newly formed progeny virions contain the genetic information necessary for replicating in new cells of the same plant or in another susceptible host. Virions also protect the encapsidated genome from both the intracellular and extracellular environment and, as well, may assist in cell-to-cell movement, systemic movement and vector transmission (55, 278).

In many cases packaging of ssRNA viruses involves recognition of specific packaging signals (PS) on viral RNA and CP or CP oligomers (for details see Section 1.19.6). This recognition nucleates the virion assembly process which is then followed by addition of further CP molecules or oligomers. This second stage of the assembly process could simply involve successive interactions between CP molecules until assembly of the virion is complete. However, numerous studies suggest that viral RNA plays a crucial scaffolding type role in facilitating further assembly by recruiting additional CP molecules via either non-specific or specific interactions with motifs on viral RNA (53, 55, 173, 174). Ionic interactions between the

[4] A version of this Chapter is under preparation for publication.

phosphate groups of viral RNA and the basic aa side chains of the CP have been found to play an important role in virion assembly and stability (51, 137, 157, 164, 166, 279). In numerous previous studies including those on *Satellite tobacco necrosis virus*, *Beet black scorch virus*, *Brome mosaic virus* (BMV), *Ourmia melon virus*, *Cucumber mosaic virus*, *Alfalfa mosaic virus*, *Red clover necrotic mosaic virus*, *Cowpea chlorotic mottle virus*, *Sesbania mosaic virus*, *Flock house virus* (FHV), *Human immunodeficiency virus*, *Macrobrachium rosenbergii nodavirus* and *Melon necrotic spot virus* (MNSV), it has been shown that basic motifs in the N-terminal inward facing portion of the CP play an important role in viral RNA interaction (51, 53, 55, 151-163). In BMV, it has been suggested that this region interacts with viral RNA promoting both assembly and virion stability partly through electrostatic interactions (157).

Cucumber necrosis virus (CNV) is an excellent model system virus for characterizing fundamental aspects of virus assembly *in vivo* as the virus multiplies to very high levels in plants and both the cryo-EM and X-ray crystal structure have been determined (13, 14). As well, an infectious cDNA clone is available for mutagenesis studies (13, 14, 31). CNV belongs to the genus *Tombusvirus* in the family *Tombusviridae*. CNV virions contain an approximate 4.7 kb positive polarity ssRNA genome that encodes five proteins. The p33 auxiliary replicase factor ORF is read through to produce the RNA dependent RNA polymerase (p92) from genomic RNA (gRNA) template (16). The internally located CP (p41), along with the silencing suppressor (p20) and the movement (p21) are translated from subgenomic RNA (sgRNA) of 2.1 kb and 0.9 kb, respectively (16). The CNV particle is a T=3 icosahedron, consisting of 180 identical copies of the 41 kDa CP.

Based on the X-ray crystal structure of CNV along with the cryoEM structure (13, 14) the CP exists in three different conformations (A, B and C) in the icosahedron. Each of the CP subunits folds into three distinct structural domains. The N-terminal RNA binding domain (R) interacts with virion RNA (vRNA) and forms the inner shell of the virion. The shell domain (S) constitutes the capsid backbone and forms the outer shell of the virion. The protruding domain (P) is the C-terminal domain and forms 90 dimeric protrusions on the surface of the particle. The P and the S domains are connected by a short five aa hinge (h). The arm region of 34 amino acids (aa) flexibly connects the R and S domains thereby contributing to T=3 icosahedral symmetry (16, 22). The CP arm consists of a β region rich in hydrophobic aa residues as well as an ε region rich in basic aa (22).

The arm is ordered in the C subunit and disordered in the A and B subunits. The β regions of the arms of three C subunits intertwine to form a β-annulus at the particle 3-fold axis that contributes to particle stability and forms a bridge to the inner shell (22, 59). The ε region of the C subunit arm lies along the inner face of the S domain antiparallel to the first β-sheet. The A and B subunit arms are flexible and can extrude from the particle interior upon virion breathing (13, 21).

The cryo EM structure of the CNV particle was the first to show that it consists of an outer shell and a structured inner shell as described above (13). It has been suggested that the highly structured inner shell which is formed, at least in part, from the R domain that serves as a scaffold important in the assembly of T=3 particles (21). CNV vRNA is sandwiched between the outer and the inner shells likely, in part, through interactions with the R domain (13, 21).

Previous work in Dr. Rochon's lab has identified a highly basic "KGKKGK" sequence in the C-terminus of the R domain as playing an important role in virus assembly and in the encapsidation of the full-length genome during infection (164). The ε region, may, like the R domain, bind vRNA as it is also rich in basic aa and its position in the particle is co-incident with vRNA based on neutron scattering studies of the related *Tombusvirus, Tomato bushy stunt virus* (TBSV) (280). The complete ε region has also previously been found to be essential for formation of particles (22). I wished to test the hypothesis that the basic aa sequences in the CNV CP arm region of the C/C dimer as well as A/B dimers might play an important role in binding RNA within virions and promoting virus particle assembly and stability. The ε region of the CNV CP arm contains a highly basic "KGRKPR" sequence that consists of four basic aa residues. Hence, I postulate that the "KGRKPR" sequence of the C subunit arm, which colocates with vRNA may play an important role in vRNA encapsidation and particle assembly.

In the present study I extend previous studies on the role of basic aa in the N-terminal region of the CNV CP in particle assembly. I have analyzed the role of specific basic aa in the ε region of the CNV CP arm in encapsidation of RNA during infection. I have found that replacement of one or two of the basic aa in the "KGRKPR" sequence of the ε region results in a lower level of virion accumulation and replacement of all four aa results in a near loss of virion formation demonstrating the essential role of this sequence in CNV assembly. I have also shown that replacement of one, two or four aa results in increased formation of particles having T=1 icosahedral symmetry. Additionally, I have found that these replacements are also associated with reduced encapsidation of vRNA as well as increased relative encapsidation of host RNA

suggesting that the ε region of the CP arm plays an important role, either directly or indirectly, in selection of CNV RNA over host RNA for encapsidation during particle assembly.

4.2 Materials and methods

4.2.1 Structural analysis of CNV CP C/C dimer

The protein data bank (PDB) file for the CNV CP C/C dimer was kindly provided by Dr. Thomas Smith (Biochemistry and Molecular Biology, UTMB). The location of the basic aa residues in the "KGRKPR" sequence in the CNV CP C/C dimer was analysed using RasMol software VERSION 2.7.5.2 (http://rasmol.org/OpenRasMol.html).

4.2.2 Site-directed mutagenesis

All mutations in the ε region of the CNV CP arm mutants M1-M7 (see Figure 4.2A) were generated using a PCR-based method (281). Two 5' phosphorylated diverging primers (Table 4.1) were used that contained the substituted bases required for converting the desired K or R residue to A. All mutagenic PCR reactions were conducted using a WT CNV cDNA sub-clone in pUC19 that encompasses the complete CP ORF. The mutated CNV CP region was sequenced for the desired mutation and cloned back into the WT CNV clone using EcoRI and BglII which cleave upstream of the CP ORF and within the CP ORF, respectively, and contain the mutated CP arm ε region. The region between the EcoRI and BglII sites was resequenced to confirm the presence of the mutation and to ensure that no unintended mutations were introduced. See Table 4.1 for a list of mutagenic primers for each mutant.

4.2.3 Transcript inoculation

Equal amounts of T7 polymerase run-off transcripts of WT CNV or mutants M1-M7 were produced and used to inoculate carborundum dusted 4-6 week old *N. benthamiana* leaves as previously described (31).

4.2.4 TLR extraction and electrophoresis

Two to three comparable leaves on 6-10 *N. benthamiana* plants were inoculated with WT CNV or mutant transcripts as described above. At 4 dpi, infected leaf tissue was collected and combined and ground to a fine powder in liquid nitrogen. TLR was extracted from 100 mg of ground material using the RNeasy Plant Mini Kit (Qiagen) according to the manufacturer's instructions. RNA was analyzed by electrophoresis through 1% agarose gels buffered in 0.5 X TBE and visualized by staining with EtBr as previously described (30).

4.2.5 SDS-PAGE and Western blot analysis

TLP samples were obtained by grinding leaf tissue to a fine powder in liquid nitrogen as described previously (122). For Western blot analysis equal amounts of TLP obtained from equal masses of leaf tissue were electrophoresed through NuPAGE 4-12% Bis-Tris gels (Thermo Fisher Scientific), blotted onto PVDF membranes (Bio-Rad) and probed with the CNV CP antibody made to the bacterially expressed shell and protruding domains (SP antibody) as described in the figure legends. Western blots of virion proteins were conducted similarly using approximately equivalent masses of virions and the blot was probed with SP antibody.

4.2.6 Virus purification by “midiprep” procedure

Infected leaf material (~4.5 to 6 g) at 4-5 dpi was collected, ground in liquid nitrogen and added to at least 5 volumes of 100 mM NaOAc pH 5.0 containing 20 mM β-mercaptoethanol. The slurry was gently rotated at 4°C for at least 1 h and then centrifuged at 8000 x g for 15 min at 4°C to remove plant debris. The supernatant was passed through two layers of Miracloth (Calbiochem) and the solution was adjusted to 8% polyethylene glycol (PEG 8000, Sigma-Aldrich) followed by incubation for at least 2 h at 4°C with constant stirring. Virus was pelleted at 10,000 x g for 20 min at 4°C then resuspended in 10 mM NaOAc, pH 5.0. The virus was subjected to constant rotation at 4°C overnight, and then centrifuged again at 15,000 x g for 20 min at 4°C to remove residual debris. The supernatant (containing virions) was collected and stored at 4°C until further use. For large scale virus extraction (greater than 10 g of tissue) a similar method was employed except infected material was homogenised in a blender.

4.2.7 Agarose gel electrophoresis of purified particles

For comparative analysis of the accumulation level of virions produced by mutants M1-M7 and WT CNV, virus extraction was performed using equal amounts of leaf tissue and the final virus pellet was resuspended in equal volumes of 10 mM NaOAc, pH 5.0 as described above. Virus particles were electrophoresed through 2% (w/v) agarose gels in TB buffer (45 mM Tris, 45 mM borate, pH 8.3) for 2 h as described previously (30). Virions were stained with EtBr in the presence of TB buffer containing 1 mM EDTA and photographed under ultraviolet illumination (Gel Doc, Alpha Innotech Corporation) to visualize vRNA (59). To visualize virion protein, SYPRO Ruby (Thermo Fisher Scientific) was used as the stain. To stain, the gel was submerged

in SYPRO Ruby protein gel stain (Thermo Fisher Scientific) overnight and then destained in wash buffer (10% methanol, 7% acetic acid) for 1 h.

4.2.8 Virus yield

The following formula was used for the calculation of % yield of mutant virions. % yield of mutant virions = µg virions produced/g of infected leaf tissue divided by that of WT CNV X 100. The mass of virions was determined by electrophoresis of several dilutions of the virions followed by staining with SYPRO Ruby as described above using WT CNV as a standard.

4.2.9 Percent RNA encapsidation

The following formula was used for the calculation of % RNA encapsidated by mutant virions. % RNA encapsidation of mutant virions = yield of vRNA obtained in ng from pancreatic ribonucleaseA (RNaseA) treated virions /µg of virus divided by that obtained for WT CNV X 100. RNaseA was used to remove any contaminating host RNA that may have co-purified with virions during the extraction procedure. The yield of vRNA was obtained by measuring the concentration of RNA at A_{260nm} spectrophotometrically using a NanoDrop® ND-1000 spectrophotometer V3.3 (Thermo Fisher Scientific). The mass of virions was determined by electrophoresis of several dilutions of the virions followed by staining with SYPRO Ruby as described above using known concentrations of highly purified WT CNV as a standard. The concentration of highly purified CNV RNA was determined spectrophotometrically where the absorbance at 260 nm of a 1 mg/ml suspension of CNV = 4.5.

4.2.10 Transmission electron microscopy

Electron microscopy using approximately 600 ng of purified virus particles per grid was conducted as described previously. Uranyl acetate (2%) was used as the negative stain (22).

4.2.11 Thermostability assay

Thermal stability of the double "KGRKPR" mutants and WT CNV particles was determined as described previously (22).

4.2.12 RNaseA treatment of virions

WT CNV and "KGRKPR" mutant virions (13-251 µg) were treated with pancreatic RNaseA (Thermo Fisher Scientific), when indicated, at a concentration of 0.02 ng/ul in10 mM NaOAc pH 5.0 for 30 min at RT in a 400 µl reaction volume. Prior to vRNA extraction, as described below, the mixtures were adjusted to 20 mM β-mercaptoethanol to inhibit RNaseA activity during the purification procedure. Purified RNA was subjected to the RNeasy Mini protocol as recommended by the manufacturer (Qiagen) to remove residual RNaseA from the vRNA preparation.

4.2.13 vRNA extraction

Five hundred µl of water-saturated phenol, equilibrated with 1X vRNA extraction buffer (200 mM Tris, 50 mM EDTA, pH 8.8) containing 1% SDS, was mixed with 100 µl of 5X vRNA extraction buffer containing 5% SDS and 1% β-mercaptoethanol (BME). Four hundred µl of solution containing 10-50 µg of virions in 10 mM NaOAc, pH 5.0 was added to the above and vigorously mixed for 5 min. The mixture was centrifuged at 15,000 x g for 2 min at 4°C and the aqueous phase was removed. To increase the yield of vRNA, the organic phase was back extracted with 200 ul of water. This aqueous phase was combined with the previous aqueous phase and re-extracted with phenol/chloroform/isoamyl alcohol (25:24:1) followed by extraction of the aqueous phase from this treatment with chloroform/isoamyl alcohol (25:1). vRNA was precipitated using 0.1 volumes of 2 M NaOAc pH 5.8 and 2.5 vol of absolute ethanol and placed at -80°C for 1 h. Following centrifugation at 20,000 x g for 15 min the pellet was washed with 70% ethanol, briefly dried, resuspended in sterile water and stored at -80°C until use.

4.2.14 Northern blot analysis

vRNA extracted from RNaseA treated WT CNV or "KGRKPR" mutant virions M1-M7 were electrophoresed through 1% formaldehyde containing agarose gels (135) and transferred to Zeta-Probe GT blotting membranes (BioRad) in 10X SSC (1.5 M NaCl, 150 mM sodium citrate). For viral RNA detection, the RNA blot was hybridized with either a randomly primed ^{32}P-labelled full-length CNV cDNA (35 ng) probe of 4702 nt or a CNV cDNA probe corresponding the 3' terminal 428 nt (25 ng) of CNV RNA as indicated in the corresponding figure legends. The Random Primers DNA Labeling System was utilized for making the probe (Thermo Fisher

Scientific). For host RNA detection, the RNA blot was hybridized with a randomly primed ^{32}P-labelled cDNA probe prepared to 2 µg of TLR from uninfected *N. benthamiana* using ReadyMade Random Hexamers (Integrated DNA Technologies) and SuperScript® IV Reverse Transcriptase as recommended by the manufacturer's protocol (Thermo Fisher Scientific).

4.2.15 Percent relative encapsidation efficiency of viral versus host RNA

The peak intensity of all the bands in a single lane observed in the unsaturated image of the EtBr stained gel of WT or mutant vRNA (Figure 4.5A, panel i) or of unsaturated images of the Northern blots of similar gels probed with full-length WT CNV cDNA (Figure 4.5A, panel iii) or uninfected *N. benthamiana* cDNA (Figure 4.5A, panel iv, omitting the non-specific hybridization signal to WT CNV as indicated by the arrow) was quantified using ImageJ software (https://imagej.nih.gov/ij/). The cumulative peak intensities obtained for viral RNA or host RNA for each virion type (WT CNV or the mutants) as determined from the Northern blots were standardized relative to total vRNA intensity values obtained from EtBr stained gel by dividing the former with the latter. The normalized viral RNA and host RNA intensities were then added to obtain total normalized vRNA followed by determining the percentage of viral versus host RNA encapsidated.

Table 4.1: Oligonucleotides used for PCR

Primer name[a]	Sequence from 5' to 3' direction[b]	Description of use[c]	pK2/M5 binding position
CNV354F	**GC**ACCTAGGTTTCAAA CAGCAAAAGGATCTGT GC	5' IVM primer used in combination with CNV355R to mutate "KGRKPR" to "KGRAPR" (M1)	2878-2910
CNV355R	CCTTCCTTTAACCGCAT AGGC	3' primer used in combination with CNV354F and CNV356F to mutate "KGRKPR" to "KGRAPR" (M1) and "KGRKPA" (M2) respectively	2856-2876
CNV356F	AAACCTGCGTTTCAAAC A**GC**AAAAGGATCTGTG C	5' IVM primer used in combination with CNV355R to mutate "KGRKPR" to "KGRKPA" (M2)	2877-2910
CNV361F	**GC**ACCTGCGTTTCAAA CA**GC**AAAAGGATCTGT GC	5' IVM primer used in combination with CNV355R to mutate "KGRKPR" to "KGRAPA" (M3)	2877-2910
CNV362R	**CG**CTCCT**GC**AACCGCA TAGGCATAAGAGATTG G	3' IVM primer used in combination with CNV361F to mutate "KGRKPR" to "AGAAPA" (M4)	2844-2876
CNV357F	AAACCTAGGTTTCAAA CAGCAAAAGGATCTGT GC	5' primer used in combination with CNV358R and CNV362R to mutate "KGRKPR" to "KGAKPR" (M5) and "AGAKPR" (M7) respectively	2877-2910
CNV358R	**CGC**TCCTTTAACCGCAT AGGCATAAGAG	3' IVM primer used in combination with CNV357F to mutate "KGRKPR" to "KGAKPR" (M5)	2849-2876
CNV393R	CCTTCCT**GC**AACCGCAT AGGCATAAGAG	3' IVM primer used in combination with CNV357F to mutate "KGRKPR" to "AGRKPR" (M6)	2849-2876

[a] F=forward primer; R= reverse primer.

[b] Nucleotides in bold correspond to mutagenized nucleotides used to replace the basic aa in the "KGRKPR" sequence shown in Figure 4.2A with A residues.

[c] IVM=*in vitro* mutagenesis.

4.3 Results

4.3.1 The ε region of the CNV CP arm is rich in basic amino acid (aa) residues

In a previous study (22), it was found that deletion of the complete ε region of the CNV CP arm in an infectious cDNA clone of CNV resulted in the inability of the infectious transcripts to produce virions in inoculated *N. benthamiana*. This led to the possibility that the ε region contains essential information for particle assembly; however the specific amino acids responsible for particle assembly were not determined. This, in conjunction with the studies of *Timmins et al.* (1994) (280), which showed by neutron scattering studies that vRNA lies predominantly beneath C/C dimers (which correspond to the ε region), suggested that that the ε region may contain residues that are essential for encapsidation of vRNA.

Figure 4.1A shows the aa sequence of the ε region of the CNV CP arm where it can be seen that five of the 16 aa residues are either lysine (K) or arginine (R) residues making this region highly basic. Additionally, all other sequenced members of the *Tombusvirus* genus also contain a high proportion of basic aa residues in the ε region. Such conservation of basic aa residues was also observed in several other members of the *Tombusviridae* family (data not shown). Additionally, a similar region in the MNSV CP has been shown to play a role in RNA binding (163). Also, as described above, a previously identified RNA binding region in the CNV CP R domain (164), which bears the sequence "KGKKGK", is highly similar to the basic sequence "KGRKPR" in the ε region of the arm. These observations led us to hypothesize that this portion of the ε region of the CP arm may play a role in particle assembly and stability by mediating RNA protein interactions during the assembly process and maintaining the structural integrity of virions.

The spatial positioning of the "KGRKPR" sequence in the ε region of the C subunit of CNV CP arm is shown in Figure 4.1B. In the C subunit, but not the A and B subunits, the arm is structured and lies antiparallel to the first β sheet of the S domain and thus the position of basic residues in the arm can be readily determined (13). Figure 4.1B demonstrates that the "KGRKPR" sequences of the two C subunits of the C/C dimer are clustered and next to each other below the two shell domains of the C/C dimer and thus within the interior of the capsid as expected. This positioning points to a role for the basic aa of the "KGRKPR" region in interacting with virion RNA within the CNV particle possibly promoting viral RNA assembly and/or particle stability.

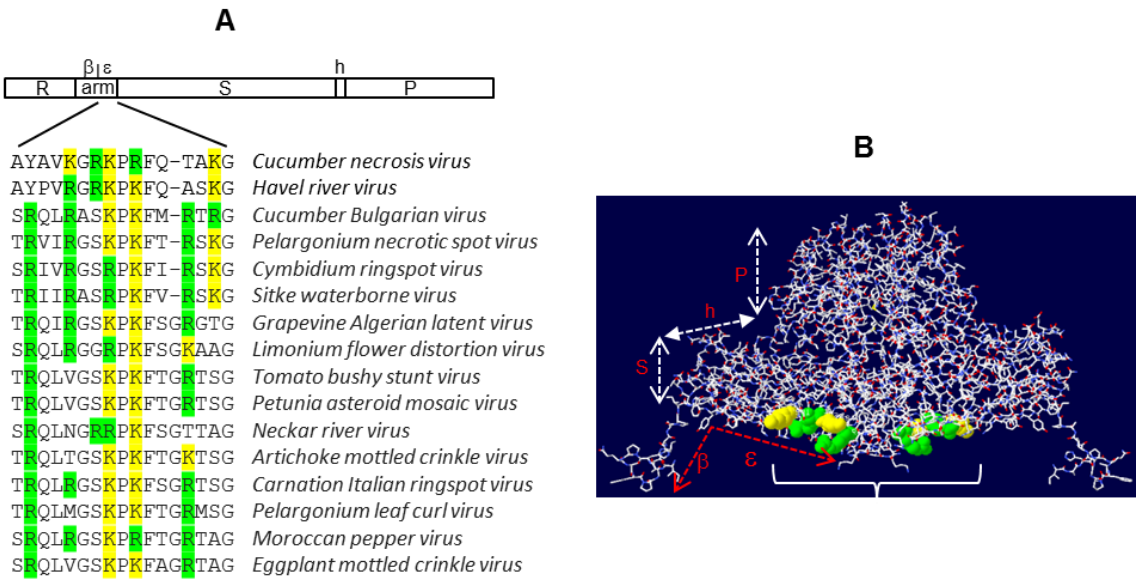

Figure 4.1: The epsilon (ε) region of the CNV CP is conserved among *Tombusviruses*, being rich in basic amino acid residues which lie under the C/C dimer facing the interior of the particle.

(A) A diagrammatic linear representation of the CNV CP showing the three major domains R, S and P as well as the arm and h regions. The two structural regions of the arm, β and ε, are indicated. The expanded region shows an aa sequence alignment of the CP ε region of several sequenced members of the *Tombusvirus* genus. The basic aa residues [lysine (K) and arginine (R)] are highlighted in yellow and green, respectively. (B) The tertiary structure of a C/C dimer of the CNV CP showing the K and R residues of the "KGRKPR" sequence in yellow and green respectively. The position of the CP arm is shown in red (indicating the β and ε regions). The shell (S), hinge (h) and protruding (P) domains in one of the two subunits are indicated by the dashed white lines. The approximate portion of the C/C dimer where the density of vRNA is hypothesized to be maximum according to *Timmins et al.* (1994) (280) is shown with a white bracket. The R domain is unstructured in the X-ray structure and therefore is not shown.

4.3.2 Mutations in basic residues in the "KGRKPR" sequence affect genomic RNA, CP and particle accumulation

To assess the importance of basic aa in the "KGRKPR" sequence in particle formation and assembly of viral RNA, I performed mutational analyses on a full-length infectious CNV cDNA clone [pK2/M5; (31)] referred to here as WT CNV. Seven different mutants were constructed as shown in Figure 4.2A where the basic amino acids (K or R; shown in yellow or green, respectively) of the "KGRKPR" sequence were replaced by alanine indicated in red. Four single substitution mutants (M1, M2, M5 and M6), two double substitution mutants (M3 and M7) and one quadruple substitution mutant affecting all four basic aa residues (M4) were constructed. Equal amounts of transcripts from WT CNV and the seven different "KGRKPR" mutants were used to inoculate *N. benthamiana* leaves followed by collection of infected leaf tissue at 4 dpi. The collected samples were analysed for levels of CNV gRNA in total leaf RNA (TLR) preparations, for levels of CNV CP in total leaf extracts and for the levels and electrophoretic profiles of virions. The results are summarised in Figure 4.2B-4.2E.

We first wished to examine the levels of gRNA present in total leaf RNA extracts of the various "KGRKPR" mutants relative to CNV. Figure 4.2B, panel i, shows one such experiment where equal quantities (500 ng) of TLR obtained from leaf tissue infected with the seven different "KGRKPR" mutants and WT CNV were electrophoresed through an agarose gel and stained with EtBr. It can be seen that the gRNA for the different mutants (lanes 2-8) accumulates to apparently similar levels relative to WT CNV gRNA (lane 1). To examine this further, I conducted additional similar experiments and analyzed the data using densitometry. Figure 4.2B, panel ii, is a graphical representation of the percent gRNA accumulation of "KGRKPR"

mutants relative to WT CNV from two or more independent experiments. It can be seen that the mutants M1-M7 accumulate at slightly lower levels compared to WT CNV (i.e., approximately 96%, 94%, 83%, 73%, 80%, 79% and 90%, respectively). The lower levels of accumulation are especially evident for the latter four mutants (M3-M6), with mutant M4 showing the lowest level of gRNA accumulation (73%). The slightly lower level of accumulation of the mutant gRNAs could suggest that the mutations in the "KGRKPR" sequence are affecting viral RNA replication and/or accumulation. However, a lower level of accumulation of gRNA might be expected if the CP does not assemble with gRNA as efficiently, as this would render the gRNA more susceptible to RNAase. Thus, the presented data are consistent with the possibility that the mutations in the "KGRKPR" sequence affect virion assembly, but other possible effects of the mutations such as decreasing viral RNA replication cannot be ruled out.

We also conducted Western blot analyses of total leaf extracts obtained from equal masses of infected leaf tissue using a CNV CP antibody in order to assess the levels of accumulation of CP in the "KGRKPR" mutants relative to WT CNV. One such experiment is shown in Figure 4.2C, panel i, where it can be seen that generally lower levels of CP accumulate in mutant infected leaves as compared to WT CNV. Similar additional experiments were conducted and the data were examined by densitometric analyses. Figure 4.2C shows a graphical representation of the compiled data showing that CP accumulation is generally lower in mutants M1-M7 relative to WT CNV (i.e, approximately 88%, 80%, 72%, 50%, 86%, 89% and 71%, respectively). Again, the most striking difference in the level of CP accumulation was in mutant M4 which is only on average ~50% that of WT CNV. The generally lower level of accumulation of CP is not surprising given that gRNA accumulation levels are lower. However, in general, the %CP

accumulation levels are lower than the %gRNA accumulation levels (with the exception of mutants M5 and M6 which show slightly higher levels of accumulation of CP relative to genomic RNA accumulation (compare Figure 4.3B, panel 11 with Figure 4.3C, panel ii). Overall, it can be stated that CP accumulation is also affected in most of the mutants. It is possible that the mutation in the various "KGRKPR mutants affect translation of the CP or the production of sgRNA but experiments were not conducted to test these possibilities. It is also possible, as described above, that if the CP mutations negatively affect particle assembly then the accumulation of less CP would be expected since unassembled CP is likely to become degraded if not used for particle assembly.

We then extracted virions from equal masses of infected leaf tissue and electrophoresed the virions in duplicate gels, followed by staining with either EtBr or SYPRO Ruby to visualize vRNA and virion protein levels, respectively. It can be seen that virions of the "KGRKPR" mutants accumulated at significantly lower levels than that of WT CNV (Figure 4.2D, panel i, compare lane 1 with lanes 2-8). To facilitate visualization of the virions, 2X the volume of virions of the double mutants M3 and M7 (lanes 4 and 8) and 8X the volume of virions of the quadruple mutant M4 (lane 5) was loaded. I then conducted densitometric analysis of two or more independent experiments using SYPRO Ruby stained gels (SYPRO Ruby stained gel results were chosen over that of EtBr since it is possible that particles may encapsidate lesser amounts of RNA if the mutations in the "KGRKPR" sequence affect the amount of RNA that can be encapsidated as described further below). The compiled data are shown graphically in Figure 4.2D, panel ii. It can be seen that each of the mutants, M1-M7, show a lower level of accumulation of virions relative to WT CNV (i.e., approximately 56%, 64%, 35%, 1%, 59%,

60% and 26%, respectively). Moreover, the level of accumulation of virions is consistently lower than the level of accumulation of CP (Figure 4.2E), consistent with the notion that the changes in the basic aa of the "KGRKPR" sequence affect particle assembly and/or accumulation. The loss of particle accumulation in the M4 mutant is particularly striking as the level of CP accumulation is 58% but the level of virion accumulation is approximately 1% on average (i.e., 2% virion accumulation with respect to CP accumulation). The loss of particle accumulation in the double mutants M3 and M7 are also significant as particle accumulation is approximately 48.6% and 22.5% of CP accumulation, respectively. In the remaining single aa substitution mutants the reduction in on particle accumulation versus CP accumulation are less dramatic, being approximately 64%, 80%, 69%, and 86% for mutants M1, M2, M5 and M6, respectively.

It is to be noted that a faster migrating diffuse protein species indicated by an asterisk in lane 5 in the lower panel of Figure 4.2D, panel i was observed in mutant M4. This species was detected when SYPRO Ruby was used as the stain (lane 5, lower panel) but was not detected when EtBr was used as the stain (lane 5, upper panel) suggesting that the CP species detected by SYPRO Ruby may correspond to empty CNV particles. The faster migration of these particles could suggest that they correspond to previously described T=1 particles that have been found to be associated with certain CNV R domain mutants (21, 164). Alternatively, the particles may be T=3 particles but migrate faster since they lack detectable RNA and thus would have a lower net negative charge (282). The results of electron microscopic analyses of M4 particles will be described further below to clarify the nature of the particles. It also is noted that a low level of T=3-sized particles is observed in the SYPRO Ruby stained gel containing M4 particles (Figure 4.2D, panel i, lower panel, lane 5). A very low, but detectable level of staining is also observed

in the EtBr stained gel (Figure 4.2D, panel i, upper panel, lane 5) suggesting that the M4 mutant produced T=3 particles and that at least some of the T=3 particles produced by mutant M4 encapsidate RNA.

4.3.3 "KGRKPR" mutants encapsidate less RNA compared to WT CNV

I also determined the percent RNA encapsidated by "KGRKPR" mutants relative to WT CNV from independent experiments using spectrophotometric measurements and found that all the mutants encapsidated lower amounts of RNA (Figure 4.2F). When compared to CNV, the level of encapsidation of RNA by the single aa substitution mutants (M1, M2, M5 and M6) was only approximately 43-45% that of WT CNV particles, whereas that of the double aa substitution mutants (M3 and M7) was approximately 16-35.5%. RNA encapsidation efficiency was most significantly compromised in the quadruple mutant M4 which encapsidated RNA at only about ~0.86% compared to the level observed in WT CNV.

It is noted that the percent RNA accumulation in the "KGRKPR mutants (~0.86-45%) is lower than the percent yield of mutant virions (~0.98-64%) when compared to WT CNV (100%). This might suggest that some of the particles formed by the "KGRKPR" mutants might be empty (see TEM analysis in Figure 4.3). Also, some particles lacking RNA might be accumulate in mutant M4 as the particles stain with SYPRO Ruby but not significantly with EtBr (Figure 4.2D, panel i, lane 5). Overall, the results suggest that mutations of basic aa residues in the "KGRKPR" sequence of the CP, not only affects particle accumulation but also plays a role in the mass of RNA that can be encapsidated. This is not surprising since it has previously been shown in several cases that elimination of basic residues in virus particles results in less RNA being

encapsidated possibly in part due to balancing of electrostatic interactions between basic residues within the particle and phosphate residues of vRNA (157) (described in details in Section 1.19.2).

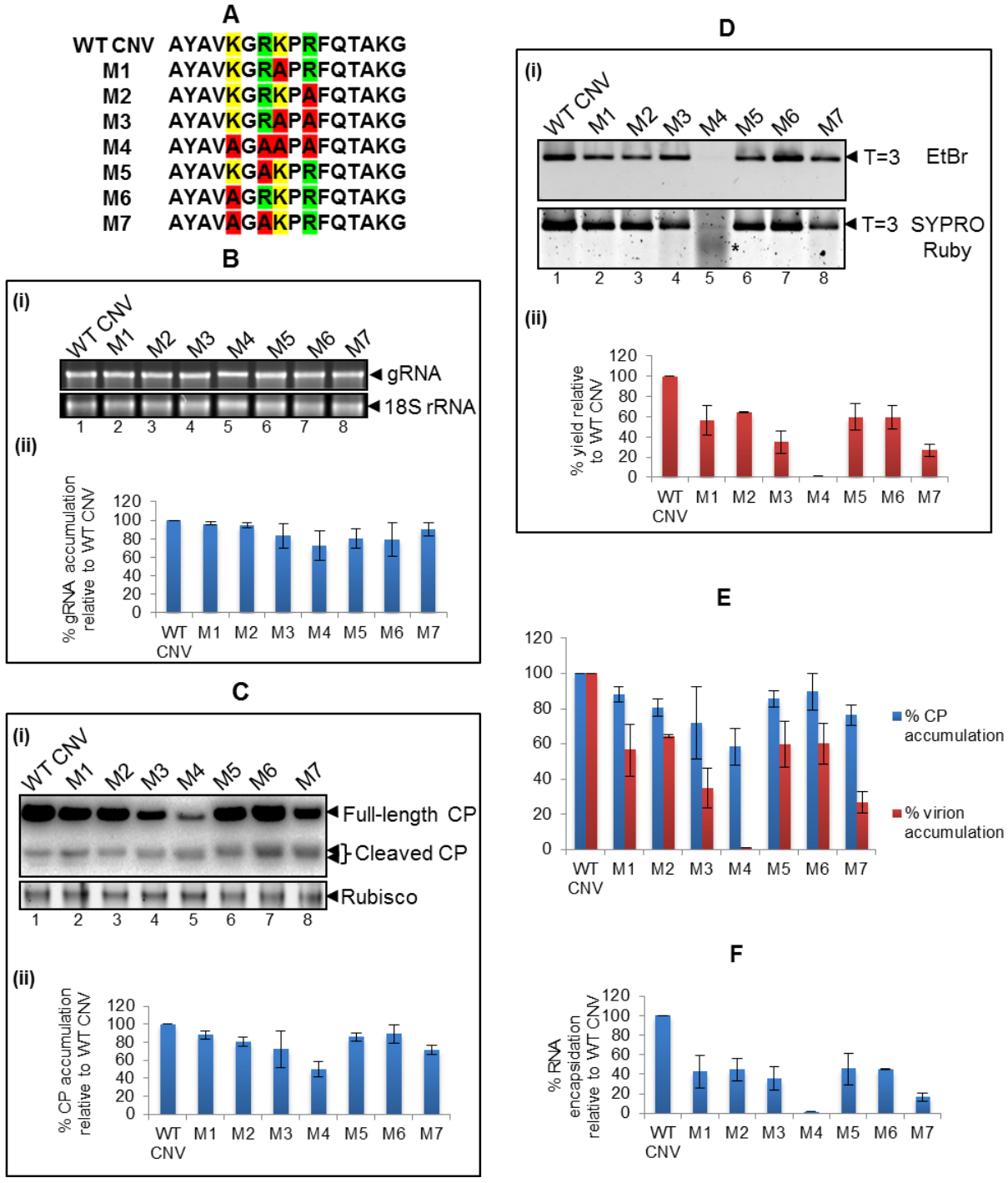

Figure 4.2: Mutations of basic residues in the "KGRKPR" sequence of the CNV CP arm ε region affect CNV particle accumulation.

(A) Diagrammatic representation of the CP ε region mutants (M1-M7) in the "KGRKPR" sequence. Mutations were introduced by site-directed mutagenesis where selected lysine (K) or

arginine (R) residues were mutated to alanine (A, shown in red). The WT CNV sequence is shown where K residues are highlighted in yellow and R residues in green. Mutated K or R residues in M1-M7 are highlighted in red. (B-D) Accumulation of CNV gRNA, CP and virions in mutants M1-M7. Equal amounts of transcripts of mutants M1 to M7 and of WT CNV were used to inoculate three leaves of seven *N. benthamiana* plants (21 leaves in total for each inoculation). The combined samples for each inoculation were ground in liquid nitrogen and equivalent portions were analysed at 4 dpi for the level of gRNA (B), CP (C) and virions (D). (B, panel i) Total leaf RNA (TLR) (500 ng) from mutants M1-M7 as indicated was electrophoresed through an agarose gel and then stained with EtBr. The upper panel shows gRNA and the lower panel cytoplasmic18S rRNA used as a loading standard. (B, panel ii) Graphical representation of % gRNA accumulation normalized to 18S rRNAs in mutants M1-M7 relative to WT CNV where WT CNV is arbitrarily assigned a value of 100%. The data are compiled from densitometric analysis from at least two independent experiments. The standard error is shown by the brackets above the bars. (C, panel i) Equal amounts of total leaf extract from equal masses of leaf tissue were subjected to SDS-PAGE in duplicate followed by Western blot analysis using the CNV CP antibody SP (upper panel) or by staining with SYPRO Ruby (lower panel). Levels of Rubisco in the lower panel were used to standardize the amount loaded onto the gel. Full-length CNV CP as well as cleaved CP species are indicated by arrows on the right side of the blot. (B, panel ii) Graphical representation of the % CP accumulation (normalized using Rubisco) relative to WT CNV where WT CNV is arbitrarily assigned a value of 100%. The data were taken from at least two independent experiments using densitometric analysis. Both the full-length and cleaved CP species are included in the total mass of CP. The standard error is shown by the brackets above the bars. (D, panel i) Virions were extracted from equal masses of WT CNV infected (lane 1) or from mutant infected (M1-M7; lanes 2-8, respectively) leaf tissue. Following extraction, pellets were resuspended in equal volumes and samples were subjected to agarose gel electrophoresis in duplicate followed by EtBr staining to visualize vRNA (upper panel) or SYPRO Ruby stain to visualize virion protein (lower panel). To permit better visualization, 2X the volume of virions were loaded for mutants M3 (lane 4) and M7 (lane 8) and 8X the volume of virions were loaded for mutant M4. The arrow head in the upper and lower panels indicate the electrophoretic position of CNV T=3 particles. The asterisk in lane 5 in the lower panel points to the position of putative T=1 particles (see text). (D, panel ii) Graphical representation of the average percent yield of mutant virions relative to WT CNV where WT CNV is arbitrarily assigned a value of 100%. The data were obtained by densitometric analysis and were compiled from at least two independent experiments. The standard error is shown by the brackets above the bars. The % yield was calculated using SYPRO Ruby stained virions. For mutant M4, both the upper and diffuse lower band (shown by the asterisk) was combined for densitometric analysis. (E) Comparison of the percent CP accumulation versus % virion accumulation relative to WT CNV. Data for the graphs were obtained from C, panel ii and D, panel ii. (F) Graphical representation of the average percent total RNA encapsidated in mutant virions relative to WT CNV virions where WT CNV is arbitrarily assigned a value of 100%. The data were obtained by spectrophotometric analysis of vRNA obtained from at least two independent experiments. The standard error is shown by the brackets above the bars. See Figure 4.5 for an analysis of the RNA species present in virions as determined by agarose gel electrophoresis and Northern blot analysis.

4.3.4 Virions of "KGRKPR" mutants are polymorphic

To examine the particle morphology of virions produced by "KGRKPR" mutants, I conducted transmission electron microscopy (TEM) of uranyl acetate stained virus preparations. Figure 4.3A, shows that while WT CNV predominantly produces T=3 particles, virions of the "KGRKPR" mutants are polymorphic consisting of both T=3 and T=1 particles, respectively. T=1 particles were previously found to be associated with specific CNV R domain deletion mutants as well as arm region mutants and have also been described in detail by cryo-electron microscopy (13, 21, 164).

Virions of mutants M3 and M4 contained some T=3 sized particles with darkly stained centers (see arrowheads in Figure 4.3A, panels ix and x). It is possible that these may correspond to empty particles (EPs). Since the assembly of CNV is believed to be RNA dependent, this observation may indicate that the RNA within these virions has become partly degraded following encapsidation, especially if the particles are not formed properly and are therefore permeable to ribonuclease. It is also possible that the structure of the particle has allowed uranyl acetate to become incorporated into the particle, unlike that observed with WT CNV virions. As described below, it is interesting that mutants M3 and M4 encapsidate a relatively high proportion of host RNA and encapsidate only a low level of full-length CNV RNA (see below; Figure 4.5A, lanes 4, 5, 8). The particles with darkly staining centers may therefore reflect encapsidation of host RNA a process which may produce malformed particles (173, 174). Further research is required to determine the nature of these particles.

A determination of the average percent of T=1 sized particles was conducted using TEM of uranyl acetate stained virions. Figure 4.3B summarizes the results. WT CNV was found to consist of only about 0.45% T=1 particles. Mutants M1, M2, M5 and M6 (containing single aa substitutions) were found to consist of ~4%, ~3%, ~3% and ~1% T=1 particles respectively. Thus in the case of M1, M2, M5 and M6 an increase in the number of T=1 particles over that of WT CNV is observed but only slightly so. The double mutant M7 contained ~6% T=1 particles. Mutants M3 and M4 (containing two or four aa substitutions, respectively) were found to consist of a dramatically higher percentage of T=1 particles, being ~26% and ~95%, respectively. Thus, in general, substitution of basic aa in the "KGRKPR" mutants correlates with the formation of particles having T=1 symmetry with substitution of all four basic aa leading to the greatest proportion of T=1 particles. Together, these results suggest that the basic aa residues in the "KGRKPR" sequence play an important role in determining particle morphology. The basis for the formation of T=1 particles is currently not known, however, it is possible that mutations in the "KGRKPR" region affect the ability of the CP arm to adopt the two distinct conformations (i.e., that found in C subunits and that found in A and B subunits) that are required for T=3 particle formation as has been previously suggested for other CNV CP arm mutants, including a mutant at the proline residue in the "KGRKPR" sequence (21, 60).

As has been previously described, CNV CP is targeted to chloroplasts and mitochondria during infection and during agroinfiltration (24, 243). Targeting to chloroplasts involves an initial cytoplasmic cleavage of the CP to an approximate ~34.7 kDa species which lacks the R domain and subsequent further cleavages to a ~32.9 kDa protein that lacks a portion of the arm and the complete R domain followed by a third cleavage at the junction of arm and shell to yield a 31.1

kDa species (24, 135, 243). So it is possible that mutant CP that cannot assemble into T=3 particles (particularly mutants M3 and M4 whose mutations flank the above described proline residue) becomes cleaved in the cytoplasm and during organellar uptake, and that these cleaved species are responsible for forming T=1 particles.

It is interesting that total leaf extracts of mutants M3 and M4 contain a relatively higher proportion of cleaved CP relative to full-length CP when compared to WT CNV and the other mutants (Figure 4.2C, panel i, compare cleaved with full-length CP in lanes 1 and 5). These cleaved products may therefore be the protein species that give rise to T=1 particles. Also, as will be described below, the CP species of virion preparations of M3 and M4 contain a relatively abundant amount of cleaved CP which likely derives from the T=1 particles present in these virion preparations.

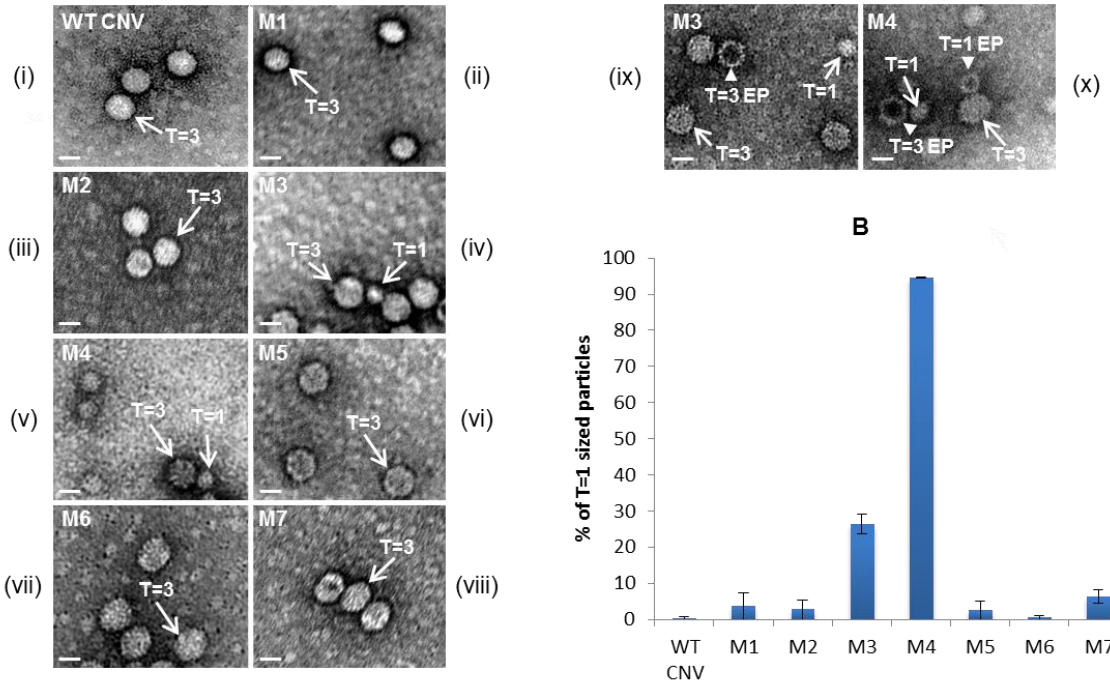

Figure 4.3: Virions of "KGRKPR" mutants are polymorphic.

(A) TEM analysis of virions extracted from *N. benthamiana* plants inoculated with "KGRKPR" mutants M1-M7 (panels ii-viii respectively) or WT CNV (panel i) as indicated. Particles were negatively stained with uranyl acetate. T=3 and T=1 particles are indicated with arrows and are assigned as such based on their estimated sizes of 34 nm and 23 nm, respectively. Panels ix and x are images containing empty particles (EP) found in virion preparations of mutants M3 and M4. The scale bar in panels i-x represents 34 nm. (B) Graphical representation of the % of T=1 sized particles for each mutant and WT CNV from two independent experiments. The standard error is shown as brackets above the bars.[(Set 1; WT CNV, N = 931; M1, N =136; M2, N = 452; M3, N = 566; M4, N = 925; M5, N = 510; M6, N = 240; M7, N = 619), (Set 2; WT CNV, N = 364; M1, N =165; M2, N = 219; M3, N = 334; M4, N = 203; M5, N = 180; M6, N = 171; M7, N = 154); N represents number of particles counted for statistical analyses].

4.3.5 Virion proteins of WT CNV and "KGRKPR" mutants contain cleaved species which may correspond to CP subunits of T=1 particles

Virions of each of the seven "KGRKPR" mutants along with WT CNV virions were subjected to SDS-PAGE followed by Western blotting to analyze the size of the CP species present in virions. Figure 4.4A shows that WT CNV as well as each of the mutants contains the full-length 41 kDa species (not visible in the short exposure in the M4 lane) as well as cleavage products of 34.7 kDa and 32.9 kDa. These cleavage products have been mapped by Edman degradation analysis (data not shown) and are consistently observed in CNV virion preparations subjected to denaturing gel electrophoresis [(135);unpublished observations], however, their origin has been unclear except the 34.7 kDa species corresponds to the complete CNV CP minus the R domain and the 32.9 kDa species to the complete CNV CP minus the R domain and the β region of the arm. Strikingly, M4 mutant virions consist predominantly of the 32.9 kDa species (lane 5) with a longer autoradiographic exposure showing a small amount of the full-length 41 kDa CP species.

I further conducted densitometric analyses of Western blots obtained from at least two independent experiments to determine the percentage of cleaved CP species relative to total CP in WT CNV and the "KGRKPR" mutants. As shown in Figure 4.4B, I found that the single "KGRKPR" mutants M1, M2, M5 and M6 contain slightly higher relative proportions of the cleaved CP species (approximately 15%, 17%, 20.78%, and 20.74%, respectively) when compared to WT CNV (~11%). A significant increase in the levels of cleaved CP species exists in mutant in M4 (~91%) relative to WT CNV (~11%). Also the CP of virions of the double mutants M3 and M7 contain a much higher proportion of the cleaved CP compared to WT CNV being approximately 44% and 28%, respectively. The percentage of cleaved CP species is

largely consistent with the percentage of T=1 particles formed by the different mutants (see Figure 4.3B). Neither the 34.7 kDa species nor the 32.9 kDa species are able on their own to form T=3 particles but could form T=1 particles (21). I therefore suggest that the higher level of the cleaved CP species in mutants M3 and M7 (in this case predominantly the 32.9 kDa species) is due to the presence of T=1 particles in the virion preparations which are composed of the cleaved species.

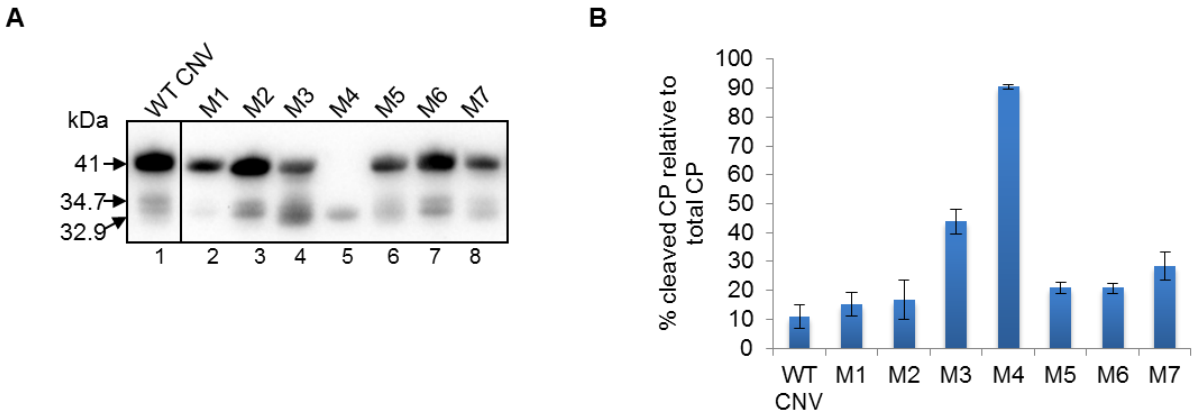

Figure 4.4: Western blot analysis of proteins extracted from virions of mutants M1-M7.

(A) Virions were purified from leaves inoculated with transcripts of the indicated mutants. WT CNV or the indicated M1-M7 virions (0.5 µl each) were loaded and subjected to SDS-PAGE followed by Western blotting. The blot was probed with CNV CP antibody SP. The full-length 41 kDa protein is indicated on the left as well as the cleavage products previously described to be associated with CNV virions. A longer exposure of M4 virion protein in this experiment and others showed that a small amount of full-length CP is visible. (B) Graphical representation of the percentage of cleaved CP relative to total CP (Full-length CP + both the cleaved CP species) from at least two independent experiments. The standard error is shown as brackets above the bars. The data were compiled from densitometric analysis of at least two independent experiments.

4.3.6 Virions produced by "KGRKPR" mutants encapsidate full-length as well as truncated RNA of viral origin

Virion RNA was extracted from ribonuclease treated virions of mutants M1-M7 as well as WT CNV virions and analyzed by denaturing agarose gel electrophoresis as shown in Figure 4.5A, panel i. It can be seen that the major species encapsidated by the single aa substitution mutants M1, M2, and M5 are similar to those encapsidated by WT CNV with the major RNA species co-migrating with CNV gRNA (~4.7 kb). The single aa substitution mutant M6, similarly encapsidates predominantly gRNA but a ~3.1 kb species not detected in WT CNV is also readily apparent. This species is also present, but at relatively lower levels in mutants M1, M2 and M5. The double aa substitution mutants M3 and M7 encapsidate predominantly truncated RNA species (Figure 4.5A, panel i, lanes 4 and 8) of ~4.4 kb, ~3.3 kb and ~1.5 kb (observed using a higher exposure, not shown). Detectable, but lower levels of ~1.9 kb and ~1.8 kb RNA species are also apparent. Quadruple mutant M4, from which it was difficult to obtain sufficient vRNA to readily observe the various encapsidated RNA species due to the low level of virions produced and the low level of encapsidated RNA (see above), encapsidates predominantly ~3.3 and ~1.9 kb species and slightly lesser amounts of ~1.8 and ~1.5 kb species as well as a low level of full-length RNA (Figure 4.5A, panels i and ii, lane 5). Together, the results suggest that mutation of basic aa residues in the "KGRKPR" sequence of the arm affects the ability of virions to encapsidate full-length RNA and that the greater the reduction in the number of basic residues, the greater the propensity for encapsidation of truncated RNA species.

This observation was also validated by densitometric analyses from at least two independent experiments as shown in Figure 4.5A, panel ii. It can be seen that the single aa mutants M1, M2,

M5 and M6 encapsidate more truncated RNA (being approximately 28%, 23%, 38% and 57% respectively) than WT CNV (~3%). The double aa mutants M3 and M7 encapsidate relatively more truncated RNA (being approximately 71% and 76%) than the single aa mutants. The quadruple mutant M4 shows the greatest % of encapsidation for truncated RNA (being approximately 83%) compared to WT CNV and all the mutants. Similar truncated species were observed in virion preparations that were not treated with ribonuclease (data not shown). Similar observations have previously been described for BMV and other viruses where electrostatic interactions between basic amino acid side chains of the CP and phosphate groups of the RNA were found to play a role, at least in part, in this phenomenon (157).

Northern blot analyses of species encapsidated in mutants M1-M7 (ribonuclease treated prior to RNA extraction) show that the majority of the RNA species observed in EtBr stained gels are of viral origin, since most hybridize to a probe prepared to CNV (Figure 4.5A, panel iii). An exception to this is the vRNAs in the M4 mutant. Specifically, whereas the major encapsidated species in mutant M4 as detected by EtBr staining are ~3.3 and ~1.9 kb along with lesser amounts of ~1.8 and ~1.5 kb species (see above), numerous faintly hybridizing bands of approximate equal signal intensity and with sizes of approximately 4.7, 4.0, 3.1, 2.1 and 1.8 kb are observed in the Northern blot (Figure 4.5A, panel iii, lane 5). Thus, it would appear that the major 3.3 and 1.9 kb species present in the EtBr stained gel of mutant M4 are not of viral origin. Similar truncated RNAs of viral origin were also apparent in vRNA preparation extracted from ribonuclease untreated virions (data not shown).

4.3.7 Virions produced by "KGRKPR" mutants encapsidate relatively more host RNA than WT CNV

Previous work in Dr. Rochon's lab has shown that a small proportion of CNV RNA (~0.1-0.7%) is of host origin, predominantly ribosomal RNAs (rRNAs) (135). To assess the possibility that some of the species encapsidated in the "KGRKPR" mutants are of host origin, WT CNV and each of the "KGRKPR" mutants were treated with ribonuclease to remove any residual contaminating host RNA from virions preparations and then extracted virion RNA was electrophoresed through a denaturing agarose gel.

Northern blot analysis using a cDNA probe to TLR from uninfected *N. benthamiana* leaves was then conducted with the results shown in Figure 4.5A, panel iv. It can be readily seen that the host cDNA probe hybridizes strongly in mutant M4 (lane 5), with the major hybridizing species being ~3.3 kb and ~1.9 kb along with weaker signals to bands of approximately 1.5, 1.3 and 1.1 kb. Since each of these species co-migrate with the major rRNAs species present in TLR extracts, it would appear that at least some of the RNA encapsidated in mutant M4 corresponds to rRNAs. Interestingly the double aa substitution mutants M3 and M7 also encapsidate similar host RNAs when compared to mutant M4, however, the levels appear lower as indicated by the weaker autoradiographic signal (Figure 4.5A, panel iv, lanes 4 and 8). It is noted that the ~3.3 kb RNA band observed in the EtBr stained gel in Figure 4.5A, panel i, in mutants M3, M4 and M7 is likely a mixture of truncated CNV RNA and the host ~3.3 kb RNA species as it hybridizes to both the CNV probe (Figure 4.5A, panel iii) and the host RNA probe (Figure 4.5A, panel iv) in these mutants.

To obtain quantitative data regarding the relative levels of host RNA species versus viral RNA species present in the "KGRKPR" mutants, densitometric analyses was conducted on the EtBr stained gel of RNA extracted from WT CNV and the "KGRKPR" mutant virions (Figure 4.5A, panel i), as well as Northern blots using WT CNV (Figure 4.5A, panel iii) or host cDNA (Figure 4.5A, panel iv) as the probe. In particular, it can be seen in Figure 4.5B that "KGRKPR" mutants M3 and M7, which are double aa substitution mutants, and mutant M4, which is a quadruple aa substitution mutant, encapsidate predominantly host RNA versus viral RNA, with host RNA representing ~56%, ~66% and ~90% of the total RNA encapsidated, respectively. The single aa mutants M1, M2, M5 and M6 contain a lower proportion of host RNA (~10%, ~14%, ~22% and ~29%, respectively). These results are interesting since they suggest that the "KGRKPR" sequence plays an important role in selective encapsidation of viral RNA over host RNA during the WT CNV particle assembly process.

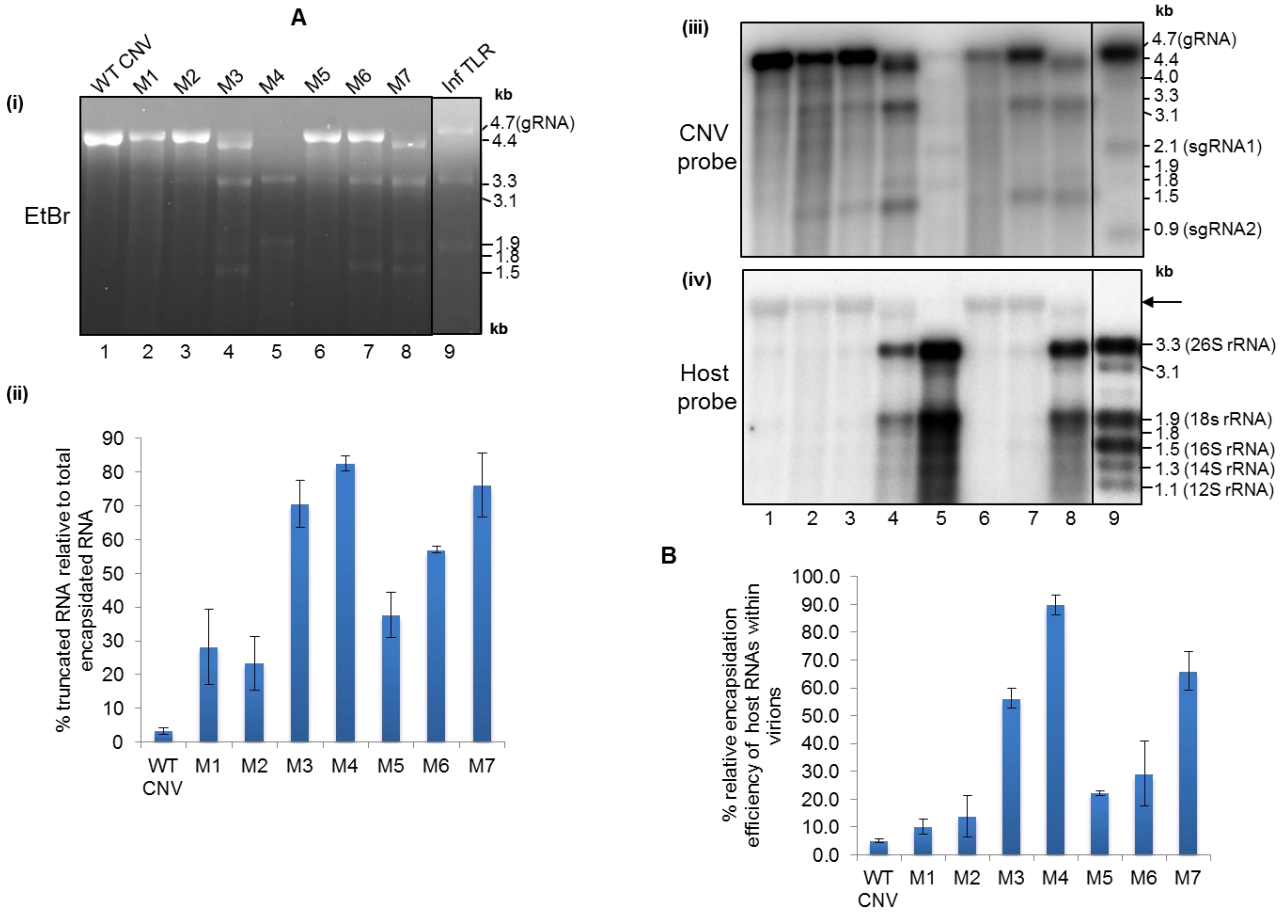

Figure 4.5: Virions produced by "KGRKPR" mutants encapsidate full-length and truncated viral RNA as well as host RNA species.

(A) (i) Denaturing agarose gel electrophoresis of vRNA extracted from mutants M1-M7. RNA extracted from virions of WT CNV (400 ng) and RNA extracted from "KGRKPR" mutants M1-M7 (131 ng, 246 ng, 124 ng, 75 ng, 199 ng, 240 ng and 156 ng, respectively) was electrophoresed though a 1% denaturing formaldehyde agarose containing EtBr. CNV infected TLR (Inf TLR) was included for use as a size marker along with Millenium RNA Markers (Ambion) (not shown). The sizes of major encapsidated RNAs and CNV gRNA are indicated in kb on the right hand side of the gel. (ii) Densitometric analyses of % truncated RNA relative to total encapsidated RNA from at least two independent experiments. Truncated RNA species were defined as all the density below full-length CNV gRNA. The standard error is shown as brackets above the bars. (iii) Northern blot analyses of RNA species present in virions of mutants M1-M7 using a CNV cDNA probe. WT CNV RNA (20 ng) and RNA of the indicated M1-M7 mutants (6.5 ng, 12.3 ng, 6.2 ng, 3.8 ng, 9.9 ng, 12 ng and 7.8 ng respectively) along with CNV infected total leaf RNA (Inf TLR) was electrophoresed as in A, panel i above, blotted and then probed with a WT CNV probe corresponding to the complete CNV genome. The sizes of major hybridizing species are indicated on the right of the blot in kb. Also included are the 2.1 kb and

0.9 kb sgRNAs of CNV which were used as size markers. (iv) Northern blot analysis of host RNA species present in virions of mutants M1-M7 using a cDNA probe synthesized using total uninfected *N. benthamiana* leaf RNA as template. RNA (400 ng) extracted from WT CNV or different "KGRKPR" mutants (see panel i for amounts) were subjected to denaturing agarose gel electrophoresis as described in A, panel i. The gel was blotted and then probed with a randomly-primed cDNA to total uninfected *N. benthamiana* leaf RNA. The sizes of the major detected RNA species are indicated on the right in kb along with the sizes of the various rRNAs which include cytoplasmic 26S and 18S rRNA and chloroplastic 16S rRNA along with 23S rRNA breakdown products of 1.3 kb and 1.1 kb (283). In this experiment, faint non-specific hybridization to CNV genomic RNA also occurred in several of the mutants except M3, M4 and M7 and is indicated with the arrow. (B) Graphical representation of the average % of relative encapsidation efficiency of host RNAs within virions from at least two independent experiments. The standard error is shown as brackets above the bars. The % of relative encapsidation efficiency was determined by densitometric analyses using ImageJ software (https://imagej.nih.gov/ij/) as described in the Materials and Methods.

4.3.8 Host RNAs detected in vRNA extracted from "KGRKPR" mutant preparations are contained within virions

As stated above, the virions used in the experiments in Figure 4.5 were treated with RNaseA prior to RNA extraction in order to eliminate any potentially contaminating host RNAs from the vRNA preparations. Therefore the Northern blot results with the host cDNA probe indicate that host RNA is contained within CNV virions. This could indicate that the "KGRKPR" sequence plays an important role in selecting CNV RNA for encapsidation (as described above in Figure 4.5B). To further assess the possibility that the host RNA signals in Figure 4.5A, panel iii, do not correspond to contaminating host RNA, I conducted a "mock virus" extraction from equal amounts of uninfected *N. benthamiana* leaves using conditions identical to that used for extraction of virions from the double mutants M3 and M7, respectively, including the volume that the virions were resuspended in. I then treated the resulting virions with RNaseA followed by RNA extraction and resuspended the pellets in volumes equal to that used for M3 and M7.

Figure 4.6, panel i, shows the results of an EtBr stained gel using equivalent amounts of vRNA extracted from RNaseA-treated "mock virions" along with RNaseA-treated M3 and M7 virions. Figure 4.6, panel ii, represents the Northern blot using uninfected *N. benthamiana* cDNA as the probe. It can be seen that vRNA extracted from RNaseA-treated "mock virions" do not contain detectable RNA species as evident by the absence of any signal in the EtBr stained agarose gel as well as the Northern blot (panels i and ii, see lanes 1 and 3) compared to that of the double "KGRKPR" mutants M3 (lane 2) and M7 (lane 4). These results suggest that the RNA species detected in mutants M3 and M7 in Figure 4.5A, panel iv, lanes 4 and 8 respectively, are

encapsidated within virions and do not merely co-purify as a contaminant during the virus and vRNA extraction procedures.

To demonstrate whether host RNAs would be present using more rigorously purified virus, a purification procedure using differential centrifugation was utilised for WT CNV, mutant M3 and "mock virions" as described previously (117). Virion RNA was then extracted from RNaseA-treated virions and subjected to Northern blot analysis using a host cDNA probe. It can be seen in Figure 4.6 that "mock virions" contain no detectable RNA, whereas M3 virions as well as WT CNV virions contain host RNA (Figure 4.6, panel i and ii, lanes 5-7). It is noted that the EtBr stained gel of M3 vRNA extracted from virions purified by differential centrifugation indicates that slightly less vRNA was loaded onto the gel when compared to WT CNV vRNA (Figure 4.6, panel i, compare lanes 7 and 6, respectively). Nevertheless, hybridization to host RNA appears to be slightly stronger (about 3-4 fold), suggesting that mutant M3 encapsidates host RNA more readily than CNV.

When densitometric analysis was conducted to determine the relative increase in host RNA encapsidated by mutant M3 compared to that of WT CNV following purification of virions by the differential centrifugation procedure, a similar result was obtained (62 fold in "midiprep" procedure extracted virions versus 35.5 fold in differential centrifugation purified virions), thus confirming that the basic aa substitutions in M3 may play an important role in selection of viral RNA during the assembly process.

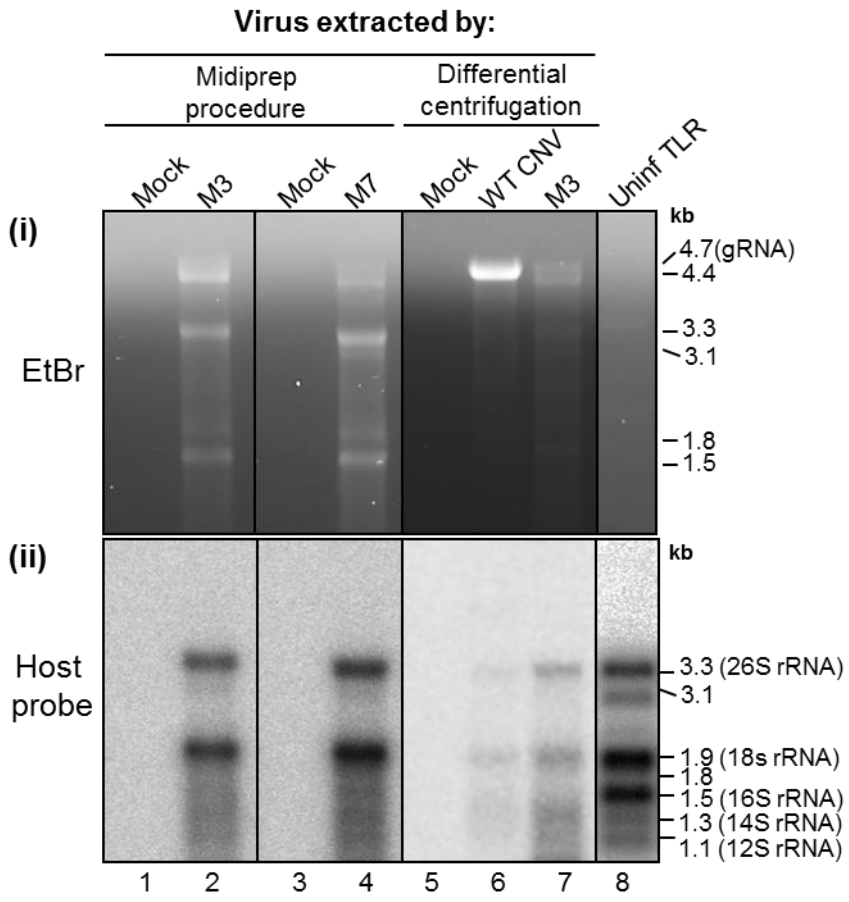

Figure 4.6: Host RNAs detected in vRNA extracted from "KGRKPR" mutant preparations are contained within virions.

"Mock virions" were extracted from equal amounts of uninfected *N. benthamiana* leaf tissue in a manner similar to that used for the "midiprep" purification of mutants M3 and M7 (see Materials and methods), respectively, including resuspending mock virus in an equivalent volume of buffer. RNA was extracted from equivalent volumes of RNaseA treated "mock virions" and virions of M3 or M7 and the resulting pellets were resuspended in the same volume as used for the respective mutants. Equal volumes of RNA extracted from RNaseA treated "mock virions" (lanes 1 and 3) or RNaseA treated mutants M3 (lane 2) and M7 (lane 4) (corresponding to ~400 ng of M3 or M7 virion RNA) were subjected to 1% denaturing formaldehyde agarose gel electrophoresis and EtBr staining (panel i) and Northern blot (panel ii) analyses using a randomly-primed cDNA to total uninfected *N. benthamiana* leaf RNA as described in Figure 4.5A, panel iv to detect host RNA species. WT CNV, M3 or "mock virions" were also extracted using a differential centrifugation method as described previously (38). Approximately 400 ng of WT CNV or ~60 ng of M3 RNA were subjected to agarose gel electrophoresis followed by EtBr staining (panel i) and Northern blot analysis (panel ii). In lane 8, 32 ng of TLR obtained from uninfected *N. benthamiana* (Uninf TLR) was also electrophoresed.

4.3.9 "KGRKPR" double mutants are thermally less stable than WT CNV

Previous studies on *Sesbania mosaic virus* have shown that the basic aa residues of the CP can play an important role in stability of virions by RNA-protein and protein-protein interactions (51, 138). It was postulated that encapsidation of gRNA enhances the stability of virions (14). Since, the double mutants M3 and M7 encapsidate less viral RNA compared to WT CNV (~16-35.3%) as shown in Figure 4.5A, panel i and 5B, I wished to investigate if these mutants were thermally less stable. Due to the low level of virions produced by the quadruple mutant M4 (only ~1% compared to WT CNV, Figure 4.2E, panel ii), experiments were only conducted with the double mutants M3 and M7 along with WT CNV.

To assess the thermal stability of the "KGRKPR" double mutants, I subjected equal amount of virions extracted from WT CNV or the mutants M3 or M7 to increasing temperatures, ranging from 4 to 75°C, and then analyzed the virions by agarose gel electrophoresis followed by SYPRO Ruby staining to visualize virion proteins. It can be seen in Figure 4.7, that the double mutants M3 and M7 become unstable at 65°C (lane 6, panels ii and iii), whereas WT CNV becomes unstable at 75°C (lane 8, panel i). The higher molecular weight species were also stained with EtBr in a duplicate gel (data not shown), suggesting that these represent ribonucleoprotein (RNP) complexes. These higher molecular weight RNP complexes perhaps might have originated from loss of CP subunits during the heating process due to loose CP-RNA interactions, thus imparting a distinct electrophoretic mobility pattern due to altered charge on the particle. These results suggest that RNA-protein interactions contribute to particle stability of CNV. In this specific case, M3 and M7 virions lack two basic aa residues that could impart stability to the CP-RNA interactions in the particle.

I also noted that a significant proportion of the RNA encapsidated by mutants M3 and M7 is of host origin (Figure 4.5A, panel iii and 5B). So the decrease in stability of the M3 and M7 virions may relate to the fact that some of the encapsidated RNA is of host origin and may not interact with the virion in the same stabilizing manner that viral RNA might confer. For example, it is believed that during assembly of viral RNA, a high affinity interaction occurs between a specific region on viral RNA and specific CP residues (53) (described in details in Section 1.19.6). Particles assembling host RNA may not possess these same high affinity interactions.

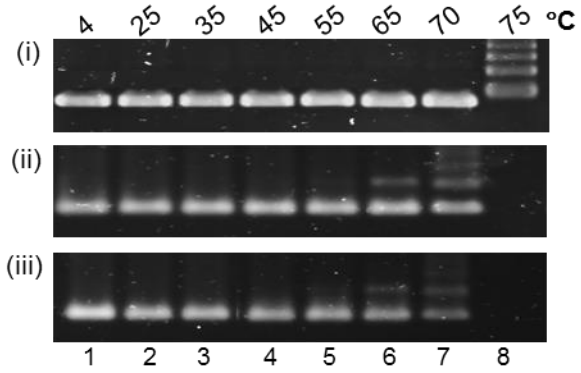

Figure 4.7: "KGRKPR" double mutants M3 and M7 are thermally less stable than WT CNV.

WT CNV (panel i) along with the "KGRKPR" double mutants M3 (panel ii) and M7 (panel iii) were subjected to increasing temperatures ranging from 4 to 75 °C. Virions were then analyzed by agarose gel electrophoresis followed by SYPRO Ruby staining. Note that double mutants M3 and M7 become unstable at 65°C (lane 6) as indicated by the additional slower migrating species and at 75°C (lane 8) no virions are apparent. In contrast, WT CNV remains stable at 65°C but doesn't become unstable until 75°C, where multiple bands are present. Similar trends in the staining pattern were also observed in a duplicate gel stained with EtBr to visualize RNA (not shown), suggesting that the high molecular weight bands are ribonucleoprotein complexes.

4.4 Discussion

One of the major steps in production of an infectious virion is the encapsidation of viral RNA by CP subunits into a stable structure that provides the viral genome with a protective coat which prevents host ribonuclease digestion. The CPs of several positive strand RNA viruses have been shown to possess an arginine-rich RNA binding motif (ARM) at the N-terminus (49, 53, 151-163, 284-286) that assists in viral RNA encapsidation and particle assembly. In previous studies we have shown that CNV too contains a highly basic N-terminus which includes a lysine rich "KGKKGK" sequence in the R domain of the CP. The "KGKKGK" sequence has been found to be involved in the encapsidation of full-length RNA and assembly of T=3 vs T=1 virions (164).

In the current study, I wished to investigate and map the location of other potential RNA binding sites in the CNV CP, in particular a "KGRKPR" sequence in the ε region of the arm which mapped to a location within the virion previously determined by neutron scattering to have high RNA density (280). Mutational analyses of the "KGRKPR" sequence suggested the importance of the basic aa residues in accumulation and/or assembly of CNV virions (Figure 4.2). A major line of evidence was the observation that the percent virion accumulation relative to WT CNV was lower than the percent CP accumulation relative to WT CNV for each mutant (Figure 4.2E). This was especially so for the quadruple mutant M4 where the % CP accumulation (relative to WT CNV) was 58% whereas the % virion accumulation (relative to WT CNV) was less than 1%. The double mutants M3 and M7 also showed significantly affected virion accumulation. For example, M3 virion accumulation is ~35% whereas CP accumulation is ~72% (relative to WT CNV). For M7, virion accumulation is ~27% whereas the CP accumulation is 76% (relative to WT CNV). In the remaining single aa substitution mutants the reduction in particle accumulation

versus CP accumulation was less dramatic, but significant, being approximately 56% versus 88%, 64% versus 81%, 60% versus 86%, and 60% versus 89% for mutants M1, M2, M5 and M6, respectively (Figure 4.2E).

When vRNA of the different "KGRKPR" mutants was analysed by agarose gel electrophoresis, a variety of truncated species (as well as full-length CNV RNA species) was observed (Figure 4.5A, panel i). An interesting observation was that the "KGRKPR" mutant virions were found to encapsidate relatively more truncated RNA species (~23-83%, Figure 4.5A, panel ii) when compared to WT CNV (~3%). This being especially so for the double (~71-76%) and quadruple (83%) mutants. These observations suggest the importance of basic residues of the "KGRKPR" sequence in encapsidation of full-length CNV RNA over truncated RNA species as has been shown for BMV and several other viruses (51, 53, 55, 151-163). It is known that many viruses in which basic aa have been removed encapsidate truncated RNA species (51, 53, 55, 151-163). This has been attributed in part to electrostatic interactions which prohibit an excess of viral RNA relative to basic amino acids.

Viruses generally selectively package their own RNA preferentially over host RNA. In many cases, virus capsid proteins have been found to bind specific high affinity sequences and/or structures on viral RNA which helps to preclude packaging or co-packaging of host RNAs (173, 174, 191, 199, 200, 287-299). The presence of specific interactions between CP and viral RNA species, as well as their co-localization within a cellular compartment ensures that majority of the virions contains viral RNA (180, 299). To determine the origin and nature of encapsidated RNA, Northern blot analyses was conducted using a full-length CNV cDNA probe and vRNA

extracted from WT CNV or the different "KGRKPR" mutant virions. I found that some of the truncated RNAs encapsidated by the "KGRKPR" mutants are of viral origin (Figure 4.5A, panel iii). However, not all the truncated RNA observed in the agarose gel hybridized to the full-length CNV cDNA probe suggesting that some of the encapsidated RNA may be of host origin.

To determine if this is so, a Northern blot was conducted using a cDNA probe to TLR of *N. benthamiana*. An interesting observation was that the quadruple and double mutants encapsidated significantly more host RNA (~90% and 56-66%, respectively) than single aa substitution mutants or WT CNV (Figure 4.5B), suggesting the importance of the "KGRKPR" sequence in selective encapsidation of viral RNA over host RNA during particle assembly.

I have found using co-immunoprecipitation analyses that the CNV CP interacts either directly or indirectly with the auxiliary replicase protein p33 (S.B. Alam and D. Rochon, unpublished observations). Also, previous work in Dr. Rochon's lab has shown that CNV preferentially encapsidates its own RNA (>99%) over host RNA (0.1-0.7%) (135). An intriguing hypothesis is that CNV CP interacts with the replicase to ensure selective encapsidation of viral RNA over host RNA as has been suggested for other viruses such as FHV and BMV (47, 48). Additionally, a recent report on *Satellite tobacco mosaic virus* shows that the interaction between the N-terminal basic motif of the coat protein with the helper TMV replicase plays an important role in replication and packaging (151). Hence, it is possible that mutations of basic aa residues in the ε region of the CNV CP arm not only preclude encapsidation of full-length RNA due to loss of electrostatic interactions or specificity of interaction with viral RNA but also interferes with potential interaction with the replicase. If so, the CNV CP mutants may not be in a cellular

location where predominantly viral RNA occurs and this could result in "mis-encapsidation" of host RNAs. The mutations in the "KGRKPR" sequence may therefore indirectly affect specific encapsidation of viral RNA through its interaction with p33. However, given the basic nature of the substituted aa and their co-incident location with vRNA it would seem likely that these aa are also at least directly involved in specific recognition of viral RNA. To my knowledge, CP aa sequences involved in selective encapsidation of viral RNA over host RNA have not yet been identified.

To gain structural insight into the nature of virions formed by the "KGRKPR" mutants, TEM studies were conducted. It was found that virions produced by the double and quadruple "KGRKPR" mutants were polymorphic likely having T=1 as well as T=3 icosahedral symmetry based on the size of the particles (Figure 4.3A). Also the "KGRKPR mutants were found to contain greater proportion of T=1-sized particles relative to WT CNV (Figure 4.3B). This being more pronounced in the double (~6-26%) and quadruple (94.5%) mutants.

The T=1 particles produced by mutant M4 appear to be predominantly empty as determined by agarose gel electrophoresis, where the T=1 particles are visible following SYPRO Ruby staining but are not visible following EtBr staining (Figure 4.2D, panel i, lane 5). Some T=3 particles having darkly stained centers were also observed in mutants M3 and M4 that have been designated as EPs (Figure 4.3A, panels ix and x, arrowhead). Although it is possible that the EPs result from formation of particles in the absence of RNA it is more likely that particles are assembled in the presence of RNA but that the RNA degraded at least partially following assembly. On the other hand, it is possible that assembly occurred in the presence of RNA as

usual but the architecture of the assembled particle was such that it allowed penetration of the uranyl acetate negative stain. Also, encapsidation of host RNA might lead to unstable CP-host RNA interaction due to dispositioning of the packaging signals as described previously (174, 192) and that, in turn, might lead to formation of unstable particles that allow the stain to penetrate into virions making them appear like EPs.

We observe that mutant M4 encapsidates a high proportion of host RNAs that have sizes of primarily ~3.4 and ~1.9 kb along with smaller species ranging from ~1.8 to ~1.1 kb (Figure 4.5A, panel iv, lane 5). The 3.4, 1.9 and ~1.8 kb species are most likely encapsidated by the few T=3 particles present in M4 preparations as the T=1 particles would likely not be able to encapsidate species larger than 1.1 kb. Additionally, the vast majority if not all of the T=1 particles of M4 mutants are empty as determined by their inability to stain with EtBr (Figure 4.2D, panel i, lane 5). This explanation is likely also applicable to mutants M3 and M7; that is, it is the T=3 particles that encapsidate the host RNA species observed in Figure 4.5A, panel iv.

We note that the mutant M3 virions consist of approximately 26.4% T=1 particles as determined by TEM analysis (Figure 4.3B). In addition, approximately 23% of CP of virions is the 32.9 kDa species which I have suggested to comprise T=1 particles. However, virion agarose gel electrophoresis suggests that such a high level of T=1 particles are not present since a band co-migrating with T=1 particles is not apparent (compare Figure 4.2D, upper and lower panel i, lane 4). The basis for this observation is not known. It is possible however, that not enough CP was loaded onto the gel to observe a band comprising only ~26.4% of the total. Alternatively, or in

conjunction, it could be that the M3 T=1 particles co-migrate with WT CNV T=3 particles due to an unusual morphology and/or charge of the T=1 particles.

Mutants M3 and M7 show reduced thermal stability compared to WT CNV (Figure 4.7). These two mutants each show encapsidation of slightly less RNA compared to WT CNV (~16-36%; Figure 4.2F). Also the encapsidated RNA predominantly consists of host RNA (~56% and ~66%, respectively; Figure 4.5B) and truncated viral RNA (Figure 4.5A, panel iii). Which or how many of these factors contributes to decreased thermal stability is not known. Factors that could contribute to weaker thermal stability include weaker overall electrostatic interactions due to less RNA being encapsidated or a loss of the specific RNA/CP interactions that might normally occur in a virion that has selectively encapsidated viral RNA through specific RNA sequence/viral CP interactions. Also, these aa may in WT CNV interact with other aa in the particle, which in the mutants could negatively affect particle stability. Such aa could include those of the first β strand of the S domain which is antiparallel to the beta strand of the ε region in C/C subunits.

Based on previous and current research in Dr. Rochon's lab and on the results of NMR studies of TBSV RNA binding sites (280), I present a pictorial representation of the location of RNA binding sites in CNV (280). Figure 4.8 shows that there are two highly basic sequences in the C subunit of CNV that bind vRNA. The first putative site is the "KGKKGK" in the C-terminus of the R domain of the CP that is shown by the green circles and the second sequence is the "KGRKPR" sequence in the ε region of the CP arm as shown by blue bars. This model is likely applicable to other *Tombusviruses* as well, since all sequenced *Tombusviruses* contain a highly

basic region in the C-terminus of the R domain (164) as well as a highly basic sequence in the ε region (Figure 4.1A).

Also, in the *Carmovirus*, MNSV, I noted that a highly basic sequence "KLSKAAKRR" exists in the C-terminus of the R domain of the CP and an identified highly basic RNA binding sequence also exists in the ε region of the arm (163) as described above. It has been suggested by *Sorger et al*. (1986) (49) that assembly of TCV occurs via the interaction of a trimer of C/C dimers with specific TCV RNA sequences (296). The presence of highly basic residues in the C-terminal region of the R domain and the ε region of *Tombusviruses* could suggest that a trimer of C/C dimers is also important for the initiation of assembly of *Tombusviruses* as well, as this would allow for 12 potential viral RNA binding sites in a single nucleation event. This hypothesis is discussed in more detail in the general discussion (Section 5.4.2). My findings that the double and quadruple "KGRKPR" mutants encapsidate host RNA raises the question as to whether this sequence plays a role in the selective encapsidation of CNV RNA. Although we have previously found that CNV encapsidates host RNA at a low level (135), the significantly higher relative level of encapsidation of host versus viral RNA in the double and quadruple "KGRKPR" mutants (~56-90% of total encapsidated RNA is host RNA) strongly suggests a role for the "KGRKPR" sequence in selecting viral RNA during the assembly process. Further research will need to be conducted to further assess the basis for the observed increase in host RNA encapsidation.

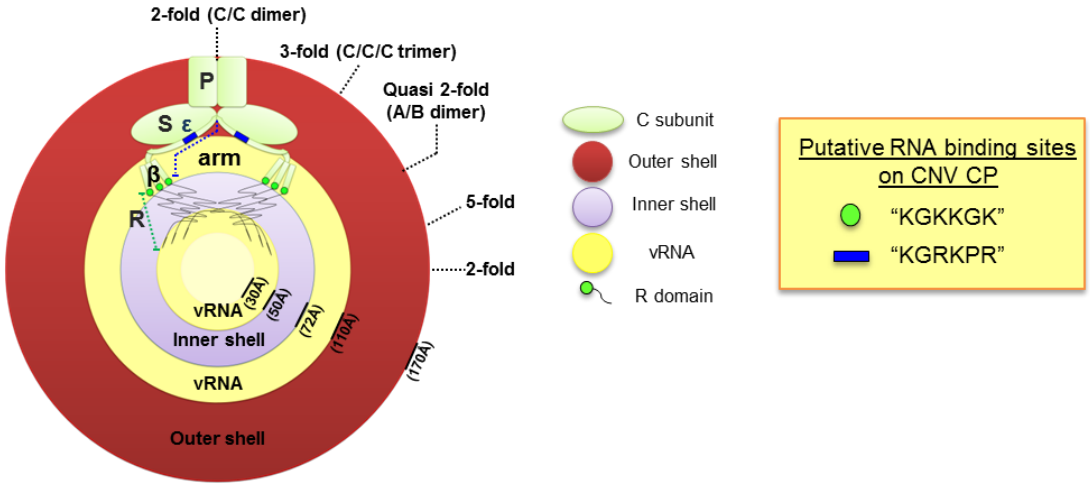

Figure 4.8: Pictorial representation showing the location of two putative RNA binding sites on the CP in CNV virions.

A diagrammatic illustration of a cross section of the CNV virion, showing the outer (red) and inner (purple) protein shells along with the layer of vRNA (yellow) sandwiched between the two concentric shells as previously proposed (6). According to the presented illustration there are two highly basic sequences in the C subunit (green) of CNV that bind vRNA. One putative site is the "KGRKPR" sequence (blue bar) in the ε region of the CP arm (arm shown by the dotted blue bars) and the second RNA binding site is a previously described "KGKKGK" sequence (green circles) (300) in the R domain. This model is in agreement with that of *Timmins et al.* (1994) (280), as determined by neutron scattering studies. RNA density was not found under AB dimers in *Timmins et al.* (1994) (280), likely due to the disordered arms and R domain in these subunits (not shown). A colour key is shown on the right hand side. The locations of the different icosahedral axes are shown by black dotted lines. The radii in Å of the outer boundary of the different concentric shells from the virion center is shown based on previous studies (13).

Chapter 5: General discussion and future perspectives[5]

A main objective of this thesis was to further examine aspects of CNV particle assembly and disassembly with an emphasis on the involvement of host factors, in particular, HSP70 homologs. During the course of my research it was found that CNV CP co-opts the host factor HSP70 for assembly and disassembly of virions. This is the first time host HSP70 homologs have been implicated in plant virus particle disassembly. HSP70 homologs were also found to promote several other aspects of the CNV multiplication (see below).

I also discovered that a highly basic sequence in the arm domain of the CNV CP promotes particle assembly and encapsidation of full-length viral RNA. The highly basic sequence is also important for assembly of viral rather than host RNA, which is important for the assembly of infectious virions. To my knowledge, this is the first time that a specific CP aa sequence has been implicated in specific recognition of viral RNA for assembly.

Data in my thesis also shows that CNV infection induces specific heat shock inducible retrotransposons such as ONSEN-like retrotransposons. This may occur through the ability of CNV infection to promote a heat shock-like response and particularly the synthesis of heat shock factors which are known to induce ONSEN retrotransposons. . I find the fact that CNV can induce retrotransposons particularly intriguing because retrotransposons are known for promoting genome variation. Thus the induction of heat shock factors by CNV might ultimately be beneficial to future generations of plants under stress conditions.

[5] [5] A version of information presented in this Chapter is under preparation for publication.

5.1 Multiple roles played by the host factor HSP70 during CNV infection

During the course of my thesis research I found that CNV infection induces several isoforms of the host factor HSP70 (Figures 2.2 and 2.3, respectively), some of which are co-opted by the virus at different stages of infection. Overexpression of HSP70 homologs was found to increase gRNA, CP and particle accumulation, whereas its downregulation was associated with a corresponding decrease in CNV multiplication (Figures 2.4 and 2.5). Also, using co-immunoprecipitation analyses, I determined that a direct or indirect physical association exists between CNV CP and HSP70 homologs *in vivo* (Figure 2.7). I also found that Hsc70-2 can promote the solubilisation of CNV CP *in vitro* (Figure 2.8), suggesting a role of Hsc70-2 in preventing CP aggregate formation in plants. CP aggregate formation is likely to occur during CNV infection due to the very high concentration of CP that accumulates (up to 0.3 mg/g of leaf tissue; Rochon Lab, unpublished results). Prevention of aggregation may assist in more efficient particle accumulation by preventing CP aggregates from forming during assembly, and as described below, in preventing proteosomal degradation of denatured or aggregated CNV CP.

Using silencing experiments, I found that downregulation of HSP70 homologs interfere with the ability of the CNV CP to target chloroplasts during infection (Figure 2.9), which is consistent with the known role of HSP70 homologs in targeting cytoplasmically synthesized chloroplast preproteins (99, 247). Chloroplasts play a prominent role in plant defense and there is emerging evidence that pathogenic effectors target this compartment for attenuating host defense (206, 301-303). I hypothesize that HSP70-mediated targeting of CNV CP to chloroplasts may interfere with chloroplast mediated defense responses. In this light, the ability of CNV CP to be targeted to chloroplast with the aid of HSP70 homologs could also be a strategy the virus utilizes to

promote multiplication and spread. One of the interesting observations that I made in this regard was that overexpression of HSP70 homologs in the CNV local lesion host, *C. quinoa*, produced larger local lesions compared to plants having a basal level of HSP70 when inoculated with CNV (Figure 2.4F). One reason for this could be that HSP70 directly enhances replication by promoting replication complex formation (17). Thus enhanced RNA production would lead to a greater propensity for spread due to a higher level of viral RNA. In addition, however, these results could suggest that the enhanced entry of CP into the chloroplasts might ameliorate symptoms and hence promote the spreading of virus which would lead to larger lesions. In this regard, local lesion experiments could be conducted on HSP70-downregulated plants to determine if smaller local lesions are produced and if that correlates with reduced entry of CP into the chloroplasts. This indeed is supported by an experiment where a mutant defective in chloroplast stromal entry was inoculated onto *C. quinoa*. In this experiment, it was found that lesion size was significantly smaller, thus suggesting a correlation between the inability to enter chloroplasts and smaller lesion size.

Figure 5.1 shows a pictorial representation of the multiple roles played by the HSP70 homologs at several stages of the CNV multiplication cycle. According to this model, HSP70 homologs play an important role in CNV disassembly as described in Chapter 3 and Section 5.2 (a). It plays a prominent role in increasing replication as described by *Wang et al.* (2009) (17) and in Chapter 2 (c). HSP70 homologs also interacts with CP, likely preventing the formation of non-native intermediates or aggregates or possibly even the formation of premature virions (although the latter remains speculative) (55). However, if true, this phenomenon would promote viral RNA replication/accumulation. Once progeny viral RNAs have been formed through multiple

rounds of replication, HSP70 becomes involved in subsequent stages of the infection cycle. HSP70 may initiate capsid nucleation events by increasing the effective local concentration of CP (55) (d). However in order to have controlled regulation over the assembly process and to prevent the formation of kinetically trapped premature CP aggregates, HSP70 promotes protein folding and keeps the CP in a solubilized form until the proper nucleation events have occurred (d). HSP70 homologs also assist in the assembly of CNV virions by participating in some aspect of the assembly process possibly by assisting in CP oligomer formation (e). It is speculated that CNV may also co-opt HSP70 that is known to be associated with the replicase complex for assembly of virions. This would not only promote the assembly phase of the multiplication cycle while attenuating the replication phase, but, would also ensure the specificity of encapsidation as has been described for other viruses (47, 48). Finally, with the development of infection, the plant mounts a defense response against the virus by inducing necrosis, a phenomenon that will restrict the virus from spreading. CNV in turn recruits HSP70 to target CP to chloroplasts possibly to ameliorate symptom development to ensure more efficient spread and multiplication (f).

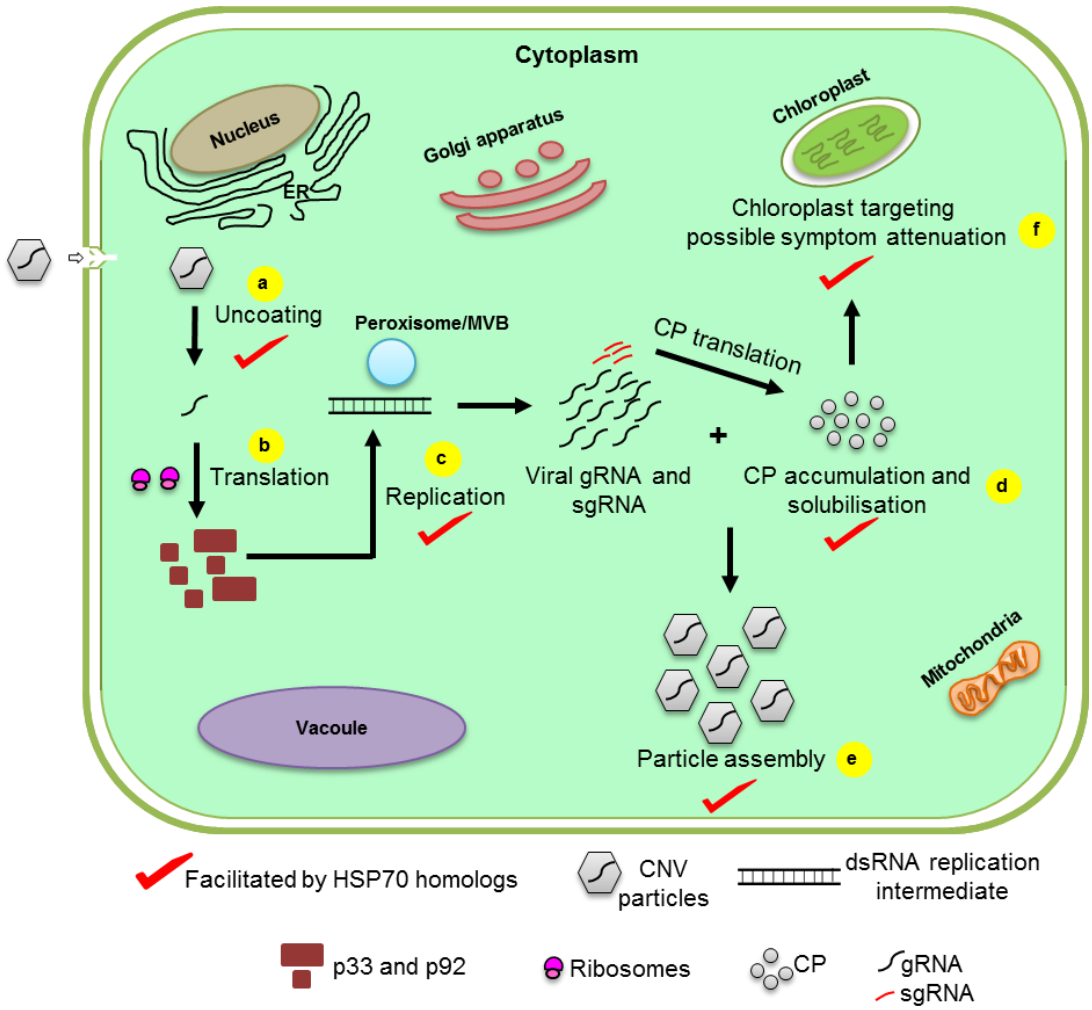

Figure 5.1: Hypothetical model for multiple roles played by HSP70 homologs during CNV infection.

Virions enter cells either with the help of a zoospore vector, systemically through the vascular tissue or by mechanical inoculation of the leaf. (a) As described in Chapter 3, HSP70 homologs assist in the uncoating process of CNV virions. (b) After the particles disassemble, the encapsidated gRNA is used as a template for the translation of the replication proteins, p33 and p92 (see Figure 1.1). (c) The replication proteins with the assistance of HSP70 homologs and other host factors initiate the formation of replicase complex. Replication occurs in induced spherules of peroxisomes (forming multivesicular bodies or MVBs) to replicate gRNA into multiple copies of progeny RNA and to form sgRNA species via a double stranded RNA intermediate. sgRNA2 is then translated to CP. (d) HSP70 homologs also assist in the solubilisation of CP and also its accumulation thereby preventing proteasomal degradation of aggregated or denatured CP. (e) Apart from that, HSP70 homologs promote the assembly of virus particles by interacting with CP molecules either directly or indirectly. (f) Finally, HSP70 homologs promote the targeting of CP to the chloroplast stroma likely to attenuate the necrosis response induced by the virus and this results in further virus spread.

5.2 Role of Hsc70-2 in CNV particle disassembly

To further investigate my observation that HSP70 homologs are induced during CNV infection and are recruited by the CP at several stages of infection to promote multiplication and spread, I conducted several lines of research to determine if HSP70 homologs are involved in the CNV uncoating process during the establishment of infection. I found that the HSP70 homologue, Hsc70-2 is present in CNV virion preparations (Figures 3.1A and C). I quantified the amount of Hsc70-2 present in CNV particle preparations and determined that ~18 molecules of Hsc70-2 are present per 1000 CNV particles (Figure 3.1D and E). It is speculated that the low level of HSP70 homologs in purified virion preparations is likely due to virion-associated HSP70 molecules being extracted from away from CNV particles during the purification procedure. I next conducted experiments to show that the association between Hsc70-2 and CNV occurs both *in vivo* and *in vitro* (Figure 3.3). I performed immunogold labelling experiments to directly assess that a physical interaction occurred between HSP70 and CNV particles (Figure 3.4) in a CNV virion preparation. Using, trypsin digestion assays, I also found that the bound Hsc70-2 is partially protected by the virus (Figure 3.5). I also determined that another member of the *Tombusviridae* family, the *Aureusvirus*, CLSV is associated with HSP70 and the relative proportion of HSP70 molecules to CLSV virions is similar to that of CNV (Figure 3.2), reinforcing a potential biological significance of virion bound HSP70 homologs in some aspect of the CNV and CLSV infection process.

To determine the biological significance of CNV/Hsc70-2 interaction in the CNV uncoating process, I developed a local lesion assay to investigate disassembly efficiency (Figure 3.6A). I

found that significantly fewer local lesions were produced on *C. quinoa* plants that were inoculated with CNV incubated with HSP70 antibody compared to the prebleed control. This suggested a possible role of virion bound Hsc70-2 in virion disassembly (Figure 3.6B). I also found that virions containing undetectable amounts of Hsc70-2 produced significantly fewer local lesions compared to virion preparations having a detectable amount of Hsc70-2, providing strong evidence for a role of virion bound Hsc70-2 in promoting CNV disassembly (Figure 3.6C). In both *C. quinoa* (Figure 3.8A) and *N. benthamiana* (Figure 3.7B) using local lesion assays, I found that the disassembly efficiency of CNV is enhanced in plants overexpressing HSP70 homologs resulting in a significantly greater number of local lesions compared to controls. A similar increase in the number of local lesions was not observed when plants were inoculated with viral RNA suggesting that it is particle disassembly efficiency that is enhanced rather than any other aspect of the CNV multiplication cycle (Figure 3.8B).

In order to determine if particles incubated with HSP70 homologs undergo a conformational change, I performed a chymotrypsin sensitivity assay and found that a small fraction of the particles undergo a conformational change as evident from the chymotrypsin digestion profile (Figure 3.9C). When Hsc70-2 incubated particles were subjected to transmission electron microscopy, 8% of particles were found to be deformed or conformationally altered compared to particles incubated with BSA (Figures 3.9A and B). All of these data are consistent with a role of Hsc70-2 in CNV particle disassembly. Importantly, this is the first time that a host HSP70 homolog has been shown to be involved in uncoating of a plant virus.

Previously, others have shown that some filamentous and spherical plant viruses uncoated on ribosomes during translation of viral RNA associated with partially disassembled virions (36, 37, 255). However, I was unable to duplicate these results with CNV following several attempts under different conditions. Therefore it will be of interest to determine how commonly plant viruses utilize HSP70 homologs for particle disassembly. It is known that several plant viruses induce HSP70 homologs during infection (214). These viruses might be the first ones to investigate since copious levels of HSP70 homologs might be available to the virus in the infected plant.

5.2.1 Hypothetical model for CNV disassembly in the presence of HSP70 homologs

Figure 5.2 represents a hypothetical model for CNV disassembly facilitated by HSP70 homologs and is described as follows. (a) Virions enter cells either with the help of a vector (zoospores) or following systemic movement through the vascular tissue or by mechanical inoculation under laboratory condtions. (b) The disassembly process is facilitated by the bound Hsc70-2 which helps to conformationally change CP subunits along with the higher pH environment of the cytoplasm which is known to result in CNV expansion. Cellular HSP70 may also be envisioned to assist in this process. Particle expansion, as a result of repulsion of A, B and C subunits, creates an opening in the particle at the quasi three-fold axis which has been well-described in the closely related TBSV (see text in Chapter 4). (c) As the disordered arm and R domains of the A and B subunits of the CP externalize through this opening, virion RNA bound to the highly basic “KGRKPR” and “KGKKGK” sequences may exit the virion. This will result in a partially disassembled virion.Cytoplasmic HSP70 homologs may further assist in “untangling” the

partially uncoated CNV beyond that facilitated by the virion associated Hsc70-2 (d). (f) This may allow for a more complete disassembly and release of viral RNA although it may not be necessary for all CP to become stripped from the viral RNA as it is possible that translating ribosomes could help achieve this.Finally, it is possible that the Hsc70-2 associated with the original incoming particle, as well as the sequestered or cytoplasmic HSP70 homologs, may assist in the formation of the replication complex (g) since it is known that cellular HSP70 homologs assist in CNV replication. (h) The cytoplasmic or the originally virion bound HSP70 homologs may then assist in the replication process to initiate replication.

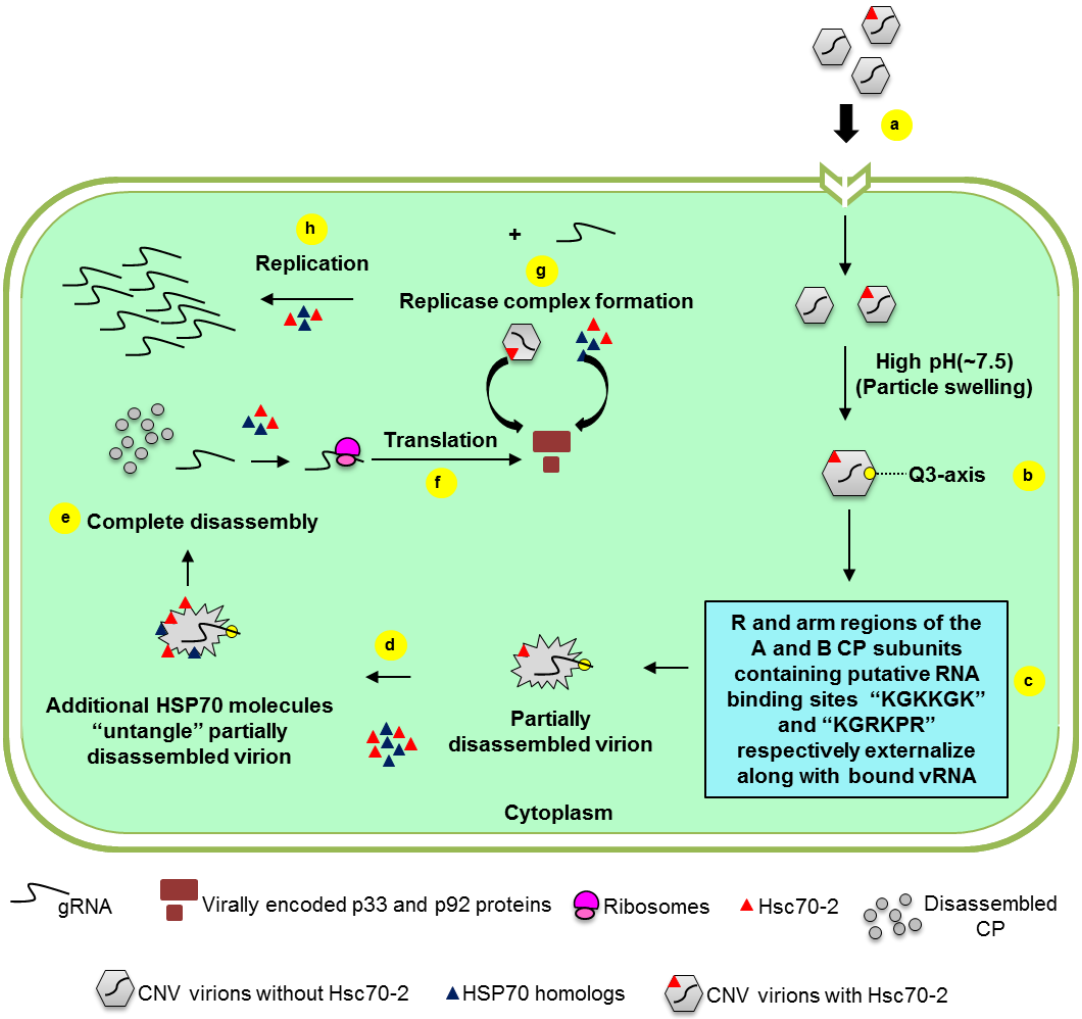

Figure 5.2: Hypothetical model for CNV disassembly facilitated by HSP70 homologs.

For details on the various steps of this model see section 5.2.1.

5.3 Evaluation of potential HSP70 binding sites on CNV CP

HSP70 homologs are known to bind a short stretch of hydrophobic aa flanked on both sides by positively charged residues (56, 268, 269). The CNV CP contains such a stretch of hydrophobic residues in the β region of the arm and this region is flanked by positive aa in the R domain as well as the ε region of the arm. In order to assess if HSP70 homologs bind the β region of the CP, I conducted a local lesion assay on *C. quinoa* overexpressing HSP70 homologs using particles of a mutant lacking the CP β region [β(-) mutant]. From five independent local lesion assays, I found that there was an insignificant difference in the number of local lesions between untreated and heat-shocked plants containing elevated levels of HSP70. These results are consistent with the possibility that in the absence of the β region, CNV CP is not able to recruit the induced HSP70 homologs for promoting disassembly. Hence, it is possible that the β region of the CP interacts with HSP70 homologs during infection. However, it is also possible that β(-) mutants are less stable than CNV mutant particles and thus may not establish infection as readily so further experiments are required to help determine if the β region of the CP is an HSP70 binding site.

I also performed four independent local lesion assays and found that significantly fewer local lesions were produced in plants inoculated with the β(-) mutant compared to WT CNV (data not shown). This is a further suggestion that the β region of the CP could be important for HSP70 binding and thus disassembly. Further research could be conducted to determine if a similar effect is observed when plants are inoculated with equal inoculums of vRNA extracted from β(-) mutant or WT CNV to rule out the possibility that the observed effect on number of local lesions

is due to reduced disassembly efficiency of β(-) mutant rather than reduced infectivity of the β(-) mutant RNA.

Also, experiments could be conducted to determine if there is a difference in the amount of HSP70 homologs detected in virion preparations of β(-) mutant particles versus WT CNV particles. Also, it could be determined if β(-) particles treated with Hsc70-2 become conformationally altered as determined by TEM and as shown previously for WT CNV particles. It is interesting that the β region is part of the chloroplast transit peptide of the CNV CP and we have recently determined that the CNV β(-) mutant does not enter chloroplasts very efficiently (Rochon lab, unpublished). Transit peptides are believed in many cases to bind HSP70 as part of the chloroplast import process (99). This observation provides circumstantial evidence that the β region could be an HSP70 binding site but further experiments are required to provide definitive evidence.

5.4 Role of basic residues in the CNV CP in CNV particle assembly

I conducted further research to characterize the role of CNV CP in promoting particle assembly, particularly with respect to binding viral RNA during the assembly process and within the completed particle. In particular, I found that there is a conservation of basic aa in the ε region of the CP arm of different *Tombusviruses,* and in CNV the sequence is "KGRKPR" (Figure 4.1A). This sequence is spatially located below the C/C dimers where the density of viral RNA is maximum as determined by previous neutron diffraction studies on the related *Tombusvirus,* TBSV (Figure 4.1B) (280).

I also found that when plants were inoculated with equal concentrations of WT CNV and "KGRKPR" mutants bearing mutations in basic residues, particle accumulation as well as RNA encapsidation was significantly compromised in the double and quadruple mutants compared to WT CNV (Figure 4.2E and F).

By TEM analysis, I found that "KGRKPR" mutants produce a greater relative proportion of particles having T=1 symmetry or a distinct morphology as indicated by darkly stained centers (Figure 4.3). Cryo EM experiments can be conducted on these mutants, which could shed light into the detailed structure of the capsids as well as help to provide an explanation for the nature of the distinct morphology.

The thermal stability of the double "KGRKPR" mutants was assessed. I found that the double "KGRKPR" mutants are thermally less stable than WT CNV (Figure 4.7). This may be due to weaker virion RNA-CP interactions.

I found that the basic aa residues in the "KGRKPR" sequence of the CP ε region likely play an important role in encapsidation of full-length viral RNA over truncated RNA (Figure 4.5A, panel ii) as described previously for positively charged regions in the CP of other viruses such as STMV, *Beet black scorch virus*, BMV, *Ourmia melon virus*, CMV, AMV, RCNMV, CCMV, SeMV, FHV, HIV, *Macrobrachium rosenbergii nodavirus* and MNSV (51, 53, 151-163). This may be in part due to balancing electrostatic interactions; i.e., particles with fewer basic residues would have a lesser capacity for encapsidating larger RNA species as described in Chapter 4.

An interesting observation made was that the "KGRKPR" mutant virions encapsidated a relatively greater proportion of host RNA over viral RNA when compared to WT CNV (Figure 4.5B). These results suggest the importance of basic amino acids in the "KGRKPR" sequence in selection of vRNA over host RNA during assembly. In this regard future experiments could be conducted to determine the specificity of binding of the ε region with CNV RNA. Experiments could also be conducted to determine if the "KGRKPR" region binds p33 which might also affect the specificity of binding as described above for STMV. Our results would also suggest that the RNA of CNV virions likely plays a role in particle stability as it is intimately associated with specific amino acids of the CP.

5.4.1 Examination of CP species that form T=1 particles

I wished to analyse the size of the CP in M4 virions to assess why M4 virions are primarily T=1 particles. I found that the quadruple mutant M4 predominantly contained a cleaved CP species of 32.9 kDa (Figure 4.4B). Also the double mutants contained a relatively greater proportion of the 32.9 kDa as well as 34.7 kDa cleaved CP species relative to full-length CP when compared to WT CNV and the single aa mutants (Figure 4.4B). This observation suggested that the T=1 particles may be formed from cleaved CP.

Previous work in Dr. Rochon's lab suggests that certain R domain deletion mutants (that correspond to the 34.7 kDa cleaved CP species) fail to form T=3 particles and form T=1 virions instead (21, 164). Also, *Ghoshal et al.* (2014) (135), found that protein of particles formed from agroinfiltration (VLPs) which were predominantly T=1 particles consisted mostly of 32.9 kDa and 34.7 kDa cleaved CP species. It was postulated that in the absence of a full-length replicating

CNV RNA, that likely contains a PS(s) for CP binding and hence particle assembly, the majority of the full-length 41 kDa CP cannot efficiently assemble into T=3 particles. Hence, the unassembled CP is either targeted to mitochondria to produce a truncated 32.9 kDa species or cleaved to yield a 34.7 kDa species that is targeted to chloroplasts to yeild a 32.9 kDa truncated CP species. These CP species likely assembles into the T=1 particles predominantly found in VLP preparations.

In my studies on CNV CP, as described in Chapter 4, Section 4.3.4, I found that the "KGRKPR" mutants, even in the presence of a replicating CNV RNA and full-length CP, produced significantly greater amounts of T=1 over T=3 particles likely because the mutated CP is unable to bind CNV RNA and assemble into T=3 particles. This would allow for enhanced targeting of unassembled full-length CP to mitochondria and chloroplasts to yield the cleaved 34.7 kDa or 32.9 kDa species. In light of previous and current findings, I speculate that mutant M4 that predominantly consists of T=1 particles are made of the 32.9 kDa cleaved CP species. Conversely, it can be stated that the 32.9 kDa cleaved CP species is the species that forms the T=1 particles. Edman degradation analysis of the 32.9 kDa species shows that it corresponds to cleavage of the CP within the arm just upstream of the ε region (135). Such a CP species could not form a T=3 particle since it lacks the R domain which would form the inner shell of the particle. Also, its size and nature would suggest that it could form T=1 particles which correspond to 60 subunits of CP of the A/B conformation.

5.4.2 Proposed hypothetical model for CNV assembly

Based on previous work conducted by *Reade et al.* (2010) (164) as well as neutron scattering studies by *Timmins et al.* (1994) (280) and current research conducted by me (Chapter 4), I was able to map putative RNA binding sites on the CNV CP in virions (Figure 4.8). It is indeed interesting that the two major binding sites can be seen to exist in virions near the β-annulus which is an important stability determinant in CNV and is the place at which trimers of C/C dimers adjoin at the particle 3-fold axis. It has previously been suggested that the related virus TCV assembles initially via interaction between viral RNA and trimers of C/C dimers (Figure 5.3A). However, in the case of SBMV and SeMV it has been suggested that particle assembly might originate from pentamers of A/B dimers (Figure 5.3B) (50, 51).

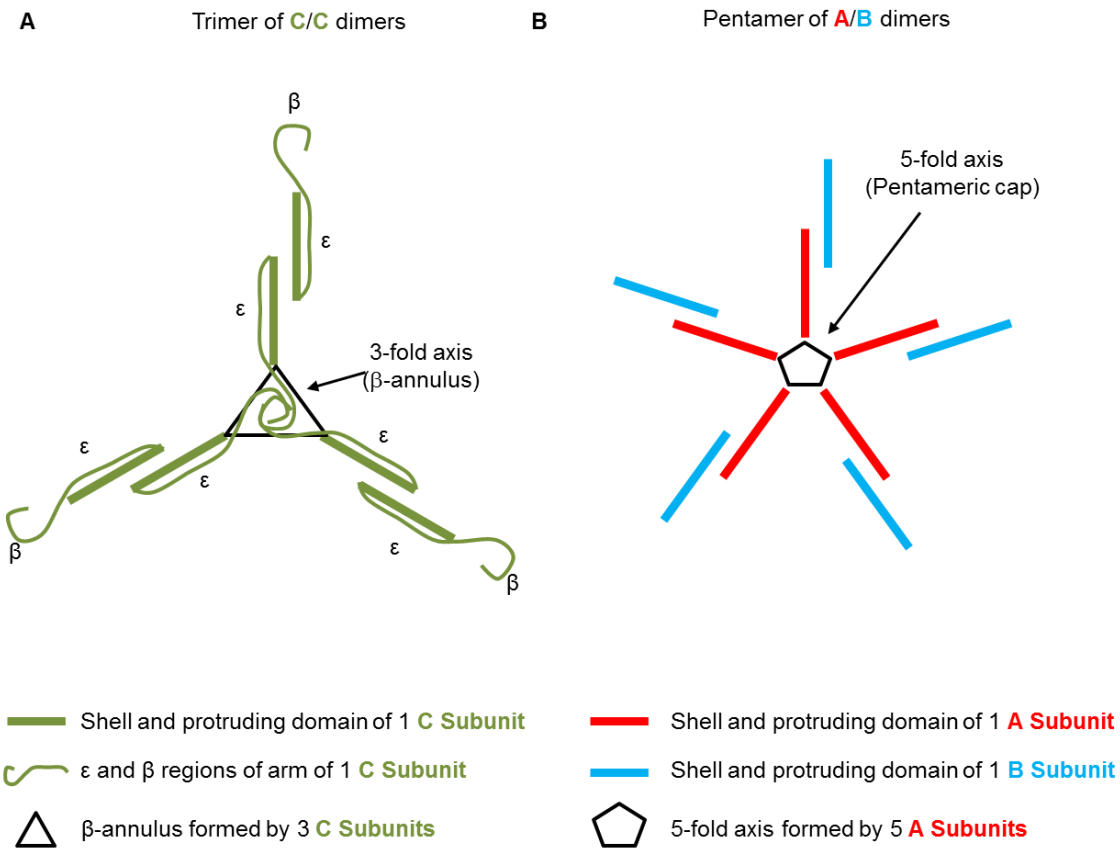

Figure 5.3: Diagrammatic representation of a trimer of C/C dimers and a pentamer of A/B dimers.

To meet the criteria for quasi-equivalence (different conformations of the same protein which is required for formation of T=3 particle symmetry) and for the formation of an icosahedral T=3 shell, CNV CP exists in three distinct conformations A (red), B (blue) and C (green). The arm as well as the R domains are ordered and structured in the C subunit, however they are disordered in the A and B subunits. The CNV particle is made up of 30 C/C dimers that lie at the 2-fold axis and 60 A/B dimers that lie at the quasi 2-fold axis. (A) In a trimer of a C/C dimers, the ordered β regions of the three C subunits extend towards the centre of the virion at the 3-fold axis to produce a stable structure termed the β-annulus. (B) On the other hand five A/B pentamers meet at the 5-fold axis to produce a pentameric cap. The arm as well as the R domain of A and B subunits are not shown because they are disordered within the virion.

Our findings would agree with the importance and structure of a trimer of C/C dimers in CNV assembly initiation. Specifically, as described in Chapter 4, Section 4.4, we propose that a trimer of C/C dimers binds six sites on CNV RNA using the C subunits most proximal to the β-annulus and the RNA binding sites "KGKKGK" and "KGRKPR". An additional six sites corresponding to the "KGKKGK" sequence and the "KGRKPR" sequence in the remaining C subunits of the trimer of C/C dimers may also be involved in binding RNA (see Figure 4.8). The requirement for at least six distinct binding sites on CNV RNA to nucleate assembly would be expected to contribute greatly to the specificity of viral RNA selectivity. Should the additional six binding events also be required, this would further enhance the selectivity process.

Following nucleation, we propose as for TCV (49) that CP dimers would attach to the nucleating complex and thereby adopt an A/B conformation. The RNA could then interact with additional sets of "KGKKGK" and "KGRKPR" sequences present in the A/B dimers. Also, apart from the two sequences bearing clustered basic aa (in the "KGKKGK" and "KGRKPR" sequences), the CNV CP contains 12 additional positively charged residues in the R (5 aa) and S (6 aa) domain and in the arm (1 aa) region. These residues could serve as additional RNA binding sites.

Hence, I propose that CNV assembly likely is a combined effect of at least two CP-RNA interactions (with the help of "KGKKGK" and "KGRKPR" sequences that assist in nucleating the assembly process) and additional CP-RNA interactions. This hypothesis raises the possibility of multiple PSs on CNV RNA for binding to the multiple CP sequences likely with different affinities. As described above, the most important aspect of the selectivity may reside in the

nucleation event of encapsidation (see above) where six distinct sites on viral RNA (or possibly even 12) may be required to initiate the assembly of particles.

As described in Chapter 1, Section 1.19.6, it has been suggested, as well as described in the literature, that viral RNA contains a PS or multiple PSs that are recognized by the CP during the initiation of assembly. Our proposed model for CNV assembly would therefore be consistent with the requirement for more than one such signal and that, in turn, would increase the selectivity process by requiring several specific viral RNA sequences.

Previous work in the Rochon lab [K. Ghoshal, Ph.D. thesis, (201)] showed that a 1227 nt region (R3) corresponding to CNV nt 2202-3427 encompassing 404 nt of the 3' terminal region of the replicase ORF, 23 nt of the intergenic region between the replicase and CP ORF and the 5' terminal 800 nt region of the CP ORF may represent a PS in CNV RNA, however, further experiments are required to demonstrate this. It was further found that many other regions throughout CNV RNA can be recognized for assembly, *albeit* with lower apparent affinity than the R3 region. Thus the notion that CNV RNA contains a single PS was not strongly supported by previous data (201). Our model, invoking several PSs is consistent with these studies. Also, numerous PSs on viral RNA this would facilitate the compaction of viral RNA that would help to reduce the hydrodynamic radii and accommodate RNA within the limited area of a sphere having a T=3 icosahedral symmetry as suggested previously for other viruses (173, 174).

Also, as described in Section 1.17.2 and in Chapter 2, HSP70 homologs might act as a scaffold protein or auxiliary host factor to promote the initiation of capsid nucleation event or any other

aspect of the particle assembly process by increasing the accumulation of CP molecules as well as preventing the aggregation of CP oligomers. However, further experiments are required to ascertain this possibility. In this regard, it would be of interest to perform *in vitro* assembly reactions using recombinant CNV CP, RNA and HSP70 homologs under optimised conditions. Assembly intermediates could be collected at different time points post-reaction start time. Assembly intermediates could be analysed either by structural studies or by native PAGE followed by Western blotting to detect at which stage of the assembly process, HSP70 homologs associates with CP. However, as described previously in Section 2.3.7, particles might not be assembled or observed *in vitro* in the presence or absence of HSP70 homologs due to the low level of soluble CP produced under the optimised *in vitro* system. Hence, further optimization of *in vitro* solubilisation of CP is required to assist in resolving this question.

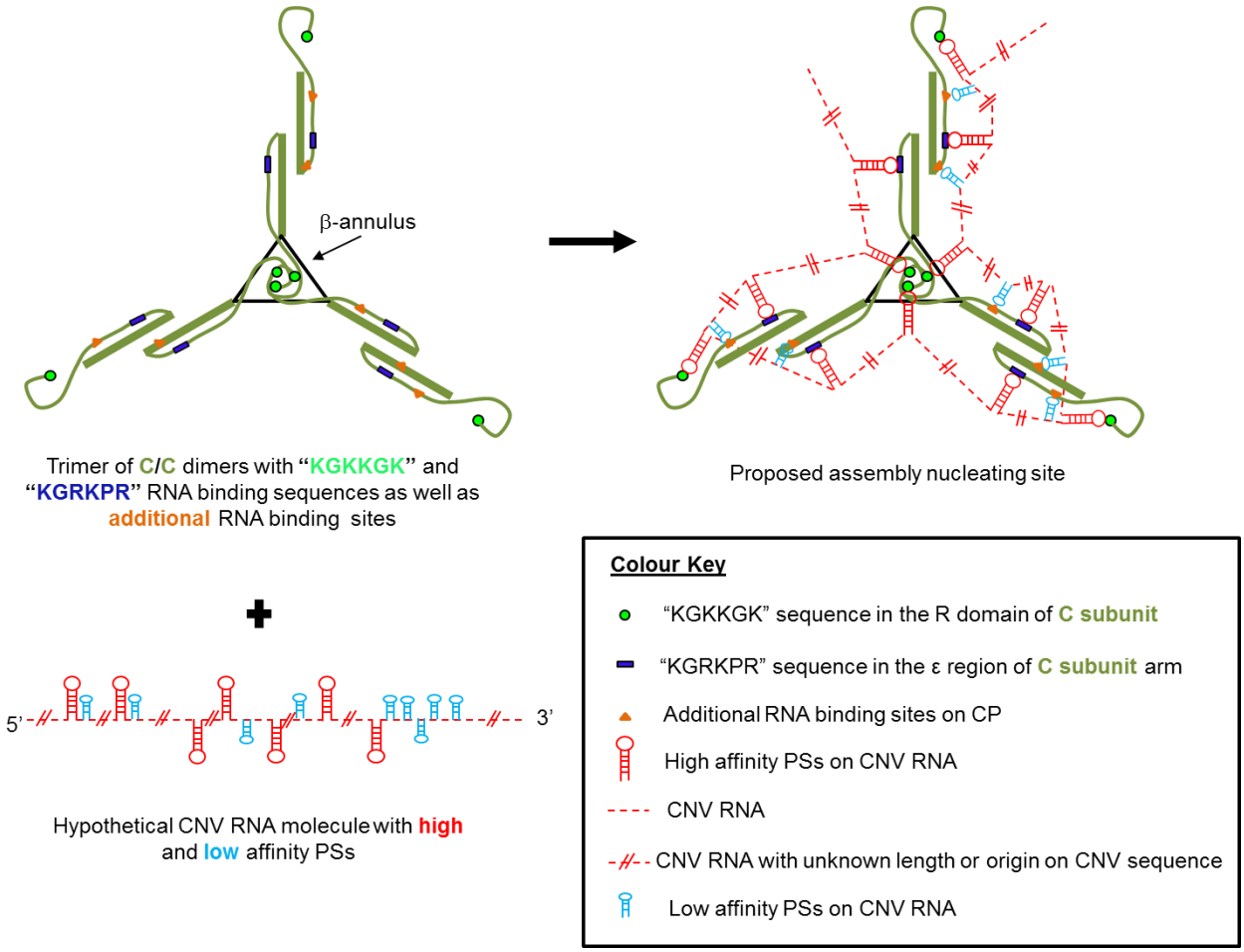

Figure 5.4: Hypothetical model for CNV assembly.

According to this model, assembly initiates from a trimer of C/C dimers (left) bearing at least six but up to 12 RNA binding sites. The CNV RNA on the other hand might contain several high or low affinity PSs as previously suggested for other viruses (174). Assembly initiates when the 6-12 CP binding sites on the trimer of C/C dimers interact with the high affinity PSs on the viral RNA (right). The interaction of CP molecules with RNA at several sites would likely increase the specificity of CNV RNA binding (over that of host RNA) and as well might enhance the compaction of RNA as suggested by *Borodavka et al.* (2013) (173). Once the initial nucleation event occurs additional CP subunits bind in a co-operative manner facilitating formation of the complete virion.

5.4.3 Host RNA encapsidation by WT CNV and "KGRKPR" mutants

CNV has been found to encapsidate a low level (~0.1-0.7%) of host RNA during natural infection (135). As described in Chapter 4, Section 4.3.7, when all four basic aa residues in the "KGRKPR" sequence, are mutated, there is a significantly greater relative encapsidation of host RNA over viral RNA. In light of the current proposed model for CNV assembly (see above), I speculate that mutation of sites on the CP that impart selectivity of viral RNA during assembly (i.e., the "KGRKPR" sequence) disrupts the specific CP-viral RNA interaction leading to formation of virions containing cellular RNA.

A recent report on STMV shows that interaction between the N-terminal basic motif of the CP with the helper TMV replicase plays an important role in replication and encapsidation (151). Also, in a preliminary experiment by co-immunoprecipitation analyses, I have shown that the CNV CP associates with the replication protein p33 either directly or indirectly (S.B. Alam, data not shown). Hence, it is also possible that the "KGRKPR" sequence of the CP plays an important role in interacting with p33. It will be interesting to see if this association is abolished by mutating the basic aa residues of the "KGRKPR" sequence. If an association between this sequence and the replicase normally occurs in a WT CNV infection the CNV CP mutants may not be in a cellular location where predominantly viral RNA occurs and this could result in "mis-encapsidation" of host RNAs.

On the other hand, in the quadruple "KGRKPR" mutant M4, since the other RNA binding site "KGKKGK" is intact, it could potentially participate in a CP-RNA interaction (See Section 5.4.2). This perhaps could lead to the formation of some viral RNA containing virions (~10%,

Figure 4.5). However, the majority of the encapsidated RNA is of host origin (~90%), suggesting the importance of "KGRKPR" sequence in selectivity of viral RNA during particle assembly.

However, as described in Chapter 4, another possible reason for encapsidation of host RNA could be the loss of CP's location from the site of viral RNA encapsidation and particle assembly in the (particularly in the double and quadruple "KGRKPR" mutants) that could lead to mis-encapsidation of host RNAs. Further *in vitro* binding experiments could shed light on this possibility. It will be interesting to examine the encapsidation profile of a mutant lacking both the "KGRKPR" and "KGKKGK" sequences. However, due to the loss of two clustered RNA binding sites from the CP that comprises ~47% of the total basic aa content, it might be difficult to obtain virions. However, if any virions are obtained, they would likely be exclusively comprised of cellular RNAs.

5.5 Does the ability of CNV CP to target the stroma interfere with chloroplast-mediated plant defense response?

Previous work in the Rochon lab has shown that ~1-5% of the CP is targeted to chloroplasts during infection and that the CP arm region functions as a chloroplast transit peptide, targeting the CP S and P domains to the chloroplast stroma (24). Previous studies have shown that chloroplasts play important roles in plant defense responses including the hypersensitive response (HR) response (304). For example, salicylic acid, which is required for the induction of the HR marker gene *PR1a,* is synthesized in chloroplasts and, chloroplasts also produce reactive oxygen species which assist in limiting pathogen infection (305-308). Indeed, some pathogenic effectors of bacteria and fungi target chloroplasts to attenuate host defense responses (223, 301-

303, 309). Also, some reports have shown the involvement of viral proteins in attenuation of host defense responses (310, 311). Hence, my work as well as the work of others in Dr. Rochon's lab led to the hypothesis that CNV CP targets the chloroplast stroma resulting in the attenuation of symptoms during infection (manuscript in preparation).

The "KGRKPR" sequence in the ε region of the CP arm is encompassed within the CP transit peptide-like region responsible for chloroplast targeting of CNV CP. I therefore, tested if the "KGRKPR" mutants produce severe symptoms compared to WT CNV. At 4 dpi, plants infected with equal inoculum concentrations of WT CNV and the "KGRKPR" mutants, showed that most of the latter produced more severe symptoms that appeared earlier in infection when compared to CNV. Also, the symptoms were more localised compared to that of WT CNV. This suggests a potential role for the CNV CP to enter chloroplasts and interfere with components of the host defense machinery.

It was further found that "KGRKPR" mutants M3, M4 and M7, do not enter the chloroplast stroma as efficiently as WT CNV (S.B. Alam, data not shown) although they do target the chloroplast intermembrane space. I also found that the "KGRKPR" mutant inoculated plants were undergoing a stronger defense response as suggested by higher and sustained levels of the defense response gene *PR1a* relative to the housekeeping gene *PP2a*.

Trypan blue staining could be conducted to determine if inoculation of plants with CP mutants defective in efficient stromal uptake leads to more cell death compared to WT CNV. Furthermore, DAB staining could be performed to estimate the amount of peroxide accumulation

in leaves inoculated with WT CNV or CP mutants defective in efficient stromal entry. Further research will be conducted to further characterize the role of CP in attenuating symptoms during infection. In this regard, it has recently been found that local lesion assays on the CNV local lesion host *C. quinoa* showed that "KGRKPR" mutants that inefficiently enter the chloroplast stroma produce significantly smaller lesions compared to WT CNV.

It has previously been shown that TBSV p19 induces necrosis in *N. tabacum* (312). To determine whether CNV CP could reduce p19-induced necrosis in *N. tabacum*, leaves can be co-agroinfiltrated with different concentrations of TBSV p19 along with either pGFP/pBin(+) or pCNVCP/pBin(+) followed by analysis of symptoms,assessment of *PR1a* levels and trypan blue and DAB staining. If the p19 induced symptoms are attenuated in the presence of CNV CP, further experiments could be conducted to directly test if symptom attenuation is correlated with the ability of CP to target chloroplasts. In this regard a CP mutant lacking 16 aa of the CP transit peptide-like region will be cloned into a binary vector [pCPβ(-)/pBin(+)]. A similar experiment as described above will be performed in the presence of p19 followed by symptom analyses and *PR1a* levels assessment. Confocal experiments could further be conducted by making GFP fusion constructs to correlate the results with the ability of CP to target chloroplasts. Also, I participated in a collaborative project in Dr. Rochon's lab, where it was found that the CNV auxiliary replicase protein p33 induces necrosis in *N. benthamiana* upon agroinfiltration (32). To test if the ability of CP to target chloroplasts interferes with p33 induced necrosis, similar types of experiments can be conducted as described above for TBSV p19.

5.6 Does CNV acts as a beneficial microparasite for plants?

During the end of my Ph.D. tenure I became interested in how plants have evolved to utilise some of the virus-induced host factors for their own benefit, and if viruses can thereby act as a beneficial microbe in this regard (248). As described in Section 2.4, previous studies have shown that TMV, BMV, TRV and CMV can confer drought or cold tolerance to their plant hosts (248). In addition, several plant viruses such as TMV and CMV along with CNV are known to induce HSP70 homologs (122, 214). It was hypothesized in Chapter 2 that induction of heat shock proteins by CNV and other plant viruses may confer heat tolerance to their hosts in natural environments.

My work in conjunction with others in the Rochon lab showed that specific types of retrotransposons (RTn) are induced during CNV infection.Among the most highly induced are specific *Ty-1/Copia*-type RTns (Figure B.1, Dr. Rochon lab, personal communication). Interestingly, these retrotransposons group phylogenetically with a previously described heat inducible retrotransposon, ONSEN. The 5' LTRs of four different RTns induced during CNV infection were analysed and found to contain several putative heat-shock elements (HSEs) (Figure B.2) raising the possibility that heat-shock factors (HSFs) induced by heat stress can activate these RTns.

Previous work (122) described in this thesis showed that CNV infection results in a strong upregulation of HSP70 homolog mRNAs and proteins (Chapter 2). The promoters of the HSP70 family of genes contain HSEs to which the transcription factors HSFs bind and promote the transcription of downstream *HSP70* genes and other HSP genes (for details see Section 1.10).

Also HSFA2 is known to regulate the expression of the heat inducible ONSEN RTn (313). By RNA-seq analysis and quantitative PCR, current research in Dr. Rochon's lab shows that HSFA2 mRNA as well as other HSFs are upregulated both during CNV infection and heat stress (Rochon lab, personal communication).

Based on the above described work I tested whether the RTns induced by CNV infection can be induced by heat treatment and found that indeed heat induces these RTns and that the level of induction strongly parallels that found during CNV infection. Moreover, I found that the transcript abundance of these RTns was significantly increased with severity of the stress (i.e., higher temperature) (Figure B.3), which suggests a temperature-sensitive response as previously described for RTns in rice (*Oryza sativa*) (314). To rule out the possibility that heat treatment induces RTns non-specifically, I also determined the transcript levels of the *Ty-1/Copia* element RTnNbTnt which is not induced during CNV infection and not reported to be heat inducible (Rochon Lab, personal communication). I found that RTnNbTnt is not induced by heat treatment at 42°C or 48°C suggesting that RTn induction by heat treatment is specific.

I also tested if heat-shocked plants only containing the LTRs of two ONSEN-like RTns induced by CNV infection and placed upstream of the GFP reporter coding region were activated by heat-shock. Both LTRs were strongly activated as determined by ddPCR analysis of GFP levels in total leaf RNA of heat-shocked plants. In addition, heat-shocked plants containing the two LTR-GFP constructs also contained elevated levels of GFP as determined by Western blot analysis of total leaf protein and by confocal microscopy of agroinfiltrated leaves (Figures B.4 and B.5). Current research in Dr. Rochon's lab suggests that agroinfiltrated plants also show a

similar activation of GFP mRNA transcription and expression when infected with CNV (Rochon Lab, personal communication). To determine the specificity of CNV and heat stress mediated LTR activation, future experiments could be conducted by cloning the LTR sequence of RTnNbTnt which does not become induced by heat or CNV infection (see above), upstream of the GFP reporter coding region [pRTnNbTnt-LTR/GFP/pBin(+)]. Heat shock as well as CNV inoculation experiments could be conducted on pRTnNbTnt-LTR/GFP/pBin(+) agroinfiltrated plants followed by analyses of GFP expression levels, to rule out the possibility that activation of ONSEN-like RTn LTRs by heat stress and CNV infection is a non-specific process.

It is speculated that CNV induces ONSEN-like RTns during infection due to the induction of the heat-shock response which activates the LTRs of the RTns, possibly through HSFA2 or other HSF induction. As stated above, HSFA2 could bind the HSEs in the LTRs of ONSEN-like RTn to increase the transcription of downstream genes. In this regard, *N. benthamiana* HSFA2 will be cloned into a bacterial expression vector such as pET24D(+) and expressed in *Escherichia coli* cells (NbHSFA2). The purified NbHSFA2 will be utilised in gel electrophoretic mobility shift assays (GEMSAs). GEMSA will be performed by incubating increasing amounts of recombinant NbHSFA2 with DNA corresponding to the 5' LTR of specific heat stress and CNV inducible RTn, followed by gel electrophoresis and EtBr staining to look for mobility shift. Apart from this, competition assays could also be performed using NbHSFA2 and DNA fragments that do not contain any HSEs. BSA would also be utilised instead of NbHSFA2 to assess the specificity of binding with HSEs containing LTRs. To directly assess which of the putative HSEs interact with NbHSFA2, a similar type of GEMSA experiment will be conducted using oligonucleotides corresponding to individual HSEs or by using LTR DNA fragments in which specific HSE

elements are mutated. However, the latter experiment may be difficult to interpret since the LTRs of specific heat and CNV inducible RTn contain several putative HSEs and mutating one of the elements may still allow efficient binding of NbHSFA2 and thereby result in inconclusive data.

DNase I Footprint analysis can be conducted to identify the HSEs in the LTRs. 5' radiolabelled LTR fragments containing putative HSEs or their mutated versions could be incubated with the bacterially expressed and purified NbHSFA2 followed by DNase I digestion, gel electrophoresis and phosphorimaging. Regions that are resistant to DNase I digestion would likely represent the HSEs with bound HSFs. However, protection will not occur if the sites did not represent authentic HSEs.

Transposition of the ONSEN-like RTns induced during CNV infection has not yet been demonstrated. To assess this *N. benthamiana* plants will be either mock inoculated or inoculated with CNV followed by extraction of total DNA at 5 dpi. A similar experiment would be performed on plants heat-shocked at both 42°C and 48°C, again followed by total DNA extraction. Equal amounts of DNA from mock inoculated, CNV inoculated, untreated and heat-shocked plants would then be subjected to gel electrophoresis followed by Southern blotting using a probe made to a RTn induced by CNV such as the strongly CNV and heat-induced RTn5533 (see Figures B.1 and B.3). If replication of the RTn is occurring then an approximate 5 kb DNA band (the size of RTn5533) should be detected in CNV inoculated and heat treated plants, but not in uninoculated and untreated plants. To ensure that the band corresponds to DNA

and not contaminating RNA in the DNA preparation, the DNA preparations will be treated with RNaseA during the extraction procedure.

It is noted that, if transposition occurs, it could indicate that CNV infection may contribute to modification of the infected plant genome. However, such modifications would have to be present in the germ line cells in order to be transmitted to the next generation. In this regard future experiments could be conducted on second generation plants obtained from the seeds of CNV inoculated leaves. However, since CNV infects the plants systemically and the plant does not survive up to the flowering stage (plants collapse at about 9-12 dpi and don't flower), it might not be possible to conduct such an experiment. Recent work in Dr. Rochon's lab has shown that a full-length infectious mutant of CNV bearing a stop codon in the silencing suppressor ORF, p20 (20K-stop), induces retrotransposons to high levels (Rochon Lab, personal communication). It is interesting that the CNV 20K-stop mutant does not cause death of the infected plants (Rochon Lab, Unpublished). Hence, plants could either be mock inoculated or inoculated with the CNV 20K-stop mutant. The infection would be allowed to proceed up to the flowering stage until seeds are produced. From the collected seeds, second generation plants will be germinated followed by total DNA extraction and Southern blot analyses as described above. If retrotransposition is demonstrated then that would indicate that RTn sequences have a potential to alter the host genome. These experiments would probably need to be conducted from a large number of second generation plants to observe retrotransposition if this event is not frequent in the inoculated plant. Also, it would be of interest to conduct these experiments on the natural host of CNV, cucumber, as this would shed light on the possibility that generation of retrotransposons is part of the co-evolution of CNV with its host (see below).

5.7 Evolution of a plant virus and its susceptible host

In the light of current research and findings, I propose a hypothetical model for evolution of CNV and its host plants (Figure 5.5). According to this model, when CNV infects the plant (a), HSFs are upregulated resulting in an increase in the transcription and expression of HSP70 homologs and other heat shock proteins (b). CNV has evolved to multiply at a high rate in plants through its interaction with HSP70 homologs and possibly other heat shock proteins (c). In particular, the CNV CP evolved to interact with the HSP70 homologs and to utilize it in several stages of the infection such as disassembly of virions, gRNA accumulation, CP accumulation and preventing CP aggregate formation as well as promoting particle assembly. Overall, the CP utilises the host factor HSP70 to promote virus spread and multiplication (c_1). As infection proceeds, the plant responds by restricting the virus to localised lesions. The viral CP, in turn, has evolved further, to target and enter chloroplasts with the aid of HSP70 homologs. This and the induced HSP70 homologs likely interfere with plant defense, thus both contributing to the attenuation of symptoms and thereby allowing CNV to spread and to invade plants systemically.

To facilitate selective packaging of viral RNA from the pool of cellular RNAs, the CP itself has evolved to bear a sequence "KGRKPR" that facilitates interaction specifically with viral RNA and to avert interaction with host RNAs which would be a "dead" end as far as virus infection is concerned. The "KGRKPR" sequence along with the previously described basic "KGKKGK" residues in the R domain (164), along with additional sequences on the CP, helps to initiate the virion assembly nucleation event from the trimers of C/C dimers (c_2) and helps in the assembly of infectious virions (c_2).

The plant in turn, has adapted to utilise the virus induced host factors, such as HSFA2, to facilitate the transcription of ONSEN-like RTns. It is possible that the induced RTns in turn render plant genome variation, allowing for adaptation of the plants under changing environmental conditions. In particular, 5’ or 3’ LTRs of the integrated RTn could cause induction of gene expression in the corresponding upstream or downstream genes under heat stress conditions and if positioned optimally could result in transcription of genes that could help the plant resist heat stress or other stresses.

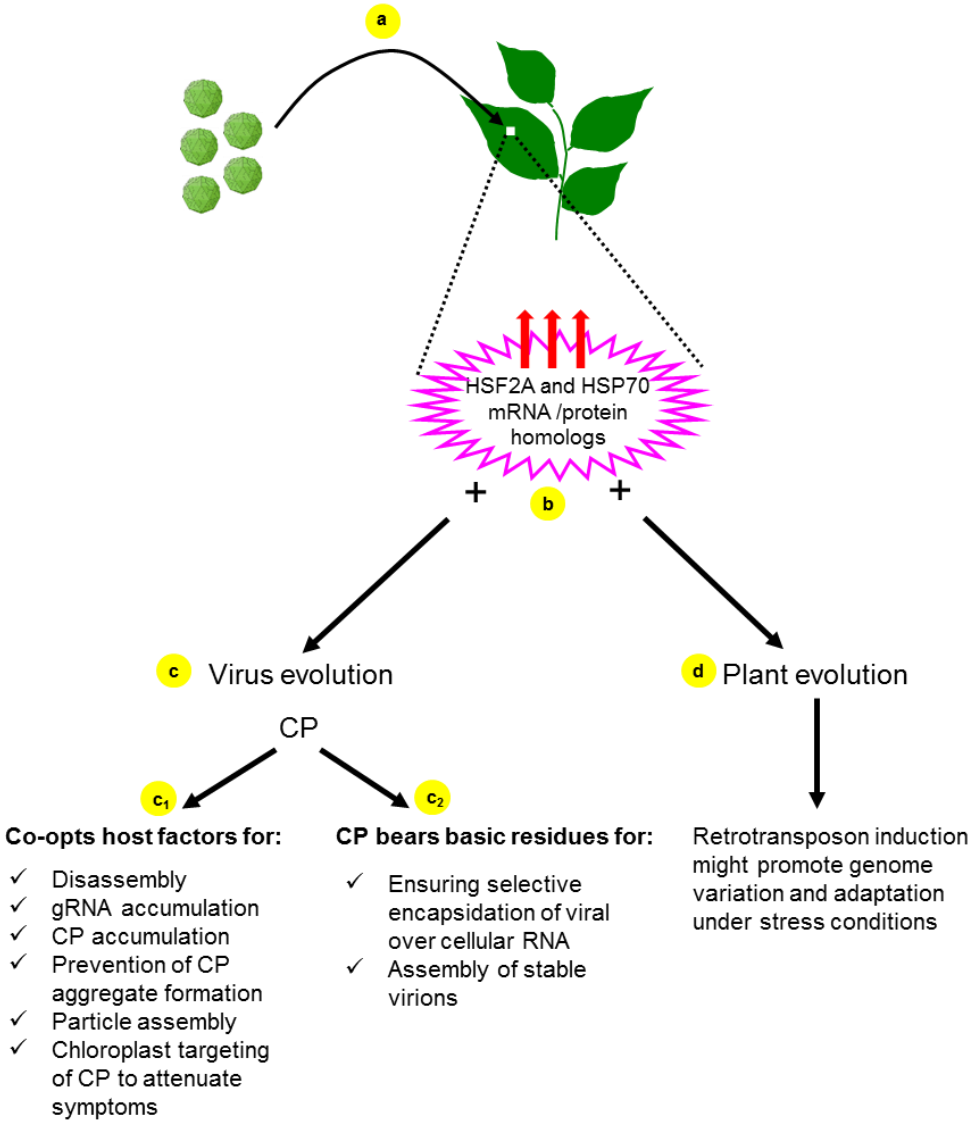

Figure 5.5: Hypothetical model showing evolution of CNV and plants.

For details see Section 5.7.

Bibliography

1. **Roger H.** 2009. Comparative plant virology. 2. edition. Amsterdam : Elsevier, 2009.
2. **Lucas WJ.** 2006. Plant viral movement proteins: agents for cell-to-cell trafficking of viral genomes. Virology **344:**169-184.
3. **McKeen CD.** 1959. CUCUMBER NECROSIS VIRUS. Canadian Journal of Botany **37:**913-925.
4. **Babos P, Kassanis B.** 1963. SEROLOGICAL RELATIONSHIPS AND SOME PROPERTIES OF TOBACCO NECROSIS VIRUS STRAINS. Journal of general microbiology **32:**135-144.
5. **Dias HF, Doane FW.** 1968. Evidence for lack of relationship between Canadian cucumber necrosis and tobacco necrosis viruses. Canadian Journal of Botany **46:**47-50.
6. **TREMAINE DARAJH.** 1988. Cucumber Necrosis Virus Is a Member of the Tombusvirus Group. J. gen. Virol **69:**395-400.
7. **King AMQ, Adam, M.J., Carstens, E.B., Lefkowitz, E.J. (Ed.).** 2012. Virus Taxonomy: Ninth Report of the International Committee on the Taxonomy of Viruses. . Elsevier Academic Press, London, **:**pp. 1111-1138.
8. **Wydro M, Kozubek E, Lehmann P.** 2006. Optimization of transient Agrobacterium-mediated gene expression system in leaves of Nicotiana benthamiana. Acta biochimica Polonica **53:**289-298.
9. **Clemente T.** 2006. Nicotiana (Nicotiana tobaccum, Nicotiana benthamiana). Methods in molecular biology (Clifton, N.J.) **343:**143-154.
10. **Fabian MR, White KA.** 2006. Tombusvirus replication: an overview of essential processes. *In* Hefferon KL (ed.). Transworld Research Network, Trivandrum.
11. **Nagy PD.** 2011. The roles of host factors in tombusvirus RNA recombination. Advances in virus research **81:**63-84.
12. **Nagy PD, Pogany J.** 2010. Global genomics and proteomics approaches to identify host factors as targets to induce resistance against Tomato bushy stunt virus. (Special Issue: Natural and engineered resistance to plant viruses, Part II.). Advances in virus research **76:**123-177.
13. **Katpally U, Kakani K, Reade R, Dryden K, Rochon D, Smith TJ.** 2007. Structures of T = 1 and T = 3 Particles of Cucumber Necrosis Virus: Evidence of Internal Scaffolding. Journal of Molecular Biology **365:**502-512.
14. **Li M, Kakani K, Katpally U, Johnson S, Rochon D, Smith TJ.** 2013. Atomic structure of Cucumber necrosis virus and the role of the capsid in vector transmission. J Virol **87:**12166-12175.
15. **Scholthof KB, Scholthof HB, Jackson AO.** 1995. The tomato bushy stunt virus replicase proteins are coordinately expressed and membrane associated. Virology **208:**365-369.
16. **White KA, Nagy PD.** 2004. Advances in the molecular biology of tombusviruses: gene expression, genome replication, and recombination. Progress in nucleic acid research and molecular biology **78:**187-226.
17. **Wang RY, Stork J, Nagy PD.** 2009. A key role for heat shock protein 70 in the localization and insertion of tombusvirus replication proteins to intracellular membranes. J Virol **83:**3276-3287.

18. **Pogany J, Stork J, Li Z, Nagy PD.** 2008. In vitro assembly of the Tomato bushy stunt virus replicase requires the host Heat shock protein 70. Proceedings of the National Academy of Sciences of the United States of America **105:**19956-19961.
19. **Nagy PD, Wang RY, Pogany J, Hafren A, Makinen K.** 2011. Emerging picture of host chaperone and cyclophilin roles in RNA virus replication. Virology **411:**374-382.
20. **Johnston JC, Rochon DM.** 1995. Deletion analysis of the promoter for the cucumber necrosis virus 0.9-kb subgenomic RNA. Virology **214:**100-109.
21. **Kakani K, Reade R, Katpally U, Smith T, Rochon D.** 2008. Induction of particle polymorphism by Cucumber necrosis virus coat protein mutants in vivo. Journal of Virology **82:**1547-1557.
22. **Hui E, Rochon D.** 2006. Evaluation of the roles of specific regions of the Cucumber necrosis virus coat protein arm in particle accumulation and fungus transmission. Journal of Virology **80:**5968-5975.
23. **Chauvin C, Witz J, Jacrot B.** 1978. Structure of the tomato bushy stunt virus: a model for protein-RNA interaction. J Mol Biol **124:**641-651.
24. **Xiang Y, Kakani K, Reade R, Hui E, Rochon D.** 2006. A 38-amino-acid sequence encompassing the arm domain of the Cucumber necrosis virus coat protein functions as a chloroplast transit peptide in infected plants. Journal of Virology **80:**7952-7964.
25. **Kakani K.** 2009. Molecular and biochemical characterization of viral and vector components required for cucumber necrosis virus transmission. Text. University of British Columbia, UBCV.
26. **Harrison SC, Olson AJ, Schutt CE, Winkler FK, Bricogne G.** 1978. Tomato bushy stunt virus at 2.9 A resolution. Nature **276:**368-373.
27. **Erk I, Huet JC, Duarte M, Duquerroy S, Rey F, Cohen J, Lepault J.** 2003. A zinc ion controls assembly and stability of the major capsid protein of rotavirus. J Virol **77:**3595-3601.
28. **Rochon D, Kakani K, Reade R.** 2002. Partial characterization of Cucumber necrosis virus binding sites on zoospores of the fungal vector Olpidium bornovanus. Proceedings of the Fifth Symposium of the International Working Group on Plant Viruses with Fungal Vectors, Institute of Plant Sciences, Swiss Federal Institute of Technology, Zurich, Switzerland.
29. **Kakani K, Robbins M, Rochon D.** 2003. Evidence that binding of cucumber necrosis virus to vector zoospores involves recognition of oligosaccharides. Journal of Virology **77:**3922-3928.
30. **Kakani K, Sgro J-Y, Rochon DA.** 2001. Identification of specific cucumber necrosis virus coat protein amino acids affecting fungus transmission and zoospore attachment. Journal of Virology **75:**5576-5583.
31. **Rochon DM, Johnston JC.** 1991. Infectious transcripts from cloned cucumber necrosis virus cDNA: evidence for a bifunctional subgenomic mRNA. Virology **181:**656-665.
32. **Rochon D, Singh B, Reade R, Theilmann J, Ghoshal K, Alam SB, Maghodia A.** 2014. The p33 auxiliary replicase protein of Cucumber necrosis virus targets peroxisomes and infection induces de novo peroxisome formation from the endoplasmic reticulum. Virology **452-453:**133-142.
33. **Laliberte JF, Sanfacon H.** 2010. Cellular remodeling during plant virus infection. Annu Rev Phytopathol **48:**69-91.

34. **Sanfaçon H.** 2005. Replication of positive-strand RNA viruses in plants: contact points between plant and virus components. Canadian Journal of Botany **83:**1529-1549.
35. **Rochon D, Kakani K, Robbins M, Reade R.** 2004. Molecular aspects of plant virus transmission by olpidium and plasmodiophorid vectors, p. 211-241, vol. 42.
36. **Shaw JG, Plaskitt KA, Wilson TM.** 1986. Evidence that tobacco mosaic virus particles disassemble contranslationally in vivo. Virology **148:**326-336.
37. **Bakker SE, Ford RJ, Barker AM, Robottom J, Saunders K, Pearson AR, Ranson NA, Stockley PG.** 2012. Isolation of an asymmetric RNA uncoating intermediate for a single-stranded RNA plant virus. J Mol Biol **417:**65-78.
38. **Fabian MR, White KA.** 2006. Analysis of a 3'-translation enhancer in a tombusvirus: a dynamic model for RNA-RNA interactions of mRNA termini. RNA (New York, N.Y.) **12:**1304-1314.
39. **Nicholson BL, White KA.** 2011. 3' Cap-independent translation enhancers of positive-strand RNA plant viruses. Curr Opin Virol **1:**373-380.
40. **Serva S, Nagy PD.** 2006. Proteomics analysis of the tombusvirus replicase: Hsp70 molecular chaperone is associated with the replicase and enhances viral RNA replication. J Virol **80:**2162-2169.
41. **Kovalev N, Pogany J, Nagy PD.** 2012. A Co-Opted DEAD-Box RNA helicase enhances tombusvirus plus-strand synthesis. PLoS Pathog **8:**e1002537.
42. **Wang X, Ahlquist P.** 2008. Filling a GAP(DH) in asymmetric viral RNA synthesis. Cell Host Microbe **3:**124-125.
43. **Wang RY, Nagy PD.** 2008. Tomato bushy stunt virus co-opts the RNA-binding function of a host metabolic enzyme for viral genomic RNA synthesis. Cell Host Microbe **3:**178-187.
44. **Choi IR, Ostrovsky M, Zhang G, White KA.** 2001. Regulatory activity of distal and core RNA elements in Tombusvirus subgenomic mRNA2 transcription. The Journal of biological chemistry **276:**41761-41768.
45. **Jiwan SD, White KA.** 2011. Subgenomic mRNA transcription in Tombusviridae. RNA biology **8:**287-294.
46. **Sztuba-Solinska J, Stollar V, Bujarski JJ.** 2011. Subgenomic messenger RNAs: mastering regulation of (+)-strand RNA virus life cycle. Virology **412:**245-255.
47. **Seo JK, Kwon SJ, Rao AL.** 2012. A physical interaction between viral replicase and capsid protein is required for genome-packaging specificity in an RNA virus. J Virol **86:**6210-6221.
48. **Annamalai P, Rao AL.** 2006. Packaging of brome mosaic virus subgenomic RNA is functionally coupled to replication-dependent transcription and translation of coat protein. J Virol **80:**10096-10108.
49. **Sorger PK, Stockley PG, Harrison SC.** 1986. Structure and assembly of turnip crinkle virus. II. Mechanism of reassembly in vitro. J Mol Biol **191:**639-658.
50. **Savithri HS, Erickson JW.** 1983. The self-assembly of the cowpea strain of southern bean mosaic virus: formation of T = 1 and T = 3 nucleoprotein particles. Virology **126:**328-335.
51. **Satheshkumar PS, Lokesh GL, Murthy MR, Savithri HS.** 2005. The role of arginine-rich motif and beta-annulus in the assembly and stability of Sesbania mosaic virus capsids. J Mol Biol **353:**447-458.

52. **Hafren A, Hofius D, Ronnholm G, Sonnewald U, Makinen K.** 2010. HSP70 and its cochaperone CPIP promote potyvirus infection in Nicotiana benthamiana by regulating viral coat protein functions. Plant Cell **22:**523-535.
53. **Rao AL.** 2006. Genome packaging by spherical plant RNA viruses. Annu Rev Phytopathol **44:**61-87.
54. **Hildenbrand ZL, Bernal RA.** 2012. Chaperonin-mediated folding of viral proteins. Adv Exp Med Biol **726:**307-324.
55. **Mateu MG.** 2013. Assembly, stability and dynamics of virus capsids. Archives of biochemistry and biophysics **531:**65-79.
56. **Mayer MP.** 2005. Recruitment of Hsp70 chaperones: a crucial part of viral survival strategies. Reviews of physiology, biochemistry and pharmacology **153:**1-46.
57. **Beachy RN, Heinlein M.** 2000. Role of P30 in replication and spread of TMV. Traffic (Copenhagen, Denmark) **1:**540-544.
58. **McLean MA, Hamilton RI, Rochon DM.** 1993. Symptomatology and movement of a cucumber necrosis virus mutant lacking the coat protein protruding domain. Virology **193:**932-939.
59. **Kakani K, Reade R, Rochon D.** 2004. Evidence that vector transmission of a plant virus requires conformational change in virus particles. J Mol Biol **338:**507-517.
60. **Kakani K, Rochon DA.** 2002. Mutation of Pro-73 in the arm region of the Cucumber necrosis virus coat protein results in particles with an altered swollen conformation and loss of fungus transmissibility. Proceedings of the Fifth Symposium of the International Working Group on Plant Viruses with Fungal Vectors, Institute of Plant Sciences, Swiss Federal Institute of Technology, Zurich, Switzerland.
61. **Rochon DA, Kakani K, Robbins M, Reade R.** 2004. Molecular aspects of plant virus transmission by olpidium and plasmodiophorid vectors. Annual Review of Phytopathology **42:**211-241.
62. **Ritossa F.** 1962. A new puffing pattern induced by temperature shock and DNP in drosophila. Experientia **18:**571-573.
63. **Tissiéres A, Mitchell HK, Tracy UM.** 1974. Protein synthesis in salivary glands of Drosophila melanogaster: Relation to chromosome puffs. Journal of Molecular Biology **84:**389-398.
64. **Jones C.** 1984. Heat Shock: From bacteria to man: Edited by M J Schlesinger, M Ashburner and A Tissières. pp 440. Cold Spring Harbor Laboratory. 1982. ISBN 0–87969–158–1. Biochemical Education **12:**45-45.
65. **Schlesinger MJ.** 1990. Heat shock proteins. The Journal of biological chemistry **265:**12111-12114.
66. **Ritossa F.** 1996. Discovery of the heat shock response. Cell stress & chaperones **1:**97-98.
67. **Lindquist S.** 1986. The heat-shock response. Annual review of biochemistry **55:**1151-1191.
68. **Young JC.** 2010. Mechanisms of the Hsp70 chaperone system. Biochemistry and cell biology = Biochimie et biologie cellulaire **88:**291-300.
69. **Akerfelt M, Morimoto RI, Sistonen L.** 2010. Heat shock factors: integrators of cell stress, development and lifespan. Nature reviews. Molecular cell biology **11:**545-555.
70. **Åkerfelt M, Morimoto RI, Sistonen L.** 2010. Heat shock factors: integrators of cell stress, development and lifespan. Nature Reviews. Molecular Cell Biology **11:**545-555.

71. **Wu C.** 1995. Heat shock transcription factors: structure and regulation. Annual review of cell and developmental biology **11:**441-469.
72. **Morimoto RI.** 1998. Regulation of the heat shock transcriptional response: cross talk between a family of heat shock factors, molecular chaperones, and negative regulators. Genes & development **12:**3788-3796.
73. **Pirkkala L, Nykanen P, Sistonen L.** 2001. Roles of the heat shock transcription factors in regulation of the heat shock response and beyond. FASEB journal : official publication of the Federation of American Societies for Experimental Biology **15:**1118-1131.
74. **Sakurai H, Enoki Y.** 2010. Novel aspects of heat shock factors: DNA recognition, chromatin modulation and gene expression. The FEBS journal **277:**4140-4149.
75. **Sakurai H, Takemori Y.** 2007. Interaction between heat shock transcription factors (HSFs) and divergent binding sequences: binding specificities of yeast HSFs and human HSF1. The Journal of biological chemistry **282:**13334-13341.
76. **Flores-Perez U, Jarvis P.** 2013. Molecular chaperone involvement in chloroplast protein import. Biochimica et biophysica acta **1833:**332-340.
77. **Bukau B, Weissman J, Horwich A.** 2006. Molecular chaperones and protein quality control. Cell **125:**443-451.
78. **Mayer MP, Bukau B.** 2005. Hsp70 chaperones: cellular functions and molecular mechanism. Cellular and molecular life sciences : CMLS **62:**670-684.
79. **Sun Y, Zhao J, Sheng Y, Xiao YF, Zhang YJ, Bai LX, Tan Y, Xiao LB, Xu GC.** 2014. Identification of heat shock cognate protein 70 gene (Alhsc70) of Apolygus lucorum and its expression in response to different temperature and pesticide stresses. Insect science.
80. **Luo S, Ahola V, Shu C, Xu C, Wang R.** 2015. Heat shock protein 70 gene family in the Glanville fritillary butterfly and their response to thermal stress. Gene **556:**132-141.
81. **Chong KY, Lai CC, Su CY.** 2013. Inducible and constitutive HSP70s confer synergistic resistance against metabolic challenges. Biochem Biophys Res Commun **430:**774-779.
82. **Kim YE, Hipp MS, Bracher A, Hayer-Hartl M, Hartl FU.** 2013. Molecular chaperone functions in protein folding and proteostasis. Annual review of biochemistry **82:**323-355.
83. **Fourie AM, Sambrook JF, Gething MJ.** 1994. Common and divergent peptide binding specificities of hsp70 molecular chaperones. The Journal of biological chemistry **269:**30470-30478.
84. **Takenaka IM, Leung SM, McAndrew SJ, Brown JP, Hightower LE.** 1995. Hsc70-binding peptides selected from a phage display peptide library that resemble organellar targeting sequences. The Journal of biological chemistry **270:**19839-19844.
85. **Shiber A, Ravid T.** 2014. Chaperoning proteins for destruction: diverse roles of Hsp70 chaperones and their co-chaperones in targeting misfolded proteins to the proteasome. Biomolecules **4:**704-724.
86. **Finka A, Sharma SK, Goloubinoff P.** 2015. Multi-layered molecular mechanisms of polypeptide holding, unfolding and disaggregation by HSP70/HSP110 chaperones. Frontiers in molecular biosciences **2:**29.
87. **Dodson M, Roberts J, McMacken R, Echols H.** 1985. Specialized nucleoprotein structures at the origin of replication of bacteriophage lambda: complexes with lambda O protein and with lambda O, lambda P, and Escherichia coli DnaB proteins. Proc Natl Acad Sci U S A **82:**4678-4682.

88. **Eisenberg E, Greene LE.** 2007. Multiple roles of auxilin and hsc70 in clathrin-mediated endocytosis. Traffic (Copenhagen, Denmark) **8:**640-646.
89. **Pishvaee B, Costaguta G, Yeung BG, Ryazantsev S, Greener T, Greene LE, Eisenberg E, McCaffery JM, Payne GS.** 2000. A yeast DNA J protein required for uncoating of clathrin-coated vesicles in vivo. Nature cell biology **2:**958-963.
90. **Newmyer SL, Schmid SL.** 2001. Dominant-interfering Hsc70 mutants disrupt multiple stages of the clathrin-coated vesicle cycle in vivo. The Journal of cell biology **152:**607-620.
91. **Bocking T, Aguet F, Harrison SC, Kirchhausen T.** 2011. Single-molecule analysis of a molecular disassemblase reveals the mechanism of Hsc70-driven clathrin uncoating. Nature structural & molecular biology **18:**295-301.
92. **Jinwal UK, O'Leary JC, 3rd, Borysov SI, Jones JR, Li Q, Koren J, 3rd, Abisambra JF, Vestal GD, Lawson LY, Johnson AG, Blair LJ, Jin Y, Miyata Y, Gestwicki JE, Dickey CA.** 2010. Hsc70 rapidly engages tau after microtubule destabilization. The Journal of biological chemistry **285:**16798-16805.
93. **French JB, Zhao H, An S, Niessen S, Deng Y, Cravatt BF, Benkovic SJ.** 2013. Hsp70/Hsp90 chaperone machinery is involved in the assembly of the purinosome. Proc Natl Acad Sci U S A **110:**2528-2533.
94. **Hutchison KA, Dittmar KD, Czar MJ, Pratt WB.** 1994. Proof that hsp70 is required for assembly of the glucocorticoid receptor into a heterocomplex with hsp90. The Journal of biological chemistry **269:**5043-5049.
95. **Murphy PJ, Morishima Y, Chen H, Galigniana MD, Mansfield JF, Simons SS, Jr., Pratt WB.** 2003. Visualization and mechanism of assembly of a glucocorticoid receptor.Hsp70 complex that is primed for subsequent Hsp90-dependent opening of the steroid binding cleft. The Journal of biological chemistry **278:**34764-34773.
96. **Hutchison KA, Dittmar KD, Stancato LF, Pratt WB.** 1996. Ability of various members of the hsp70 family of chaperones to promote assembly of the glucocorticoid receptor into a functional heterocomplex with hsp90. The Journal of steroid biochemistry and molecular biology **58:**251-258.
97. **Chen S, Prapapanich V, Rimerman RA, Honore B, Smith DF.** 1996. Interactions of p60, a mediator of progesterone receptor assembly, with heat shock proteins hsp90 and hsp70. Molecular endocrinology (Baltimore, Md.) **10:**682-693.
98. **Pratt WB, Gehring U, Toft DO.** 1996. Molecular chaperoning of steroid hormone receptors. Exs **77:**79-95.
99. **Lee DW, Jung C, Hwang I.** 2013. Cytosolic events involved in chloroplast protein targeting. Biochimica et biophysica acta **1833:**245-252.
100. **Ivey RA, 3rd, Subramanian C, Bruce BD.** 2000. Identification of a Hsp70 recognition domain within the rubisco small subunit transit peptide. Plant Physiol **122:**1289-1299.
101. **Zhang XP, Glaser E.** 2002. Interaction of plant mitochondrial and chloroplast signal peptides with the Hsp70 molecular chaperone. Trends in plant science **7:**14-21.
102. **Rial DV, Arakaki AK, Ceccarelli EA.** 2000. Interaction of the targeting sequence of chloroplast precursors with Hsp70 molecular chaperones. European journal of biochemistry / FEBS **267:**6239-6248.
103. **Richter S, Lamppa GK.** 1999. Stromal processing peptidase binds transit peptides and initiates their ATP-dependent turnover in chloroplasts. The Journal of cell biology **147:**33-44.

104. **Goloubinoff P, De Los Rios P.** 2007. The mechanism of Hsp70 chaperones: (entropic) pulling the models together. Trends in biochemical sciences **32:**372-380.
105. **Ziemienowicz A, Zylicz M, Floth C, Hubscher U.** 1995. Calf thymus Hsc70 protein protects and reactivates prokaryotic and eukaryotic enzymes. The Journal of biological chemistry **270:**15479-15484.
106. **Sousa RJ.** 2014. Structural Mechanisms of Chaperone Mediated Protein Disaggregation. Frontiers in Molecular Biosciences **1**.
107. **Lomonossoff GP.** 1995. Pathogen-derived resistance to plant viruses. Annu Rev Phytopathol **33:**323-343.
108. **Wilson TM.** 1985. Nucleocapsid disassembly and early gene expression by positive-strand RNA viruses. The Journal of general virology **66 (Pt 6):**1201-1207.
109. **Chromy LR, Oltman A, Estes PA, Garcea RL.** 2006. Chaperone-mediated in vitro disassembly of polyoma- and papillomaviruses. Journal of Virology **80:**5086-5091.
110. **Ivanovic T, Agosto MA, Chandran K, Nibert ML.** 2007. A role for molecular chaperone Hsc70 in reovirus outer capsid disassembly. The Journal of biological chemistry **282:**12210-12219.
111. **Guerrero CA, Bouyssounade D, Zarate S, Isa P, Lopez T, Espinosa R, Romero P, Mendez E, Lopez S, Arias CF.** 2002. Heat shock cognate protein 70 is involved in rotavirus cell entry. J Virol **76:**4096-4102.
112. **Saphire AC, Guan T, Schirmer EC, Nemerow GR, Gerace L.** 2000. Nuclear import of adenovirus DNA in vitro involves the nuclear protein import pathway and hsc70. The Journal of biological chemistry **275:**4298-4304.
113. **Niewiarowska J, D'Halluin JC, Belin MT.** 1992. Adenovirus capsid proteins interact with HSP70 proteins after penetration in human or rodent cells. Exp Cell Res **201:**408-416.
114. **Chroboczek J, Gout E, Favier AL, Galinier R.** 2003. Novel partner proteins of adenovirus penton. Curr Top Microbiol Immunol **272:**37-55.
115. **Chang JS, Chi SC.** 2015. GHSC70 Is Involved in the Cellular Entry of Nervous Necrosis Virus. J Virol **89:**61-70.
116. **Napuli AJ, Falk BW, Dolja VV.** 2000. Interaction between HSP70 homolog and filamentous virions of the Beet yellows virus. Virology **274:**232-239.
117. **Alam SB, Rochon D.** 2017. Evidence that Hsc70 is associated with CNV particles and plays a role in CNV particle disassembly. J Virol.
118. **Mine A, Hyodo K, Tajima Y, Kusumanegara K, Taniguchi T, Kaido M, Mise K, Taniguchi H, Okuno T.** 2012. Differential roles of Hsp70 and Hsp90 in the assembly of the replicase complex of a positive-strand RNA plant virus. J Virol **86:**12091-12104.
119. **Gao J, Xiao S, Liu X, Wang L, Ji Q, Mo D, Chen Y.** 2014. Inhibition of HSP70 reduces porcine reproductive and respiratory syndrome virus replication in vitro. BMC microbiology **14:**64.
120. **Lahaye X, Vidy A, Fouquet B, Blondel D.** 2012. Hsp70 protein positively regulates rabies virus infection. J Virol **86:**4743-4751.
121. **Mathioudakis MM, Rodriguez-Moreno L, Sempere RN, Aranda MA, Livieratos I.** 2014. Multifaceted Capsid Proteins: Multiple Interactions Suggest Multiple Roles for Pepino mosaic virus Capsid Protein. Mol Plant Microbe Interact **27:**1356-1369.
122. **Alam SB, Rochon D.** 2016. Cucumber Necrosis Virus Recruits Cellular Heat Shock Protein 70 Homologs at Several Stages of Infection. J Virol **90:**3302-3317.

123. **Chromy LR, Pipas JM, Garcea RL.** 2003. Chaperone-mediated in vitro assembly of Polyomavirus capsids. Proceedings of the National Academy of Sciences of the United States of America **100:**10477-10482.
124. **Yu L, Ye L, Zhao R, Liu YF, Yang SJ.** 2009. HSP70 induced by Hantavirus infection interacts with viral nucleocapsid protein and its overexpression suppresses virus infection in Vero E6 cells. Am J Transl Res **1:**367-380.
125. **Li PP, Itoh N, Watanabe M, Shi Y, Liu P, Yang HJ, Kasamatsu H.** 2009. Association of simian virus 40 vp1 with 70-kilodalton heat shock proteins and viral tumor antigens. J Virol **83:**37-46.
126. **Alzhanova DV, Napuli AJ, Creamer R, Dolja VV.** 2001. Cell-to-cell movement and assembly of a plant closterovirus: roles for the capsid proteins and Hsp70 homolog. Embo J **20:**6997-7007.
127. **Macejak DG, Sarnow P.** 1992. Association of heat shock protein 70 with enterovirus capsid precursor P1 in infected human cells. J Virol **66:**1520-1527.
128. **Gurer C, Hoglund A, Hoglund S, Luban J.** 2005. ATPgammaS disrupts human immunodeficiency virus type 1 virion core integrity. Journal of Virology **79:**5557-5567.
129. **Florin L, Becker KA, Sapp C, Lambert C, Sirma H, Mueller M, Streeck RE, Sapp M.** 2004. Nuclear translocation of papillomavirus minor capsid protein L2 requires Hsc70. Journal of Virology **78:**5546-5553.
130. **Cobbold C, Windsor M, Wileman T.** 2001. A virally encoded chaperone specialized for folding of the major capsid protein of African swine fever virus. J Virol **75:**7221-7229.
131. **Bol JF.** 2008. Role of capsid proteins. Methods in molecular biology (Clifton, N.J.) **451:**21-31.
132. **Coombs KM.** 2006. Reovirus structure and morphogenesis. Curr Top Microbiol Immunol **309:**117-167.
133. **Siegel A.** 1971. Pseudovirions of tobacco mosaic virus. Virology **46:**50-59.
134. **Routh A, Domitrovic T, Johnson JE.** 2012. Host RNAs, including transposons, are encapsidated by a eukaryotic single-stranded RNA virus. Proc Natl Acad Sci U S A **109:**1907-1912.
135. **Ghoshal K, Theilmann J, Reade R, Maghodia A, Rochon D.** 2015. Encapsidation of Host RNAs by Cucumber Necrosis Virus Coat Protein during both Agroinfiltration and Infection. J Virol **89:**10748-10761.
136. **Stockley PG, Twarock R, Bakker SE, Barker AM, Borodavka A, Dykeman E, Ford RJ, Pearson AR, Phillips SE, Ranson NA, Tuma R.** 2013. Packaging signals in single-stranded RNA viruses: nature's alternative to a purely electrostatic assembly mechanism. Journal of biological physics **39:**277-287.
137. **Patel N, Dykeman EC, Coutts RH, Lomonossoff GP, Rowlands DJ, Phillips SE, Ranson N, Twarock R, Tuma R, Stockley PG.** 2015. Revealing the density of encoded functions in a viral RNA. Proc Natl Acad Sci U S A **112:**2227-2232.
138. **Satheshkumar PS, Lokesh GL, Sangita V, Saravanan V, Vijay CS, Murthy MR, Savithri HS.** 2004. Role of metal ion-mediated interactions in the assembly and stability of Sesbania mosaic virus T=3 and T=1 capsids. J Mol Biol **342:**1001-1014.
139. **Loo L, Guenther RH, Lommel SA, Franzen S.** 2007. Encapsidation of nanoparticles by red clover necrotic mosaic virus. Journal of the American Chemical Society **129:**11111-11117.

140. **Polisky B, McCarthy B.** 1975. Location of histones on simian virus 40 DNA. Proc Natl Acad Sci U S A **72:**2895-2899.
141. **Sung MT, Cao TM, Coleman RT, Budelier KA.** 1983. Gene and protein sequences of adenovirus protein VII, a hybrid basic chromosomal protein. Proceedings of the National Academy of Sciences of the United States of America **80:**2902-2906.
142. **Green TJ, Cox R, Tsao J, Rowse M, Qiu S, Luo M.** 2014. Common mechanism for RNA encapsidation by negative-strand RNA viruses. J Virol **88:**3766-3775.
143. **Smith TJ, Chase E, Schmidt T, Perry KL.** 2000. The structure of cucumber mosaic virus and comparison to cowpea chlorotic mottle virus. J Virol **74:**7578-7586.
144. **Silva AM, Rossmann MG.** 1985. The refinement of southern bean mosaic virus in reciprocal space. Acta Crystallographica Section B **41:**147-157.
145. **Choi HK, Lu G, Lee S, Wengler G, Rossmann MG.** 1997. Structure of Semliki Forest virus core protein. Proteins **27:**345-359.
146. **Fisher AJ, Johnson JE.** 1993. Ordered duplex RNA controls capsid architecture in an icosahedral animal virus. Nature **361:**176-179.
147. **Tong L, Wengler G, Rossmann MG.** 1993. Refined structure of Sindbis virus core protein and comparison with other chymotrypsin-like serine proteinase structures. J Mol Biol **230:**228-247.
148. **Speir JA, Munshi S, Wang G, Baker TS, Johnson JE.** 1995. Structures of the native and swollen forms of cowpea chlorotic mottle virus determined by X-ray crystallography and cryo-electron microscopy. Structure (London, England : 1993) **3:**63-78.
149. **Belyi VA, Muthukumar M.** 2006. Electrostatic origin of the genome packing in viruses. Proc Natl Acad Sci U S A **103:**17174-17178.
150. **Hu T, Zhang R, Shklovskii BI.** 2008. Electrostatic theory of viral self-assembly. Physica A: Statistical Mechanics and its Applications **387:**3059-3064.
151. **Sivanandam V, Mathews D, Garmann R, Erdemci-Tandogan G, Zandi R, Rao ALN.** 2016. Functional analysis of the N-terminal basic motif of a eukaryotic satellite RNA virus capsid protein in replication and packaging. Scientific reports **6:**26328.
152. **Zhang X, Zhao X, Zhang Y, Niu S, Qu F, Zhang Y, Han C, Yu J, Li D.** 2013. N-terminal basic amino acid residues of Beet black scorch virus capsid protein play a critical role in virion assembly and systemic movement. Virology Journal **10:**200.
153. **Yi G, Vaughan RC, Yarbrough I, Dharmaiah S, Kao CC.** 2009. RNA binding by the Brome mosaic virus capsid protein and the regulation of viral RNA accumulation. J Mol Biol **391**.
154. **Rossi M, Vallino M, Abba S, Ciuffo M, Balestrini R, Genre A, Turina M.** 2015. The Importance of the KR-Rich Region of the Coat Protein of Ourmia melon virus for Host Specificity, Tissue Tropism, and Interference With Antiviral Defense. Mol Plant Microbe Interact **28:**30-41.
155. **Schmitz I, Rao AL.** 1998. Deletions in the conserved amino-terminal basic arm of Cucumber mosaic virus coat protein disrupt virion assembly but do not abolish infectivity and cell-to-cell movement. Virology **248**.
156. **Yusibov V, Loesch-Fries LS.** 1998. Functional significance of three basic N-terminal amino acids of Alfalfa mosaic virus coat protein. Virology **242**.
157. **Ni P, Wang Z, Ma X, Das NC, Sokol P, Chiu W, Dragnea B, Hagan M, Kao CC.** 2012. An examination of the electrostatic interactions between the N-terminal tail of the Brome Mosaic Virus coat protein and encapsidated RNAs. J Mol Biol **419:**284-300.

158. **Park SH, Sit TL, Kim KH, Lommel SA.** 2013. The red clover necrotic mosaic virus capsid protein N-terminal amino acids possess specific RNA binding activity and are required for stable virion assembly. Virus Res **176:**107-118.
159. **Annamalai P, Apte S, Wilkens S, Rao ALN.** 2005. Deletion of highly conserved arginine-rich RNA binding motif in Cowpea chlorotic mottle virus capsid protein results in virion structural alterations and RNA packaging constraints. J Virol **79**.
160. **Venter PA, Marshall D, Schneemann A.** 2009. Dual roles for an arginine-rich motif in specific genome recognition and localization of viral coat protein to RNA replication sites in flock house virus-infected cells. J Virol **83:**2872-2882.
161. **Calnan BJ, Biancalana S, Hudson D, Frankel AD.** 1991. Analysis of arginine-rich peptides from the HIV Tat protein reveals unusual features of RNA-protein recognition. Genes & development **5:**201-210.
162. **Goh ZH, Mohd NA, Tan SG, Bhassu S, Tan WS.** 2014. RNA-binding region of Macrobrachium rosenbergii nodavirus capsid protein. J Gen Virol **95:**1919-1928.
163. **Serra-Soriano M, Antonio Navarro J, Pallas V.** 2016. Dissecting the multifunctional role of the N-terminal domain of the Melon necrotic spot virus coat protein in RNA packaging, viral movement and interference with antiviral plant defence. Mol Plant Pathol.
164. **Reade R, Kakani K, Rochon DA.** 2010. A highly basic KGKKGK sequence in the RNA-binding domain of the Cucumber necrosis virus coat protein is associated with encapsidation of full-length CNV RNA during infection. Virology **403:**181-188.
165. **Schneemann A, Marshall D.** 1998. Specific Encapsidation of Nodavirus RNAs Is Mediated through the C Terminus of Capsid Precursor Protein Alpha. Journal of Virology **72:**8738-8746.
166. **Lokesh GL, Gowri TD, Satheshkumar PS, Murthy MR, Savithri HS.** 2002. A molecular switch in the capsid protein controls the particle polymorphism in an icosahedral virus. Virology **292:**211-223.
167. **Dong XF, Natarajan P, Tihova M, Johnson JE, Schneemann A.** 1998. Particle Polymorphism Caused by Deletion of a Peptide Molecular Switch in a Quasiequivalent Icosahedral Virus. Journal of Virology **72:**6024-6033.
168. **Zlotnick A, Aldrich R, Johnson JM, Ceres P, Young MJ.** 2000. Mechanism of Capsid Assembly for an Icosahedral Plant Virus. Virology **277:**450-456.
169. **Choi YG, Rao ALN.** 2000. Molecular studies on bromovirus capsid protein: VII. Selective packaging of BMV RNA4 by specific N-terminal arginine residues. Virology **275**.
170. **Choi YG, Grantham GL, Rao ALN.** 2000. Molecular studies on bromovirus capsid protein: VI. Contributions of the N-terminal arginine-rich motif of BMV capsid protein to virion stability and RNA packaging. Virology **270**.
171. **Calhoun SL, Speir JA, Rao AL.** 2007. In vivo particle polymorphism results from deletion of a N-terminal peptide molecular switch in brome mosaic virus capsid protein. Virology **364:**407-421.
172. **Calhoun SL, Rao AL.** 2008. Functional analysis of brome mosaic virus coat protein RNA-interacting domains. Arch Virol **153:**231-245.
173. **Borodavka A, Tuma R, Stockley PG.** 2013. A two-stage mechanism of viral RNA compaction revealed by single molecule fluorescence. RNA biology **10:**481-489.

174. **Borodavka A, Tuma R, Stockley PG.** 2012. Evidence that viral RNAs have evolved for efficient, two-stage packaging. Proc Natl Acad Sci U S A **109:**15769-15774.
175. **Fisher AJ, Johnson JE.** 1993. Ordered duplex RNA controls capsid architecture in an icosahedral animal virus. Nature **361:**176-179.
176. **Tihova M, Dryden KA, Le T-vL, Harvey SC, Johnson JE, Yeager M, Schneemann A.** 2004. Nodavirus Coat Protein Imposes Dodecahedral RNA Structure Independent of Nucleotide Sequence and Length. Journal of Virology **78:**2897-2905.
177. **Nugent CI, Johnson KL, Sarnow P, Kirkegaard K.** 1999. Functional coupling between replication and packaging of poliovirus replicon RNA. J Virol **73:**427-435.
178. **Liu Y, Wang C, Mueller S, Paul AV, Wimmer E, Jiang P.** 2010. Direct interaction between two viral proteins, the nonstructural protein 2C and the capsid protein VP3, is required for enterovirus morphogenesis. PLoS Pathog **6:**e1001066.
179. **Jiang P, Liu Y, Ma HC, Paul AV, Wimmer E.** 2014. Picornavirus morphogenesis. Microbiology and molecular biology reviews : MMBR **78:**418-437.
180. **Rao AL, Chaturvedi S, Garmann RF.** 2014. Integration of replication and assembly of infectious virions in plant RNA viruses. Curr Opin Virol **9:**61-66.
181. **Chaturvedi S, Rao AL.** 2014. Live cell imaging of interactions between replicase and capsid protein of Brome mosaic virus using Bimolecular Fluorescence Complementation: implications for replication and genome packaging. Virology **464-465:**67-75.
182. **Annamalai P, Rofail F, DeMason DA, Rao ALN.** 2008. Replication-Coupled Packaging Mechanism in Positive-Strand RNA Viruses: Synchronized Coexpression of Functional Multigenome RNA Components of an Animal and a Plant Virus in Nicotiana benthamiana Cells by Agroinfiltration. Journal of Virology **82:**1484-1495.
183. **Venter PA, Krishna NK, Schneemann A.** 2005. Capsid protein synthesis from replicating RNA directs specific packaging of the genome of a multipartite, positive-strand RNA virus. J Virol **79:**6239-6248.
184. **Khromykh AA, Varnavski AN, Sedlak PL, Westaway EG.** 2001. Coupling between replication and packaging of flavivirus RNA: evidence derived from the use of DNA-based full-length cDNA clones of Kunjin virus. J Virol **75:**4633-4640.
185. **Qu F, Morris TJ.** 1997. Encapsidation of turnip crinkle virus is defined by a specific packaging signal and RNA size. Journal of Virology **71:**1428-1435.
186. **Hacker DL.** 1995. Identification of a coat protein binding site on southern bean mosaic virus RNA. Virology **207:**562-565.
187. **Junker-Niepmann M, Bartenschlager R, Schaller H.** 1990. A short cis-acting sequence is required for hepatitis B virus pregenome encapsidation and sufficient for packaging of foreign RNA. The EMBO Journal **9:**3389-3396.
188. **Guogas LM, Filman DJ, Hogle JM, Gehrke L.** 2004. Cofolding organizes alfalfa mosaic virus RNA and coat protein for replication. Science (New York, N.Y.) **306:**2108-2111.
189. **Zimmern D.** 1977. The nucleotide sequence at the origin for assembly on tobacco mosaic virus RNA. Cell **11:**463-482.
190. **Basnayake VR, Sit TL, Lommel SA.** 2009. The Red clover necrotic mosaic virus origin of assembly is delimited to the RNA-2 trans-activator. Virology **384:**169-178.
191. **Zhong W, Dasgupta R, Rueckert R.** 1992. Evidence that the packaging signal for nodaviral RNA2 is a bulged stem-loop. Proc Natl Acad Sci U S A **89:**11146-11150.

192. **Weiss B, Geigenmüller-Gnirke U, Schlesinger S.** 1994. Interactions between Sindbis virus RNAs and a 68 amino acid derivative of the viral capsid protein further defines the capsid binding site. Nucleic acids research **22:**780-786.
193. **Annamalai P, Rao ALN.** 2007. In Vivo Packaging of Brome Mosaic Virus RNA3, but Not RNAs 1 and 2, Is Dependent on a cis-Acting 3′ tRNA-Like Structure. Journal of Virology **81:**173-181.
194. **Choi YG, Dreher TW, Rao AL.** 2002. tRNA elements mediate the assembly of an icosahedral RNA virus. Proc Natl Acad Sci U S A **99:**655-660.
195. **Annamalai P, Rao ALN.** 2005. Dispensability of 3′ tRNA-like sequence for packaging cowpea chlorotic mottle virus genomic RNAs. Virology **332:**650-658.
196. **Rolfsson O, Toropova K, Ranson NA, Stockley PG.** 2010. Mutually-induced conformational switching of RNA and coat protein underpins efficient assembly of a viral capsid. J Mol Biol **401:**309-322.
197. **Choi YG, Rao ALN.** 2003. Packaging of Brome Mosaic Virus RNA3 Is Mediated through a Bipartite Signal. Journal of Virology **77:**9750-9757.
198. **Bunka DH, Lane SW, Lane CL, Dykeman EC, Ford RJ, Barker AM, Twarock R, Phillips SE, Stockley PG.** 2011. Degenerate RNA packaging signals in the genome of Satellite Tobacco Necrosis Virus: implications for the assembly of a T=1 capsid. J Mol Biol **413:**51-65.
199. **McBride MS, Schwartz MD, Panganiban AT.** 1997. Efficient encapsidation of human immunodeficiency virus type 1 vectors and further characterization of cis elements required for encapsidation. J Virol **71:**4544-4554.
200. **Kemler I, Barraza R, Poeschla EM.** 2002. Mapping the encapsidation determinants of feline immunodeficiency virus. J Virol **76:**11889-11903.
201. **Ghoshal K.** 2016. Studies toward the identification of the origin of assembly on cucumber necrosis virus RNA and encapsidation of host RNA. Thesis/Dissertation. University of British Columbia, UBCV.
202. **Hui E, Rochon D.** 2006. Evaluation of the roles of specific regions of the Cucumber necrosis virus coat protein arm in particle accumulation and fungus transmission. J Virol **80:**5968-5975.
203. **Li Z, Nagy PD.** 2011. Diverse roles of host RNA binding proteins in RNA virus replication. RNA biology **8:**305-315.
204. **Verchot J.** 2012. Cellular chaperones and folding enzymes are vital contributors to membrane bound replication and movement complexes during plant RNA virus infection. Frontiers in plant science **3:**275.
205. **Chen Z, Zhou T, Wu X, Hong Y, Fan Z, Li H.** 2008. Influence of cytoplasmic heat shock protein 70 on viral infection of Nicotiana benthamiana. Mol Plant Pathol **9:**809-817.
206. **Kim C, Meskauskiene R, Zhang S, Lee KP, Ashok ML, Blajecka K, Herrfurth C, Feussner I, Apela K.** 2012. Chloroplasts of Arabidopsis are the source and a primary target of a plant-specific programmed cell death signaling pathway. Plant Cell **24:**3026-3039.
207. **Pastorino B, Boucomont-Chapeaublanc E, Peyrefitte CN, Belghazi M, Fusai T, Rogier C, Tolou HJ, Almeras L.** 2009. Identification of cellular proteome modifications in response to West Nile virus infection. Mol Cell Proteomics **8:**1623-1637.

208. **Aranda MA, Escaler M, Wang D, Maule AJ.** 1996. Induction of HSP70 and polyubiquitin expression associated with plant virus replication. Proc Natl Acad Sci U S A **93:**15289-15293.
209. **Whitham SA, Quan S, Chang HS, Cooper B, Estes B, Zhu T, Wang X, Hou YM.** 2003. Diverse RNA viruses elicit the expression of common sets of genes in susceptible Arabidopsis thaliana plants. The Plant journal : for cell and molecular biology **33:**271-283.
210. **Whitham SA, Yang C, Goodin MM.** 2006. Global impact: elucidating plant responses to viral infection. Mol Plant Microbe Interact **19:**1207-1215.
211. **Babu M, Griffiths JS, Huang TS, Wang A.** 2008. Altered gene expression changes in Arabidopsis leaf tissues and protoplasts in response to Plum pox virus infection. BMC genomics **9:**325.
212. **Richter K, Haslbeck M, Buchner J.** 2010. The heat shock response: life on the verge of death. Molecular cell **40:**253-266.
213. **Mathioudakis MM, Veiga R, Ghita M, Tsikou D, Medina V, Canto T, Makris AM, Livieratos IC.** 2012. Pepino mosaic virus capsid protein interacts with a tomato heat shock protein cognate 70. Virus Res **163:**28-39.
214. **Aparicio F, Thomas CL, Lederer C, Niu Y, Wang D, Maule AJ.** 2005. Virus induction of heat shock protein 70 reflects a general response to protein accumulation in the plant cytosol. Plant Physiol **138:**529-536.
215. **Mayer MP.** 2010. Gymnastics of molecular chaperones. Molecular cell **39:**321-331.
216. **Avisar D, Prokhnevsky AI, Dolja VV.** 2008. Class VIII myosins are required for plasmodesmatal localization of a closterovirus Hsp70 homolog. J Virol **82:**2836-2843.
217. **Gorovits R, Moshe A, Ghanim M, Czosnek H.** 2013. Recruitment of the host plant heat shock protein 70 by Tomato yellow leaf curl virus coat protein is required for virus infection. PLoS One **8:**e70280.
218. **Jiang S, Lu Y, Li K, Lin L, Zheng H, Yan F, Chen J.** 2014. Heat shock protein 70 is necessary for Rice stripe virus infection in plants. Mol Plant Pathol **15:**907-917.
219. **Chotewutmontri P, Bruce BD.** 2015. Non-native, N-terminal Hsp70 molecular motor recognition elements in transit peptides support plastid protein translocation. The Journal of biological chemistry **290:**7602-7621.
220. **Xiang Y, Kakani K, Reade R, Hui E, Rochon D.** 2006. A 38-amino-acid sequence encompassing the arm domain of the cucumber necrosis virus coat protein functions as a chloroplast transit Peptide in infected plants. J Virol **80:**7952-7964.
221. **Cognat V, Pawlak G, Duchene AM, Daujat M, Gigant A, Salinas T, Michaud M, Gutmann B, Giege P, Gobert A, Marechal-Drouard L.** 2013. PlantRNA, a database for tRNAs of photosynthetic eukaryotes. Nucleic acids research **41:**D273-279.
222. **Nakasugi K, Crowhurst RN, Bally J, Wood CC, Hellens RP, Waterhouse PM.** 2013. De novo transcriptome sequence assembly and analysis of RNA silencing genes of Nicotiana benthamiana. PLoS One **8:**e59534.
223. **Jelenska J, van Hal JA, Greenberg JT.** 2010. Pseudomonas syringae hijacks plant stress chaperone machinery for virulence. Proc Natl Acad Sci U S A **107:**13177-13182.
224. **Voinnet O, Rivas S, Mestre P, Baulcombe D.** 2003. An enhanced transient expression system in plants based on suppression of gene silencing by the p19 protein of tomato bushy stunt virus. The Plant journal : for cell and molecular biology **33:**949-956.

225. **Robbins MA, Reade RD, Rochon DM.** 1997. A cucumber necrosis virus variant deficient in fungal transmissibility contains an altered coat protein shell domain. Virology **234:**138-146.
226. **Gibson DG, Young L, Chuang RY, Venter JC, Hutchison CA, 3rd, Smith HO.** 2009. Enzymatic assembly of DNA molecules up to several hundred kilobases. Nature methods **6:**343-345.
227. **Lu Z, Cyr DM.** 1998. Protein folding activity of Hsp70 is modified differentially by the hsp40 co-chaperones Sis1 and Ydj1. The Journal of biological chemistry **273:**27824-27830.
228. **Johnson BD, Schumacher RJ, Ross ED, Toft DO.** 1998. Hop modulates Hsp70/Hsp90 interactions in protein folding. The Journal of biological chemistry **273:**3679-3686.
229. **Gandia M, Conesa A, Ancillo G, Gadea J, Forment J, Pallas V, Flores R, Duran-Vila N, Moreno P, Guerri J.** 2007. Transcriptional response of Citrus aurantifolia to infection by Citrus tristeza virus. Virology **367:**298-306.
230. **Ventelon-Debout M, Delalande F, Brizard JP, Diemer H, Van Dorsselaer A, Brugidou C.** 2004. Proteome analysis of cultivar-specific deregulations of Oryza sativa indica and O. sativa japonica cellular suspensions undergoing rice yellow mottle virus infection. Proteomics **4:**216-225.
231. **Brosens JJ, Salker MS, Teklenburg G, Nautiyal J, Salter S, Lucas ES, Steel JH, Christian M, Chan YW, Boomsma CM, Moore JD, Hartshorne GM, Sucurovic S, Mulac-Jericevic B, Heijnen CJ, Quenby S, Koerkamp MJ, Holstege FC, Shmygol A, Macklon NS.** 2014. Uterine selection of human embryos at implantation. Scientific reports **4:**3894.
232. **Sun HK, Hyun SL, Won YS, Kwan SC, Hur Y.** 2007. Chloroplast-targeted BrMT1 (Brassica rapa type-1 metallothionein) enhances resistance to cadmium and ROS in transgenic Arabidopsis plants. Journal of Plant Biology **50:**1-7.
233. **Wilke N, Sganga MW, Gayer GG, Hsieh KP, Miles MF.** 2000. Characterization of promoter elements mediating ethanol regulation of hsc70 gene transcription. The Journal of pharmacology and experimental therapeutics **292:**173-180.
234. **Lyupina YV, Zatsepina OG, Timokhova AV, Orlova OV, Kostyuchenko MV, Beljelarskaya SN, Evgen'ev MB, Mikhailov VS.** 2011. New insights into the induction of the heat shock proteins in baculovirus infected insect cells. Virology **421:**34-41.
235. **Yan F, Xia D, Hu J, Yuan H, Zou T, Zhou Q, Liang L, Qi Y, Xu H.** 2010. Heat shock cognate protein 70 gene is required for prevention of apoptosis induced by WSSV infection. Arch Virol **155:**1077-1083.
236. **Noel LD, Cagna G, Stuttmann J, Wirthmuller L, Betsuyaku S, Witte CP, Bhat R, Pochon N, Colby T, Parker JE.** 2007. Interaction between SGT1 and cytosolic/nuclear HSC70 chaperones regulates Arabidopsis immune responses. Plant Cell **19:**4061-4076.
237. **Guzik K, Bzowska M, Dobrucki J, Pryjma J.** 1999. Heat-shocked monocytes are resistant to Staphylococcus aureus-induced apoptotic DNA fragmentation due to expression of HSP72. Infection and immunity **67:**4216-4222.
238. **Cronje MJ, Weir IE, Bornman L.** 2004. Salicylic acid-mediated potentiation of Hsp70 induction correlates with reduced apoptosis in tobacco protoplasts. Cytometry. Part A : the journal of the International Society for Analytical Cytology **61:**76-87.
239. **Ye C, Dickman MB, Whitham SA, Payton M, Verchot J.** 2011. The unfolded protein response is triggered by a plant viral movement protein. Plant Physiol **156:**741-755.

240. **Byth-Illing HA, Bornman L.** 2014. Heat shock, with recovery, promotes protection of Nicotiana tabacum during subsequent exposure to Ralstonia solanacearum. Cell stress & chaperones **19:**193-203.
241. **Kanzaki H, Saitoh H, Ito A, Fujisawa S, Kamoun S, Katou S, Yoshioka H, Terauchi R.** 2003. Cytosolic HSP90 and HSP70 are essential components of INF1-mediated hypersensitive response and non-host resistance to Pseudomonas cichorii in Nicotiana benthamiana. Mol Plant Pathol **4:**383-391.
242. **Elia G, Santoro MG.** 1994. Regulation of heat shock protein synthesis by quercetin in human erythroleukaemia cells. The Biochemical journal **300 (Pt 1):**201-209.
243. **Hui E, Xiang Y, Rochon D.** 2010. Distinct regions at the N-terminus of the Cucumber necrosis virus coat protein target chloroplasts and mitochondria. Virus Research **153:**8-19.
244. **Kyratsous CA, Panagiotidis CA.** 2012. Heat-shock protein fusion vectors for improved expression of soluble recombinant proteins in Escherichia coli. Methods in molecular biology (Clifton, N.J.) **824:**109-129.
245. **Ailor E, Betenbaugh MJ.** 1998. Overexpression of a cytosolic chaperone to improve solubility and secretion of a recombinant IgG protein in insect cells. Biotechnology and bioengineering **58:**196-203.
246. **Zietkiewicz S, Lewandowska A, Stocki P, Liberek K.** 2006. Hsp70 chaperone machine remodels protein aggregates at the initial step of Hsp70-Hsp100-dependent disaggregation. The Journal of biological chemistry **281:**7022-7029.
247. **Jackson-Constan D, Akita M, Keegstra K.** 2001. Molecular chaperones involved in chloroplast protein import. Biochimica et biophysica acta **1541:**102-113.
248. **Roossinck MJ.** 2011. The good viruses: viral mutualistic symbioses. Nat Rev Micro **9:**99-108.
249. **Maham A, Tang Z, Wu H, Wang J, Lin Y.** 2009. Protein-based nanomedicine platforms for drug delivery. Small (Weinheim an der Bergstrasse, Germany) **5:**1706-1721.
250. **Lai YT, Reading E, Hura GL, Tsai KL, Laganowsky A, Asturias FJ, Tainer JA, Robinson CV, Yeates TO.** 2014. Structure of a designed protein cage that self-assembles into a highly porous cube. Nature chemistry **6:**1065-1071.
251. **Loebenstein G.** 2009. Local lesions and induced resistance. Adv Virus Res **75:**73-117.
252. **Suomalainen M, Greber UF.** 2013. Uncoating of non-enveloped viruses. Curr Opin Virol **3:**27-33.
253. **Lanzrein M, Schlegel A, Kempf C.** 1994. Entry and uncoating of enveloped viruses. Biochemical Journal **302:**313-320.
254. **Tsai B.** 2007. Penetration of nonenveloped viruses into the cytoplasm. Annual review of cell and developmental biology **23:**23-43.
255. **Hiscox JA, Ball LA.** 1997. Cotranslational disassembly of flock house virus in a cell-free system. J Virol **71:**7974-7977.
256. **Sun Y, Zhao J, Sheng Y, Xiao YF, Zhang YJ, Bai LX, Tan Y, Xiao LB, Xu GC.** 2016. Identification of heat shock cognate protein 70 gene (Alhsc70) of Apolygus lucorum and its expression in response to different temperature and pesticide stresses. Insect science **23:**37-49.
257. **Robinson IK, Harrison SC.** 1982. Structure of the expanded state of tomato bushy stunt virus. Nature **297:**563-568.

258. **Wang CY, Zhang QF, Gao YZ, Xie L, Li HM, Hong J, Zhang CX.** 2015. Uncoating Mechanism of Carnation Mottle Virus Revealed by Cryo-EM Single Particle Analysis. Scientific reports **5:**14825.
259. **Sherman MB, Guenther RH, Tama F, Sit TL, Brooks CL, Mikhailov AM, Orlova EV, Baker TS, Lommel SA.** 2006. Removal of divalent cations induces structural transitions in red clover necrotic mosaic virus, revealing a potential mechanism for RNA release. J Virol **80:**10395-10406.
260. **Perkins DN, Pappin DJ, Creasy DM, Cottrell JS.** 1999. Probability-based protein identification by searching sequence databases using mass spectrometry data. Electrophoresis **20:**3551-3567.
261. **Sambrook J, Russell DW.** 2006. Southern blotting: capillary transfer of DNA to membranes. CSH protocols **2006**.
262. **Gurer C, Cimarelli A, Luban J.** 2002. Specific incorporation of heat shock protein 70 family members into primate lentiviral virions. J Virol **76:**4666-4670.
263. **Matthews REF.** 1991. 2 - Methods for Assay, Detection, and Diagnosis, p. 11-52, Plant Virology (Third Edition). Academic Press, San Diego.
264. **Pruss GJ, Nester EW, Vance V.** 2008. Infiltration with Agrobacterium tumefaciens induces host defense and development-dependent responses in the infiltrated zone. Mol Plant Microbe Interact **21:**1528-1538.
265. **Perez-Vargas J, Romero P, Lopez S, Arias CF.** 2006. The peptide-binding and ATPase domains of recombinant hsc70 are required to interact with rotavirus and reduce its infectivity. J Virol **80:**3322-3331.
266. **Jiang R, Gao B, Prasad K, Greene LE, Eisenberg E.** 2000. Hsc70 chaperones clathrin and primes it to interact with vesicle membranes. The Journal of biological chemistry **275:**8439-8447.
267. **Chromy LR, Pipas JM, Garcea RL.** 2003. Chaperone-mediated in vitro assembly of Polyomavirus capsids. Proc Natl Acad Sci U S A **100:**10477-10482.
268. **Rudiger S, Germeroth L, Schneider-Mergener J, Bukau B.** 1997. Substrate specificity of the DnaK chaperone determined by screening cellulose-bound peptide libraries. Embo J **16:**1501-1507.
269. **Rudiger S, Buchberger A, Bukau B.** 1997. Interaction of Hsp70 chaperones with substrates. Nature structural biology **4:**342-349.
270. **Hewat EA, Neumann E, Blaas D.** 2002. The concerted conformational changes during human rhinovirus 2 uncoating. Molecular cell **10:**317-326.
271. **Racaniello VR.** 1996. Early events in poliovirus infection: virus-receptor interactions. Proc Natl Acad Sci U S A **93:**11378-11381.
272. **Jiang M, Abend JR, Tsai B, Imperiale MJ.** 2009. Early Events during BK Virus Entry and Disassembly. Journal of Virology **83:**1350-1358.
273. **Brisco M, Hull R, Wilson TM.** 1986. Swelling of isometric and of bacilliform plant virus nucleocapsids is required for virus-specific protein synthesis in vitro. Virology **148:**210-217.
274. **Matthews RE, Witz J.** 1985. Uncoating of turnip yellow mosaic virus RNA in vivo. Virology **144:**318-327.
275. **Martin SL, He L, Meilleur F, Guenther RH, Sit TL, Lommel SA, Heller WT.** 2013. New insight into the structure of RNA in red clover necrotic mosaic virus and the role of divalent cations revealed by small-angle neutron scattering. Arch Virol **158:**1661-1669.

276. **Aramayo R, Merigoux C, Larquet E, Bron P, Perez J, Dumas C, Vachette P, Boisset N.** 2005. Divalent ion-dependent swelling of tomato bushy stunt virus: a multi-approach study. Biochimica et biophysica acta **1724:**345-354.
277. **Brisco M, Haniff C, Hull R, Wilson TM, Sattelle DB.** 1986. The kinetics of swelling of southern bean mosaic virus: a study using photon correlation spectroscopy. Virology **148:**218-220.
278. **Katen S, Zlotnick A.** 2009. Chapter 14 The Thermodynamics of Virus Capsid Assembly, p. 395-417, Methods in Enzymology, vol. Volume 455. Academic Press.
279. **Krol MA, Olson NH, Tate J, Johnson JE, Baker TS, Ahlquist P.** 1999. RNA-controlled polymorphism in the in vivo assembly of 180-subunit and 120-subunit virions from a single capsid protein. Proc Natl Acad Sci U S A **96:**13650-13655.
280. **Timmins PA, Wild D, Witz J.** 1994. The three-dimensional distribution of RNA and protein in the interior of tomato bushy stunt virus: a neutron low-resolution single-crystal diffraction study. Structure (London, England : 1993) **2:**1191-1201.
281. **Fisher CL, Pei GK.** 1997. Modification of a PCR-based site-directed mutagenesis method. BioTechniques **23:**570-571, 574.
282. **Saunders K, Sainsbury F, Lomonossoff GP.** 2009. Efficient generation of cowpea mosaic virus empty virus-like particles by the proteolytic processing of precursors in insect cells and plants. Virology **393:**329-337.
283. **Nishimura K, Ashida H, Ogawa T, Yokota A.** 2010. A DEAD box protein is required for formation of a hidden break in Arabidopsis chloroplast 23S rRNA. The Plant journal : for cell and molecular biology **63:**766-777.
284. **Erickson JW, Rossmann MG.** 1982. Assembly and crystallization of a T = 1 icosahedral particle from trypsinized southern bean mosaic virus coat protein. Virology **116:**128-136.
285. **Vriend G, Hemminga MA, Verduin BJM, Wit JLD, Schaafsma TJ.** 1981. Segmental mobility involved in protein—RNA interaction in cowpea chlorotic mottle virus. FEBS letters **134:**167-171.
286. **Satheshkumar PS, Lokesh GL, Murthy MRN, Savithri HS.** 2005. The role of arginine-rich motif and β-annulus in the assembly and stability of Sesbania mosaic virus capsids. J Mol Biol **353**.
287. **Annamalai P, Rao AL.** 2007. In vivo packaging of brome mosaic virus RNA3, but not RNAs 1 and 2, is dependent on a cis-acting 3' tRNA-like structure. J Virol **81:**173-181.
288. **Basnayake VR, Sit TL, Lommel SA.** 2009. The Red clover necrotic mosaic virus origin of assembly is delimited to the RNA-2 trans-activator. Virology **384:**169-178.
289. **Bink HH, Schirawski J, Haenni AL, Pleij CW.** 2003. The 5'-proximal hairpin of turnip yellow mosaic virus RNA: its role in translation and encapsidation. J Virol **77:**7452-7458.
290. **Choi YG, Rao AL.** 2003. Packaging of brome mosaic virus RNA3 is mediated through a bipartite signal. J Virol **77:**9750-9757.
291. **Damayanti TA, Tsukaguchi S, Mise K, Okuno T.** 2003. cis-acting elements required for efficient packaging of brome mosaic virus RNA3 in barley protoplasts. J Virol **77:**9979-9986.
292. **Frolova E, Frolov I, Schlesinger S.** 1997. Packaging signals in alphaviruses. J Virol **71:**248-258.

293. **Hemmer O, Dunoyer P, Richards K, Fritsch C.** 2003. Mapping of viral RNA sequences required for assembly of peanut clump virus particles. The Journal of general virology **84:**2585-2594.
294. **Johnson SF, Telesnitsky A.** 2010. Retroviral RNA dimerization and packaging: the what, how, when, where, and why. PLoS Pathog **6:**e1001007.
295. **Kwon SJ, Park MR, Kim KW, Plante CA, Hemenway CL, Kim KH.** 2005. cis-Acting sequences required for coat protein binding and in vitro assembly of Potato virus X. Virology **334:**83-97.
296. **Qu F, Morris TJ.** 1997. Encapsidation of turnip crinkle virus is defined by a specific packaging signal and RNA size. J Virol **71:**1428-1435.
297. **Zimmern D, Butler PJ.** 1977. The isolation of tobacco mosaic virus RNA fragments containing the origin for viral assembly. Cell **11:**455-462.
298. **Rochon D, Siegel A.** 1984. Chloroplast DNA transcripts are encapsidated by tobacco mosaic virus coat protein. Proc Natl Acad Sci U S A **81:**1719-1723.
299. **Osman F, Choi YG, Grantham GL, Rao ALN.** 1998. Molecular Studies on Bromovirus Capsid Protein. Virology **251:**438-448.
300. !!! INVALID CITATION !!!
301. **de Torres Zabala M, Littlejohn G, Jayaraman S, Studholme D, Bailey T, Lawson T, Tillich M, Licht D, Bölter B, Delfino L, Truman W, Mansfield J, Smirnoff N, Grant M.** 2015. Chloroplasts play a central role in plant defence and are targeted by pathogen effectors. Nature Plants **1:**15074.
302. **Petre B, Saunders DG, Sklenar J, Lorrain C, Win J, Duplessis S, Kamoun S.** 2015. Candidate Effector Proteins of the Rust Pathogen Melampsora larici-populina Target Diverse Plant Cell Compartments. Mol Plant Microbe Interact **28:**689-700.
303. **Petre B, Lorrain C, Saunders DGO, Win J, Sklenar J, Duplessis S, Kamoun S.** 2015. Rust fungal effectors mimic host transit peptides to translocate into chloroplasts. Cellular Microbiology**:**n/a-n/a.
304. **Nomura H, Komori T, Uemura S, Kanda Y, Shimotani K, Nakai K, Furuichi T, Takebayashi K, Sugimoto T, Sano S, Suwastika IN, Fukusaki E, Yoshioka H, Nakahira Y, Shiina T.** 2012. Chloroplast-mediated activation of plant immune signalling in Arabidopsis. Nature communications **3:**926.
305. **Serrano M, Wang B, Aryal B, Garcion C, Abou-Mansour E, Heck S, Geisler M, Mauch F, Nawrath C, Metraux JP.** 2013. Export of salicylic acid from the chloroplast requires the multidrug and toxin extrusion-like transporter EDS5. Plant Physiol **162:**1815-1821.
306. **Loake G, Grant M.** 2007. Salicylic acid in plant defence--the players and protagonists. Current opinion in plant biology **10:**466-472.
307. **Dempsey DA, Vlot AC, Wildermuth MC, Klessig DF.** 2011. Salicylic Acid biosynthesis and metabolism. The Arabidopsis book / American Society of Plant Biologists **9:**e0156.
308. **Chen Z, Zheng Z, Huang J, Lai Z, Fan B.** 2009. Biosynthesis of salicylic acid in plants. Plant Signal Behav **4:**493-496.
309. **Li G, Froehlich JE, Elowsky C, Msanne J, Ostosh AC, Zhang C, Awada T, Alfano JR.** 2014. Distinct Pseudomonas type-III effectors use a cleavable transit peptide to target chloroplasts. The Plant journal : for cell and molecular biology **77:**310-321.

310. **Donze T, Qu F, Twigg P, Morris TJ.** 2014. Turnip crinkle virus coat protein inhibits the basal immune response to virus invasion in Arabidopsis by binding to the NAC transcription factor TIP. Virology **449:**207-214.
311. **Love AJ, Geri C, Laird J, Carr C, Yun BW, Loake GJ, Tada Y, Sadanandom A, Milner JJ.** 2012. Cauliflower mosaic virus protein P6 inhibits signaling responses to salicylic acid and regulates innate immunity. PLoS One **7:**e47535.
312. **Scholthof HB, Scholthof KB, Jackson AO.** 1995. Identification of tomato bushy stunt virus host-specific symptom determinants by expression of individual genes from a potato virus X vector. Plant Cell **7:**1157-1172.
313. **Cavrak VV, Lettner N, Jamge S, Kosarewicz A, Bayer LM, Mittelsten Scheid O.** 2014. How a retrotransposon exploits the plant's heat stress response for its activation. PLoS genetics **10:**e1004115.
314. **Chen C, Begcy K, Liu K, Folsom JJ, Wang Z, Zhang C, Walia H.** 2016. Heat stress yields a unique MADS box transcription factor in determining seed size and thermal sensitivity. Plant Physiol **171:**606-622.
315. **Callinan PA, Batzer MA.** 2006. Retrotransposable elements and human disease. Genome dynamics **1:**104-115.
316. **Hedges DJ, Deininger PL.** 2007. Inviting instability: Transposable elements, double-strand breaks, and the maintenance of genome integrity. Mutation research **616:**46-59.
317. **Naito K, Cho E, Yang G, Campbell MA, Yano K, Okumoto Y, Tanisaka T, Wessler SR.** 2006. Dramatic amplification of a rice transposable element during recent domestication. Proc Natl Acad Sci U S A **103:**17620-17625.
318. **Naito K, Zhang F, Tsukiyama T, Saito H, Hancock CN, Richardson AO, Okumoto Y, Tanisaka T, Wessler SR.** 2009. Unexpected consequences of a sudden and massive transposon amplification on rice gene expression. Nature **461:**1130-1134.
319. **Kanazawa A, Liu B, Kong F, Arase S, Abe J.** 2009. Adaptive evolution involving gene duplication and insertion of a novel Ty1/copia-like retrotransposon in soybean. Journal of molecular evolution **69:**164-175.
320. **Ito H, Kim J-M, Matsunaga W, Saze H, Matsui A, Endo TA, Harukawa Y, Takagi H, Yaegashi H, Masuta Y, Masuda S, Ishida J, Tanaka M, Takahashi S, Morosawa T, Toyoda T, Kakutani T, Kato A, Seki M.** 2016. A Stress-Activated Transposon in Arabidopsis Induces Transgenerational Abscisic Acid Insensitivity. Scientific reports **6:**23181.
321. **Civ, #xe1, #x148, P, #x160, vec M, Hauptvogel P.** 2011. On the Coevolution of Transposable Elements and Plant Genomes. Journal of Botany **2011:**9.
322. **Alzohairy AM, Gyulai G, Jansen RK, Bahieldin A.** 2013. Transposable elements domesticated and neofunctionalized by eukaryotic genomes. Plasmid **69:**1-15.
323. **Kumar A, Bennetzen JL.** 1999. Plant retrotransposons. Annu Rev Genet **33:**479-532.
324. **Le QH, Wright S, Yu Z, Bureau T.** 2000. Transposon diversity in Arabidopsis thaliana. Proceedings of the National Academy of Sciences of the United States of America **97:**7376-7381.
325. **Finnegan DJ.** 2012. Retrotransposons. Current Biology **22:**R432-R437.
326. **Kumar A.** 1996. The adventures of the Ty1-copia group of retrotransposons in plants. Trends in Genetics **12:**41-43.
327. **Jiang J, Birchler JA, Parrott WA, Dawe RK.** 2003. A molecular view of plant centromeres. Trends in plant science **8:**570-575.

328. **Sinzelle L, Izsvak Z, Ivics Z.** 2009. Molecular domestication of transposable elements: from detrimental parasites to useful host genes. Cellular and molecular life sciences : CMLS **66:**1073-1093.
329. **Lisch D.** 2013. How important are transposons for plant evolution? Nat Rev Genet **14:**49-61.
330. **Lippman Z, May B, Yordan C, Singer T, Martienssen R.** 2003. Distinct mechanisms determine transposon inheritance and methylation via small interfering RNA and histone modification. PLoS biology **1:**E67.
331. **Wierzbicki AT, Haag JR, Pikaard CS.** Noncoding Transcription by RNA Polymerase Pol IVb/Pol V Mediates Transcriptional Silencing of Overlapping and Adjacent Genes. Cell **135:**635-648.
332. **Gao Z, Liu H-L, Daxinger L, Pontes O, He X, Qian W, Lin H, Xie M, Lorkovic ZJ, Zhang S, Miki D, Zhan X, Pontier D, Lagrange T, Jin H, Matzke AJM, Matzke M, Pikaard CS, Zhu J-K.** 2010. An RNA polymerase II- and AGO4-associated protein acts in RNA-directed DNA methylation. Nature **465:**106-109.
333. **Ito H, Gaubert H, Bucher E, Mirouze M, Vaillant I, Paszkowski J.** 2011. An siRNA pathway prevents transgenerational retrotransposition in plants subjected to stress. Nature **472:**115-119.
334. **Capy P, Gasperi G, Biemont C, Bazin C.** 2000. Stress and transposable elements: co-evolution or useful parasites? Heredity **85:**101-106.
335. **Alzohairy AM, Sabir JSM, Gyulai G, Younis RAA, Jansen RK, Bahieldin A.** 2014. Environmental stress activation of plant long-terminal repeat retrotransposons. Functional Plant Biology **41:**557-567.
336. **Slotkin RK, Martienssen R.** 2007. Transposable elements and the epigenetic regulation of the genome. Nat Rev Genet **8:**272-285.
337. **Mhiri C, Morel JB, Vernhettes S, Casacuberta JM, Lucas H, Grandbastien MA.** 1997. The promoter of the tobacco Tnt1 retrotransposon is induced by wounding and by abiotic stress. Plant Mol Biol **33:**257-266.
338. **Latif HH, Mohamed HI.** 2016. Exogenous applications of moringa leaf extract effect on retrotransposon, ultrastructural and biochemical contents of common bean plants under environmental stresses. South African Journal of Botany **106:**221-231.
339. **Roy M, Ghosh B.** 1996. Polyamines, both common and uncommon, under heat stress in rice (Oryza sativa) callus. Physiologia Plantarum **98:**196-200.
340. **Liu J, Feng L, Li J, He Z.** 2015. Genetic and epigenetic control of plant heat responses. Frontiers in plant science **6:**267.
341. **Matsunaga W, Kobayashi A, Kato A, Ito H.** 2012. The effects of heat induction and the siRNA biogenesis pathway on the transgenerational transposition of ONSEN, a copia-like retrotransposon in Arabidopsis thaliana. Plant & cell physiology **53:**824-833.
342. **Ito H, Yoshida T, Tsukahara S, Kawabe A.** 2013. Evolution of the ONSEN retrotransposon family activated upon heat stress in Brassicaceae. Gene **518:**256-261.
343. **Voronova A, Belevich V, Jansons A, Rungis D.** 2014. Stress-induced transcriptional activation of retrotransposon-like sequences in the Scots pine (Pinus sylvestris L.) genome. Tree Genetics & Genomes **10:**937-951.
344. **Angelika Voronova1* ĀJ, Dainis Ruņģis1.** 2011. Expression of retrotransposon-like sequences in Scots pine (Pinus sylvestris) in response to heat stress. Environmental and Experimental Biology **9:**121–127.

345. **Alzohairy AM, Yousef, M. A, Edris, S, Kerti, B, Gyulai, G, Bahieldin, A.** 2012 Detection of LTR Retrotransposons Reactivation induced by in vitro Environmental Stresses in Barley (Hordeum vulgare) via RT-qPCR. LIFE SCIENCE JOURNAL-ACTA ZHENGZHOU UNIVERSITY OVERSEAS EDITION MARSLAND PRESS **9:**5019-5026.
346. **Ni JZ, Kalinava N, Chen E, Huang A, Trinh T, Gu SG.** 2016. A transgenerational role of the germline nuclear RNAi pathway in repressing heat stress-induced transcriptional activation in C. elegans. Epigenetics & Chromatin **9:**3.
347. **Ikeda K, Nakayashiki H, Takagi M, Tosa Y, Mayama S.** 2001. Heat shock, copper sulfate and oxidative stress activate the retrotransposon MAGGY resident in the plant pathogenic fungus Magnaporthe grisea. Molecular genetics and genomics : MGG **266:**318-325.
348. **Strand DJ, McDonald JF.** 1985. Copia is transcriptionally responsive to environmental stress. Nucleic acids research **13:**4401-4410.
349. **Deininger PL, Batzer MA.** 2002. Mammalian retroelements. Genome research **12:**1455-1465.
350. **Goodier JL, Kazazian HH, Jr.** 2008. Retrotransposons revisited: the restraint and rehabilitation of parasites. Cell **135:**23-35.
351. **Jang KL, Latchman DS.** 1989. HSV infection induces increased transcription of Alu repeated sequences by RNA polymerase III. FEBS letters **258:**255-258.
352. **Panning B, Smiley JR.** 1989. Regulation of cellular genes transduced by herpes simplex virus. Journal of Virology **63:**1929-1937.
353. **Panning B, Smiley JR.** 1993. Activation of RNA polymerase III transcription of human Alu repetitive elements by adenovirus type 5: requirement for the E1b 58-kilodalton protein and the products of E4 open reading frames 3 and 6. Molecular and cellular biology **13:**3231-3244.
354. **Williams WP, Tamburic L, Astell CR.** 2004. Increased levels of B1 and B2 SINE transcripts in mouse fibroblast cells due to minute virus of mice infection. Virology **327:**233-241.
355. **Sengupta S, Powell E, Kong L, Blackard JT.** 2013. Effects of HCV on Basal and Tat-Induced HIV LTR Activation. PLoS ONE **8:**e64956.
356. **Doi A, Iijima K, Kano S, Ishizaka Y.** 2015. Viral protein R of HIV type-1 induces retrotransposition and upregulates glutamate synthesis by the signal transducer and activator of transcription 1 signaling pathway. Microbiology and immunology **59:**398-409.
357. **Liu D, Shi L, Han C, Yu J, Li D, Zhang Y.** 2012. Validation of reference genes for gene expression studies in virus-infected Nicotiana benthamiana using quantitative real-time PCR. PLoS One **7:**e46451.
358. **Pietzenuk B, Markus C, Gaubert H, Bagwan N, Merotto A, Bucher E, Pecinka A.** 2016. Recurrent evolution of heat-responsiveness in Brassicaceae COPIA elements. Genome biology **17:**209.
359. **Enoki Y, Sakurai H.** 2011. Diversity in DNA recognition by heat shock transcription factors (HSFs) from model organisms. FEBS letters **585:**1293-1298.
360. **Goldsbrough AP, Albrecht H, Stratford R.** 1993. Salicylic acid-inducible binding of a tobacco nuclear protein to a 10 bp sequence which is highly conserved amongst stress-inducible genes. The Plant journal : for cell and molecular biology **3:**563-571.

361. **Kobayashi S, Goto-Yamamoto N, Hirochika H.** 2004. Retrotransposon-induced mutations in grape skin color. Science (New York, N.Y.) **304:**982.
362. **Kashkush K, Feldman M, Levy AA.** 2002. Gene loss, silencing and activation in a newly synthesized wheat allotetraploid. Genetics **160:**1651-1659.
363. **Kashkush K, Feldman M, Levy AA.** 2003. Transcriptional activation of retrotransposons alters the expression of adjacent genes in wheat. Nature genetics **33:**102-106.
364. **Grandbastien MA, Audeon C, Bonnivard E, Casacuberta JM, Chalhoub B, Costa AP, Le QH, Melayah D, Petit M, Poncet C, Tam SM, Van Sluys MA, Mhiri C.** 2005. Stress activation and genomic impact of Tnt1 retrotransposons in Solanaceae. Cytogenetic and genome research **110:**229-241.
365. **Feschotte C, Jiang N, Wessler SR.** 2002. Plant transposable elements: where genetics meets genomics. Nat Rev Genet **3:**329-341.
366. **Sabot F, Schulman AH.** 2006. Parasitism and the retrotransposon life cycle in plants: a hitchhiker's guide to the genome. Heredity (Edinb) **97:**381-388.
367. **Ramallo E, Kalendar R, Schulman AH, Martinez-Izquierdo JA.** 2008. Reme1, a Copia retrotransposon in melon, is transcriptionally induced by UV light. Plant Mol Biol **66:**137-150.
368. **Law JA, Jacobsen SE.** 2010. Establishing, maintaining and modifying DNA methylation patterns in plants and animals. Nature reviews. Genetics **11:**204-220.
369. **Becker C, Hagmann J, Muller J, Koenig D, Stegle O, Borgwardt K, Weigel D.** 2011. Spontaneous epigenetic variation in the Arabidopsis thaliana methylome. Nature **480:**245-249.
370. **Lippman Z, Gendrel A-V, Black M, Vaughn MW, Dedhia N, Richard McCombie W, Lavine K, Mittal V, May B, Kasschau KD, Carrington JC, Doerge RW, Colot V, Martienssen R.** 2004. Role of transposable elements in heterochromatin and epigenetic control. Nature **430:**471-476.
371. **Grandbastien M-A.** 1998. Activation of plant retrotransposons under stress conditions. Trends in plant science **3:**181-187.
372. **Karijolich J, Abernathy E, Glaunsinger BA.** 2015. Infection-Induced Retrotransposon-Derived Noncoding RNAs Enhance Herpesviral Gene Expression via the NF-kappaB Pathway. PLoS Pathog **11:**e1005260.
373. **Shukla R, Upton Kyle R, Muñoz-Lopez M, Gerhardt Daniel J, Fisher Malcolm E, Nguyen T, Brennan Paul M, Baillie J K, Collino A, Ghisletti S, Sinha S, Iannelli F, Radaelli E, Dos Santos A, Rapoud D, Guettier C, Samuel D, Natoli G, Carninci P, Ciccarelli Francesca D, Garcia-Perez Jose L, Faivre J, Faulkner Geoffrey J.** 2013. Endogenous Retrotransposition Activates Oncogenic Pathways in Hepatocellular Carcinoma. Cell **153:**101-111.
374. **Castro-Diaz N, Ecco G, Coluccio A, Kapopoulou A, Yazdanpanah B, Friedli M, Duc J, Jang SM, Turelli P, Trono D.** 2014. Evolutionally dynamic L1 regulation in embryonic stem cells. Genes & development **28:**1397-1409.
375. **Ehrlich M.** 2002. DNA methylation in cancer: too much, but also too little. Oncogene **21:**5400-5413.
376. **Shitani M, Sasaki S, Akutsu N, Takagi H, Suzuki H, Nojima M, Yamamoto H, Tokino T, Hirata K, Imai K, Toyota M, Shinomura Y.** 2012. Genome-wide analysis of DNA methylation identifies novel cancer-related genes in hepatocellular carcinoma.

Tumour biology : the journal of the International Society for Oncodevelopmental Biology and Medicine **33:**1307-1317.

377. **Stief A, Brzezinka K, Lamke J, Baurle I.** 2014. Epigenetic responses to heat stress at different time scales and the involvement of small RNAs. Plant Signal Behav **9:**e970430.

Appendices

Appendix A: Various HSP70 mRNA homologs are induced during CNV infection

A.1 Summary of induction levels of HSP70 mRNA homologs in CNV versus mock inoculated plants at 3 dpi

Transcript ID	Description	CNV RPKM	Mock RPKM	CNV to Mock RPKM ratio
Nbv5tr6313114	Heat shock cognate 70 kDa protein (similar to)	218.0	0.04	5491.0
Nbv5tr6313115	Heat shock cognate 70 kDa protein (similar to)	183.4	0.04	4293.1
Nbv5tr6237742	Heat shock cognate 70 kDa protein (similar to)	270.9	0.07	4049.9
Nbv5tr6262864	Heat shock 70 kDa protein 5 (probable)	192.6	0.05	4018.7
Nbv5tr6217195	Heat shock 70 kDa protein (probable)	44.4	0.01	3526.5
Nbv5tr6340970	Heat shock cognate 70 kDa protein (similar to)	203.9	0.06	3275.0
Nbv5tr6248470	Heat shock 70 kDa protein (probable)	113.4	0.04	2913.9
Nbv5tr6274820	Heat shock 70 kDa protein 5 (probable)	95.8	0.03	2740.5
Nbv5tr6411059	Heat shock 70 kDa protein 5 (probable)	49.0	0.02	2658.9
Nbv5tr6263838	Heat shock 70 kDa protein (probable)	59.3	0.03	2269.4
Nbv5tr6343294	Heat shock 70 kDa protein (probable)	25.9	0.01	1931.2
Nbv5tr6239778	Heat shock 70 kDa protein 5 (probable)	113.1	0.07	1548.0
Nbv5tr6263036	Heat shock 70 kDa protein (probable)	75.9	0.05	1534.7
Nbv5tr6315459	Heat shock 70 kDa protein (probable)	47.4	0.03	1483.4
Nbv5tr6228252	Heat shock 70 kDa protein (probable)	293.5	0.23	1286.9
Nbv5tr6240566	Heat shock 70 kDa protein (probable)	76.6	0.07	1174.0
Nbv5tr6316161	Heat shock 70 kDa protein 5 (probable)	69.3	0.08	913.0
Nbv5tr6292801	Heat shock 70 kDa protein (probable)	62.9	0.07	859.9
Nbv5tr6239164	Heat shock cognate 70 kDa protein (similar to)	160.2	0.22	729.0
Nbv5tr6315458	Heat shock 70 kDa protein (probable)	36.3	0.05	712.5
Nbv5tr6369540	Heat shock 70 kDa protein (probable)	16.5	0.03	629.7
Nbv5tr6409725	Heat shock 70 kDa protein (probable)	23.7	0.05	494.5
Nbv5tr6399865	Heat shock cognate 70 kDa protein 1 (probable)	61.9	0.13	459.1
Nbv5tr6206844	Heat shock cognate 70 kDa protein 2 (probable)	153.6	0.46	330.9
Nbv5tr6379485	Heat shock cognate 70 kDa protein 1 (probable)	47.8	0.15	326.4
Nbv5tr6421447	Heat shock cognate 70 kDa protein 1 (probable)	54.0	0.17	321.2
Nbv5tr6379484	Heat shock cognate 70 kDa protein 1 (similar to)	50.6	0.16	317.5
Nbv5tr6233770	Heat shock cognate 70 kDa protein 2 (probable)	47.7	0.18	262.3
Nbv5tr6379480	Heat shock cognate 70 kDa protein 1 (probable)	48.5	0.19	255.4
Nbv5tr6379482	Heat shock cognate 70 kDa protein 1 (probable)	49.4	0.21	240.2
Nbv5tr6379483	Heat shock cognate 70 kDa protein 2 (probable)	57.7	0.25	231.8
Nbv5tr6379481	Heat shock cognate 70 kDa protein 1 (probable)	53.4	0.24	226.9
Nbv5tr6399864	Heat shock cognate 70 kDa protein 1 (probable)	57.5	0.28	208.1

Transcript ID	Description	CNV RPKM	Mock RPKM	CNV to Mock RPKM ratio
Nbv5tr6243057	Heat shock cognate 70 kDa protein 2 (probable)	9.4	0.05	172.6
Nbv5tr6317174	Heat shock cognate 70 kDa protein 2 (probable)	76.5	0.92	82.9
Nbv5tr6371458	Heat shock cognate 70 kDa protein 2 (probable)	79.9	1.06	75.4
Nbv5tr6424932	Heat shock cognate 70 kDa protein 2 (probable)	110.0	1.48	74.3
Nbv5tr6371455	Heat shock cognate 70 kDa protein 2 (probable)	86.1	1.17	73.8
Nbv5tr6371456	Heat shock cognate 70 kDa protein 2 (probable)	82.9	1.15	72.0
Nbv5tr6345618	Heat shock cognate 70 kDa protein 2 (similar to)	68.8	0.96	71.9
Nbv5tr6371457	Heat shock cognate 70 kDa protein 2 (probable)	71.1	1.03	68.7
Nbv5tr6393155	Heat shock cognate 70 kDa protein 2 (probable)	96.7	1.47	66.0
Nbv5tr6393153	Heat shock cognate 70 kDa protein 2 (probable)	90.0	1.36	66.0
Nbv5tr6233193	Heat shock cognate 70 kDa protein 2 (probable)	99.5	1.51	65.8
Nbv5tr6241746	Heat shock cognate 70 kDa protein 2 (probable)	35.7	0.55	65.5
Nbv5tr6393156	Heat shock cognate 70 kDa protein 2 (probable)	72.9	1.13	64.5
Nbv5tr6345619	Heat shock cognate 70 kDa protein 2 (probable)	70.5	1.10	64.0
Nbv5tr6393154	Heat shock cognate 70 kDa protein 2 (probable)	87.2	1.37	63.6
Nbv5tr6393157	Heat shock cognate 70 kDa protein 2 (probable)	88.5	1.42	62.4
Nbv5tr6412958	Heat shock cognate 70 kDa protein 2 (probable)	104.9	1.70	61.7
Nbv5tr6393152	Heat shock cognate 70 kDa protein 2 (probable)	91.9	1.49	61.7
Nbv5tr6206845	Heat shock cognate 70 kDa protein 2 (probable)	82.6	3.35	24.7
Nbv5tr6432353	Heat shock 70 kDa protein 15 (probable)	5.6	0.27	20.5
Nbv5tr6378082	Heat shock 70 kDa protein 15 (probable)	5.1	0.25	20.2
Nbv5tr6324733	Heat shock 70 kDa protein 15 (probable)	8.2	0.43	19.3
Nbv5tr6209761	Heat shock 70 kDa protein (probable)	0.6	0.03	18.7
Nbv5tr6217644	Heat shock 70 kDa protein (probable)	2.4	0.14	17.8
Nbv5tr6351467	Heat shock 70 kDa protein 8 (probable)	3.1	0.17	17.8
Nbv5tr6261004	Heat shock 70 kDa protein 15 (probable)	19.9	1.14	17.5
Nbv5tr6324732	Heat shock 70 kDa protein 15 (probable)	7.6	0.46	16.6
Nbv5tr6261142	Heat shock 70 kDa protein 15 (probable)	5.8	0.38	15.0
Nbv5tr6376015	Heat shock 70 kDa protein 15 (probable)	5.9	0.39	14.8
Nbv5tr6317727	Heat shock 70 kDa protein 15 (probable)	3.3	0.22	14.8
Nbv5tr6345470	Heat shock 70 kDa protein 15 (probable)	4.9	0.33	14.7
Nbv5tr6376014	Heat shock 70 kDa protein 15 (probable)	7.8	0.54	14.5
Nbv5tr6432349	Heat shock 70 kDa protein 15 (similar to)	4.9	0.35	13.8
Nbv5tr6262602	Heat shock 70 kDa protein 15 (similar to)	3.6	0.26	13.6
Nbv5tr6345471	Heat shock 70 kDa protein 15 (probable)	4.3	0.32	13.5
Nbv5tr6371283	Heat shock 70 kDa protein 15 (probable)	4.3	0.32	13.5
Nbv5tr6351465	Heat shock 70 kDa protein 8 (probable)	2.9	0.21	13.4
Nbv5tr6393848	Heat shock 70 kDa protein 15 (probable)	4.6	0.35	13.4

Transcript ID	Description	CNV RPKM	Mock RPKM	CNV to Mock RPKM ratio
Nbv5tr6393853	Heat shock 70 kDa protein 15 (probable)	8.3	0.62	13.3
Nbv5tr6393856	Heat shock 70 kDa protein 15 (probable)	3.9	0.30	13.1
Nbv5tr6432348	Heat shock 70 kDa protein 15 (probable)	4.5	0.34	13.1
Nbv5tr6432352	Heat shock 70 kDa protein 15 (probable)	4.7	0.37	12.9
Nbv5tr6393849	Heat shock 70 kDa protein 15 (probable)	6.7	0.53	12.8
Nbv5tr6345472	Heat shock 70 kDa protein 15 (probable)	4.1	0.32	12.6
Nbv5tr6317732	Heat shock 70 kDa protein 15 (similar to)	3.1	0.24	12.6
Nbv5tr6351466	Heat shock 70 kDa protein 8 (probable)	4.1	0.33	12.5
Nbv5tr6345469	Heat shock 70 kDa protein 15 (probable)	5.3	0.44	12.3
Nbv5tr6317730	Heat shock 70 kDa protein 15 (similar to)	4.5	0.37	12.2
Nbv5tr6317725	Heat shock 70 kDa protein 15 (similar to)	3.1	0.26	12.1
Nbv5tr6274281	Heat shock 70 kDa protein 15 (probable)	3.2	0.27	11.9
Nbv5tr6274279	Heat shock 70 kDa protein 15 (probable)	3.4	0.28	11.9
Nbv5tr6371287	Heat shock 70 kDa protein 15 (probable)	7.0	0.60	11.8
Nbv5tr6345468	Heat shock 70 kDa protein 15 (probable)	5.4	0.46	11.7
Nbv5tr6393854	Heat shock 70 kDa protein 15 (probable)	7.2	0.62	11.7
Nbv5tr6293307	Heat shock 70 kDa protein 15 (probable)	4.6	0.39	11.6
Nbv5tr6378081	Heat shock 70 kDa protein 15 (similar to)	6.3	0.55	11.5
Nbv5tr6371288	Heat shock 70 kDa protein 15 (probable)	5.6	0.49	11.5
Nbv5tr6317729	Heat shock 70 kDa protein 15 (similar to)	3.1	0.27	11.2
Nbv5tr6294799	Heat shock 70 kDa protein 15 (probable)	3.2	0.29	11.2
Nbv5tr6274280	Heat shock 70 kDa protein 15 (probable)	3.1	0.28	11.1
Nbv5tr6229442	Heat shock 70 kDa protein 15 (probable)	6.2	0.56	11.0
Nbv5tr6257763	Heat shock 70 kDa protein 15 (probable)	15.1	1.37	11.0
Nbv5tr6317726	Heat shock 70 kDa protein 15 (similar to)	3.1	0.28	10.9
Nbv5tr6432346	Heat shock 70 kDa protein 15 (similar to)	2.9	0.27	10.9
Nbv5tr6293305	Heat shock 70 kDa protein 15 (probable)	2.7	0.25	10.8
Nbv5tr6233529	Heat shock 70 kDa protein 15 (probable)	15.3	1.43	10.7
Nbv5tr6393850	Heat shock 70 kDa protein 15 (probable)	3.5	0.33	10.6
Nbv5tr6274276	Heat shock 70 kDa protein 15 (probable)	3.4	0.32	10.6
Nbv5tr6274278	Heat shock 70 kDa protein 15 (similar to)	2.4	0.23	10.5
Nbv5tr6293306	Heat shock 70 kDa protein 15 (probable)	3.0	0.29	10.3
Nbv5tr6394155	Heat shock 70 kDa protein 8 (probable)	3.7	0.36	10.3
Nbv5tr6371285	Heat shock 70 kDa protein 15 (probable)	5.0	0.49	10.2
Nbv5tr6393852	Heat shock 70 kDa protein 15 (probable)	4.1	0.41	10.1
Nbv5tr6345467	Heat shock 70 kDa protein 15 (probable)	3.3	0.33	10.1
Nbv5tr6206842	Heat shock cognate 70 kDa protein 2 (probable)	69.3	6.93	10.0
Nbv5tr6432351	Heat shock 70 kDa protein 15 (probable)	2.1	0.21	9.9

Transcript ID	Description	CNV RPKM	Mock RPKM	CNV to Mock RPKM ratio
Nbv5tr6371289	Heat shock 70 kDa protein 15 (probable)	4.3	0.44	9.8
Nbv5tr6274277	Heat shock 70 kDa protein 15 (probable)	2.9	0.30	9.8
Nbv5tr6432350	Heat shock 70 kDa protein 15 (probable)	2.9	0.30	9.6
Nbv5tr6393000	Heat shock 70 kDa protein 15 (probable)	8.5	0.88	9.6
Nbv5tr6371284	Heat shock 70 kDa protein 15 (probable)	4.6	0.49	9.3
Nbv5tr6393855	Heat shock 70 kDa protein 15 (probable)	4.9	0.54	9.2
Nbv5tr6274275	Heat shock 70 kDa protein 15 (similar to)	2.1	0.23	9.1
Nbv5tr6351468	Heat shock 70 kDa protein 8 (probable)	2.1	0.23	9.1
Nbv5tr6211369	Heat shock 70 kDa protein 15 (probable)	1.8	0.20	9.0
Nbv5tr6317728	Heat shock 70 kDa protein 15 (similar to)	3.4	0.38	8.9
Nbv5tr6393847	Heat shock 70 kDa protein 15 (probable)	4.1	0.46	8.8
Nbv5tr6371286	Heat shock 70 kDa protein 15 (probable)	4.7	0.54	8.8
Nbv5tr6293308	Heat shock 70 kDa protein 15 (probable)	2.5	0.29	8.8
Nbv5tr6317731	Heat shock 70 kDa protein 15 (similar to)	2.7	0.31	8.7
Nbv5tr6274282	Heat shock 70 kDa protein 15 (probable)	2.9	0.33	8.7
Nbv5tr6294796	Heat shock 70 kDa protein 15 (probable)	2.8	0.33	8.7
Nbv5tr6293304	Heat shock 70 kDa protein 15 (probable)	2.0	0.23	8.5
Nbv5tr6424464	Heat shock 70 kDa protein 15 (probable)	7.2	0.85	8.5
Nbv5tr6262696	Heat shock 70 kDa protein 15 (probable)	12.0	1.47	8.2
Nbv5tr6371292	Heat shock cognate 70 kDa protein 2 (probable)	36.2	4.55	7.9
Nbv5tr6394156	Heat shock 70 kDa protein 8 (probable)	3.3	0.42	7.9
Nbv5tr6256774	Heat shock 70 kDa protein 15 (probable)	6.0	0.77	7.7
Nbv5tr6393455	Heat shock cognate 70 kDa protein 2 (probable)	40.7	5.28	7.7
Nbv5tr6393851	Heat shock 70 kDa protein 15 (probable)	4.2	0.55	7.7
Nbv5tr6236060	Heat shock cognate 70 kDa protein 2 (probable)	57.1	7.46	7.7
Nbv5tr6233178	Heat shock cognate 70 kDa protein 2 (probable)	35.1	4.75	7.4
Nbv5tr6393453	Heat shock cognate 70 kDa protein 2 (probable)	30.3	4.17	7.3
Nbv5tr6345475	Heat shock cognate 70 kDa protein 2 (probable)	31.1	4.38	7.1
Nbv5tr6274274	Heat shock 70 kDa protein 15 (probable)	2.1	0.30	7.1
Nbv5tr6253085	Heat shock 70 kDa protein 15 (probable)	4.8	0.69	7.0
Nbv5tr6372659	Heat shock 70 kDa protein 8 (probable)	2.9	0.41	7.0
Nbv5tr6218543	Heat shock 70 kDa protein 18 (probable)	2.3	0.32	7.0
Nbv5tr6424962	Heat shock 70 kDa protein 15 (probable)	11.0	1.66	6.6
Nbv5tr6393454	Heat shock cognate 70 kDa protein 2 (probable)	20.9	3.31	6.3
Nbv5tr6371293	Heat shock cognate 70 kDa protein 2 (probable)	23.6	3.80	6.2
Nbv5tr6345476	Heat shock cognate 70 kDa protein 2 (probable)	26.0	4.22	6.2
Nbv5tr6259462	Heat shock 70 kDa protein 15 (similar to)	6.9	1.13	6.1
Nbv5tr6261463	Heat shock cognate 70 kDa protein 2 (probable)	54.7	9.00	6.1

Transcript ID	Description	CNV RPKM	Mock RPKM	CNV to Mock RPKM ratio
Nbv5tr6423124	Heat shock 70 kDa protein 16 (probable)	0.5	0.09	5.8
Nbv5tr6211368	Heat shock 70 kDa protein 15 (probable)	1.4	0.24	5.7
Nbv5tr6430069	Heat shock cognate 70 kDa protein 2 (similar to)	50.4	9.03	5.6
Nbv5tr6392773	Heat shock cognate 70 kDa protein 2 (probable)	123.4	22.97	5.4
Nbv5tr6276355	Heat shock 70 kDa protein 8 (probable)	1.8	0.34	5.3
Nbv5tr6392774	Heat shock cognate 70 kDa protein 2 (probable)	61.4	11.89	5.2
Nbv5tr6392772	Heat shock cognate 70 kDa protein 2 (probable)	48.8	9.56	5.1
Nbv5tr6371043	Heat shock cognate 70 kDa protein 2 (probable)	72.7	14.53	5.0
Nbv5tr6206843	Heat shock cognate 70 kDa protein 2 (probable)	48.8	9.77	5.0
Nbv5tr6206841	Heat shock cognate 70 kDa protein 2 (probable)	71.4	14.43	4.9
Nbv5tr6413030	Heat shock cognate 70 kDa protein 2 (similar to)	83.7	17.38	4.8
Nbv5tr6430068	Heat shock cognate 70 kDa protein 2 (probable)	67.5	14.33	4.7
Nbv5tr6218854	Heat shock 70 kDa protein 8 (probable)	1.6	0.34	4.7
Nbv5tr6415008	Heat shock 70 kDa protein 16 (probable)	0.6	0.13	4.7
Nbv5tr6263875	Heat shock 70 kDa protein 15 (probable)	4.7	1.03	4.6
Nbv5tr6252404	Heat shock 70 kDa protein 16 (similar to)	0.5	0.11	4.3
Nbv5tr6358738	Heat shock 70 kDa protein 16 (probable)	0.6	0.14	4.3
Nbv5tr6250450	Heat shock 70 kDa protein 17 (similar to)	0.6	0.14	4.2
Nbv5tr6279309	Heat shock 70 kDa protein 16 (probable)	0.5	0.12	4.1
Nbv5tr6421657	Heat shock 70 kDa protein 16 (probable)	1.6	0.39	4.0
Nbv5tr6294797	Heat shock 70 kDa protein 15 (probable)	2.8	0.72	3.9
Nbv5tr6218651	Heat shock 70 kDa protein 15 (similar to)	2.8	0.73	3.8
Nbv5tr6275587	Heat shock 70 kDa protein 15 (probable)	1.6	0.43	3.8
Nbv5tr6304244	Heat shock 70 kDa protein 16 (similar to)	0.4	0.12	3.7
Nbv5tr6218933	Heat shock 70 kDa protein 15 (probable)	2.1	0.58	3.6
Nbv5tr6304245	Heat shock 70 kDa protein 16 (similar to)	0.4	0.11	3.6
Nbv5tr6432347	Heat shock 70 kDa protein 15 (probable)	3.3	0.92	3.6
Nbv5tr6358739	Heat shock 70 kDa protein 16 (probable)	0.5	0.15	3.5
Nbv5tr6413804	Heat shock 70 kDa protein 16 (probable)	0.4	0.12	3.5
Nbv5tr6272294	Heat shock 70 kDa protein 16 (probable)	0.6	0.18	3.5
Nbv5tr6302558	Heat shock 70 kDa protein 17 (similar to)	0.8	0.25	3.4
Nbv5tr6294798	Heat shock 70 kDa protein 15 (probable)	2.4	0.71	3.4
Nbv5tr6358740	Heat shock 70 kDa protein 16 (probable)	0.7	0.21	3.2
Nbv5tr6200769	Heat shock 70 kDa protein 17 (probable)	0.9	0.28	3.1
Nbv5tr6318531	Heat shock 70 kDa protein 17 (probable)	0.5	0.17	3.1
Nbv5tr6226199	Heat shock 70 kDa protein 15 (probable)	3.4	1.14	3.0
Nbv5tr6304243	Heat shock 70 kDa protein 16 (probable)	0.4	0.15	2.9
Nbv5tr6302559	Heat shock 70 kDa protein 17 (probable)	0.5	0.20	2.8

Transcript ID	Description	CNV RPKM	Mock RPKM	CNV to Mock RPKM ratio
Nbv5tr6252405	Heat shock 70 kDa protein 16 (similar to)	0.7	0.26	2.8
Nbv5tr6256892	Heat shock 70 kDa protein 16 (probable)	0.7	0.25	2.8
Nbv5tr6393828	Heat shock 70 kDa protein 17 (probable)	0.4	0.14	2.7
Nbv5tr6282151	Heat shock 70 kDa protein 17 (probable)	0.4	0.17	2.7
Nbv5tr6358360	Heat shock 70 kDa protein 15 (probable)	3.2	1.21	2.6
Nbv5tr6421001	Heat shock 70 kDa protein 16 (probable)	0.5	0.19	2.5
Nbv5tr6393827	Heat shock 70 kDa protein 17 (probable)	0.6	0.27	2.4
Nbv5tr6251762	Heat shock 70 kDa protein 17 (probable)	0.9	0.38	2.4
Nbv5tr6418305	Heat shock 70 kDa protein 17 (similar to)	0.4	0.17	2.4
Nbv5tr6372230	Heat shock 70 kDa protein 17 (probable)	0.5	0.20	2.4
Nbv5tr6406432	Heat shock 70 kDa protein 16 (probable)	0.6	0.26	2.3
Nbv5tr6346382	Heat shock 70 kDa protein 17 (probable)	0.7	0.29	2.3
Nbv5tr6372228	Heat shock 70 kDa protein 17 (probable)	0.5	0.23	2.3
Nbv5tr6372229	Heat shock 70 kDa protein 17 (probable)	0.4	0.18	2.3
Nbv5tr6255771	Heat shock 70 kDa protein 17 (probable)	0.4	0.18	2.2
Nbv5tr6372232	Heat shock 70 kDa protein 17 (probable)	0.5	0.24	2.2
Nbv5tr6393830	Heat shock 70 kDa protein 17 (probable)	0.5	0.27	2.0
Nbv5tr6383512	Heat shock 70 kDa protein 16 (probable)	0.4	0.19	2.0
Nbv5tr6402731	Heat shock 70 kDa protein 15 (probable)	2.8	1.45	2.0
Nbv5tr6346381	Heat shock 70 kDa protein 17 (probable)	0.4	0.22	2.0
Nbv5tr6252281	Heat shock 70 kDa protein 17 (similar to)	0.4	0.18	1.9
Nbv5tr6358737	Heat shock 70 kDa protein 16 (probable)	0.4	0.20	1.8
Nbv5tr6253217	Heat shock 70 kDa protein 17 (similar to)	0.6	0.33	1.8
Nbv5tr6372231	Heat shock 70 kDa protein 17 (probable)	0.4	0.25	1.6
Nbv5tr6256813	Heat shock 70 kDa protein 16 (probable)	0.4	0.24	1.6
Nbv5tr6393831	Heat shock 70 kDa protein 17 (probable)	0.3	0.19	1.4
Nbv5tr6304242	Heat shock 70 kDa protein 16 (probable)	0.2	0.13	1.3
Nbv5tr6393829	Heat shock 70 kDa protein 17 (probable)	0.5	0.39	1.3
Nbv5tr6417800	Heat shock 70 kDa protein 16 (probable)	0.3	0.25	1.1
Nbv5tr6330410	Heat shock 70 kDa protein 16 (probable)	0.2	0.20	0.8
Nbv5tr6223295	Heat shock 70 kDa protein (probable)	0.1	0.43	0.3

Figure A.1: RPKM values for individual transcripts were determined and then the ratios of CNV RPKM values to mock values were obtained.

The data are ranked from the highest to the lowest ratio.

A.2 Nucleotide sequence of cloned *N. benthamiana* Hsc70-2 (NbHsc70-2)

ATGGCAGGAAAAGGAGAAGGTCCGGCGATCGGAATCGATCTCGGAACTACTTACTCTTGTGTCG
GTGTATGGCAACATGATCGTGTTGAGATTATTGCTAATGATCAAGGGAACAGGACGACGCCGTC
TTATGTTGGATTTACCGATTCTGAACGTCTCATTGGTGATGCCGCTAAGAATCAAGTCGCTATG
AATCCTATTAACACTGTCTTCGATGCCAAGAGGCTCATTGGAAGGAGGTTCAGTGATGCCTCTG
TACAAAGTGACATCAAATTGTGGCCTTTTAAGGTTATTTCTGGACCTGCTGACAAGCCAATGAT
TGTTGTCAACTACAAGGGTGAAGAGAAGCAGTTTGCTGCTGAAGAAATCTCTTCCATGGTCCTG
ATAAAGATGAAGGAAATTGCCGAGGCCTTCCTTGGATCAACTGTGAAAAATGCTGTGGTTACTG
TACCTGCATACTTCAATGACTCACAACGTCAGGCTACTAAGGATGCTGGTGTCATATCTGGCTT
GAATGTCATGCGTATTATTAATGAGCCCACAGCAGCAGCCATTGCTTATGGTCTTGACAAGAAA
GCCACAAGTGTTGGTGAGAAGAACGTTCTTATCTTTGATCTAGGTGGTGGTACTTTCGATGTGT
CCCTCCTTACTATTGAAGAAGGTATTTTTGAGGTGAAAGCCACAGCAGGAGACACTCACCTTGG
AGGTGAAGATTTTGATAACAGAATGGTGAACCACTTTGTCCAGGAGTTCAAAAGAAAGCACAAG
AAGGACATTACCGGTAACCCAAGAGCCCTTAGAAGATTGAGGACAGCATGTGAGAGGGCGAAGA
GAACTCTTTCTTCCACTGCCCAGACAACAATTGAAATTGATTCCTTGTATGAGGGAGTTGACTT
CTATTCCACCATTACTCGTGCTAGATTTGAGGAATTGAACATGGATCTTTTCAGGAAGTGTATG
GAGCCAGTAGAGAAATGTTTGAGGGACGCCAAGATGGACAAGAGCACTGTACATGATGTTGTTC
TTGTTGGTGGATCCACTAGAATTCCCAAGGTACAACAGCTGTTGCAAGACTTCTTTAATGGCAA
GGAACTTTGCAAGAGCATCAACCCAGATGAGGCTGTTGCCTATGGTGCAGCTGTGCAAGCTGCC
ATTCTAAGCGGAGAGGGTAACGAGAAGGTTCAAGACTTGTTGCTTTTGGATGTGACCCCTCTAT
CTCTTGGGTTGGAAACTGCTGGAGGAGTGATGACTGTATTGATTCCAAGGAATACCACTATTCC
TACCAAGAAAGAGCAGGTGTTCTCTACATATTCTGACAACCAACCTGGAGTGTTGATTCAGGTG
TATGAGGGTGAGAGAGCAAGAACTAGAGACAACAACTTGCTGGGTAAATTTGAGCTTTCTGGTA
TCCCTCCTGCACCTAGGGGTGTGCCTCAGATCACAGTCTGCTTTGATATTGATGCCAATGGTAT
CTTGAACGTCTCTGCTGAAGACAAGACCACTGGACAGAAGAACAAGATCACAATTACCAATGAC
AAGGGTAGGTTGTCAAAGGAAGAAATTGAAAAGATGGTCCAGGAAGCAGAGAAGTACAAGGCAG
AGGATGAAGAACACAAGAAGAAGGTAGAGGCCAAGAACGCACTGGAGAACTATGCCTACAACAT
GAGGAACACCATAAAGGATGAGAAGATTGGTTCTAAGCTAAGCCCAGACGACAAAAAGAAGATT
GAGGATGCGATTGATCAGGCAATCTCATGGCTTGACAGCAACCAGCTTGCTGAAGCTGACGAGT
TTGAAGATAAGATGAAGGAGCTCGAGAGCATCTGCAACCCCATCATTGCCAAGATGTACCAAAG
CGCTGGTGGTGAAGCAGGTGCACCTATGGATGATGATGCTCCTCCAGCTGGTGGTAGCGGTGCA
GGTCCCAAGATTGAGGAGGTCGACTAA

A.3 Alignment of various peptides obtained via Mass Spectometry of the co-immunoprecipitate and CNV virion preparation with *N. benthamiana* Hsc70-2 protein sequence

MAGKGEGPAIGIDLGTTYSCVGVWQHDRVEIIANDQGNRTTPSYVGFTDSERLIGDAAKNQVAM
NPINTVFDAKRLIGRRFSDASVQSDIKLWPFKVISGPADKPMIVVNYKGEEKQFAAEEISSMVL
IKMKEIAEAFLGSTVKNAVVTVPAYFNDSQRQATKDAGVISGLNVMRIINEPTAAAIAYGLDKK
ATSVGEKNVLIFDLGGGTFDVSLLTIEEGIFEVKATAGDTHLGGEDFDNRMVNHFVQEFKRKHK
KDITGNPRALRRLRTACERAKRTLSSTAQTTIEIDSLYEGVDFYSTITRARFEELNMDLFRKCM
EPVEKCLRDAKMDKSTVHDVVLVGGSTRIPKVQQLLQDFFNGKELCKSINPDEAVAYGAAVQAA
ILSGEGNEKVQDLLLLDVTPLSLGLETAGGVMTVLIPRNTTIPTKKEQVFSTYSDNQPGVLIQV
YEGERARTRDNNLLGKFELSGIPPAPRGVPQITVCFDIDANGILNVSAEDKTTGQKNKITITND
KGRLSKEEIEKMVQEAEKYKAEDEEHKKKVEAKNALENYAYNMRNTIKDEKIGSKLSPDDKKKI
EDAIDQAISWLDSNQLAEADEFEDKMKELESICNPIIAKMYQSAGGEAGAPMDDDAPPAGGSGA
GPKIEEVD*

Yellow- Peptides exclusively detected in Mass Spectometry of co-immunoprecipitate (see Figure 2.3.7B).

Blue- Peptides exclusively detected in Mass Spectometry of CNV virion preparation (see Figure 3.3.1C).

Red- Peptides detected in Mass Spectometry of both co-immunoprecipitate as well as CNV virion preparation (see Figures 2.3.7B and 2.3.7B).

Appendix B: Induction of specific retrotransposons by *Cucumber necrosis virus* infection likely occurs through activation of the heat-shock response[6]

B.1 Introduction

Plants must cope with environmental change to persist in the natural environment. Plant cells adapt physiologically through responses that are immediate and reversible. At the population and species levels, selection may lead to genetic changes and evolution of inherited characteristics that are not readily reversible. Transposable elements (TEs) have been described to play an important role in genome evolution. TEs are described as genetic entities capable of self-amplifying and inserting to new genomic locations and are known to alter the function of the genes with which they become associated.

Previous reports have shown that genetic variability of genomes is enhanced by induction of TEs (315, 316). A consequence of increased TE mobility is the creation of new genetic variability that can be useful in facing stressful conditions as described for the activity of *mping* DNA transposon in some rice strains. The *mping* TE rapidly increases in every generation and acts as an enhancer that renders stress responsiveness to neighbouring genes (317, 318). In soybean, the insertion of the retrotransposon (RTn) *Ty-1/Copia SORE-1* into a paralog of phytochrome A resulted in photoperiod insensitivity, allowing for soybean cultivation at high latitudes.(319). Also a recent report has shown that retrotransposition of *Ty-1/Copia* retrotransposon ONSEN into an abscisic acid (ABA) responsive gene results in ABA-insensitive phenotypes in *A. thaliana*, suggesting a role of RTns in influencing adaptive stress responses (320).

[6] A version of information presented here along with additional experiments is anticipated to be prepared for publication.

TEs are a major component of all plant genomes and represent about 4-75% of the content of the genome depending on the plant species (321). There are two major classes of TEs (322). Class I elements transpose through reverse transcription of an RNA intermediate by a "copy-and-paste" mechanism and comprise RTns and other retroelements (323). Class II elements are DNA transposons that transpose via a DNA intermediate using a non-replicative "cut-and-paste" mechanism (324). DNA transposons are less abundant in the genome than RTns (325). RTns are further grouped into long terminal repeat (LTR) RTns and non-LTR RTns (325). LTR RTns constitute a large part of the plant non-genic genomic regions (323). LTR RTns are further divided into *Ty-1/Copia* and *Ty-3/Gypsy* families according to the relative positions of the invertase and reverse transcriptase coding regions. While the former RTns are conserved in euchromatin regions of some plant species (326), the latter are enriched in the intergenic regions that constitute centromeric heterochromatin in some plants (327).

TEs often referred as "junk DNA" are programmed to amplify and insert to new genetic loci following use of the host's transcriptional machinery. New TE insertions can give rise to genetic instability as well as deleterious mutations but can also have a positive influence on gene regulation and adaptation (328, 329). Transposon derived siRNAs may introduce DNA methylation into nearby genes via RNA-directed DNA methylation (RdDM) and influence gene expression. Plants thus have evolved epigenetic silencing as the mechanism to suppress uncontrolled propagation of TEs (330-332). Reports have shown that siRNA-mediated regulation is responsible for the restriction of transcription of a heat inducible RTn, ONSEN, after heat stress (333).

Transposition is not a random process, but is controlled by host intrinsic and extrinsic factors such as environmental stress and challenges. Some TEs have co-evolved to escape the plant's repression mechanisms and maintain their ability to be activated and transposed by several biotic and abiotic stress conditions. Sequences involved in the expression of RTns such as the signals for the initiation and termination of transcription as well as stress responsive elements are located in a well-defined region of several hundred nucleotides, repeated at both ends of the RTn, in the LTRs.

There is growing evidence that environmental stress such as temperature, drought and salt stress, radiation, UV exposure, wounding, cell culture, pathogen infection and polyploidization can activate transposons (334, 335) (336). For example, the transcription of tobacco *Copia*-type Tnt1 RTn has been shown to be induced by wounding, freezing, oxidative stress as well as salicylic acid and $CuCl_2$ application (337). Also, abiotic stresses like salinity, high temperature and gamma rays have been shown to induce Ji and Opie retrotransposons of common bean plants, *Phaseolus vulgaris* (338).

High temperature and heat stress is considered to be one of the most important environmental factors that affect growth and development of plants (339). Epigenetic regulation of heat responses have recently attracted significant attention (340). Recently it has been shown that, ONSEN, a *Ty-1/Copia*-type RTn, is activated under heat stress in *A. thaliana* and some other species of *Brassicaceae* (333, 341, 342). Heat stress has also been shown to increase the expression of RTn-like sequences in Scots pine (343, 344), where it was hypothesized that heat activation and insertion of heat inducible RTns within or close to genes may confer heat

responsiveness to the flanking genes. Heat stress has been also reported to activate seven different LTR RTns in barley (345). A recent study on the nematode *Caenorhabditis elegans* also showed that many of the genes that are transcriptionally activated by heat stress are in or near the LTRs of RTns suggesting that a subset of LTR RTns are heat inducible in this organism (346). Also another group recently reported that heat stress activates TE and RTns in rice (*Oryza sativa*) (314). MAGGY a *Ty-3/Gypsy* RTn in the fungus *Pyricularia grisea* was shown to be transcriptionally activated by heat-shock (347). *Copia*-type RTn transcripts have also been found to be induced by heat stress in *Drosophila melanogaster* (348).

Short and long interspersed nuclear element (SINE and LINE respectively) retroelements are non-LTR retrotransposons that contain a poly(A) tail at the 3' terminus of the element (325). These non-LTR retrotransposons are one of the largest potential sources of host-derived non-coding RNAs and constitute >10% of the human and mouse genomes (349, 350). In general, SINE and LINE elements are transcriptionally silent in healthy somatic cells due to post transcriptional modifications. But infection by certain viruses like *Herpes simplex virus I* (351, 352), *Adenovirus type 5* (353) and *Minute virus of mice* (354) have been found to induce SINE retroelements. *Hepatitis C virus* has been reported to activate LTRs of the *Retrovirus* HIV and hence upregulates HIV gene transcription during co-infections (355). The viral protein R of HIV type 1 has been recently shown to induce retrotransposition of LINE-1 (356). However, no reports have yet been made regarding the induction of RTns or any TE by a plant virus. Previous studies of FHV have shown that RTns are packaged into virions, however, to my knowledge induction of retrotransposons by this virus has not been investigated.

CNV is a non-enveloped positive strand RNA virus in the genus *Tombusvirus*, family *Tombusviridae* (7). CNV particles have a T=3 icosahedral structure with a diameter of 34 nm. Virions predominantly encapsidate a genomic RNA of approximately 4.7 kb. However, recently, work in the Dr. Rochon's lab has shown that ~0.1% of the RNA encapsidated during infection is of host origin. Also, host RNAs were found to be encapsidated in VLPs produced following agroinfiltration of *N. benthamiana* plants with CNV coat protein (CP) (135). One of the remarkable findings was that the most predominantly encapsidated non-ribosomal cytoplasmic host RNAs were RTn-like RNA sequences.

RNA-seq analysis of RNA extracted from CNV-infected leaves revealed that specific RTns are upregulated dramatically during infection (D. Rochon, personal communication). Several of these RTns were found to be phylogenetically related to ONSEN. Also, recently I have shown that HSP70 mRNAs and proteins are significantly induced during CNV infection and that CNV co-opts HSP70 homologs to facilitate several stages of the multiplication cycle (122). The induction of HSP70 is dependent on the activation of specific transcription factors termed heat-shock factors (HSFs) which bind to heat-shock element (HSE) in the promoters of the genes encoding HSP70s (69). Unpublished work from Dr. Rochon's lab has shown that the mRNA for transcription factor HSF30 (which is phylogenetically most similar to HSFA2 involved in activation of ONSEN) is induced ~8-10 fold during CNV infection of *N. benthamiana*. These observations together prompted us to investigate if the RTns induced by CNV infection are heat inducible.

I found that several of the RTns induced by CNV during infection are heat inducible and that a greater induction is observed at a higher temperature (48°C) as compared to a lower temperature (42°C). The 5' LTR region of four major *Ty-1/Copia* RTns were analysed and found to be rich in putative HSEs. To directly assess if the LTR of CNV inducible RTns are heat responsive, a GFP reporter assay was developed. I found that heat treatment activates the LTRs of two tested CNV inducible RTns resulting in the expression of the downstream reporter gene, GFP. A similar increase in the activation of these LTR was also observed during CNV infection suggesting that induction of these LTR may be due to the heat-shock response induced during CNV infection. We speculate that CNV infection induces *Ty-1/Copia* RTn mRNAs via the HSFs induced during infection and further speculate that CNV infection may therefore impart a potential benefit to infected plants by installing retrotransposibility to heat-shock elements that may provide an evolutionary advantage to subsequent generations.

B.2 Materials and methods

B.2.1 Next generation sequencing

Next generation sequence analysis utilizing RNA-seq (Applied Biological Materials) and the Illumina platform was performed on total ribosomal RNA depleted leaf RNA obtained from mock or CNV infected plants at 4 dpi (CNV1 and Mock1) and 3 dpi (CNV2 and Mock2) in independent experiments. The data was analysed as described previously (122). This work was conducted by Dr. Rochon and members of the Rochon Lab.

B.2.2 Identification of LTRs

Briefly, the complete sequences of highly induced RTns were obtained by conducting a BLAST search of genomic DNA of *N. benthamiana* using the University of the Sydney, Au database (http://benthgenome.qut.edu.au/) and/or the Sol Genomics Network database (https://solgenomics.net/) with a partial or near complete RNA sequence of the specific RTn. DNA sequences 5' and 3' of the RTn RNA sequence were obtained and the full-length RTns including the LTRs were identified using "LTR finder" software (http://tlife.fudan.edu.cn/ltr_finder/). Sequences of the 5' LTRs obtained are shown in Figure B.2. Highly induced RTns were identified from RNA-seq data by dividing the RPKM value obtained for a particular RTn identified in RNA extracted from CNV infected leaves by the value obtained for the same RTn in RNA extracted from mock inoculated leaves. This work was conducted by Dr. Rochon.

B.2.3 Identification of HSEs in LTRs

HSFA2 consists of discrete functional domains, including a hydrophobic DBD. The DNA binding domain of each monomeric HSFA2 unit binds to the pentanucleotide unit, 5'-nGAAn- 3' (or 5'-nTTCn-3'), in the target DNA. Since, the DBD in HSFA2 binds to the pentanucleotide unit and the typical HSE is composed of 3 copies of the pentanucleotide unit this results in homotrimerization of HSFA2 (71-74).

As described for *Saccharomyces cerevisiae* (75), there are three different types of HSEs that can interact with HSF. The "perfect-type" (P type) HSE consists of continuous inverted repeats of

the pentanucleotide unit (5'-nTTCnnGAAnnTTCn-3' or 5'-nGAAnnTTCnnGAAn-3'), the "gap-type" (G type) contains one gap between the units [5'-nGAAnnTTCn(5bp)nTTCn-3' or 5'-nTTCnnGAAn(5bp)nGAAn-3' or 5'-nGAAn(5bp)nGAAnnTTCn-3' or 5'-nTTCn(5bp)nTTCnnGAAn-3'] and the "step-type" (S type) contains two gaps [5'-nGAAn(5bp)nGAAn(5bp)nGAAn-3' or 5'-nTTCn(5bp)nTTCn(5bp)nTTCn-3'].

The putative HSEs in Figure B.2 were identified manually. In *Sakurai et al.* (2007) (75), it was found that many HSEs identified by footprint analyses did not fully match the consensus sequence and up to two substitutions (one in each of two elements) in a given trimeric motif could be found. We therefore allowed two such substitutions per triplicate in our search for putative HSEs. The HSEs may also be overlapping as described in *Sakurai et al.* (2010) (74). For example, four pentanucleotide motifs spaced as in a P type would basically comprise 2 sets of HSE elements with the first three pentanucleotide motifs constituting one HSE and the second group of three pentanucleotide motifs constituting a second element and so on for motifs containing additional pentanucleotide motifs. Similar scenarios would also apply to the G type and S type motifs (74). This work was conducted by the candidate, Dr. Rochon, and Ron Reade.

B.2.4 Heat-shock experiment to determine if RTns are induced by heat treatment of *N. benthamiana*

Four 4-6 week old *N. benthamiana* plants were either heat-shocked at 42°C for 2 h or 48°C for 30 min followed by a 2 h recovery period at 24°C as described previously (122). Untreated plants were kept at 24°C throughout the course of the experiment. TLR was extracted from equal

amounts of untreated or heat-shocked leaf tissue using the RNeasy extraction kit (Qiagen) which employs on-column DNaseI treatment to remove contaminating DNA. RT-PCR was performed using 250 ng of TLR as template using the SuperScript® VILO™ Master Mix (Thermo Fisher Scientific) which contains random primers. ddPCR was subsequently performed as per the manufacturers recommended conditions (Bio-Rad QX200™ Droplet Digital™ PCR system) using primers listed in Table B.1in order to measure the level of specific RTns. Samples were standardized using the housekeeping gene *PP2a* mRNA levels as described previously (357) using the primers shown in Table B.1. This work was conducted by the candidate.

B.2.5 Reporter expression assay to determine if RTn LTRs are heat inducible

The *Agrobacterium tumefaciens* binary vector constructs pRTn5533-LTR/GFP/pBin(+) and pRTn0067-LTR/GFP/pBin(+) as described in Figure B.4 and B.5, respectively, were prepared by Ron Reade, a member of the Rochon lab. The candidate conducted the following experiment with the above mentioned binary constructs. Leaves of four *N. benthamiana* plants (4-6 weeks old) were agroinfiltrated with either pRTn5533-LTR/GFP/pBin(+) or pRTn0067-LTR/GFP/pBin(+) and at 3 dpai the plants were heat-shocked at 42°C for 2 h or 48°C for 30 min followed by 2 h of recovery at 24°C as described above. Untreated plants were kept at 24°C throughout the experiment. At 2 hours post treatment (2 hpt), TLR and TLP samples were collected.

Droplet digital PCR was conducted on TLR obtained from untreated or heat-shocked samples using GFP specific primers (Table B.1) to determine the relative levels of GFP mRNA. *PP2a* mRNA levels were used to standardize the samples. For Western blot analyses, equal amounts of

TLP obtained from untreated or heat-shocked plants were subjected to electrophoresis through a 4-12% Bis-Tris NuPAGE gel (Thermo Fisher Scientific) followed by Western blot analyses using a monoclonal HSP70 antibody (Enzo Life Science) or GFP antibody (Clontech Laboratories). Goat anti-mouse antibody (Thermo Fisher Scientific) was used as the secondary antibody. For visualizing the protein, the acrylamide gels were stained with SYPRO Ruby (Thermo Fisher Scientific) as recommended by the manufacturer's protocol. This work was conducted by the candidate and members of the Rochon Lab.

Table B.1: List of oligonucleotide primers used in this study

Primer name[a]	Sequence from 5' to 3' direction	Description of use
RTn5533 F	ATCGTCAAAGGGC AAGAAG	5' primer used in combination with RTn5533R for the ddPCR of RTn5533
RTn5533 R	TCCATGTTTGCGGA AGTG	3' primer used in combination with RTn5533F for the ddPCR of RTn5533
RTn0067 F	GCCGGAGACATTG ATGATAG	5' primer used in combination with RTn0067R for the ddPCR of RTn0067
RTn0067 R	CAGCTTCACATGTG GATAGAG	3' primer used in combination with RTn0067F for the ddPCR of RTn0067
RTn6278 F	GAGTCATTGGAGA AAGATCCG	5' primer used in combination with RTn6278R for the ddPCR of RTn6278
RTn6278 R	CTCTAGTTTCCGCC ACATTAG	3' primer used in combination with RTn6278F for the ddPCR of RTn6278
RTn7161 F	CACCGGTAAGCGA GTTAAAG	5' primer used in combination with RTn7161R for the ddPCR of RTn7161
RTn7161 R	TCTAGCATGCCAAA GTGATG	3' primer used in combination with RTn7161F for the ddPCR of RTn7161
RTn9304 F	CAACAAACCGTGG CATTATC	5' primer used in combination with RTn9304R for the ddPCR of RTn9304
RTn9304 R	TGTCCTTGCTCCAA GTTAAG	3' primer used in combination with RTn9304F for the ddPCR of RTn9304
RTnNbT ntF	AGGTAGAGGCAGG AGTTATC	5' primer used in combination with RTnNbTntR for the ddPCR of RTnNbTnt
RTnNbT ntR	CCTGGTTGATCACA GTTGTAG	3' primer used in combination with RTnNbTntF for the ddPCR of RTnNbTnt
RTn5145 F	CACATGGAAGACC GGATGTAG	5' primer used in combination with RTn5145R for the ddPCR of RTn5145
RTn5145 R	AGGCTACGGAAGTT GCATAAG	3' primer used in combination with RTn5145F for the ddPCR of RTn5145
GFP046F	GAAGTTCGAGGGC GACAC	5' primer used in combination with GFP047R for the ddPCR of GFP
GFP047 R	TGTGGCTGTTGTAG TTGTACTC	3' primer used in combination with GFP046F for the ddPCR of GFP
PP2A3F	TGCGCCTGAACATC ATTAG	5' primer used in combination with PP2A4R for the ddPCR of PP2A
PP2A4R	CCTCTGCTAGCTCA ACAATAG	3' primer used in combination with PP2A3F for the ddPCR of PP2A

[a] F=forward primer; R= reverse primer.

B.3 Results

B.3.1 Specific retrotransposon transcripts are induced during CNV infection

Previous and ongoing research in Dr. Rochon's lab has shown that specific *Copia* and *Gypsy* type RTns are induced during CNV infection and that these are the most highly upregulated of the induced retrotransposons. Figure B.1 shows a tabular representation of selected RTns induced during CNV infection and their level of induction. Also, a phylogenetic analyses conducted by Dr. Rochon has shown that CNV-induced *Ty-1/Copia* RTns RTn5533, Rtn0067, RTn6278 and RTn9304 are closely related to the heat stress inducible ONSEN retrotransposon. On the other hand the *Ty-3/Gypsy* RTn5145 is distantly related to ONSEN (D. Rochon, personal communication). This work was conducted by Dr. Rochon and members of the Rochon Lab.

Transcript ID	Designation	RTn type	Mock1 RPKM	CNV1 RPKM	CNV1 to Mock1 RPKM ratio	Mock2 RPKM	CNV2 RPKM	CNV2 to Mock2 RPKM ratio
Nbv5tr6285533	RTn5533	*Ty-1/Copia*	0.16	371.8	2349.4	0.15	183.7	1246.1
Nbv5tr6220067	RTn0067	*Ty-1/Copia*	0.36	102.8	282.4	0.72	85	118
Nbv5tr6366278	RTn6278	*Ty-1/Copia*	0.57	37.7	65.5	0.67	312	48.3
Nbv5tr6297161	RTn7161	*Ty-1/Copia*	3.5	16.1	46.4	5	95.9	19.1
Nbv5tr6199304	RTn9304	*Ty-1/Copia*	0.35	1.3	3.8	0.49	1.3	2.6
Nbv5tr6225145	RTn5145	*Ty-3/Gypsy*	0.93	110.9	118.8	0.82	157.6	192

Figure B.1: Retrotransposon (RTn) transcripts are induced during CNV infection.

Tabular representation of *Copia* (highlighted as green) and *Gypsy* (highlighted as blue) type RTn mRNAs induced during CNV infection relative to mock treatment from two independent experiments. The data were obtained from Illumina based RNA-seq analysis of total leaf RNA extracted from mock or CNV infected leaf tissue at 4 dpi (CNV1 and Mock1) and 3 dpi (CNV2 and Mock2). Data provided by Dr. D'Ann Rochon. RPKM=reads per kilobase per million transcripts as deduced from RNA-seq analyses. The CNV1 to Mock1 RPKM ratio as well as the CNV2 to Mock2 RPKM ratio indicate the level of induction of the indicated RTn.

B.3.2 LTRs of RTns induced by CNV contain putative HSEs

Previous and ongoing research in Dr. Rochon's lab has shown that the LTRs of RTns induced by CNV contain numerous putative HSEs. Figure B.2, panels (a) to (f), show the nucleotide sequences for the 5' LTRs of five major *Ty-1/Copia*-type RTns (RTn5533, RTn0067, RTn6278, RTn7161 and RTn9304) and the *Ty-3/Gypsy-type* RTn5145 induced during CNV infection along with the previously described heat inducible ONSEN RTn (panel h). Also the LTR of a *N. benthamiana Ty-1/Copia* Tnt type RTn (RTnNbTnt) which is not induced during CNV infection and has not been reported to be heat inducible is shown. The putative HSEs of the CNV inducible RTn LTRs are highlighted in yellow (see Materials and methods for details on what constitutes an HSE element). Sequences which may correspond to the core promoter "TATA box" are highlighted in grey.

The LTR of RTn5533 which is induced to the highest level during CNV infection and heat stress (Figure B.1 and Figure B.3) contains a high number of putative HSEs (i.e., 13; with 8 P type,four G type and one S type) as well as a high percentage of putative HSEs (3.6%) considering the criteria described above, including overlapping HSEs. However, RTn6278 which is induced to a lower level by both CNV infection and by heat shock (Figure B.1 and Figure B.3) contains a greater number of HSEs (i.e., 23; with 19 P type and four G type) as well as a higher percentage when considering the length of the LTR (4.3%). As well, RTn0067, which is expressed to a lower level than RTn5533 (Figure B.1 and Figure B.3) is quite similar to RTn5533 with respect to the number of HSEs (i.e., 13 with eight P type, five G type and one S type) but the percentage of HSEs is lower being about 2.6%. Notably, RTnNbTnt, which is not significantly induced during CNV infection (Figure B.1 and Figure B.3) contains the fewest number of percentage

putative HSEs compared to the *Ty-1/Copia* RTns that are induced during CNV infection (i.e., 3, with 2 P type and 1 G type) (Figure B.2). Also, RTn9304 and RTn5145 which are not induced strongly during CNV infection or by heat shock contain a relatively low number of HSEs (Figure B.2) (5 and 6, respectively with percent values of 1.5% and 1.2%, respectively).

Recently it has been shown that ONSEN contains numerous putative long HSE elements that accounts for its high level of induction by heat stress in *Arabidopsis* (358). Also it has been shown recently that longer HSEs (i.e., HSEs comprising more than 3 "nGAAn" elements) appear to be more strongly activated by HSFA2 than shorter ones or the ones that are of G or S type (75, 358). This also correlates with the low *in vitro* binding efficiency of HSFs with G or S type HSEs (359). We found that the most highly expressed CNV-induced RTns have the greatest number of putative HSEs (Figure B.2, panels a-d) and that retrotransposons not known to be induced by CNV or heat such as RTnNbTnt contain a low level of putative HSEs that consist predominantly of elements containing only 3 pentanucleotide motifs (Figure B.2, panel g). The observation that there is not a pronounced correlation between the level of induction by CNV (or heat) and the number and type of HSE may simply reflect that the identified HSEs are only putatively functioning as HSEs. Also, other factors may be operating with respect to the level of induction. Further experiments, such as footprint analysis to identify functional HSEs along with mutagenesis analyses are required to further assess the relationship between the possession of HSEs and inducibility by CNV infection and heat. Nevertheless, there appears to be a strong correlation between those RTns that are induced by CNV and heat shock and the number and length of putative HSEs. This work was conducted by the candidate along with Dr. Rochon and Ron Reade.

a. RTn5533 (13/357=3.6%) (13 HSEs; 8 P type, 4 G type, 1 S type)

tgttaagattaaacttgattaacatgaagtgTTCtaGAAtcATCttGTActagctaGAAaaATCttcataaaaatcaatgtattaaactaGACaaTTCtaGGAggaTACta
GATacTTCtcAAAtaaaattcataggcatcaATCtaGAGaaTTCtaTAAacTTGtataatcattcaagtatctagatcattccatggagtagtataaatatgtgatgttgtaactca
ttttgaaATCaaGAAatcaatаAAAtaacaaaagccttcttcaatataaagttttatcTCCattccaaTTCtctacatTTCctAAActctttccttctcattctaaatattactctccttctcc
aaca

b. RTn0067 (13/485=2.6%) (13 HSEs; 8 P type, 5 G type)

tgttgaaaataaaataaacttgattttgttataattatttggcttaagaaattatgaaaaataaatagcccaaTTCcgGAAcaTTCtaggcaaCTCtagaTTCcgGAAtgTTCtg
GAGaaCTCtagtccatttgagcttggAAAtaCTCtaGAAttCTCcatagaaTTCtaGCAcatgtacctagctagaaagtaataGAActCTCtaGACt|CTCtaGAAtt
CTCcatagaaTTCtaGCAcatgtacatagctaggaaatggtagaactctctagacactctagagcttggcaagcctcccctataaatatgggatggcatttggcatttgtataatataca
acacacaacatatcaagccaaaagaatcaaaaacaagtttgagtaataaaagtttctcttccccaaaatctttctactcttccaaaattcccttagcctaaaagcctccctccaaatattaatag
caattctcttccaaca

c. RTn6278 (23/528=4.3%) (23 HSE; 19 P type, 4 G type)

tgtgaacaataaaataaaccaaagctaGATatTACtaGAAtaTTCtaGACtaTTCtaAAAtaGTCtaGAAtgagctaGAAtgTTCtaGAAggTTCgaGAAcaT
TAtgGAGttCTCtgGAAcaTTCtaGAAgatgataGAAactcttttatgtatagtaGAGaatgtgaGAAtaTTCtaGAGtagtgGAAtaTTCtaGAAcatatgaGAAt
aggtagatatgaatattgtttaggatacttatatgGAAtaTTCtaGAAtgtcgtaGAAcatggaggttgatgcctataaatagggaagacctcctcatttgtatgatgtacaaaaggagt
gaagcaaagtgtgagcccaagtgtgtaccaaagtgatcccttgtgtaataaaagttgaagaattacaaaagtctctctccatatagctacatatattaaaccttccaaactacctccatttcttca
tttatcaactaaacaaaatctctttccttcttacatttaaaggtcttctaccttaaattgttctcctaca

d. RTn7161 (10/442=2.2%) (10 HSE; 3 P type, 6 G type, 1 S type)

tgttaAAAttaaagtGTAacttttgGAAaaTTAtaGAAtagtgtaGAAtaTTAtaGAAgttaggaGAGatatttctagattagtgtaggtgataaaaatatctagatattttgtaaG
AAaagtgtgGAGtaTTCtaGAAgatgaatctccaccgtaggattaaatagatcatgaccgtccattgaggaggtggaaagcctatatatacccaccccttcttccacatttgtaccatcc
aaaaaaatccaagtcttcttgagttaataaagtattctccaagttattcaagtaagtcttccacttttttagttctagtatttttggagctatatttaTTCttcgttcTTCttCAAttgtggttgtgagtct
tgggctagtgaagcataattcactactctaaggaagcaatttccggaatttgggaagttgtttttcttcaca

e. RTn5145 (6/496=1.2%)(6 HSE; 6 P type)

tgtcacgcccctccattttctaagaggttatgccatgcggacgatgactgggcgacatgcaggcaacgatttggcgcacgtatggcagctttctctagctaaGTCtaGATccTTCcaat
gGAAgaTTCtaGACccacctaaacttCTCttGTAtaTTCtactaggtgtagagatttgtaGAGatTTGtaGAActCTCtaGAgctttgatcttagccattgattagaatagat
cttagccgttgatttgggactctagcaactataaataggctagaggcatttggcatttgcatccaagaaacattcaagcaatccaacacttgtataaagcattctcttgtttaatacaaagcattctt
gcaagcttctcttcttagcttctcttagctttgttgtggcaatatttcggggaaaggctgacttagcacatcgcaggggcggattgtgactaaggccgcacggaagatagctagggagttatccg
gtccgtgaca

f. RTn9304 (5/336=1.5%) (5 HSE; 4 P type, 1 G type)

agatttgttaaagtataatatgtaatttgtaatttgtattagctaGAAgtCTCtaGATatatgagtataatatcaaagcatgGAGttCTCtaGAAtactagataacatgtttggaaaaata
tctatataagcaaaatatctagaGTCtaGAAtaatgtaGAActtgagaaatatctcatgtatgtgGAAaaATCtaGAActATCcaacaagtctataaatagccatgtaatccatca
tttgttaaggattaataagaagaagcattcaaagttattcccataacatttttctactctaacaatctaatatcttcttccatacacttcaccccaaca

g. RTnNbTnt (3/659=0.45%)(3 HSE; 2 P type, 1 G type)

tgtggggtccaacccacttattaaggaagaaaattcttccttgcttcttcattcaatataggcagcagcacgttttcttgtttgtcaaagaaagtaggctgcggaaatggagaagtcaagataag
ttggcaatattttgcctataaaatgagagcttcggctctcatttttttacaccaatagaaagagagaaaaagagtaaggtttcacagacagagtacaagaaaatagtctgtgaggaaaataga
gagtgagagatattgtagtgagatagaaatatcaaaaGAAggTTAttttcttTTGagtgttgtagtggtctttggagtatttTTCtcGGAccTACaaagtgnaaatagagagtgagcg
atattgtagtgaggtggaaatatcaaaagagggttatttttctttgagtgttgtagtggtctttggagtatttTTCtcGGAccTACaaagtgtaaaattccttactatagtgatatcagttgctactc
tcagggccgtggttttttccttattcagaagggttttccacgtaaaattttggtgtcgttgttactcttttattattgttaattaccgtatctcggtgctacattattattccgctttattaccgtgaatattatttt
ggtaggggaatttattcccaacaa

h. ONSEN (81/440=18.4%) (10/440=2.2%)(10 HSE; 5 P type, 5 G type)

tgttGAAagTTAaacttgaTTTtgaatcaagtttaattattggatcaattatccaataattaattatggcCAAatccaagTTCtaGAGttTTCtctaGAAatATCatcatttccacct
ccttaAAAgaTTCtaGAAatTTTctaGAAtcATCttccaccTCCttaaacataaaaatctagatactctaataGAAtaATCtaGATaatttgaataatgtaatctagatcttatg
taaGAActCTCtaGACttaggattaaaatattttagatattttgtagtttggaggctataaatacctcctcccccctctcaaatgttgcaatgttgtgaagttgtattcaagtttaaaGCAaagta
atAAAagTTCtatTTCctAAAaaactctCTCaaaacacttaaacactttctccattacctctaaaagaattttactctaaca

Figure B.2: LTRs of RTns induced by CNV contain putative HSEs.

Analyses of the 5’ to 3’ LTR regions of four major *Ty-1/Copia*-type RTns (RTn5533, RTn0067, RTn6278 and RTn7161) induced during CNV infection (panels a to d) along with the moderately induced RTn9304 (panel f). The 5’ to 3’ LTR promoter of RTnNbTnt which is not induced

during CNV infection is shown in panel g. The 5' to 3' LTR of a previously described heat inducible ONSEN RTn is also shown (panel h). Panel e represents the 5' to 3' LTR of a *Ty-3/gypsy* RTn5145 which is also significantly induced by CNV. The sequences highlighted in yellow represent putative HSEs and the sequences highlighted in grey represent putative TATA boxes. Putative HSE elements are described in more detail in the Materials and methods and text. The putative "nGAAn" and "nTTCn" pentanucleotide motifs (including those with single substitutions) comprising putative HSEs are shown in bold uppercase and the irregular ones (i.e. those with substitutions in the "nGAAn" or "nTTCn" sequence) are shown in regular uppercase. The number of HSEs is shown within parenthesis along with the proportion of each type [i.e, perfect (P), gap (G) or step (S) type] following the names of each RTn. The numbers of HSE elements were divided by the total number of nucleotides constituting the LTR and the values were multiplied by 100 to obtain the percentage value.

Unpublished work from Dr. Rochon's lab has also shown that the *N. benthamiana* transcription factor HSF30 (gene ID Nbv5tr6215455; a homolog of *Arabidopsis thaliana* HSFA2, henceforth referred as NbHSFA2) is induced ~ 8-10 fold during CNV infection. Also, heat treatment of *N. benthamiana* has been found to significantly induce the levels of NbHSFA2. Thus, as with ONSEN, HSFA2 may be the heat shock factor that is involved in regulating the expression of CNV induced RTns. However, this remains to be determined. Hence, the working hypothesis for this chapter is that CNV induces transcription of retrotransposons likely through activation of the heat-shock response induced during infection. More specifically, it is proposed that the highly induced RTns that are phylogenetically related to ONSEN possess functional HSEs that are likely activated by HSFA2s induced by CNV infection.

B.3.3 *Ty-1/Copia*-type RTns induced by CNV are heat-shock inducible

I wished to investigate if the RTns induced by CNV that contain HSEs in their LTRs are heat-shock inducible. To do that, *N. benthamiana* plants were either not treated or heat-shocked at 42°C (HS-42) or 48°C (HS-48) followed by TLR extraction and ddPCR as described in the Materials and methods. Figure B.3 is a graphical representation of the ddPCR results obtained using the primers described in Table B.1. It can be seen that the five major *Ty-1/Copia* RTns induced during CNV infection, i.e., RTn5533, RTn0067, RTn6278, RTn7161 and RTn9304 are each heat inducible. In addition, induction is more pronounced at 48°C than 42°C (compare blue bars with red bars, respectively). As the transcript abundance of these RTns was significantly increased with severity of the stress (i.e., higher temperature), this suggests a temperature-sensitive response as previously described for RTns in rice (*Oryza sativa*) (314).

To rule out the possibility that heat treatment induces RTns non-specifically, I also determined the transcript levels of the *Ty-1/Copia* element RTnNbTnt which is not induced during CNV infection (S.B. Alam, data not shown) and not reported to be heat inducible. It can be seen in Figure B.3 that RTnNbTnt is not induced by heat treatment at 42°C or 48°C suggesting that RTn induction by heat treatment is specific. Also, as found in CNV infection, where RTn5533 is the most strongly induced RTn followed by RTn0067, RTn6278, RTn7161 and RTn9304 (see Figure B.1), a similar pattern in the induction of RTns was observed by heat treatment suggesting a positive correlation between the levels of CNV induced RTns and RTns induced by heat treatment. I also determined the transcript levels of the *Ty-3/Gypsy* RTn (RTn5145) which is induced significantly during CNV infection and found that it is also induced by heat treatment, but only mildly so (Figure B.3B), consistent with the low level of HSE elements observed in the LTR region (Figure B.2). The basis for the high level of induction of RTn5145 by CNV infection requires further exploration. This work was conducted by the candidate.

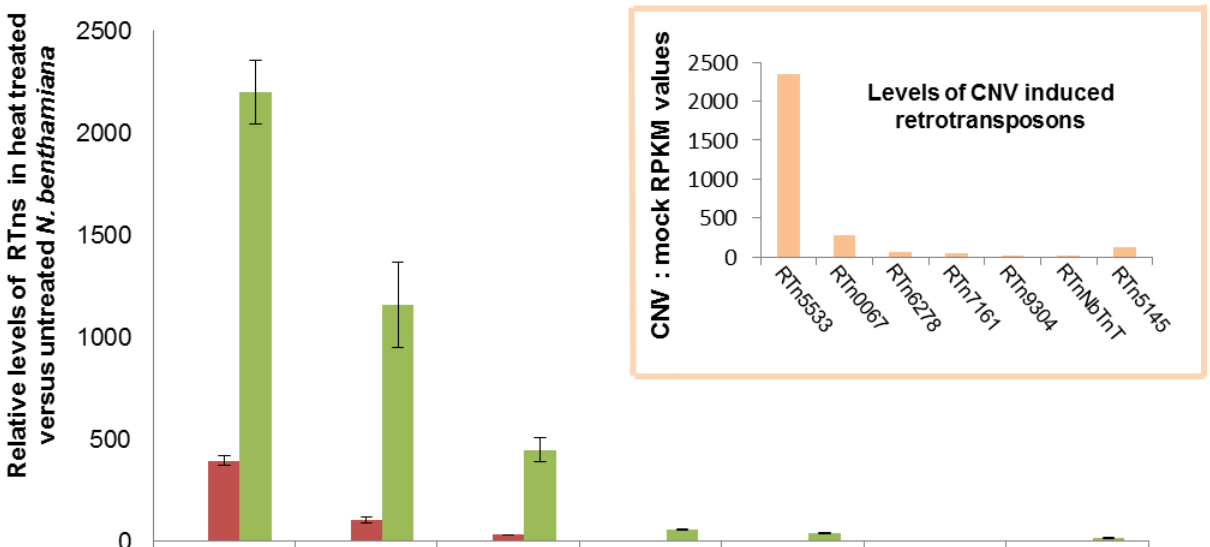

	RTn5533	RTn0067	RTn6278	RTn7161	RTn9304	RTnNbTnt	RTn5145
Untreated	1	1	1	1	1	1	1
42°C-HS	395.027	107.06	31.72	4.816	4.394	1.349	2.754
48°C-HS	2201.033	1159.00837	448.724823	57.8896221	39.680972	1.33882715	16.267

Figure B.3: *Ty-1/Copia*-type RTns induced by CNV are heat shock inducible.

Graphical representation of the mRNA levels of *Copia*-type or *Gypsy*-type RTns induced by heat treatment. *N. benthamiana* plants were heat-shocked at 42°C (42°C-HS) or 48°C (48°C-HS) as described in Materials and methods. Control samples were not subjected to any heat stress (Untreated) and were kept at 24°C throughout the course of the experiment. TLR was extracted from untreated or heat-shocked leaf tissue and subjected to ddPCR using primers specific to the indicated RTn (See Table B.1). *PP2a* mRNA levels were used to standardize samples. The inset shows the levels of the same RTns induced by CNV infection as deduced from RNA-seq analyses (see Materials and methods) (Personal communication; D. Rochon). The ratio of the RPKM value determined for a specific RTn in CNV infected leaf tissue compared to that in mock inoculated tissue (CNV:mock RPKM values) was determined and plotted as shown.

B.3.4 Heat treatment activates the LTR of CNV inducible RTn5533 resulting in the expression of the downstream reporter gene, GFP

Since the LTRs of the most strongly induced RTns contain numerous putative HSEs, I wished to directly assess the possibility that heat treatment can activate the 5' LTR of the RTns. A reporter expression assay was therefore developed in the Rochon lab. Since the RTn5533 LTR was found to contain several HSE motifs and as described above is most highly induced by CNV infection and by heat treatment, I wished to determine if the LTR sequence is sufficient for heat induction. To do this, an *Agrobacterium tumefaciens* binary vector construct pRTn5533-LTR/GFP/pBin(+) was prepared in which the 5'LTR of RTn5533 was placed upstream of the reporter gene GFP (Figure B.4A). *N. benthamiana* plants were agroinfiltrated with pRTn5533-LTR/GFP/pBin(+) and at 3 dpai the plants were either not subjected to any heat stress (untreated) or heat-shocked at 42°C or 48°C as described in Materials and methods. At 2 hpt, TLR and TLP samples were collected and subjected to ddPCR and Western blot analyses to determine the relative levels of GFP mRNA (Figure B.4B) and protein (Figure B.4C) respectively.

Figure B.4B shows that GFP mRNA levels are significantly increased following heat treatment relative to agroinfiltrated, untreated samples. Also, the GFP mRNA induction levels are more pronounced at 48°C (166 fold) than at 42°C (118 fold) which suggests that a parallel exists between the extent of heat stress and the extent of activation of the RTn5533 LTR. Figure B.4C shows a Western blot of TLP probed with either a HSP70 (upper panel) or GFP (middle panel) monoclonal antibody. The upper panel shows that, as expected, heat treatment at both 42°C and 48°C significantly increases the levels of HSP70 homologs. The middle panel shows that heat

treatment of pRTn5533-LTR/GFP/pBin(+) agroinfiltrated leaves increases the expression of GFP consistent with the increased levels of GFP mRNA as shown by ddPCR.

To further confirm activation of the pRTn5533 LTR by heat, confocal microscopy was conducted on untreated or heat-shocked pRTn5533-LTR/GFP/pBin(+) agroinfiltrated leaves at 2 hpt. Figure B.4D summarizes the results. The first panel shows GFP fluorescence (green), the middle panel chloroplast autofluorescence (red) and the third panel shows a merge of the first and the middle panels. It can be seen that while untreated samples do not show any detectable levels of GFP fluorescence, heat-shocked samples show substantial GFP fluorescence which is more pronounced at 48°C compared to 42°C. These results are consistent with those of Figure B.4B and 4.4C and suggest that heat-shock can activate the 5'LTR of RTn5533 that in turn can promote the expression of the downstream reporter gene GFP. Since the 5' LTR of RTn5533 is sufficient for heat-shock induction this suggests that the putative HSE elements may actually function as such during heat treatment. It is to be noted that similar types of results were obtained in pRTn5533-LTR/GFP/pBin(+) agroinfiltrated, CNV infected plants (personal communication, D. Rochon lab) suggesting that CNV infection may similarly activate the RTn5533 LTR via its possession of HSEs. Although highly unlikely, it is still possible that induction of GFP could occur in this binary vector in the absence of the RTn5533 LTR. Such an experiment remains to be conducted. This work was conducted by the candidate.

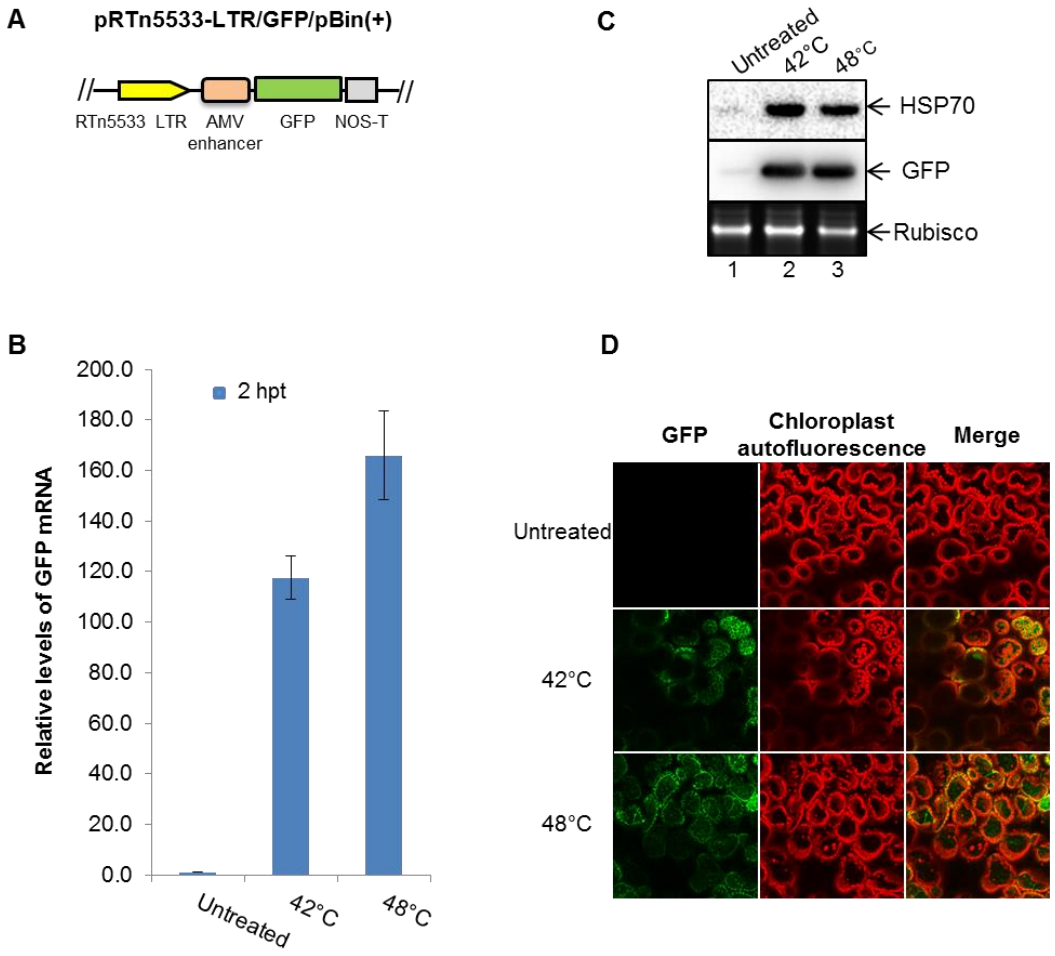

Figure B.4: Heat treatment activates the LTR of CNV inducible RTn5533 inducing the expression of the downstream reporter gene, GFP.

(A) Schematic diagram of the structure of the construct pRTn5533-LTR/GFP/pBin(+). The duplicate 35S promoter from a previously described clone pGFP/pBin(+) was replaced with the RTn5533 LTR (shown in yellow). The positions of the AMV translational enhancer (shown in orange) and the NOS transcriptional terminator (shown in grey) are also shown. *N. benthamiana* plants were agroinfiltrated with a culture of pRTn5533-LTR/GFP/pBin(+) at an OD_{600}=1.0 and at 3 dpai, the plants were heat-shocked at 42°C or 48°C as described in the Materials and methods. Untreated plants agroinfiltrated with pRTn5533-LTR/GFP/pBin(+) were kept at 24°C throughout the course of experiment. At 2 hpt, agroinfiltrated leaf samples from untreated or heat-shocked plants were collected. B) Total leaf RNA was extracted from collected samples. GFP mRNA levels were analysed by ddPCR using *PP2a* as the reference gene for standardizing the samples. The ddPCR value obtained in untreated samples was arbitrarily assigned a value of 1 and the relative levels of induction at 42°C and 48°C are shown. (C) Equal amounts of total leaf protein were subjected SDS-PAGE in triplicate followed by Western blot analyses (upper and middle panel) or SYPRO Ruby staining (lower panel). The blots were probed with either a HSP70 (upper panel) or GFP monoclonal antibody (middle panel). Rubisco levels, used as the

loading control, are shown in the bottom panel. (D) Agroinfiltrated leaf sectors that were either untreated or heat-shocked at 42°C or 48°C as indicated were analysed by confocal microscopy at 2 hpt. The first column represents GFP fluorescence (green) and the middle column shows chloroplast autofluorescence (red). The third column is a merge of the first and the middle columns.

B.3.5 Heat treatment activates the LTR of CNV inducible RTn0067 resulting in the expression of the downstream reporter gene, GFP

I wished to determine if heat-shock can activate the 5' LTR of another highly CNV induced retrotransposon with a high number of HSEs, RTn0067 (Figs B.1 and B.2). To do this an experimental approach similar to that described above for RTn5533 was taken. The construct pRTn0067-LTR/GFP/pBin(+) was produced as described for pRTn5533-LTR/GFP/pBin(+) (Figure B.5A) and used to agroinfiltrated *N. benthamiana* plants. At 3 dpai, the plants were either not subjected to any heat stress (untreated) or heat-shocked as described above. The activation of the RTn0067 LTR was analysed using ddPCR, Western blot analysis and confocal microscopy.

Figure B.5B shows that GFP mRNA levels are significantly induced by heat treatment. Also, as for pRTn5533-LTR/GFP/pBin(+), GFP mRNA levels are relatively more abundant at 48°C (215 fold) compared to 42°C (45fold). Figure B.5C shows a Western blot analysis of TLP obtained at 2 hpt from equal masses of untreated or heat-shocked, pRTn0067-LTR/GFP/pBin(+) agroinfiltrated leaves, probed with either a HSP70 (upper panel) or GFP (middle panel) monoclonal antibody. The upper panel shows that, as expected, heat treatment at both 42°C and 48°C significantly increases the levels of HSP70 homologs. The middle panel shows that heat treatment of pRTn0067-LTR/GFP/pBin(+) agroinfiltrated leaves significantly increases the expression of GFP. Lastly, confocal microscopy results show that GFP is induced at both 42°C and 48°C. Although highly unlikely, it is still possible that induction of GFP could occur in this binary vector in the absence of the RTn0067 LTR. Such experiments remain to be conducted. This work was conducted by the candidate.

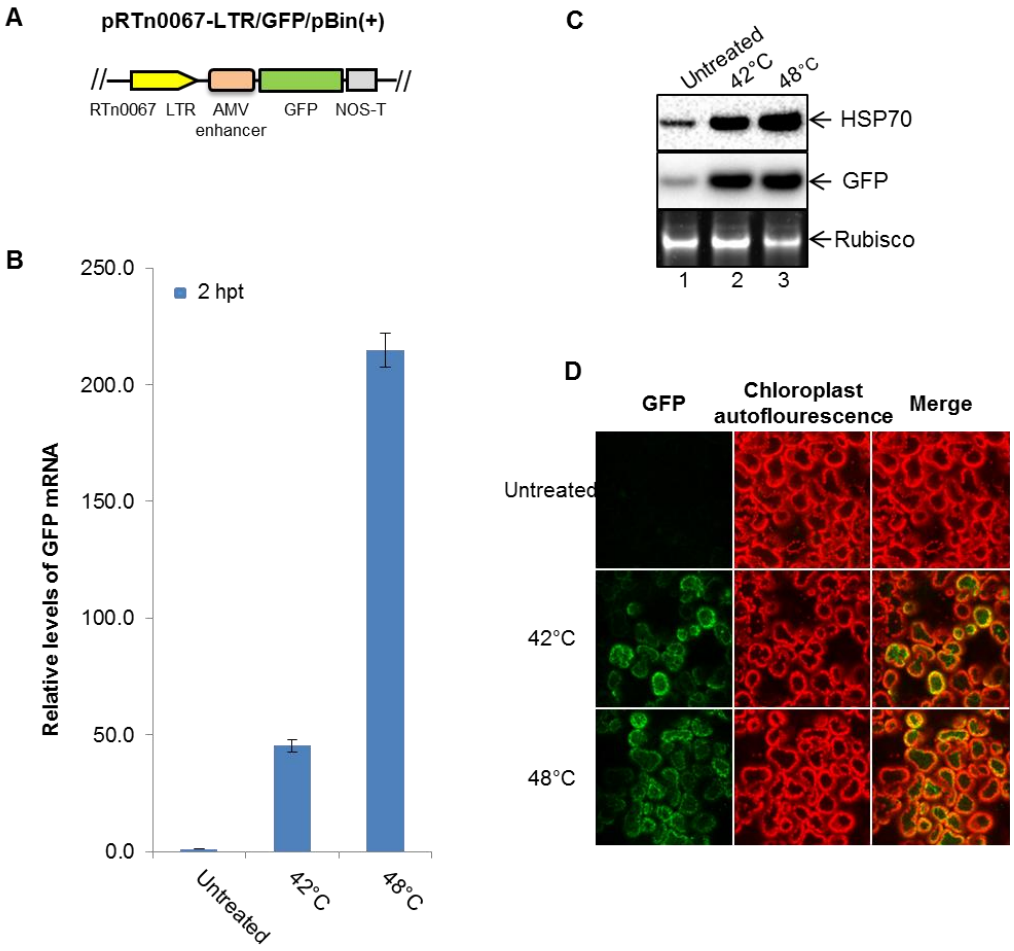

Figure B.5: Heat treatment activates the LTR of CNV inducible RTn0067 promoting the expression of the downstream reporter gene, GFP.

(A) Schematic diagram of the structure of construct pRTn0067-LTR/GFP/pBin(+). The duplicate *Cauliflower mosaic virus* 35S promoter from a previously described *A. tumefaciens* binary vector clone pGFP/pBin(+) was replaced with the RTn0067 LTR (shown in yellow). The positions of the AMV translational enhancer (shown in orange) along with the nopaline synthase (NOS) transcriptional terminator (shown in grey) are also shown. *N. benthamiana* plants were agroinfiltrated with a culture of pRTn0067-LTR/GFP/pBin(+) at an OD_{600}=1.0 and at 3 dpai, the plants were heat-shocked at 42°C or 48°C as described in the Materials and methods. Untreated plants, agroinfiltrated with pRTn0067-LTR/GFP/pBin(+) were kept at 24°C throughout the course of experiment. At 2 hpt, agroinfiltrated leaf samples from untreated or heat-shocked plants were collected. (B) Total leaf RNA was extracted from collected samples. GFP mRNA levels were analysed by ddPCR using *PP2a* as the reference gene for standardizing the samples. The ddPCR value obtained in untreated samples was arbitrarily assigned a value of 1 and the relative levels of induction at 42°C and 48°C are shown. (C) Equal amounts of total leaf protein were subjected SDS-PAGE in triplicate followed by Western blot analyses (upper and middle panel) or SYPRO Ruby staining (lower panel). The blots were probed with either a HSP70

(upper panel) or GFP monoclonal antibody (middle panel). Rubisco levels, used as the loading control, are shown in the bottom panel. (D) Agroinfiltrated leaf sectors that were either untreated or heat-shocked at 42°C or 48°C as indicated were analysed by confocal microscopy at 2 hpt. The first column represents GFP fluorescence (green) and the middle column shows chloroplast autofluorescence (red). The third column is a merge of the first and the middle columns.

B.4 Discussion

In the present study I have found a possible mechanism for induction of RTns during CNV infection. In Figure B.3, I found that several CNV induced retrotransposons are induced by heat treatment. Interestingly, the relative levels of induction of the retrotransposons by heat treatment roughly parallels that induced by CNV infection suggesting perhaps that the heat-shock response induced by CNV during infection may be responsible, at least in part, for the induction of specific CNV induced retrotransposons. I have also found that the level of heat-shock induction of several retrotransposons correlates well with the number and extent of concatenation of putative HSEs in the respective LTRs of the RTns (Figure B.2). Finally, I have shown that the LTRs of 2 CNV-induced retrotransposons can be activated by heat to induce downstream expression of a reporter gene, indicating that the LTR component of the RTn is sufficient for heat inducibility of the respective RTn (Figures B.4 and B.5). This is the first report that retrotransposons are induced by a plant virus and also the first report that induction of retrotransposons during virus infection may be related to the heat-shock response induced by the virus.

With regards to the *Ty-3/Gypsy* RTn5145 which is significantly induced during CNV infection but not significantly induced by heat treatment, it is plausible that the HSFA2 induced during CNV infection does not efficiently bind the HSEs since they are not long (see Figure B.2, panel e). However, when I analysed the LTR of RTn5145, I found that it contains other putative stress responsive consensus motifs that might be responsible for its activation during CNV infection. For example, I found that the RTn5145 LTR contains two "TCA" motifs. This motif is highly

conserved among stress-inducible genes and binds salicylic acid-inducible tobacco nuclear proteins in *N. tabacum* (360).

RTns are a major component of plant genomes. They can spread and insert at new locations throughout the genome by retrotransposition. Retrotransposition involves reverse transcription of the RTn mRNA into cDNA by reverse transcriptase encoded by the RTn and reinsertion of copied elements into new genomic loci randomly by a copy-and-paste mechanism (323). The transposition of RTns to new locations in the genome may interrupt a gene (361), change its expression (362, 363) and genome organisation (364) on a large scale. Hence, RTns represent a threat to the integrity of plant genomes when their propagation is uncontrolled.

The LTR RTns are the most abundant class of TEs in plants genomes comprising 15% of the nuclear DNA of *A. thaliana*, 90% of the DNA of some *Liliaceae* species and 50-80% of the genomic DNA of *Poaceae* genomes (365, 366). LTR RTns are flanked at both the 5' and 3' ends by LTR sequences which are a few hundred to several hundred base pairs in length. LTRs contain gene promoters and regulatory sequences for controlling transcription and replication of RTns(367). Plants in turn, have evolved to keep a check on the activity of retrotransposons by epigenetic modification. Unlike animals, plants do not erase DNA methylation patterns during meiosis (368) and hence DNA methylation is inherited and acts to maintain TE suppression across generations (369).

Nearly all TEs including the LTR RTns are dormant in plants and are not transcribed generally when biotic and abiotic stresses are absent (370). RTns on the other hand have co-evolved to

escape the plant suppressive response by acquiring *cis*-regulatory sequences in their LTRs that mimic stress responsive elements. Due to possession of the stress responsive elements in the promoter regions, RTns can become activated and multiply under different stress conditions (371). RTn activation under stress might be a driving force for adaptation, while simultaneously removing unfit variants if adjacent host genes become dysregulated (334).

In the current study, we identified that a *Tombusvirus*, CNV, induces specific *Ty-1/Copia* RTns during infection. It is also possible that like other stress inducible RTns such as ONSEN (320), CNV inducible RTns may play a positive role in conferring stress tolerance and may positively influence adaptation of the genome. In this light, it is possible that CNV infection itself may confer a beneficial advantage to plants by inducing a heat stress response and thereby confer heat tolerance to plants. Moreover, induction of retrotransposons carrying LTRs that are heat responsive could be a mechanism that allows the plant to retain heat responsiveness following virus infection.

A study on *Herpesvirus* has shown that infection induced RTn expression contributes to innate immune signaling during infection. However, *Herpesvirus* can exploit that to enhance viral gene expression (372). It was reported that during *Murine gammaherpesvirus 68* (MHV68) infection, SINE RNAs are induced that activate the antiviral NF-κB signaling pathway. However, the SINE RNAs also stimulate the activity of the IKKβ component of the NF-κB signaling pathway and this results in phosphorylation of MHV68RTA, which is the viral transcriptional activator. Thus activation of SINE RNAs by the virus promotes viral gene expression and replication.

Previous work in this thesis has shown that CNV has evolved to co-opt different homologs of HSP70 proteins at several stages of the multiplication cycle for its own benefit (Chapters 2 and 3) (117, 122). I have also shown that *C. quinoa* plants that are subjected to heat stress can result in enhanced replication of CNV (122). Hence it might be possible that CNV utilizes the heat stress inducible RTns for enhanced multiplication. It is possible that components of the RTn reverse transcriptase complex may be co-opted by the CNV replicase for enhanced CNV RNA replication. Hence, I hypothesize that CNV has evolved to co-opt some aspect of the RTn multiplication cycle during infection for enhanced CNV accumulation. For example, the type 2 cleavage site of the *Retrovirus* protease cleaves between hydrophobic residues. It is known that CNV CP is must be cleaved prior to its entry into chloroplasts (24) which is associated with attenuation of CNV induced necrosis (Rochon Lab, unpublished observations), however, it is unknown how this occurs as CNV does not encode a protease. It is possible that the RTn protease may assist in this cleavage process.

A recent report suggests that endogenous retrotransposition of LINE-1 RTns were found to play a potential role in *Hepatitis virus*-related hepatocellular carcinoma (HCC) (373). LINE-1 RTns are usually silenced in most somatic cells by DNA methyltransferase-mediated DNA methylation of its promoter (374). But, in cancer cells infected with Hepatitis B and C, DNA hypomethylation occurs at various genomic loci (375) including loci containing LINE-1 RTns allowing for LINE-1 retrotransposition (376). LINE-1 mediated retrotransposition was postulated to be a critical source of mutations that could depress tumour suppressive capacity of somatic cells in HCC (373). In analogy to LINE-1 RTn, perhaps CNV inducible RTns can be used as a source of mutations to depress tumour suppressive activities.

Previous work in Dr. Rochon's lab has shown that CNV CP when expressed in *N. benthamiana* plants can produce virus-like particles or VLPs that encapsidate host RNA (135). Of the encapsidated RNA the most abundantly encapsidated host RNAs are the cytoplasmic rRNAs possibly due to their abundance in the cytoplasm. Hence, it is possible that if CNV VLPs can encapsidate LINE-1 RTns introduced transgenically from cancer cells and expressed to high levels in plants, the resulting CNV VLPs which may encapsidate the LINE- RTns can be utilized as a vector to deliver RTns for therapeutic purposes to treat cancer. Also, CNV CP can be cloned into an expression vector capable of replicating in human cancer cell lines which express LINE-1 RTns to a significantly high level. CNV CP can then form VLPs which would be expected to encapsidate abundant LINE-1 RNAs. VLPs containing LINE-1 RTns can then be extracted and delivered as vector to treat cancer.

There is a growing attention towards the hypothesis that plants have a cellular memory of biotic and abiotic stress exposure (377). For example, the heat inducible ONSEN RTn has been described to confer heat inducibility into neighbouring genes via retrotransposition that can be transmitted to the next generation (333). Like ONSEN, CNV inducible RTns might too have hijacked the plant heat stress response. The plants, in turn may take advantage of new transpositions to cope with heat stress conditions in the long term. CNV inducible RTns might similarly play an important role in conferring long term heat stress memory as alluded to above.